Université du Québec
Institut national de la recherche scientifique
Centre Eau Terre Environnement

Géologie du Quaternaire, modélisation géologique 3D et courants glaciaires dans l'estuaire moyen du Saint-Laurent : Applications du LiDAR aéroporté

Par

Guillaume Légaré-Couture

Thèse présentée pour l'obtention du grade de

Philosophiae Doctor, Ph.D.

en sciences de la Terre

Jury d'évaluation

Président du jury et	Richard Martel
examinateur interne	INRS Centre Eau Terre Environnement
Examinateur externe	Michel Lamothe
	Université du Québec à Montréal
Examinateur externe	Hugo Dubé-Loubert
	Ministère de l'Énergie et des Ressources naturelles du Québec
Directeur de recherche	Michel Parent
	Commission géologique du Canada
Codirecteur de recherche	René Lefebvre
	INRS Centre Eau Terre Environnement

" Opportunity is most often missed
because it is dressed in overalls
and looks like work. "

- Anonyme

REMERCIEMENTS

Je tiens tout d'abord à remercier les membres du jury d'évaluation pour avoir accepté de lire cette thèse.

Je me dois de remercier mon directeur Michel Parent pour son support tout au long de ma thèse, pour nos longues conversations sur la géologie quaternaire du sud du Québec ainsi que ses nombreuses contributions lors de nos sorties sur le terrain. Merci de m'avoir donné l'opportunité de travailler sur cette thèse, pour ta confiance et pour ta participation active à mon projet. Mes remerciements les plus sincères vont également à mon co-directeur René Lefebvre. Merci pour ton soutien, ta disponibilité, ta rigueur scientifique et tes commentaires toujours constructifs.

Merci à Jean-Marc Ballard pour les sondages au piézocône, les forages et ta patience sur le terrain, même quand c'était moins facile que prévu! Merci à Marc-André Carrier pour tes conseils judicieux pendant mes premières années de thèse. Je remercie Miroslav Nastev (CGC) pour nos discussions toujours intéressantes (et aussi pour m'avoir remplacé une journée sur un chantier de forage !). Merci à Jean-Pierre Guilbault pour les analyses de foraminifères et pour nos discussions sur la paléofaune de la Mer de Champlain. Un grand merci va aussi à l'équipe complète du PACES-Chaudières Appalaches, qui a réalisé une partie de la compilation des données de forages utilisées dans le cadre du deuxième chapitre de cette thèse.

Merci à Christophe Kinnard (UQTR) de m'avoir donné la chance de pouvoir contempler des glaciers ailleurs que dans des livres. Merci à mon collègue et ami Yves Leblanc pour tes conseils judicieux et pour les nombreuses opportunités que tu m'as données au fil des années. Merci à mes amis du 2401 & 2402 d'avoir mis de la vie et de la couleur dans nos bureaux blanc cassé : Marc, Simon, Jean-Sébastien, Gabriel, Shiva, Pierre, Cecilia, Nehed, Marie-Amélie, Maria-Isabel, Mafalda, Claude, Antoine, Matthieu, Ronan, Élise, Marie-Pierre, Cynthia et tous ceux qui sont passés moins longtemps. Merci à mes parents qui m'ont toujours encouragé à poursuivre mes études, et merci à Roxanne de m'avoir supporté!

RÉSUMÉ

La cartographie de la géologie du Quaternaire des terrains glaciaires par photo-interprétation comporte un lot de défis lorsque la région ciblée a une forte densité du couvert végétal, une grande anthropisation, un relief montrant peu de variation ou encore très accidenté et difficilement accessible. Cette thèse montre que l'utilisation de la technologie LiDAR aéroporté permet la production de modèles numériques de terrain à haute résolution dont les produits dérivés peuvent être utilisés directement dans un environnement numérique pour l'interprétation de la géologie et de la paléogéographie à l'échelle régionale.

Le premier volet de recherche présente une démarche permettant d'obtenir une image cartographique qui montre l'essentiel de la variabilité du terrain et qui permet de cartographier la géologie de surface avec un niveau de détails essentiellement impossible à obtenir par photo-interprétation classique. Cette méthode a été appliquée à la cartographie de la géologie de surface de la rive sud de la vallée du Saint-Laurent entre les régions de Lotbinière et Rivière-du-Loup à l'aide d'une mosaïque de divers levés LiDAR aéroportés. Cette application a permis de préciser plusieurs aspects de la géologie des formations superficielles de la région d'étude. La limite de submersion des mers de Champlain et Goldthwait a pu être cartographiée avec précision. Une série de moraines mineures ont été identifiées dans le secteur de Lotbinière, incluant une portion de la moraine de Saint-Édouard. Finalement, des anciens glissements de terrain sous des zones de couvert forestier important ont été identifiés dans le secteur de Kamouraska.

Le deuxième volet propose un modèle géologique 3D du même secteur, où la cartographie réalisée au premier volet sert de jalon afin de contraindre les relations stratigraphiques. La réalisation de forages, de sondages, de levés géophysiques, de coupes géologiques et d'analyses paléoécologiques a permis la reconstruction de la colonne stratigraphique, de la surface du roc jusqu'à la surface du sol. La nature, la distribution et l'architecture d'une succession de 12 unités géologiques a été ainsi reconstruite. Ce modèle géologique a été appliqué à la définition du potentiel aquifère des dépôts meubles, en fournissant des cibles d'aquifères, notamment dans le secteur de Saint-Henri.

Le troisième volet de recherche porte sur l'étude d'une partie de l'empreinte du Courant glaciaire du Saint-Laurent, un épisode d'écoulement rapide de la glace en direction nord-est dans l'axe du fleuve Saint-Laurent. Les résultats de la cartographie des méga-linéations glaciaires dans cette partie de la vallée montrent que cette phase a été un événement majeur de la déglaciation du secteur nord-est de l'Inlandsis Laurentidien. Une grande variété de formes diagnostiques de paléo-courants glaciaires a été identifiée au-dessus de la limite marine. Diverses zones d'alimentation sont identifiées dans les Laurentides, alors que des zones de cisaillement ont été reconnues sur le piémont appalachien.

Le quatrième volet de recherche revisite l'hypothèse d'une réavancée glaciaire dans la Mer de Champlain au Dryas récent. Un nouvel ensemble de moraines, cartographiées dans la région de Lotbinière et identifiées sur la base de données de terrain à haute résolution, est présenté. Ces moraines représentent vraisemblablement les positions récessionnelles d'un front de glace laurentidien suite à une réavancée dans un bassin précoce de la Mer de Champlain. Leur découverte soutient et renforce l'hypothèse de la phase d'écoulement glaciaire dite de Saint-Nicolas.

Mots-clés : Wisconsinien supérieur, géologie du quaternaire, courants glaciaires, modélisation géologique 3D, LiDAR, modèles numériques de terrain haute-résolution, Courant glaciaire du Saint-Laurent, méga-linéations glaciaires, réavancée glaciaire.

ABSTRACT

Mapping the Quaternary geology of glaciated terrains by photo-interpretation presents a number of challenges when the targeted region has a high-density vegetation cover, a significant degree of anthropization, a relief showing little variation or a very rugged and poorly accessible terrain. This thesis shows that the use of airborne LiDAR addresses these problems and allows the production of high-resolution digital terrain models whose derivatives can be used directly in a digital environment for the interpretation of geology, geomorphology and paleogeography at a regional scale.

The first section of the thesis presents a workflow to obtain images that include most of the terrain variability and that allow the mapping of the surficial geology with a level of detail that is essentially impossible to obtain by photo-interpretation. This method was applied to the mapping of the surficial geology of the south shore of the St. Lawrence River valley between the Lotbinière and Rivière-du-Loup areas, using a mosaic of various airborne LiDAR surveys. This application helped to clarify several aspects of the surficial geology of the study area. The submergence limit of the Champlain and Goldthwait seas was precisely defined. A series of minor moraines have been identified in the Lotbinière area, including a portion of the Saint-Édouard moraine. Finally, old landslides under areas of dense forest cover have been identified in the Kamouraska area.

The second part proposes a 3D geological model of the same region, where the surficial mapping carried out in the first section of the thesis serves as a constraint to establish stratigraphic relationships. Drilling, soundings, geophysical surveys, geological sections and paleoecological analyses have allowed the reconstruction of the geology from the bedrock surface to the ground surface, thus exposing the nature, distribution and architecture of a succession of 12 surficial geologic units. This geological model was applied to the definition of the aquifer potential of unconsolidated deposits, providing aquifer targets, particularly in the Saint-Henri area.

The third research section presents a major part of the footprint of the St. Lawrence Ice Stream, an episode of rapid northeastward ice flow along the axis of the St. Lawrence River. The results of the mapping of mega-scale glacial lineations in this part of the valley show that this phase was

a prominent event in the deglaciation of the northeastern sector of the Laurentide Ice Sheet. A wide variety of diagnostic paleo-ice streams landforms was identified above the local marine limit. Various onset zones have been recognized in the Laurentians, while shear margin zones have been identified on the Appalachian foothills.

The fourth research theme revisits the hypothesis of an ice margin readvance in the Champlain Sea during the Younger Dryas. A new set of moraines mapped in the Lotbinière region, and identified on the basis of high-resolution topographic data, are presented. These moraines likely represent the recessional positions that followed a readvance of the Laurentide ice front into an early Champlain Sea embayment. Their discovery supports and reinforces the hypothesis of the Saint-Nicolas ice flow.

Keywords : Late Wisconsinan, Quaternary geology, ice streams, 3D geological modeling, LiDAR, high-resolution digital terrain models, St. Lawrence Ice Stream, mega-scale glacial lineations, glacial readvance, St. Nicholas ice flow.

TABLE DES MATIÈRES

LISTE DES FIGURES

LISTE DES TABLEAUX

LISTE DES ABRÉVIATIONS

BP	Avant aujourd'hui ; *Before present*
DSM	Modèle numérique de surface ; *Digital surface model*
DTM	Modèle numérique de terrain ; *Digital terrain model*
Hz	Hertz
Ka	Milliers d'années ; *Thousand years*
kHz	Kilohertz
LGM	Dernier Maximum Glaciaire ; *Last Glacial Maximum*
LiDAR	Détection et estimation de la distance par la lumière ; *Light Detection and Ranging*
mASL	Mètres au-dessus du niveau de la mer ; *Meters above sea level*
MNT	Modèle numérique de terrain
MRC	Municipalité régionale de comté
MSGL	Méga-linéation glaciaire *; Mega-scale glacial lineation*
PACES	Programme d'Acquisition de Connaissances sur les Eaux Souterraines
SIH	*Système d'Information Hydrogéologique*
SLIS	Courant glaciaire du Saint-Laurent ; *St. Lawrence Ice Stream*
YD	Dryas récent *; Younger Dryas*

1 INTRODUCTION GÉNÉRALE

1.1 Problématique

Dans le sud du Québec, une bonne compréhension de la géologie des formations superficielles (aussi appelés dépôts meubles, ou géologie du Quaternaire) contribue de manière remarquable à notre compréhension des systèmes aquifères, particulièrement dans le cadre d'études régionales (Paradis *et al.,* 2000; Ross *et al.,* 2005a; Légaré-Couture *et al.,* 2018). La nature, la distribution et l'architecture des dépôts meubles exercent un contrôle important sur des paramètres hydrogéologiques clés tels que la conductivité hydraulique, la recharge, le confinement et la vulnérabilité des aquifères.

Cette thèse s'inscrit en partie dans le cadre du Projet de connaissances en Chaudière-Appalaches dirigé par M. René Lefebvre, Ph. D. (professeur-chercheur à l'INRS-ETE). Il s'agit de l'un des six projets de caractérisation hydrogéologique régionale effectuée dans le cadre du 3e appel du Programme d'Acquisition de Connaissances sur les Eaux Souterraines (PACES) du Ministère de l'Environnement et de la Lutte contre les changements climatiques (MELCC). Les ressources en eaux souterraines du secteur à l'étude sont de plus en plus sollicitées pour l'alimentation en eau, bien qu'aucune caractérisation régionale n'ait été effectuée jusqu'à maintenant. Dans une optique de meilleure gestion à long terme de la ressource, il est essentiel de connaître les caractéristiques de l'architecture des dépôts quaternaires puisque ceux-ci influencent directement la rétention, l'écoulement et le comportement général des aquifères en milieu granulaire.

Avant le début du projet, la cartographie des formations superficielles de cette région était fragmentaire, la carte la plus récente étant en fait une compilation de produits cartographiques réalisés à des échelles différentes sur plusieurs décennies. La zone située sous la limite maximale des mers post-glaciaires de Goldthwait et de Champlain (environ 185 mètres d'élévation dans cette région) est caractérisée par une géologie quaternaire particulièrement complexe, notamment en raison des effets du passage d'un courant glaciaire peu de temps avant la déglaciation de la vallée de même qu'à l'intense remaniement littoral ayant affecté la majorité des sédiments antérieurs à l'émersion finale de la région.

En ce qui a trait à la stratigraphie, des données géologiques sont disponibles mais elles n'ont jamais été assimilées dans un modèle géologique intégré de manière à tirer une image claire des complexités régionales et locales. Lors de travaux préliminaires dans le secteur de la Basse-Chaudière (Saint-Henri-de-Lévis), une anomalie magnétique de forme rubanée et recoupant presque perpendiculairement le patron structural régional a été identifiée, et pourrait être associée à un ancien tracé de la rivière Chaudière.

L'élaboration d'un cadre géologique adéquat dans la reconstitution de l'histoire quaternaire de la rive sud de l'estuaire moyen du fleuve Saint-Laurent permet également d'investiguer le Courant glaciaire du Saint-Laurent, un phénomène majeur d'écoulement glaciaire rapide à même le glacier Laurentidien. Cette phase d'écoulement aurait eu lieu il y a environ 17 000 ans au droit de la vallée du Saint-Laurent. Bien que son existence soit généralement acceptée, les preuves géomorphologiques concrètes de celle-ci sont restées jusqu'à présent éparses, isolées spatialement et peu documentées.

Finalement, l'hypothèse d'un épisode de réavancée glaciaire dans la Mer de Champlain au Dryas récent a été postulée dans la région de la Ville de Québec sur la base de la présence, près de la surface, d'un diamicton glaciomarin contenant les restes fossiles de mollusques marins typiques des environnements de marge glaciaire. Le manque de connaissances au niveau de la distribution spatiale de ce diamicton et l'apparente absence de formes géomorphologiques associées à cet épisode ont toutefois limité la validation de cette hypothèse qui est restée en suspens depuis plusieurs décennies.

1.2 Objectifs

L'objectif principal de cette thèse est de mettre à jour le cadre géologique quaternaire de la région de la Basse-Chaudière et de la rive sud de l'estuaire moyen du fleuve Saint-Laurent. La clef de voute permettant la réalisation de cet objectif est la disponibilité de plusieurs levés altimétriques laser (LiDAR) aéroportés couvrant entièrement la zone à l'étude. Ceux-ci contiennent des mesures d'élévation du sol très précises et de grande densité, avec souvent plus d'une mesure par m^2. Une hypothèse centrale de nos travaux est que la création de modèles numériques de terrain (MNT)

et de dérivés basés sur ces données ouvre une toute nouvelle perspective dans l'interprétation de la géologie de surface et de la morphologie associée.

La réalisation de l'objectif principal se fera par les objectifs spécifiques suivants :

1. Développer et tester une démarche de cartographie exploitant les levés LiDAR afin de faire la cartographie de précision des formations du Quaternaire de la région
2. Mieux définir la stratigraphie des dépôts meubles en définissant la distribution spatiale (3D) des unités du Quaternaire par l'intégration des données de surface et de sous-surface de l'ensemble de la région
3. Mieux comprendre la nature du Courant glaciaire du Saint-Laurent en faisant l'identification, la cartographie et l'interprétation des formes de terrain associées à son empreinte
4. Identifier les évidences d'une potentielle réavancée glaciaire au Dryas récent en reconstituant la paléogéographie des événements glaciaires de cette période dans la région de la ville de Québec

1.3 Secteur à l'étude

Le secteur à l'étude dans le cadre des travaux de cette thèse correspond globalement à la région de la Basse-Chaudière et à la rive sud de l'estuaire moyen du fleuve Saint-Laurent jusqu'à la hauteur de Rivière-du-Loup. Les données LiDAR obtenues via le projet du PACES Chaudière-Appalaches couvrent une bande de terrain restreinte en bordure du fleuve faisant généralement une dizaine de kilomètres de largeur de la rive vers l'intérieur des terres, et touchent essentiellement la zone située sous la limite de submersion des mers post-glaciaires de Champlain et de Goldthwait. Cette zone correspond approximativement aux limites de la zone appelée « Zone à l'étude - Article 2 » illustrée à la Figure 1.1. Au-delà de cette zone cotière, à de plus hautes élévations, la géologique du Quaternaire est en général moins complexe. En termes de divisions administratives, les données LiDAR couvrent partiellement, du sud-ouest au nord-est, les MRC de Lotbinière, Lévis, Bellechasse, Montmagny, L'Islet, Kamouraska, et Rivière-du-Loup. Dans l'axe de la vallée du Saint-Laurent, la limite amont est située à proximité de Deschaillons-sur-Saint-Laurent, alors que la limite aval est située à une dizaine de kilomètres au nord-est du centre

de la ville de Rivière-du-Loup. Les rivières importantes localisées sur le territoire sont, d'ouest en est, les rivières du Chêne, Chaudière, Etchemin, Boyer, du Sud, Ouelle, et du Loup.

En raison des particularités de chaque volet de recherche, le secteur à l'étude n'est pas exactement le même pour chaque thème ; la Figure 1.1 illustre ces variations. L'effort de cartographie de la géologie du Quaternaire et la modélisation géologique 3D (chapitres 2 et 3 de cette thèse) partagent essentiellement le même secteur à l'étude à l'exception de la Ville de Lévis. Les limites de celle-ci sont incluses dans le modèle géologique 3D, mais elles sont exclues de la cartographie de la géologie de surface puisque cette zone a été cartographiée récemment (Daigneault *et al.,* 2014).

Le volet de recherche sur les courants glaciaires de la vallée du Saint-Laurent et ses tributaires (chapitre 4 de cette thèse) porte également sur cette même zone, mais un élargissement considérable de la région à l'étude ainsi qu'un changement d'échelle sont nécessaires dans le but de mieux mettre en contexte ces événements glaciaires. Le secteur à l'étude entier est illustré par le cadre principal complet de la Figure 1.1. Finalement, le volet sur la paléogéographie du secteur de la ville de Québec au Dryas récent (chapitre 5 de cette thèse) se concentre sur un secteur à l'étude plus restreint : les pourtours de la ville de Québec, incluant la rive nord et la rive sud (Lotbinière) du fleuve Saint-Laurent.

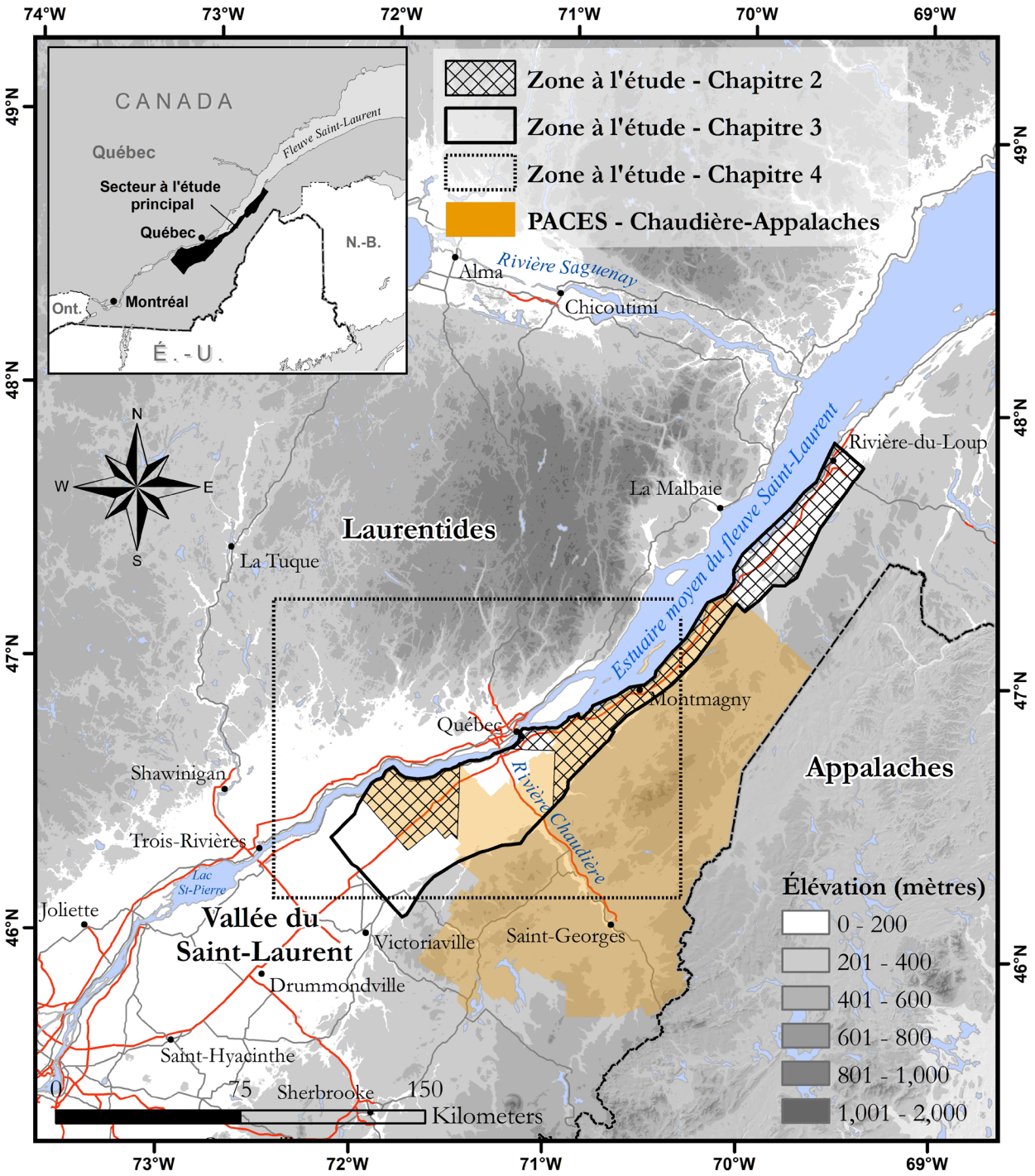

Figure 1.1 : Localisation des différentes régions étudiées dans cette thèse. Les zones à l'étude des chapitres 2, 3 et 5 sont illustrées par différents types de traits et de remplissages, alors que la zone à l'étude du chapitre 4 est contenue dans le cadre entier de la carte principale.

1.4 Géologie régionale

1.4.1 Géologie du socle

La géologie du secteur à l'étude est illustrée sur la Figure 1.2, une carte produite dans le cadre du projet de Portrait des ressources en eau souterraine en Chaudière-Appalaches (Lefebvre *et al.,* 2015), à l'aide de données fournies par la Direction générale des hydrocarbures et des biocarburants du Ministère de l'Énergie et des Ressources naturelles (MERN).

La géologie du socle et ses caractéristiques sont résumées dans la section suivante sur la base des travaux stratigraphiques de St-Julien & Hubert (1975), Globensky (1987), Slivitzky & St-Julien (1987) et Tremblay & Pinet (1994). Dans la Basse-Chaudière et le Bas-Saint-Laurent, deux provinces géologiques sont présentes : la Plate-forme du Saint-Laurent et les Appalaches. Le secteur à l'étude est presque entièrement situé sur le piémont et les hautes terres appalachiennes, exception faite de la MRC de Lotbinière au sud-ouest. Celle-ci est traversée par la ligne de Logan, qui marque le contact entre les roches autochtones de la Plate-forme du Saint-Laurent et les roches allochtones des Appalaches. Les roches sédimentaires de la Plate-forme, composées essentiellement de roches détritiques à grain fin et des roches carbonatées à faible pendage, sont d'âge Cambrien à Ordovicien et reposent en discordance sur le socle igné et métamorphique de la Province de Grenville (St-Julien & Hubert, 1975). Les Appalaches sont constituées principalement de roches sédimentaires faiblement métamorphisées et déformées lors des orogenèses taconienne et acadienne (Tremblay & Pinet, 1994). Celles-ci ont été transportées vers le nord-ouest par des nappes de chevauchement surmontant les roches de la Plate-forme du Saint-Laurent.

La portion des Appalaches située dans la zone d'étude correspond au domaine des nappes externes de la Zone de Humber. On y retrouve principalement des roches sédimentaires (grès, shale, quartzite) parfois métamorphisées en ardoises et schistes, ainsi que quelques roches volcaniques. Ces roches sont déformées par des plis et des failles essentiellement orientées SO-NE, comme l'est l'ensemble du domaine appalachien dans l'est du continent.

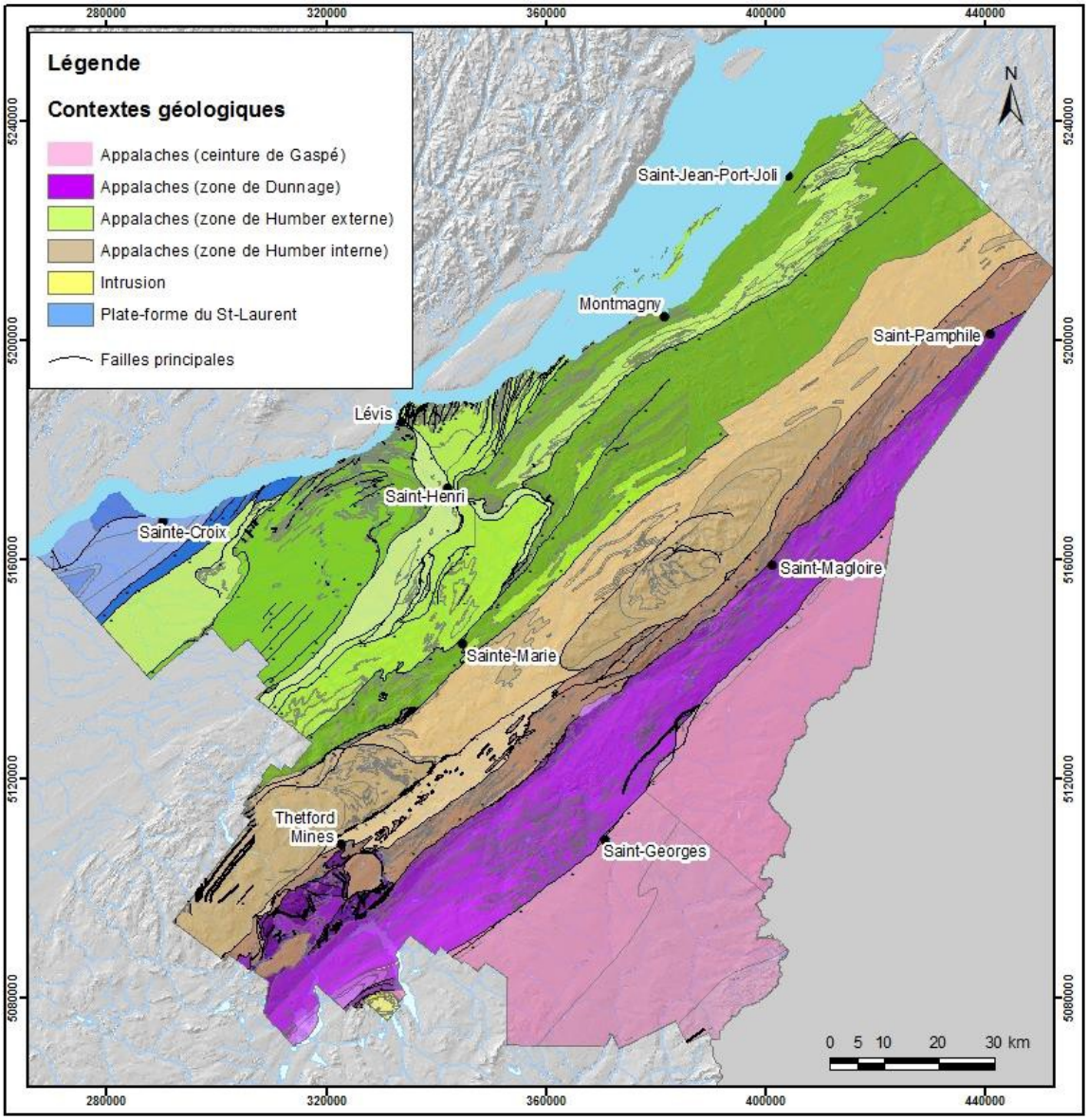

Figure 1.2 : Géologie du socle, Chaudière-Appalaches. Carte extraite de Lefebvre *et al.* (2015), géologie de Globensky (1987) et de Slivitzsky et St-Julien (1987).

La zone de la Plate-forme du Saint-Laurent occupe une faible superficie de la région étudiée, où elle est caractérisée par la présence de failles actives depuis la fin du Précambrien et qui le seraient demeurées jusqu'à la fin de l'Ordovicien. Ces failles sont principalement associées à un régime tectonique en extension engendré par la séparation du supercontinent Rodinia et l'ouverture de l'océan Iapetus (Kumarapeli & Saull, 1966).

1.4.2 Physiographie et drainage

La topographie du substratum rocheux explique en grande partie les variations topographiques du piedmont Appalachien. Celui-ci étant particulièrement accidenté dans la zone de Humber externe, il exerce un contrôle important sur l'épaisseur des dépôts meubles. Le relief de plaine caractérisant la partie centrale de la vallée du Saint-Laurent est beaucoup plus adouci, et se caractérise par la présence de rivières et des ruisseaux profondément incisés. Ceux-ci n'atteignent que rarement le roc, ce qui donne une indication sur l'épaisseur de dépôts meubles. Des forages profonds dans les dépôts sont communs dans la vallée centrale du Saint-Laurent, et pourraient témoigner de la présence d'un ancien chenal profond associé à un ancêtre du fleuve Saint-Laurent ayant existé longtemps avant la dernière époque glaciaire (Gadd *et al.*, 1971). Les cours d'eau principaux du secteur à l'étude coulent en général dans une direction perpendiculaire au fleuve sur leur portion Appalachienne dans des vallées en V, avant de se réorienter progressivement vers le N-E après avoir débouché sur la plaine argileuse et ainsi s'étaler dans des vallées plus larges. Ces cours d'eau (Rivière Boyer, Rivière des Mères, Rivière du Sud, etc.) incisent ensuite les dépôts meubles des Basses-Terres correspondant à d'anciens niveaux du fleuve Saint-Laurent (ou des mers post-glaciaires).

1.4.3 Paléogéographie et stratigraphie de la basse vallée du Saint-Laurent

La vallée du Saint-Laurent occupe un secteur critique par rapport à l'histoire glaciaire de l'Amérique du Nord puisqu'elle occupe une position centrale entre la zone d'accumulation de l'Inlandsis Laurentidien et sa zone terminale à la latitude de New York. Lors d'épisodes interstadiaires, les basses terres de la vallée du Saint-Laurent furent périodiquement envahies par des étendues d'eau associées soit à des épisodes marins ou glaciolacustres, en fonction des fluctuations du front glaciaire au niveau de Québec, des mouvements glacio-isostatiques régionaux et du niveau marin global. L'interaction de ces trois mécanismes a engendré une grande variabilité des faciès observés en coupe ou en forage (Gadd, 1971; Lamothe, 1989; Bernier & Occhietti, 1991), ce qui a contribué à complexifier le cadre stratigraphique régional et à rendre difficiles les corrélations entre les séquences de nature plus locales (Lamothe *et al.,* 1992). La vallée du Saint-Laurent comporte localement des épaisseurs de plus de 100 mètres de dépôts quaternaires, notamment dans certaines vallées enfouies (Légaré-Couture *et al.,* 2018). Les dépôts les plus

anciens retrouvés sur le territoire sont probablement illinoiens : il s'agit de tills sous-jacents à des sédiments stratifiés qui sont retrouvés à quelques endroits dans le sud du Québec (Pointe-Fortune, Veillette & Nixon (1984)).

Au dernier maximum glaciaire, la vallée était complètement occupée par les glaces laurentidiennes. Alors que l'écoulement glaciaire régional est principalement contrôlé par la dynamique d'ensemble de l'inlandsis, il semble qu'une masse glaciaire indépendante d'origine appalachienne ait bloqué la vallée à la hauteur de Québec et ait été à l'origine de l'endiguement de lacs proglaciaires dans les Basses-Terres (Lamothe *et al.*, 1992). Ce qui semble certain, c'est qu'au Wisconsinien supérieur, les masses glaciaires laurentidiennes et appalachiennes étaient amalgamées en un seul inlandsis d'échelle continentale. Quelques centaines d'années avant la déglaciation peut-être un peu davantage, un courant glaciaire orienté vers le nord-est est venu complètement perturber l'écoulement méridien de l'inlandsis (Parent & Occhietti, 1999). Ce courant s'est formé dans la vallée du Saint-Laurent, et ses limites latérales s'étendaient sur la bordure du Bouclier au nord et sur le piedmont appalachien au sud. L'importante dépression glacio-isostatique du continent a permis aux eaux marines de démanteler par vêlage rapide ce courant glaciaire et d'ensuite envahir la vallée en aval de Québec, puis en amont (Parent & Occhietti, 1999).

Les trois prochaines sous-sections résument brièvement les événements paléogéographiques et les sédiments qui y sont associés. La position stratigraphique de la grande majorité de ces unités est illustrée sur la Figure 1.3.

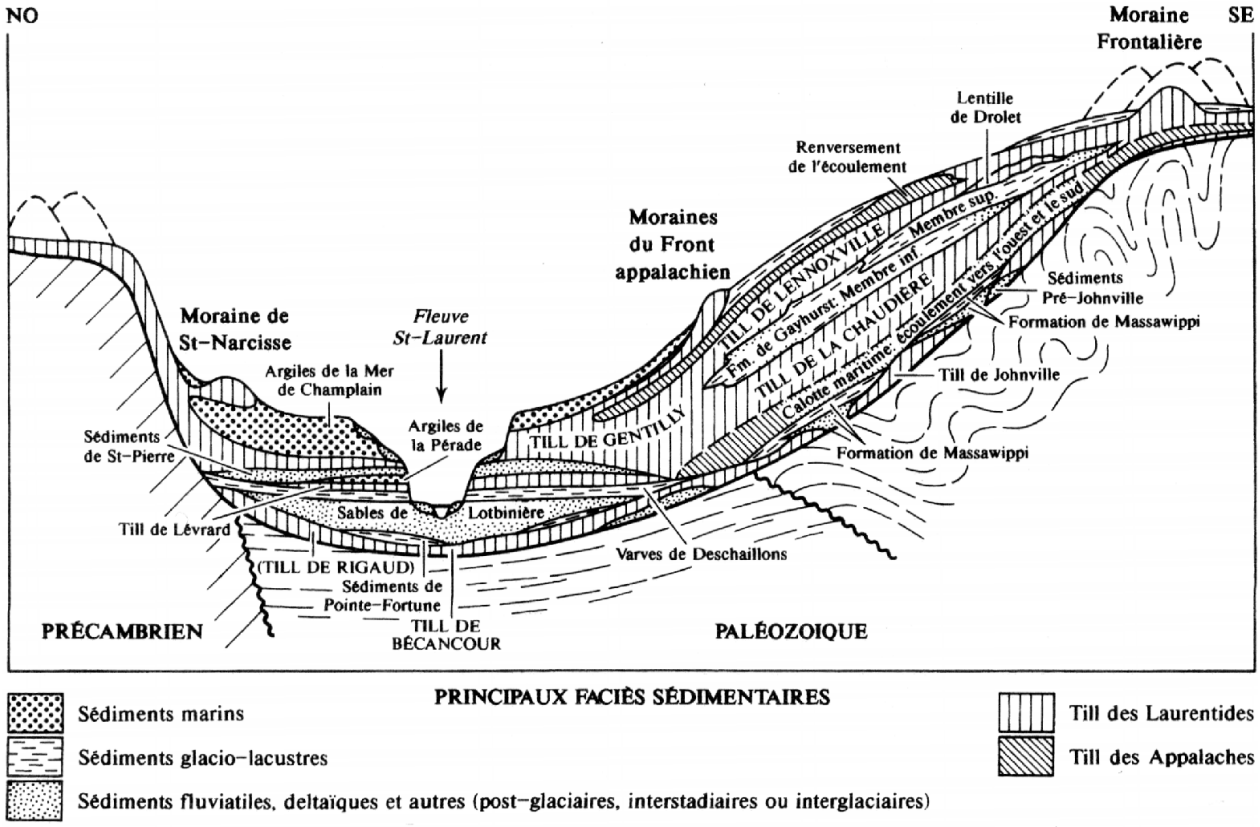

Figure 1.3 : Coupe géologique à travers le Québec méridional. Figure originale de Elson (1970) tirée de Lamarche (2011); modifiée par Shilts (1981).

1.4.3.1 Pré-Illinoien, Illinoien et Sangamonien

Sur le territoire à l'étude, la période du Quaternaire est marquée par au moins trois avancées glaciaires majeures. Les unités les plus anciennes retrouvées dans le secteur à l'étude correspondent au Till de Johnville (Appalaches) et au Till de Bécancour, tous deux des diamictons compacts et riches en clastes mis en place par un écoulement en provenance du nord-ouest (McDonald & Shilts, 1971). Ils furent jadis considérés comme d'âge Wisconsinien inférieur, mais cette théorie a été invalidée par Parent (1987) sur la base de relations stratigraphiques. Ces tills sont désormais considérés d'âge illinoien (Lamothe *et al.*, 1992). La glaciation illinoienne (stade isotopique marin 6, environ 130 à 191 ka BP ; voir Tableau 1.1) est généralement considérée comme très érosive : les sédiments pré-Johnville sont seulement observables en coupe dans quelques vallées appalachiennes à des altitudes plus hautes que celles du secteur à l'étude.

Tableau 1.1 : Stades isotopiques marins d'intérêt pour le secteur à l'étude - LR04 stack, Lisiecki & Raymo (2005). Les âges approximatifs correspondent aux périodes de transition pour les stades 1 à 5, et aux apogées pour les sous-stades 5.

Stade isotopique marin	Période approximative (Milliers d'années)
1	Présent - 14
2	14 - 29 (dernier maximum glaciaire)
3	29 – 57 (climat intermédiaire)
4	57 – 71 (climat glaciaire)
5a (apogée)	82 (sous-stade climat intermédiaire)
5b (apogée)	87 (sous-stade climat glaciaire)
5c (apogée)	96 (sous-stade climat intermédiaire)
5d (apogée)	109 (sous-stade climat glaciaire)
5e (apogée)	123 (interglaciaire Sangamonian)
6	191-130 (maximum glaciaire)

Dans les Appalaches, le Till de Johnville est surmonté par les sédiments lacustres et alluviaux de la Formation de Massawippi, qui sont considérés avoir été déposés sous un climat boréal vers la fin du dernier interglaciaire (Sangamonien). Déposés dans un contexte de drainage libre possiblement semblable au système actuel du Saint-Laurent, ces sédiments contiennent des assemblages polliniques suggérant un environnement de forêt boréale (McDonald & Shilts, 1971).

Une sous-séquence complexe de sédiments interglaciaires et glaciaires existe dans la vallée centrale du Saint-Laurent pour la période du stade isotopique marin 5 (5a à 5e). En raison de leur rare occurrence en coupe et leur identification plutôt problématique en forage, certains éléments associés à la paléogéographie et à leur position stratigraphique restent contentieux encore aujourd'hui. Une revue détaillée de ces sédiments n'est pas nécessaire ici puisque ces formations n'ont pas été observées dans le cadre de cette thèse, mais ceux-ci pourraient tout de même être présents par endroits sous les tills associés au dernier maximum glaciaire (Gentilly/Lennoxville).

Dans la vallée moyenne du Saint-Laurent, le Sable de Lotbinière surmonte généralement des varves d'âge inconnu ou encore le Till de Bécancour. Le contact érosif et la transition entre les varves sous-jacentes et le sable suggèrent un contexte de niveau eustatique en baisse (climat froid), et le

contenu pollinique de ces sables suggère aussi un environnement boréal. Les varves de Deschaillons, superposées aux Sables de Lotbinière, marquent le début d'une phase d'ennoiement progressif de la vallée par le lac proglaciaire Deschaillons (Clet & Occhietti, 1994). Une datation par la méthode de thermoluminescence optique a permis de dater la partie sommitale des Varves de Deschaillons à 69,5 ± 10,5 ka (Lamothe & Huntley, 1988), et à 80 ka par la méthode de 1'uranium-thorium sur des concrétions syngénétiques (Hillaire-Marcel & Causse, 1989). Cet ennoiement devait être causé par un barrage de glace probablement dans les environs de l'embouchure du Saguenay (Clet & Occhietti, 1994). Ces varves d'englaciation marquent ainsi le retour aux conditions glaciaires à la fin du stade 5.

1.4.3.2 Wisconsinien inférieur et moyen

Dans la vallée du Saint-Laurent, le diamicton mis en place suite à l'avancée glaciaire décrite dans la section précédente est appelé Till de Lévrard. Il est présumé corrélatif du Till de la Chaudière dans les Appalaches, et marque une avancée glaciaire au Wisconsinien inférieur (Lamothe, 1989; Lamothe *et al.*, 1992). La Formation de Massawippi est en contact supérieur avec le Till de la Chaudière, lequel est présumé avoir été mis en place par un glacier dont le centre d'englaciation était appalachien (Maine et/ou Nouveau-Brunswick). Cette glace a pu perdurer jusqu'au Wisconsinien moyen, et la direction de l'écoulement était plutôt variable (Parent, 1987).

La séquence de submersion marine, puis de drainage libre ayant suivi le dépôt du Till de Lévrard est marquée par les Argiles de la Pérade et les Sédiments de Saint-Pierre (Gadd, 1971; Lamothe, 1989; Ferland & Occhietti, 1990; Occhietti, 1990). Les argiles de la Pérade ont probablement été mises en place lors d'un épisode marin (Mer de Cartier) autour de la période de transition entre le stade isotopique marin 5b/a, où le climat dans la vallée du Saint-Laurent était en transition entre une toundra et une forêt boréale conifériennne (Occhietti *et al.,* 1996). L'âge de cette unité serait d'environ 91,000-98,000 ± 9000 ans selon la méthode de thermoluminescence optique, alors que les sédiments de Saint-Pierre sus-jacents sont datés à environ 65 ka (Lamothe, 1985). Ces unités ne sont en général pas observées sur le piémont Appalachien. Un hiatus d'une durée indéterminée est observé entre ces dépôts et l'avancée glaciaire subséquente associée au Till de

Gentilly dans la vallée du Saint-Laurent (Lamothe, 1985) et au Till de Chaudière dans les Appalaches (Godbout, 2013).

Des fluctuations de la marge glaciaire au Wisconsinien moyen ont été observées au sud dans les régions des rivières Saint-François et Chaudière (McDonald & Shilts, 1971). Cette déglaciation partielle des hautes terres appalachiennes entraîne la création d'un lac de barrage glaciaire dans lequel sont déposés les sédiments de la Formation de Gayhurst, principalement sous forme de varves silteuses, mais aussi d'épandages subaquatiques sablo-graveleux (Caron *et al.,* 2013). Les limites du Lac Gayhurst ne devraient toutefois pas recouper celles du secteur à l'étude principal. Cette unitée sépare le Till de Chaudière du till supérieur, bien qu'il s'agisse d'unités couvrant globalement le même épisode d'englaciation et sont donc tous deux corrélés au Till de Gentilly (McDonald & Shilts, 1971; Shilts, 1981), dans la plaine du Saint-Laurent ; le Till de la Chaudière et le Till de Lennoxville ne correspondant qu'à une seule unité dans la vallée, celle du Till de Gentilly (Shilts, 1981). La présence de gneiss dans le till indique généralement une provenance laurentienne, alors que la présence de roches ultramafiques est plutôt associée à une provenance appalachienne, ce type de roche provenant des ceintures ophiolitiques de Thetford-Mines ou d'Asbestos. Le Till de Lennoxville déposé dans des zones occupées précédemment par les lacs de l'épisode de Gayhurst est localement beaucoup plus silteux et moins perméable puisqu'il a incorporé des silts argileux glaciolacustres.

1.4.3.3 Wisconsinien supérieur et Holocène

L'histoire des événements de déglaciation dans le sud du Québec à la fin du Wisconsinien est complexe. Il y a un peu plus de 20 000 ans, le dernier maximum glaciaire a atteint la côte est américaine au sud de New York (Dyke & Prest, 1987). Cette dernière avancée a mis en place le Till de Lennoxville (équivalent stratigraphique du till de Gentilly) dans le secteur à l'étude, lequel constitue le till de surface sur la plus grande partie de l'Estrie-Beauce. Le réchauffement climatique ainsi que d'autres facteurs non climatiques, dans une certaine mesure (Occhietti *et al.,* 2001b), ont été responsables de l'amincissement et du retrait progressif de l'Inlandsis Laurentidien. Vers 18 ka BP, un important courant glaciaire, le Courant glaciaire du Saint-Laurent (*St. Lawrence Ice Stream, SLIS*), s'est développé dans cette partie de l'Inlandsis Laurentidien (LIS) dans la

vallée, en déversant une quantité massive de glace par le vêlage dans le golfe du Saint-Laurent. Parallèlement, l'Ontario-Erie Ice Stream (OEIS) a fonctionné de la même manière en canalisant la glace vers le bassin du lac Ontario (Taylor, 1913; Ross *et al.,* 2006; Sookhan *et al.,* 2018). Le recul progressif des glaces dans la zone du SLIS a permis la pénétration des eaux marines de la Mer de Goldthwait dans le Saint-Laurent, tandis que le retrait de l'OEIS a entraîné la coalescence des lacs glaciaires Iroquois et Vermont dans le lac glaciaire Candona (Parent & Occhietti, 1988, 1999; de Vernal *et al.,* 1989; Ross *et al.,* 2006) nommé en raison de la présence notable de l'ostracode d'eau douce *Candona subtriangulata* (Candona est l'équivalent de la phase de Fort Ann (Rayburn *et al.,* 2005, 2007, 2011) et du Lac St. Lawrence (Rodrigues, 1992). Le lac glaciaire Candona occupait une grande superficie dans l'est de l'Ontario et le sud-ouest du Québec, son drainage via la vallée du Saint-Laurent étant bloqué par le front glaciaire laurentidien (Parent & Occhietti, 1988). Les sédiments fins glaciolacustres observés dans la plupart des vallées du sud-est du Québec témoignent de ces lacs proglaciaires.

Le retrait de la glace dans la vallée du fleuve Saint-Laurent s'effectue graduellement selon une orientation principalement nord-ouest et nord-nord-ouest (McDonald & Shilts, 1971; Parent & Occhietti, 1988), comme en témoignent les nombreuses crêtes morainiques mineures ainsi que des moraines lobées d'orientation nord-est visibles sur le territoire (Normandeau, 2010). Parallèlement, la dépression glacioisostatique et l'élévation globale du niveau de la mer ont permis aux eaux marines de démanteler par vêlage les restes du courant glaciaire de l'estuaire et d'envahir la vallée, formant ainsi des bassins marins, appelés Mer de Goldthwait en aval de Québec et Mer de Champlain en amont (Elson, 1970).

Sur la rive sud de Québec (la région de Lotbinière), LaSalle & Shilts (1993) ont identifié des segments de moraine isolés composés d'un diamicton glaciomarin contenant des coquilles, et ont attribué leur présence à une réavancée glaciaire laurentidienne dans la Mer de Champlain au début du Dryas récent.. Cette proposition fut initialement formulée et par la suite détaillée principalement par P. LaSalle (LaSalle, 1984; LaSalle & Chapdelaine, 1990; LaSalle & Shilts, 1993), essentiellement sur la base de la découverte de plusieurs sites dans le secteur de Lotbinière montrant un diamicton glaciomarin porteur de coquilles de mollusques fossiles (*Balanus hameri*) retrouvé sous la séquence typique de la Mer de Champlain. L'importance climatique de cet épisode,

dit de Saint-Nicolas (*St-Nicolas flow*), n'a cependant jamais été démontrée, et comme la moraine de Saint-Édouard était un élément isolé, l'importance régionale de cet événement n'a jamais été véritablement évaluée au-delà des travaux de LaSalle & Shilts (1993). La géologie du roc locale est représentée abondamment dans les clastes du diamicton, mais des cailloux précambriens provenant de la rive nord du fleuve Saint-Laurent sont également observables. De plus, les structures de poussée observées dans les sédiments suggèrent un mouvement glaciaire provenant du nord. Malgré le fait que ces sédiments aient été mis en place dans un contexte marin profond, le front glaciaire devait encore être attaché à l'inlandsis lors de leur déposition (LaSalle & Shilts, 1993). Bien que cet événement n'ait pas été exclu du cadre chronostratigraphique du sud du Québec (voir Dyke, 2004; Occhietti *et al.,* 2011a), certains auteurs ont mis en doute l'importance et la portée de cet événement, en plus de minimiser l'extension de cette réavancée (Occhietti, 2007).

Dans la vallée du Saint-Laurent, la séquence des événements associés à la déglaciation est difficile à reconstituer en raison de l'absence d'indicateurs précis et fiables. Il est probable que de nombreuses caractéristiques de déglaciations aient été recouvertes ou érodées par l'action de l'invasion marine rapide qui a suivi de près la déglaciation. Les marqueurs géomorphologiques significatifs étant difficiles à trouver, la chronologie de la déglaciation s'est longtemps appuyée sur les âges radiocarbone obtenus sur des mollusques vivant autant en milieu glaciolacustres que marins. En position de vie mais plus souvent en thanatocénose, on les retrouve en abondance dans plusieurs coupes de la vallée. Cependant, les âges radiocarbone (^{14}C) obtenus sur les coquilles de la Mer de Champlain donnent généralement des âges de 350 à 1800 ans plus vieux que les âges provenant de matériaux terrestres contemporains (Occhietti et al., 2001b ; Occhietti & Richard, 2003 ; Richard & Occhietti, 2005 ; Cronin et al., 2008), ce qui rend encore plus ardu l'exercice d'établir une chronologie fiable. Cette différence d'âge a été notée et discutée pour la première fois par LaSalle (1966) et a été observée par la suite régulièrement, entre autres lorsque des âges supérieurs à 12 000 ans ^{14}C BP ont été obtenus sur des coquillages marins dans le bras ouest du bassin de la Mer de Champlain (Karrow *et al.,* 1975). Hillaire-Marcel et al.(1979) et Karrow (1981) ont attribué ce vieillissement, appelé « effet réservoir », à un appauvrissement en ^{14}C causé par l'ajout de carbone inorganique provenant des eaux de fonte des glaciers. Le vieillissement

supplémentaire a également été associé à des effets de salinité (Rodrigues, 1988), à des effets de vieux réservoirs de carbone (Hillaire-Marcel, 1981, 1988), et à des paramètres relatifs au milieu de vie des différentes espèces (Anderson, 1988; Rodrigues, 1992). Un effet potentiel supplémentaire a également été récemment exposé par Laurencelle *et al.* (2018), qui ont montré que la résurgence post-glaciaire d'anciennes eaux souterraines qui étaient auparavant pressurisées sous le lit d'une nappe glaciaire pourrait expliquer un apport important de vieux carbone dans le bassin fermé de la Mer de Champlain. En raison de l'absence de moyens permettant d'évaluer facilement l'effet de réservoir local affectant les coquillages marins, les premiers âges obtenus dans la littérature ont souvent été exprimés en "âge coquilles" (marins) ou en "âge des coquilles des mers froides" par plusieurs auteurs (Occhietti & Hillaire-Marcel, 1977 ; Parent & Occhietti, 1988, 1999) et n'ont pas pu être utilisés de manière fiable pour établir la chronologie de la déglaciation sans l'appui de la datation des matériaux terrestres.

Récemment, la chronologie du drainage du lac glaciaire Candona et de l'incursion précoce de la Mer de Champlain dans la vallée du Saint-Laurent a été établie de manière plus fiable à environ 11 100 ± 100 ^{14}C an BP (12 950 - 13 050 cal ka BP) sur la base de datations AMS basales des macrofossiles de plantes terrestres couplées à la teneur en pollen des sédiments lacustres postglaciaires sous-jacents de la tourbière Hemlock Carr au Mont Saint-Hilaire (Occhietti & Richard, 2003; Richard & Occhietti, 2005). Malgré ces nouvelles preuves, la chronologie des événements entourant le début du Dryas récent est demeurée incertaine en raison de la variabilité, de la complexité et de l'apparence plutôt brusque des changements climatiques. La grande disparité apparente des âges ^{14}C (par rapport aux âges calendaires calibrés) à la fin de l'Allerød et la contraction ultérieure au début de l'YD ajoutent à cette complexité (voir Occhietti (2007)). Ces incertitudes ont rendu difficile l'établissement d'une chronologie cohérente des événements dans la région de Québec, un secteur clé dans l'évolution quaternaire du sud du Québec. La compréhension des événements qui ont marqué cette région est d'une importance capitale pour le cycle complet de l'invasion marine dans les basses terres du Saint-Laurent après la dernière période glaciaire, car cette région contrôlait l'échange d'eau entre la vallée du fleuve Saint-Laurent et la Mer de Goldthwait.

Dans le secteur à l'étude, l'épisode marin ayant suivi la déglaciation déposa une couche de sédiments fins d'épaisseur variable, souvent contrôlée par la topographie du socle rocheux. La limite de submersion marine est située à environ 190 mASL dans le secteur de Lotbinière, et diminue graduellement vers le nord-est pour atteindre environ 150 mASL à Rivière-du-Loup (LaSalle *et al.,* 1976; Martineau, 1977). Dans les environnements marins de faible profondeur, des sables, silts et galets se sont mis en place sous forme de cordons littoraux ou de plages, et recouvrent les faciès d'eau profonde ou les affleurements rocheux près de la limite marine. À l'embouchure des rivières Chaudière, Etchemin et du Sud, des deltas se sont mis en place dans la Mer de Goldthwait. Dans la zone du piémont appalachien, l'épaisseur des dépôts meubles est fortement réduite, et les crêtes rocheuses sont nombreuses. Des plages sont souvent accrochées le long d'affleurements rocheux ou sur des zones de till mince en pente plus douce.

La régression marine a également été marquée par une oscillation majeure du niveau marin relatif au cours de laquelle le niveau de la mer est descendu d'environ cinq mètres sous le niveau actuel durant une période de 1000 à 2000 ans, avant de remonter à environ 10 mASL vers 6500 ans BP (Dionne, 1988). Ce dernier a documenté cet événement à plusieurs endroits le long de la rive sud de l'estuaire du Saint-Laurent et l'a nommé Transgression Laurentienne. Ces oscillations ont affecté l'estuaire du Saint-Laurent au moins jusqu'au niveau de la Ville de Québec (Lamarche, 2011). Suite au retrait de la mer jusqu'à son niveau actuel, le réseau hydrographique moderne s'installa graduellement, conduisant à l'incision des sédiments marins et le dépôt de sédiments alluviaux. Durant l'Holocène, des dépôts organiques se formèrent dans les régions mal drainées, et des sables éoliens sont mis en place. Ceux-ci sont particulièrement abondants dans la région de Lotbinière, où ils forment d'impressionnantes dunes longitudinales (Thiery, 2016).

Pour une revue plus approfondie de la déglaciation de la vallée du Saint-Laurent, le lecteur est invité à consulter l'article de Occhietti *et al.* (2011).

1.4.4 Courants glaciaires

Un courant glaciaire correspond à un corridor de glace à l'intérieur d'un inlandsis où l'écoulement s'effectue à une vitesse plus élevée (une magnitude de plusieurs ordres de grandeur) que la glace qui l'entoure, la transition latérale de la vitesse d'écoulement étant plutôt brusque (définition de

Cuffey & Paterson (2010)). Les courants glaciaires font typiquement plus de 20 km de largeur, et plus de 150 km de longueur, avec une zone de convergence alimentant un tronçon principal (Figure 1.4). Les courants glaciaires modernes sont associés à la déformation généralisée du till, au transport de sédiments de l'intérieur de l'inlandsis vers l'extérieur, ainsi qu'à de grandes accumulations de sédiments (*depo-centers*) au large des plateformes continentales (Margold *et al.,* 2015a). Les courants glaciaires déchargent la majeure partie de la glace et des sédiments des calottes glaciaires actuelles en Antarctique. Leur comportement et leur stabilité sont donc essentiels à la dynamique et au bilan de masse de l'inlandsis. Les courants glaciaires sont également susceptibles de varier dans le temps et dans l'espace, changeant d'emplacement et s'activant et se désactivant (Ross *et al.,* 2009). Leur déversement dans les bassins océaniques affecte la circulation océanique thermohaline, et c'est pourquoi les courants de glace ont donc fait l'objet de recherches dans le monde entier au cours des 30 dernières années.

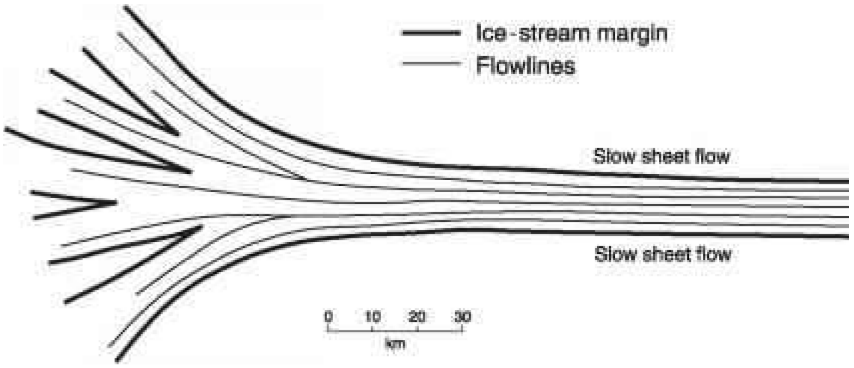

Figure 1.4 : Forme théorique simplifiée d'un courant de glace, caractérisé par des lignes d'écoulement convergentes dans une zone de formation alimentant un chenal principal. Schéma tiré de Stokes & Clark (1999).

Dans certains contextes topographiques, l'écoulement rapide peut aussi se produire par contrainte d'espace, par exemple dans un corridor bordé d'un massif rocheux. Cette distinction a amené certains auteurs à distinguer les courants glaciaires « purs », c'est-à-dire sans forçage du terrain, des courants glaciaires topographiques (voir Stokes & Clark (1999)). Les courants glaciaires ont tendance à occuper les dépressions topographiques parce qu'une glace plus épaisse entraîne une plus grande contrainte au niveau du lit et une vitesse plus rapide, car la déformation interne de la glace est contrôlée par la contrainte de cisaillement basale (Stokes, 2018). De plus, la glace plus épaisse est mieux isolée et a des températures basales plus élevées, ce qui augmente les taux de

déformation de la glace et de glissement de la couche de glace lors de la fonte basale. L'eau de fonte s'écoule et s'accumule dans les dépressions topographiques, et le taux de fonte est plus élevé sous une glace plus épaisse, ce qui favorise le glissement basal (Stokes & Clark, 2001). Ce système de rétroaction positive, avec un débit accru augmentant la température et la lubrification basale, qui à son tour augmente le débit, entraîne la formation de courants glaciaires dans certains corridors topographiques. Des courants de glace peuvent également se former dans les zones où la glace est plus fragile, ou avec un lit lubrifié qui facilite le mouvement de la base. Certains courants glaciaires sont une combinaison de topographie et de « pureté », et semblent délimités à la fois par la glace et par la topographie (Spagnolo *et al.,* 2014).

Il est de plus en plus évident que la présence des sédiments déformables, ou du moins à très faible contrainte de cisaillement, est une condition prérequise à l'écoulement glaciaire rapide (Bennett, 2003). Cependant, les mécanismes de contrôle de ce flux rapide et variable sont complexes et mal compris. Il existe un certain nombre de forçages potentiels, notamment la température de l'océan, les variations du niveau de la mer, la température de l'air, les marées océaniques, la bathymétrie sous-glaciaire, la géomorphologie sous-glaciaire, les points d'ancrage topographique, les eaux de fonte sous le courant de glace, la thermodynamique et la dimension du bassin de drainage (Bennett, 2003).

Plusieurs indices sont typiquement utilisés pour identifier les traces d'un paléo-courant glaciaire. Margold *et al.* (2015) en font une revue exhaustive :

- Empreinte physique du lit du glacier
- Empreinte topographique du réseau d'écoulement
- Zones d'accumulation sédimentaires situées au-delà de la limite continentale
- Till présentant des caractéristiques spécifiques suggérant un écoulement rapide, ou patron de dispersion distinct
- Débris transportés par la glace pouvant être retracés jusqu'à leur origine

L'étude de la géologie sous-glaciaire est donc essentielle pour déterminer l'emplacement des courants glaciaires. La géophysique permet d'obtenir de l'information importante sur les processus associés aux courants glaciaires actuels, mais l'étude du lit des paléo-courants glaciaires peut

également amener des informations cruciales à une meilleure compréhension de ces processus. En effet, les courants glaciaires étant des phénomènes d'envergure, leur empreinte physique est souvent préservée, autant pour les systèmes terrestres que les courants glaciaires marins. Celle-ci comporte typiquement un assemblage géomorphologique impressionnant, doté d'une certaine hiérarchie. La Figure 1.5 résume bien la transition typique des formes créées en amont dans la zone d'alimentation (crag-and-tails), vers un allongement progressif des formes allant du drumlin aux méga-linéations glaciaires (*mega-scale glacial lineations*, MSGLs). La présence de MSGLs est généralement l'indicateur géomorphologique prioritaire utilisé pour postuler la présence d'un paléo-courant glaciaire (Stokes & Clark, 2002), en combinaison avec le ratio d'élongation des formes sous-glaciaires.

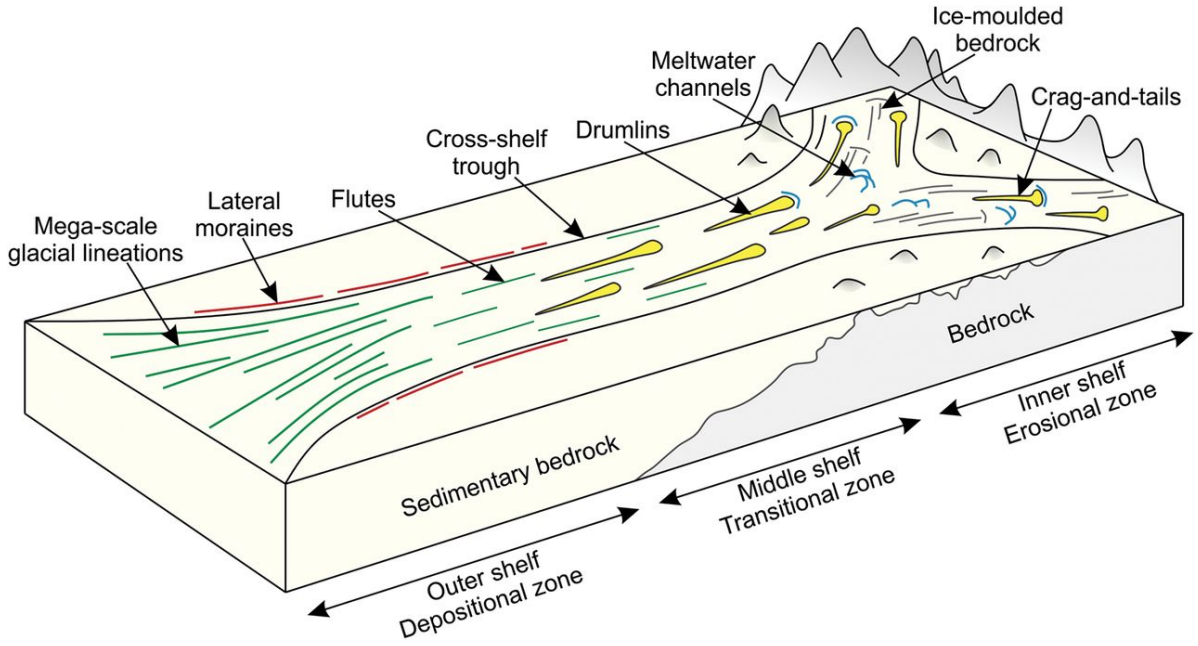

Figure 1.5 : Transition des formes du relief d'un courant glaciaire entre la marge continentale et l'océan. La glace s'écoule de l'intérieur d'un bassin de drainage continental vers un courant glaciaire marin. Les reliefs du substratum rocheux sont progressivement plus allongés vers l'aval. Figure tirée de Dowdeswell *et al.* (2016).

Cette succession morphologique idéalisée peut toutefois varier grandement lorsque le courant glaciaire est principalement terrestre. Les éléments géomorphologiques typiques sont exposés sur la Figure 1.6, et incluent des moraines récessionnelles, des terrains bosselés à géomorphologie variée et erratique, des crêtes transversales à l'écoulement, des eskers, etc. Ces éléments font partie de l'empreinte physique du courant glaciaire.

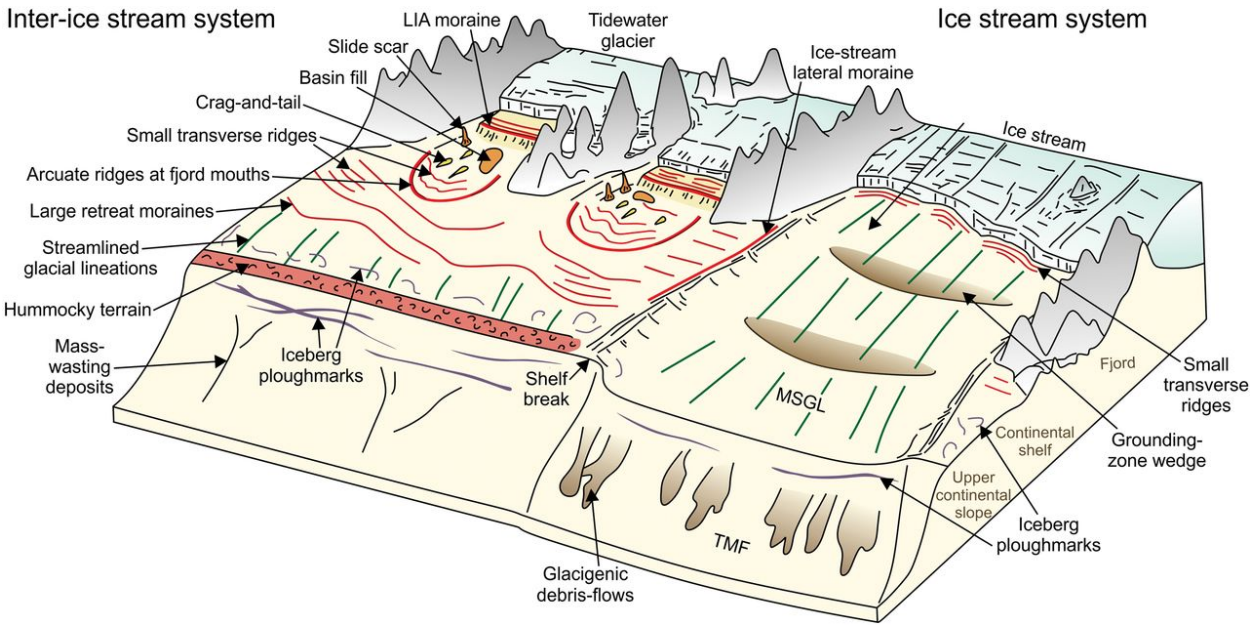

Figure 1.6 : Configuration typique de la géomorphologie associée à un courant glaciaire situé sur un plateau continental à hautes latitudes (extrait de Dowdeswell et al. (2016)).

Un assemblage de formes allongées vers le nord-est, incluant notamment des queues de rats, des roches moutonnées et des stries glaciaires a été relevé dans plusieurs secteurs de la vallée du Saint-Laurent, et l'existence d'un ou plusieurs courants glaciaires a été postulée par divers auteurs (Parent & Occhietti, 1999; Ross *et al.*, 2006). L'écoulement glaciaire dans la vallée du Saint-Laurent se serait réorienté pour emprunter un parcours et une direction d'écoulement semblable à celui du fleuve Saint-Laurent contemporain. La Figure 1.7 illustre la direction générale de l'écoulement lors du dernier maximum glaciaire, puis la réorientation du Courant glaciaire du Saint-Laurent et son écoulement vers le nord-est selon le modèle conceptuel de Parent & Occhietti (1999) basé en partie sur des relations de recoupement à partir de stries montrant un écoulement final vers le nord-est dans une région d'environ 100 km de rayon autour de la Ville de Québec et jusqu'à 300 m d'altitude. Cette reconstruction a l'avantage de tenir compte de l'inversion de l'écoulement glaciaire Appalachien mais aussi de plusieurs aspects clés des schémas régionaux de déglaciation, y compris la persistance de l'écoulement des eaux de fonte vers le sud-est dans les tunnels sous-glaciaires qui ont déposé des corps sédimentaires fluvioglaciaires tels que l'esker de Warwick-Asbestos.

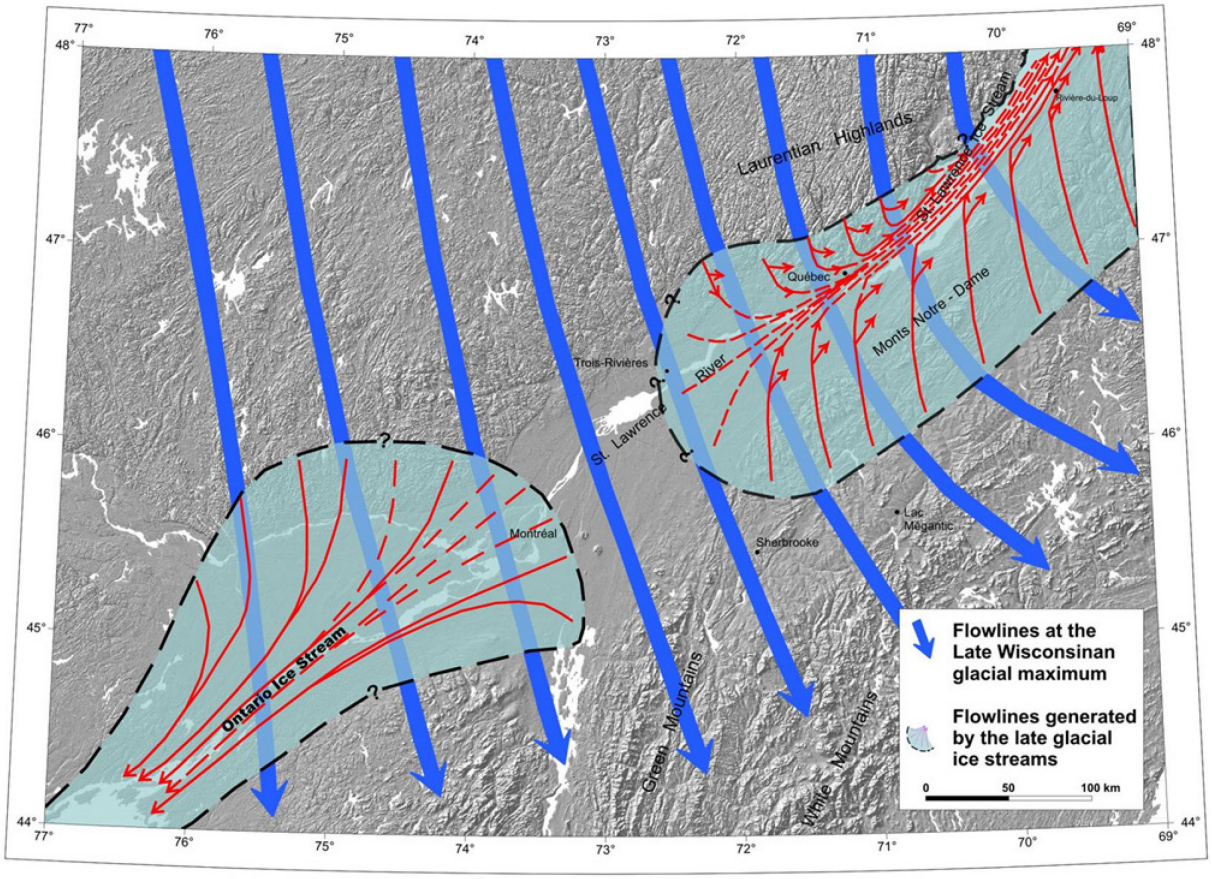

Figure 1.7 : Réorientation des lignes d'écoulements associée au Courant glaciaire du Saint-Laurent (tiré de Parent & Légaré-Couture (2018), figure modifiée de Parent & Occhietti (1999).

L'empreinte de ce mouvement de glace n'a cependant jamais été cartographiée, faute de données permettant de le faire. Selon la plus récente revue des paléo-courants glaciaires de l'Inlandsis Laurentidien (Margold *et al.*, 2015b), seulement 2 catégories d'indices seraient disponibles et documentées pour le courant glaciaire de la vallée du Saint-Laurent (identifié dans l'étude comme le courant du *Laurentian Channel*): l'empreinte topographique du réseau d'écoulement, et les débris de délestage (*ice-rafted debris*). De plus, son extension à l'intérieur de la vallée est largement sous-estimée, en comparaison avec les limites du courant proposé par Parent & Occhietti (1999).

1.5 Méthodes

1.5.1 Traitement des données LiDAR pour la cartographie géologique

La cartographie de la géologie de surface se fait traditionnellement par l'interprétation de photographies aériennes en vision stéréoscopique, en plus de campagnes de terrain exhaustives. Depuis quelques décennies, la venue de nouveaux outils numériques ainsi que de données d'élévation précises disponibles en couverture régionale amène un changement de paradigme, ainsi que de nouvelles méthodes pour cartographier les éléments géologiques de surface.

La technologie LiDAR (*Light Detection and Ranging*), un acronyme pour la détection et la télémétrie lumineuse, est un de ces outils. Cette technologie de télédétection émet des impulsions intenses et focalisées de lumière et mesure le temps nécessaire pour que les réflexions soient détectées par le capteur. Ces informations sont utilisées pour calculer les distances par rapport aux objets en utilisant la relation suivante :

$$\boldsymbol{t_{parcours} = \frac{2R}{c}}$$

où t est le temps de parcours de la lumière, c est la constante de la vitesse de la lumière (≈ 300 000 kilomètres par seconde) et R est la distance entre le capteur et la cible. Un système d'acquisition typique ainsi que quelques caractéristiques générales sont montrés conceptuellement à la Figure 1.8. Le système d'émission et de réception laser (habituellement dans les longueurs d'onde du proche infrarouge) est monté sous un avion volant à une altitude variable selon la mission et l'instrumentation à bord. Les caractéristiques des capteurs varient grandement étant donné la constante évolution des nouveaux capteurs et des avancées technologiques rapides de la présente époque. Dans le cas du système utilisé pour la prise des données du secteur à l'étude principal, le capteur émet un signal laser à une fréquence de 100 kHz, alors que la fréquence de balayage de 50 Hz (50 lignes perpendiculaires à la ligne de vol de l'avion sont balayées chaque seconde, chacun des balayages prenant 0.02 seconde). À une altitude de vol de 950 m, l'empreinte au sol du faisceau fait un diamètre d'environ 25 cm. Un système de navigation global par satellite (*Global Navigation Satellite System* (GNSS)) est utilisé afin de calculer le positionnement exact de l'avion à tout moment. L'avion possède son propre système, alors qu'une station terrestre de référence calcule

et fournit des corrections en temps réel via une mesure de la phase des ondes porteuses (Cinématique temps réel; *Real Time Kinematic* (RTK)) permet de suivre et d'enregistrer le positionnement de l'avion à chaque milliseconde permettant d'atteindre une précision nominale de l'ordre de 1 cm horizontalement et 2 cm verticalement. Une centrale inertielle (*inertial measurement unit* (IMU)) est utilisée afin d'enregistrer les paramètres de vol de l'avion, notamment son accélération, sa vitesse angulaire & linéaire, ses angles de roulis, de tangage et de cap.

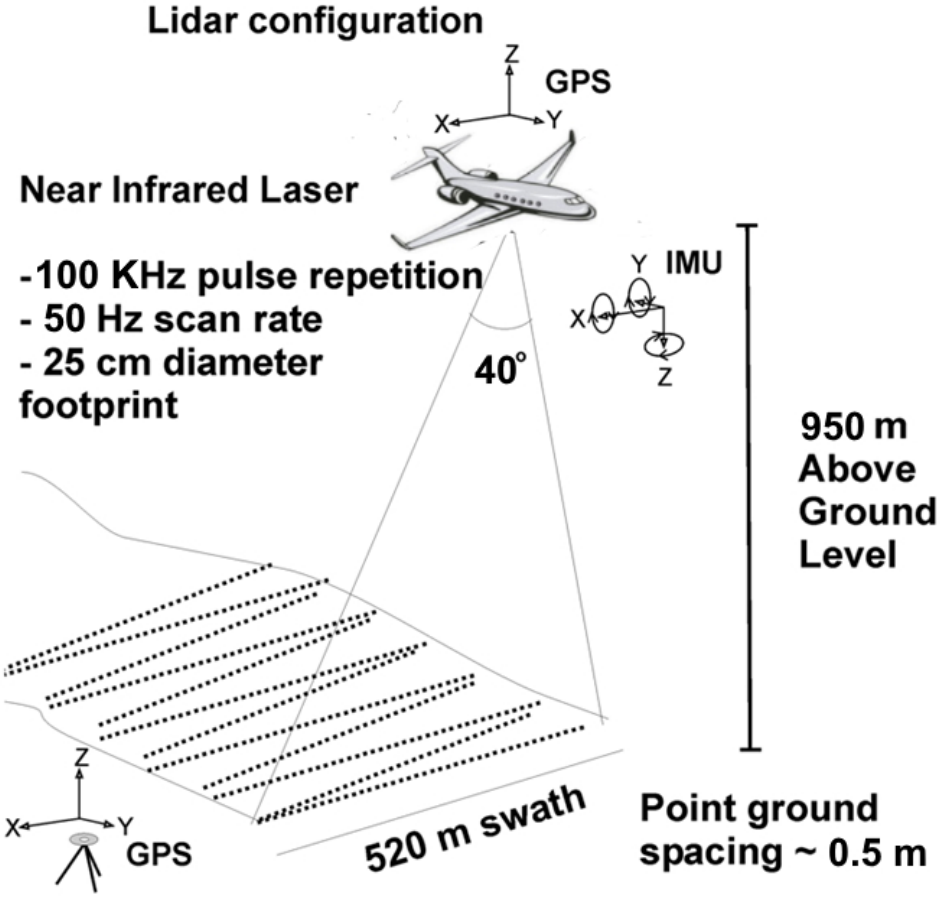

Figure 1.8 : Système d'acquisition LiDAR aéroporté typique utilisé dans le sud du Québec.

Les coordonnées géographiques (latitude, longitude, et altitude) des objets cibles sont calculées à partir de 1) la différence temporelle entre l'impulsion laser émise et retournée, 2) l'angle sous lequel l'impulsion a été émise, et 3) l'emplacement absolu du capteur sur ou au-dessus de la surface de la Terre. Un système LiDAR étant un capteur actif, il permet de recueillir des données LiDAR aussi bien la nuit que le jour.

La prise de mesure LiDAR est en quelque sorte analogue au radar (détection et télémétrie par radio), à l'exception du fait que la mesure est basée sur des impulsions discrètes de lumière focalisée plutôt qu'une onde radio. Cependant, contrairement au radar, le LiDAR ne peut pas pénétrer les nuages, la pluie ou la brume épaisse, et doit être acquis par beau temps. Le produit obtenu est un ensemble dense de points d'élévation géoréférencés de haute précision, appelé nuage de points, qui peut être utilisé pour générer de multiples représentations de la surface de la Terre et de tout ce qui s'y trouve. L'erreur absolue de positionnement de chacun des points pour les systèmes d'acquisition récents est de l'ordre de 10 cm, avec une précision verticale d'environ 15 cm. Une image typique d'un nuage de points LiDAR est illustrée à la Figure 1.9. Pour une revue plus complète du principe de fonctionnement d'un système LiDAR aéroporté, le lecteur est dirigé vers la publication de Wehr & Lohr (1999).

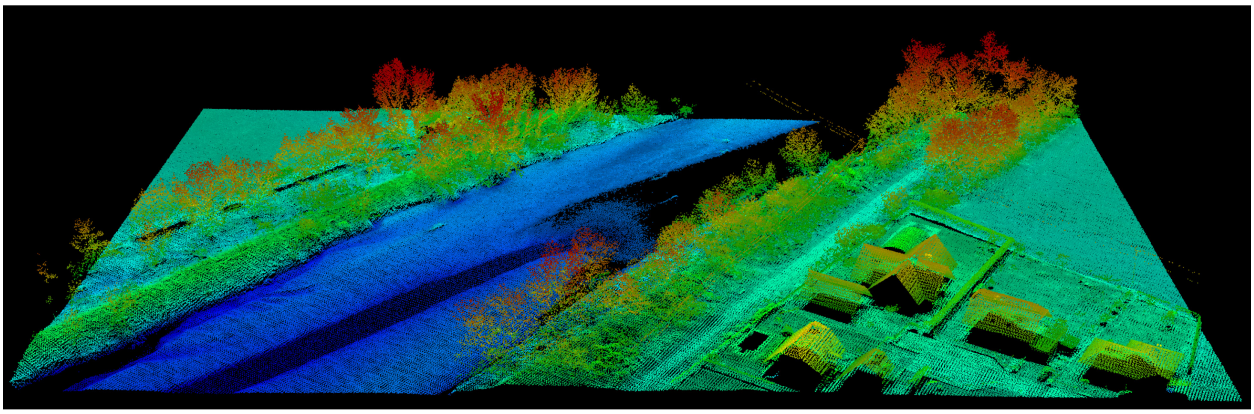

Figure 1.9 : Extrait d'une vue 3D de retours lasers dans une zone rurale partiellement végétalisée en bordure d'une rivière. Les retours individuels sont colorés en fonction de leur élévation relative à un plan horizontal, allant du bleu foncé pour les retours en basse élévation au rouge pour les retours à des élévations plus hautes.

En géologie de surface, l'élément d'intérêt est la surface du terrain. Puisque le nuage de point contient une foule de retours laser qui correspondent à des éléments situés entre le capteur et le sol (arbres, bâtiments, etc.), celui-ci doit être traité afin d'assigner une classe à chacun des retours individuels. Divers logiciels de traitement sont disponibles pour cette tâche, certains gratuits, mais la plupart payants et à source fermée. L'algorithme de classification utilisé peut avoir une influence notable sur le résultat de la classification finale. Une fois la classification terminée, le nuage de point peut être utilisé afin de créer un modèle incluant seulement les points ayant pénétré la canopée et qui représentent le sol. Il s'agit de la différence entre un modèle numérique de terrain

(MNT, *digital terrain model* (DTM)) et un modèle numérique de surface (MNS, *digital surface model* (DSM)), lequel représente la première surface rencontrée par les retours laser (Figure 1.10).

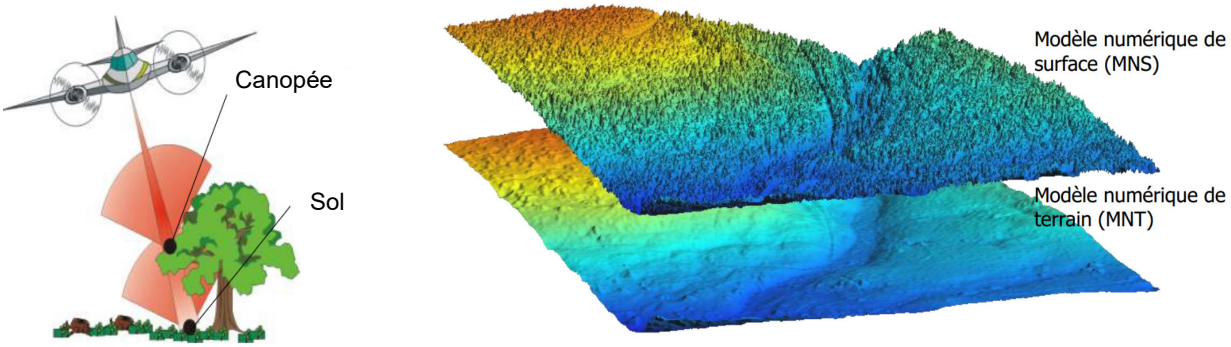

Figure 1.10 : Exemple d'utilisation des retours de la canopée versus les retours au sol pour la création d'un modèle numérique. La grille supérieure, le modèle numérique de surface (MNS) est construit à partir des premiers retours atteints par le système laser, alors que la deuxième grille, le modèle numérique de terrain (MNT), est créée à partir des retours au sol seulement.

L'un des principaux avantages de la méthode LiDAR réside dans le fait qu'elle permet de produire une image plus précise de la morphologie de surface dans les zones fortement boisées, un phénomène courant dans l'est du Canada. Dans les zones de couvert forestier dense, la proportion de réflexions laser pénétrant sous la canopée et atteignant le sol est effectivement beaucoup plus faible que dans les zones déboisées. Néanmoins, il suffit généralement pour reconstruire un modèle satisfaisant de la surface, ce qui permet de visualiser des caractéristiques microtopographiques totalement invisibles sur les photographies aériennes conventionnelles, lesquelles sont généralement prises en été au moment du développement complet de la canopée. Ces caractéristiques microtopographiques servent ensuite à identifier et délimiter des unités de géologie de surface. Un autre avantage de l'utilisation d'un MNT dérivé du LiDAR plutôt que de la photographie aérienne réside dans la nature numérique des données elles-mêmes. La création d'un MNT régional basé sur LiDAR et d'autres dérivés permet de créer une grille spatialement continue pouvant être étudiée facilement à toute échelle.

Ce type de données est utilisé depuis plusieurs années pour la cartographie géologique à plusieurs échelles. Webster *et al.* (2006) ont utilisé des modèles numériques de terrain dérivés de données LiDAR pour identifier des escarpements rocheux, des niveaux de terrasses ainsi que différencier certaines zones de till des affleurements rocheux environnants. Pawley & Atkinson (2010) ont

montré que le LiDAR était utile pour identifier des unités de granulats dans des zones forestières densément peuplées de conifères. D'autres utilisations variées sont recensées dans Smith *et al.* (2011).

1.5.2 Modélisation géologique 3D

1.5.2.1 Données géologiques

La justesse d'un modèle géologique 3D découle inévitablement de la qualité, quantité et disponibilité des données géologiques existantes. Typiquement, ces paramètres varient considérablement spatialement à l'intérieur des limites du secteur à l'étude. Lors d'une étude hydrogéologique réalisée à l'échelle régionale, la compilation, le tri et la validation de ces milliers de données archivées représentent un effort considérable et correspondent à un travail de longue haleine.

En ce qui concerne le projet proposé ici, une grande partie du travail de compilation des informations existantes a déjà été réalisée dans le cadre du projet PACES - Chaudières Appalaches (Lefebvre *et al.*, 2015). Il est important de considérer ici le travail colossal de tri et de validation d'une partie des données effectué précédemment par l'équipe entière du projet PACES-CA. Entre mai 2012 et décembre 2014, des données et des séries de données hydrogéologiques (valeurs de profondeur de la nappe dans les puits, données de stratigraphie, valeurs de profondeur au roc, données de géochimie de l'eau souterraine, valeurs de conductivité hydraulique et de transmissivité, etc.) ont été acquises et compilées dans une base de données. Les données recueillies proviennent principalement des sources suivantes :

- Système d'information hydrogéologique (SIH), MDDELCC
- Base de données géotechniques du Ministère des Transports (MTQ) du Québec
- Système d'informations géominières du Québec (SIGEOM) du Ministère des Ressources naturelles (MRN) du Québec
- Base de données géochimiques du Québec (BADGEQ) du Ministère des Ressources naturelles (MRN) du Québec
- Base de données sur la qualité du milieu aquatique (BQMA) du MDDELCC

- Données de forages géothermiques de la Coalition canadienne de l'énergie géothermique (CCEG)

Le Tableau 1.2 recense le nombre d'observations recueillies pour la région du projet PACES-CA en entier.

Tableau 1.2 : Observations hydrogéologiques compilées lors du projet PACES-CA (Lefebvre *et al.*, 2015).

Base de données	Source	Nombre d'observations
Système d'information hydrogéologique (prof. totale du puits, niveau d'eau, stratigraphie, prof. du roc, géochimie)	MDDELCC	30 189 puits ou forages
Base de données géotechniques (profondeur du forage, stratigraphie)	MTQ	1 271 forages
Système d'informations géominières (profondeur du forage, stratigraphie)	MRN-SIGEOM	2 641 forages
Données de forages géothermiques (profondeur du forage, profondeur au roc)	CCEG	148 forages
BQMA (stations, conductivité électrique, chlorures, fer, nitrates, solides en suspension, phosphore total et température)	MDDELCC	52 stations
Base de données sur les débits de rivière (stations ouvertes de jaugeage et de débits quotidiens)	CEHQ	227 stations

Les observations stratigraphiques contenues dans la base de données du SIH, par exemple, sont réputées être de fiabilité douteuse. Cette validation a permis d'accélérer considérablement le processus de construction du modèle géologique. Il est à noter qu'un effort de compilation supplémentaire a été nécessaire afin de compiler les données du secteur nord-est de la région à l'étude (Bas Saint-Laurent), située en dehors du territoire couvert par l'étude du PACES-CA.

1.5.2.2 Modélisation

Des logiciels de modélisation géologique 3D spécialisés comme gOcad (Mallet, 2002) sont souvent utilisés en raison de leur capacité à représenter des éléments ou formes géologiques complexes par dessin. Cela permet d'établir une vision intégrée de la géologie locale et d'inclure manuellement des éléments importants mais qui n'ont pas nécessairement été observés à suffisamment d'endroits pour estimer spatialement leur étendue ou leurs propriétés. Ces logiciels nécessitent cependant une

« déconnection » du reste des bases de données partagées en raison de leur fonctionnement isolé, et peuvent difficilement intégrer en temps réel les éditions apportées à la base de données centrale.

La stratégie envisagée pour la construction du modèle géologique 3D gravite autour de l'environnement QGIS (QGIS Development Team, 2014) plutôt qu'un logiciel de modélisation géologique. Ce logiciel est à la base essentiellement un système d'information géographique (SIG) 2D, mais divers modules de géostatistique permettent de créer des surfaces interpolées de type « grid » en passant par divers types d'observations géologique. Cette approche hybride à la modélisation permet de juxtaposer des méthodes géostatistiques complexes à la vision intégrée de l'expert géologue. Un avantage exclusif de cette méthode est associé au modèle géologique qui peut être construit entièrement dans un environnement SIG, et donc en relation constante avec la base de données commune à l'équipe de travail entière du projet, auxquelles des modifications sont apportées souvent sur une base quotidienne (Ross *et al.*, 2005).

L'interpolateur DSI (*discrete smooth interpolation*) de gOcad est réputé pour produire des surfaces satisfaisantes en se basant sur la réduction maximale de la rugosité de la surface, tout en respectant des contraintes définies par l'utilisateur. Bien que cet algorithme soit exclusif à gOcad, des alternatives intéressantes existent, comme l'algorithme ANUDEM (Hutchinson, 1989, 2004). Celui-ci est généralement utilisé pour construire des modèles numériques de terrain corrigés pour l'écoulement de surface à l'aide d'une variété de données de différents types (courbes de niveau, points, contraintes, etc.) et de contraintes. Ces contraintes peuvent être utilisées de manière tout aussi appropriée pour représenter des éléments géologiques. Pour pallier aux lacunes typiques des logiciels SIG pour la construction des objets géologiques discrets, des règles topologiques peuvent être utilisées afin de contraindre les surfaces créées par modélisation. Ces contraintes peuvent inclurent, par exemple pour la modélisation de la surface du roc, des données d'élévation du socle observées en forage, des données géophysiques, des observations d'affleurements en surface, des coupes interprétées, etc. Elles peuvent être réglées comme strictes ou souples ; l'interpolateur pourra ne respecter qu'approximativement certaines contraintes réglées comme souples, ce qui peut s'avérer utile lorsqu'on travaille avec différentes sources de données de fiabilité variable.

Bien que chaque série de données comporte un degré d'incertitude, cette vision intégrée permet à l'expert de créer un modèle géologique complexe tout en respectant le modèle conceptuel élaboré à priori pour la région à l'étude. Même si plusieurs outils automatisés sont disponibles afin de travailler certaines problématiques spécifiques du modèle, il est important de rappeler que l'utilisateur demeure toujours maître de son modèle. Il est libre d'imposer sa vision d'expert à toutes les étapes de la création du modèle, ce qui n'est pas nécessairement le cas avec d'autres logiciels de modélisation géologique populaires. Un autre argument pour l'utilisation de cet environnement serait celui de la diffusion des résultats. Autant les chercheurs familiers avec le domaine de la modélisation géologique 3D que les utilisateurs SIG pourront avoir un accès facile aux données étant donné la nature ouverte du type de fichier de sortie.

1.6 Structure de la thèse

Cette thèse est rédigée dans le format proposé par le service de documentation (SDIS) de l'INRS. Elle est composée de 6 chapitres. Le premier, l'introduction générale, introduit le lecteur au cadre et à la problématique de la thèse. Ce chapitre est rédigé en français, conformément aux règlements du programme. Les 4 chapitres suivants sont présentés sous forme d'articles et font état de la démarche et des travaux pour chacun des volets de recherche. Suite à ces articles, une discussion générale et une conclusion en français sont présentées. Ceux-ci mettent en contexte et résument les principaux résultats et apports scientifiques de ce projet de recherche.

Plusieurs références sont citées dans les sections en français, puis réutilisées dans un ou même plusieurs articles de cette thèse. Afin d'éviter la redondance, une seule bibliographie unifiée est présentée à la fin du document et intègre toutes les références retrouvées dans cet ouvrage.

2 Article 1: High-resolution Quaternary geology map of the south shore of the St. Lawrence Mid-estuary, Québec, Canada, using a LiDAR-derived DTM

Carte haute-résolution de la géologie du Quaternaire de la rive sud de l'estuaire moyen du fleuve Saint-Laurent, Québec, Canada, à l'aide d'un MNT dérivé d'un levé LiDAR aéroporté

Auteurs :

Guillaume Légaré-Couture[1], Michel Parent[2] & René Lefebvre[1]

[1] Institut National de la Recherche Scientifique – Centre Eau Terre Environnement (INRS-ETE), Québec, Canada

[2] Commission géologique du Canada, Ressources naturelles Canada, Québec, Canada.

Titre de la revue ou de l'ouvrage :

Journal of Maps

À soumettre en 2021

Contribution des auteurs :

Le premier auteur est responsable du développement de la méthodologie, de l'analyse, de la cartographie ainsi que de la rédaction de l'article.

Les deuxièmes et troisièmes auteurs ont contribué à la planification du travail, aux travaux sur le terrain ainsi qu'à la révision du manuscrit.

Résumé :

Une nouvelle carte géologique du Quaternaire à l'échelle de 1/50 000 a été produite pour la région du Bas-Saint-Laurent, une région rurale de l'est du Canada entourant la ville de Lévis. Cette zone d'étude, qui s'étend sur la rive sud du fleuve Saint-Laurent, est caractérisée par une géologie de surface particulièrement complexe, héritée en grande partie de la dernière glaciation et des processus de déglaciation qui ont suivi, notamment la submersion marine postglaciaire. Le faible relief topographique, combiné à une mosaïque de terres agricoles et de forêts mixtes à haute densité de feuillus et de conifères, a fait de la cartographie géologique des dépôts superficiels de la région un défi pour les méthodes traditionnelles basées sur l'interprétation de photographies aériennes. Dans le cadre de cette étude, des unités géologiques ont été identifiées et interprétées à partir de diverses dérivées d'un modèle numérique de terrain (MNT) produit à partir des données de nuages de points LiDAR (*Light Detection and Ranging*). Au total, 35 unités de géologie de surface sont différenciées sur la carte, en plus de centaines d'entités géomorphologiques ponctuelles et linéaires. Une nouvelle limite marine précise (limite maximale de submersion) pour une incursion marine postglaciaire, appelée Mer de Goldthwait, a également été interprétée. Cette étude met en évidence le grand potentiel de cette nouvelle méthode pour la cartographie de la géologie de surface des terrains glaciaires, particulièrement dans les régions à faible relief inondées par la mer, telle la vallée du Saint-Laurent.

Abstract :

A new 1:50,000 Quaternary geology map was prepared for the Lower St. Lawrence region, a rural region of eastern Canada surrounding on the city of Lévis. This study area, which extends on the south shore of the St. Lawrence River, is characterized by an especially complex surficial geology mostly inherited from the last glaciation and the ensuing deglaciation events and processes, especially the post-glacial marine invasion. The low topographic relief as well as the mosaic of agricultural lands and high-density mixed deciduous-coniferous forests make surficial geology mapping of the region a challenge for traditional methods based on air photo interpretation. In this study, geological units were identified and interpreted based on various derivatives of a digital terrain model (DTM) based on LiDAR (Light Detection and Ranging) point cloud data. A total

of 35 surficial geology units are differentiated on the map, in addition to hundreds of local and linear geomorphological features. A new precise marine limit (maximum limit of submergence) for the post-glacial Goldthwait Sea was also interpreted. This study highlights the great potential of this new approach for surficial geology mapping of glaciated terrains, especially in marine-inundated regions of low relief such as the St. Lawrence lowlands.

2.1 Introduction

Understanding the spatial distribution of surficial and near-surface Quaternary geological units is not only a key element of geological knowledge in glaciated terrains, but is also a fundamental tool for the study of regional groundwater flow systems. Such surficial mapping underpins the assessment and understanding of the associated erosional-depositional processes, as these control the properties, geometry and relationships between geological units, which in turn directly influence the properties (permeability, flow, recharge) and general flow dynamics of granular aquifers. In southern Canadian regions, significant efforts to delineate and characterize aquifers were initially undertaken by the Geological Survey of Canada (Fagnan *et al.,* 1998, 1999; Murat *et al.,* 2000; Paradis *et al.,* 2000; Rivard *et al.,* 2008b, 2008a).

During the last decade, provincial agencies such as the Québec Ministère de l'Environnement et de la Lutte contre les changements climatiques (MELCC), in collaboration with universities in various regions, took the relay and pursued these efforts. Larocque *et al.* (2018) provide details about the results of this program, whose acronym in French is PACES (Programme d'Acquisition de Connaissances sur les Eaux Souterraines). As part of the regional groundwater characterization of the Chaudière-Appalaches region of Québec (Lefebvre *et al.,* 2015), an extensive Quaternary geology mapping campaign was conducted between the fall of 2013 and the spring of 2015 in the lower Chaudière Valley and the Lower St. Lawrence region. This region has long been a challenge in regards to the surficial mapping partly due to the relatively flat topography smoothed out and altered by years of tillage, and also because of the high-density mixed deciduous-coniferous forest covering much of the region outside agricultural areas. A study was thus undertaken to assess the potential of an airborne LiDAR (Light Detection and Ranging) land surface survey covering the main region of interest as a tool to improve Quaternary geology mapping.

The main objective of this study was to produce a coherent series of surficial geology maps to help answer multiple regional hydrogeology questions, such as the estimation of groundwater recharge, the definition of hydrogeological contexts, and the assessment of aquifer vulnerability to contamination. While the main results of the regional groundwater characterization project were mostly published in a report (Lefebvre *et al.*, 2015), the resulting surficial geology maps, which had only been published in a generalized format, is herein presented in its detailed form. The map provides new insights on the Quaternary geology of the region, including a comprehensive coverage of surficial units, as well as a more precise marine submergence limit associated with the Champlain and Goldthwait seas.

2.2 Study area and geomorphological outline

The study area is located in southern Québec, Canada, and covers a part of the south shore the St. Lawrence River valley between the towns of Lyster and Rivière-du-Loup, including the city of Lévis (directly across the St. Lawrence River from Québec City) along a SW-NE axis. From a NW-SE axis, the study area lies between the St. Lawrence River and the Appalachian Uplands, up to an elevation of about 200 m, which is the approximate southern limit of farmlands in the region (Figure 2.1). The mapped area consists of two distinct parts roughly separated by the lower Chaudière River Valley. Two 1:50 000 scale map sheets, identified as 21L06 (Saint-Sylvestre) and 21L11 (Charny) in the National Topographic System (NTS), were not mapped as they were only partly included in the PACES-CA project. Moreover, a recent surficial geology map was available for the 21L11 map sheet (Bolduc, 2003). As this mapping project was limited by the availability of LiDAR data at the time, the final mapped area only includes the more densely populated area on the south shore. The mapped areas extend over 17 NTS map sheets.

From a geomorphological standpoint, this part of the St. Lawrence Valley can be described as a series of clay plains and low plateaus punctuated by a series of subparallel Appalachian ridges. The St. Lawrence Valley plays a key role in the Quaternary glacial history of North America as it constitutes a major drainage route for much of the eastern mid-continent and lies about midway between the eastern core region of the Laurentide Ice Sheet (LIS) and its terminal position at the latitude of New York. During Wisconsinan interstades, the St. Lawrence Valley was periodically

invaded by marine or glaciolacustrine water bodies as a result of the complex evolution of ice-front fluctuations, glacial isostatic adjustments and global sea level changes (Occhietti *et al.*, 1996), the details of which are beyond the scope of this paper. This complex glacial record has led to the development of an intricate Quaternary stratigraphic sequence.

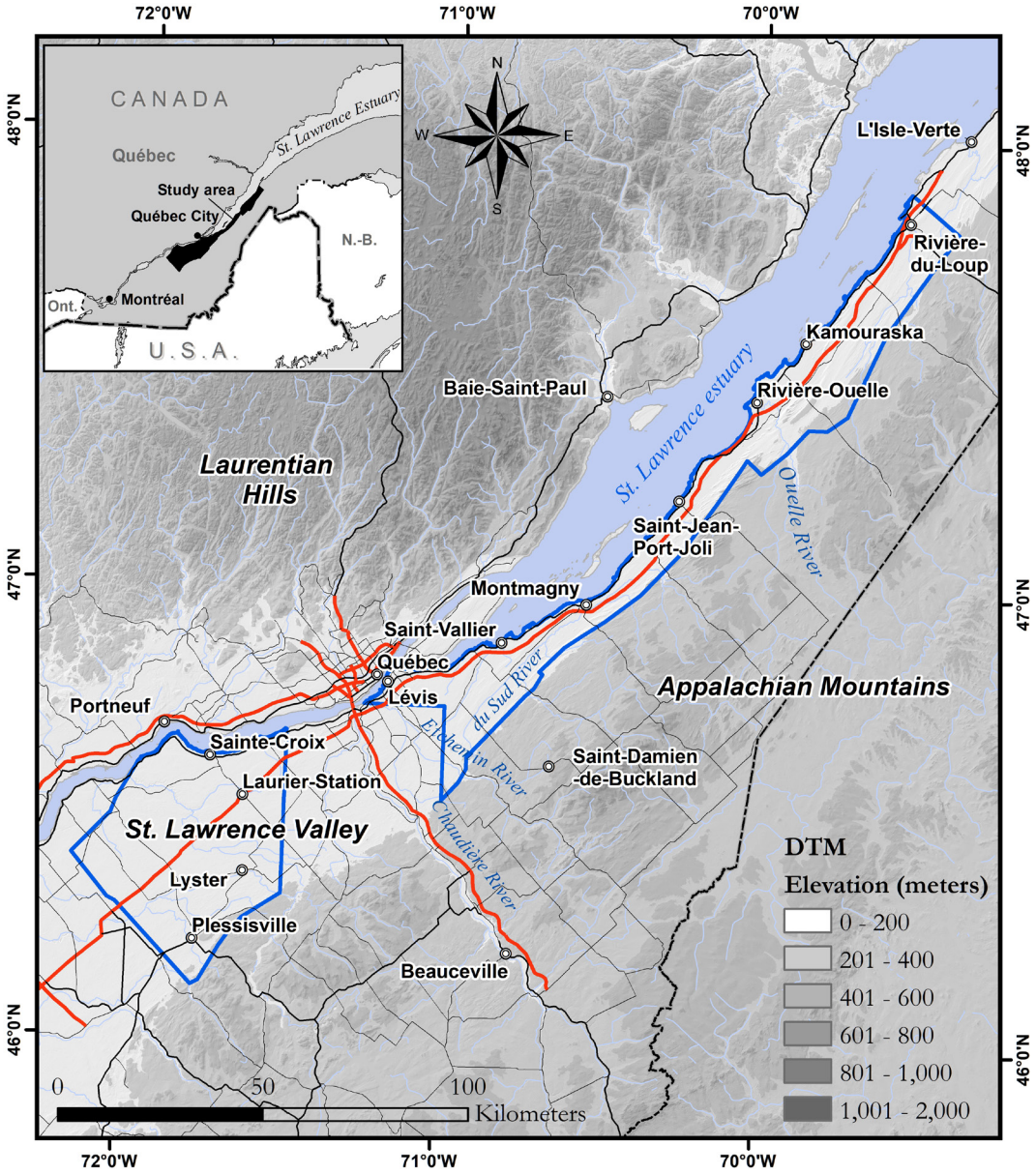

Figure 2.1 : Location of the study area, represented by a thick blue outline. The map is discontinuous in the Lévis region around the Chaudière River, as this area (NTS map sheets 21L06 (Saint-Sylvestre) and 21L11 (Charny)) had recently been mapped already (Daigneault et al., 2014).

A few previous surveys provide an outline of the main surficial geologic units and Quaternary evolution of the region. LaSalle *et al.* (1977a) focused their work on the ice-flow history and on the morphology, stratigraphy and deglaciation events of the Québec City region. This study was the basis for a first surficial geology 1: 50,000 scale map for the Québec City area (LaSalle, 1978). LaSalle *et al.* (1980) later published a 1:50,000 scale map of the Saint-Raphael region (21L15 SNRC map sheet), identifying deglacial features associated with the Highland Front system defined by Gadd (1964). While this map was in general fairly accurate, only nine surficial geology units were defined, and no distinction was made between areas of thick till cover versus areas of thin till cover, a key element for the estimation of recharge in regional groundwater characterization projects. Marine offshore/deep-sea facies were distinguished from marine beaches sediments reasonably well, but the maximum elevation limit of the Goldthwait Sea was not identified nor mapped. LaSalle *et al.* (1980) reported the presence of several landslides near the Boyer River, but these were unfortunately not mapped. Also missing were linear geomorphological features such as shorelines, raised beaches and terraces. Lee (1962) mapped the surficial geology of the Rivière-du-Loup area, while Martineau (1977) mapped the area between Saint-Denis-de-Kamouraska and Rivière-du-Loup. Rappol (1993) reported on the glacial history and striation record of the area northeast of Kamouraska. Approximately the same zone was mapped by Veillette *et al.* (2017), but at a much larger scale.

2.3 Methods and software

Our mapping effort was primarily made via the interpretation of a high-resolution digital terrain model (DTM) derived from LiDAR data. For this study, two airborne LiDAR survey datasets were used; the 2009 survey covers the northeastern part of the study area, while the 2011 survey covers the area southwest of Lévis. Both surveys were done aboard a Piper Navajo airplane flown at 950 meters above ground. An Optech ALTM Gemini laser sensor was used to take the measurements using a refreshing frequency of 100 000 Hz, a sweeping frequency of 50 Hz and a 20-degree angle of sweep on both sides of the nadir. The system reached a theoretical point density of 2 ground measurements per square meter. After geodetic corrections, the planimetric precision of the surveys was calculated to be 17 cm, while the altimetric precision was on the order of 15 cm in open areas, and 25 cm in heavily forested areas.

The recovered data were delivered in raw laser data point cloud format (LAS) as well as processed surface models: digital terrain models (DTM) representing the ground interface, and digital surface models (DSM) of the first surface encountered (canopy, buildings, etc.). The discrete individual laser returns were processed by the contractor using TerraScan software (TerraSolid, 2000) in order to classify individual pulses into ground and non-ground (vegetation, buildings, homes or other facilities) returns. Considering that no details were available on the algorithm and options used to process the raw data, it was deemed necessary to go through the same process using an open source processing algorithm in order to compare the results. Raw laser data on those tiles were thus reprocessed and classified using a PDAL point cloud library (PDAL Contributors, 2018) JSON pipeline incorporating the Simple Morphological Filter (SMRF) approach (Pingel *et al.*, 2013).

For the entire study area, the processed and classified laser returns were used to build a high resolution 1-meter cell size gridded DTM using the Lidar2dems algorithm (https://github.com/Applied-GeoSolutions/lidar2dems), and using only the ground returns. However, as DTM grids are not the most efficient way of interpreting morphological features, a hillshade function derivative was used to create an artificial illumination of the DTM. Values for each cell in a raster are determined using the slope and aspect derivative, and by using a position for an artificial light source. The resulting relative illumination value for each grid cell in relation to neighboring cells is then calculated. This process considerably enhances the visualization of a DTM. One of the caveats of using a hillshade model with a direct illumination coming from a single direction is that it restricts visualization possibilities in shaded areas. Subtle terrain variability hidden in the shade of a large steep hill, for example, would not be visible on a single illumination hillshade model. Furthermore, while structures that lie perpendicular to the direction of illumination will most of the time be well defined, elements lying parallel to the direction of illumination can be completely invisible on the resulting hillshade model, which would be quite problematic in the context of geological mapping. In order to alleviate this problem, multiple analytical hillshade models with illumination coming from 64 different directions were created using the RVT software (Zakšek *et al.*, 2011). Principal component analysis (PCA), a mathematical procedure used to summarize the information of correlated data (Davis, 1986) was

performed on the created hillshade images to determine the three illumination directions most associated with topographic variations. Multiple illumination shaded relief grids were then created using artificial illumination directions identified by PCA analysis in order to highlight the topographic features on the ground. For the purpose of the surficial geology mapping, our tests showed that the use of 3 distinct light sources has proven to be sufficient due to high autocorrelation. The visual results obtained at each step of the LiDAR data processing workflow are illustrated in Figure 2.2. More details about this methodology are provided by Webster *et al.* (2006).

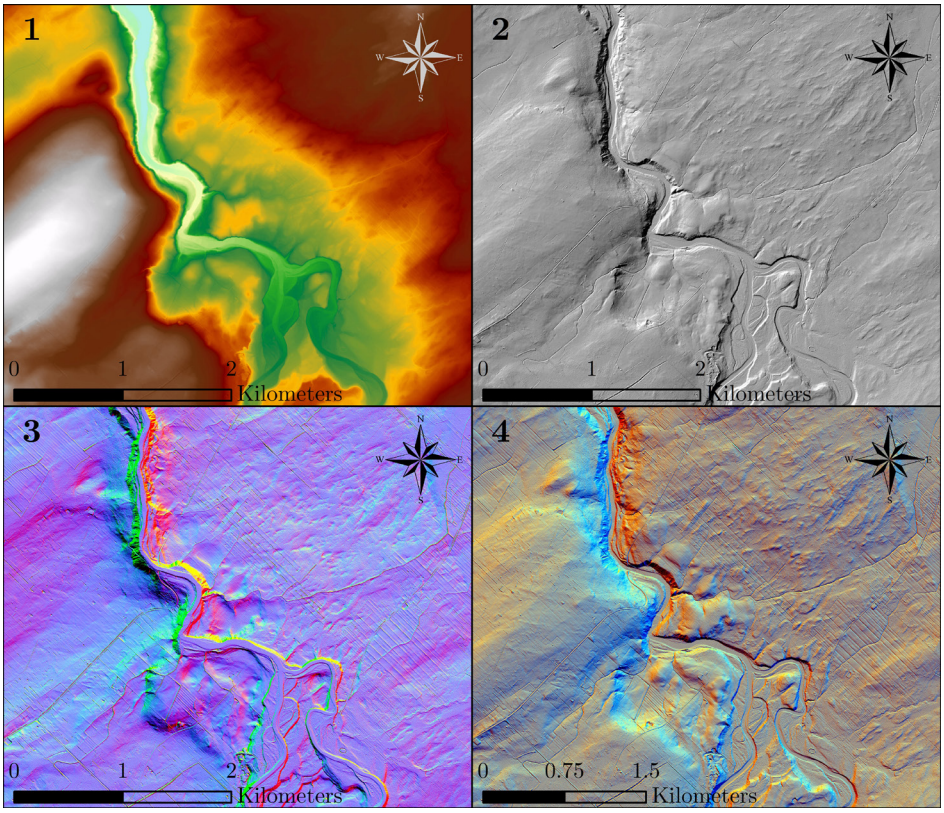

Figure 2.2 : LiDAR-derived DTM and derivatives used to interpret the surficial geology illustrated by the Ouelle River, near the village of the same name. 1: 1-meter grid cell size DTM, with elevations ranging from 90 to 210 m (white). 2: Typical grayscale shaded relief image derived from the DTM with illumination coming from a single 315° direction (0° is North, 90° is East); 3: Results of the principal component analysis (PCA) showing the 3 directional components responsible for 99% of the variability of the DTM. Each component is displayed using a single RGB inverted channel in order to highlight subtle relief features: 145.99° in green, 130.68° in blue, and 229.76° in red. Note the farmland drainage ditches in the lower right quadrant, amongst other features, becoming clearly visible in the green channel; 4: Analytical hillshaded relief with multiple direction illumination displayed as RGB channels.

Analysis and interpretation of landforms were then carried out directly over those raster images, sometimes in combination with aerial photos, in QGIS 2.8 Wien (QGIS Development Team, 2014). Polygon and polyline features were digitized at a cartographic scale varying between 1:1,000 and 1:10,000, depending on the size of the geological element. Field work was conducted in order to locally validate the interpretations from the LiDAR data. Over a period of three years, 98 sites were investigated and documented in order to confirm the results of the remote mapping.

2.4 Surficial geology of the Lower St. Lawrence Valley region, south shore

We present in this section a brief outline of the surficial and bedrock geology of the area starting with the oldest units. Figure 2.3 shows a simplified stratigraphic conceptual cross-section of the surficial geology encountered in the study area.

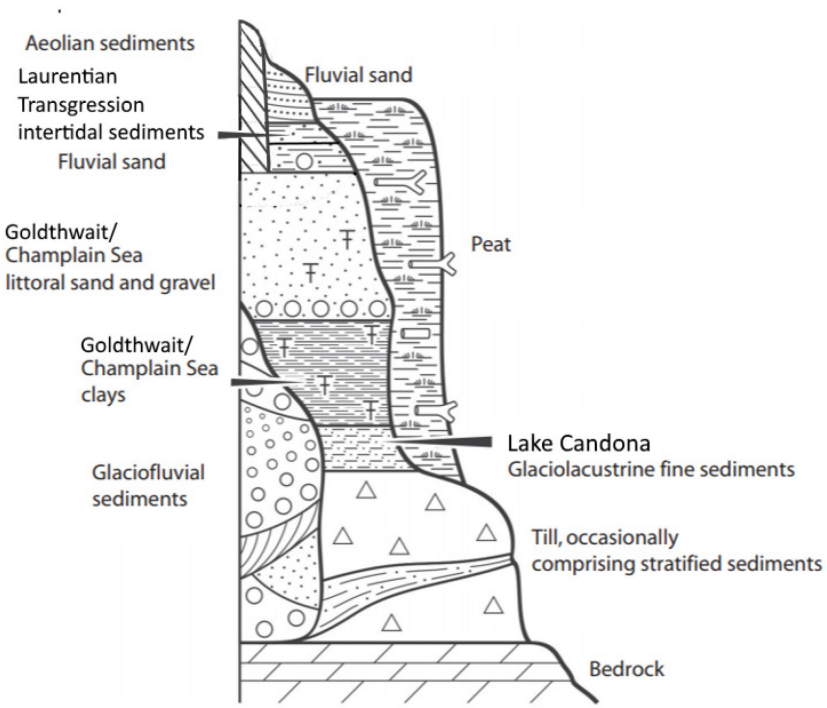

Figure 2.3 : Conceptual stratigraphic sequence of the study area (modified from Tremblay *et al.* (2010))

During the Late Wisconsinan glaciation, the eastern LIS is widely assumed to have advanced across the St. Lawrence valley toward the south and south-east, as its flow was mainly controlled by outflow from the core accumulation areas of the ice sheet. This event deposited a till blanket

over the study area. Its thickness depends on local ice flow dynamics, bedrock topography and other factors. Sometime earlier during the Middle Wisconsinan, the ice sheet had retreated significantly, allowing the development of proglacial lakes in the Appalachian uplands (McDonald and Shilts, 1972; Shilts and Caron, 2018). This event (Lake Gayhurst) is recorded through a series of varves that can often be found between till layers.

Following the Last Glacial Maximum (LGM), but prior to deglaciation of the St. Lawrence Valley, regional ice flow was disrupted and reoriented towards northeast as an ice stream, called the St. Lawrence Ice Stream (SLIS), formed in the St. Lawrence Valley depression downstream of Québec City (Parent & Occhietti, 1999). During this event, regional thinning of the LIS also led to the deglaciation of the southern part of the St. Lawrence Lowlands, where large proglacial lakes developed. The largest of these was Glacial Lake Candona, which occupied a large area in eastern Ontario and western Québec as its drainage route through the St. Lawrence Valley was blocked by retreating Laurentide ice (Parent & Occhietti, 1988, 1999). This episode is recorded through the presence of fine-grained glaciolacustrine sediments in most valleys of southeastern Quebec. Concomitantly, the post-glacial isostatic depression and global sea level rise allowed marine waters to dismantle the remains of the ice stream in the estuary and invade the valley, thus forming marine water bodies known as the Goldthwait Sea and the Champlain Sea, covering the areas respectively downstream and upstream of Québec City (Elson, 1970). The post-glacial sea in the St. Lawrence Valley allowed the deposition of a wide range of sediments, from deep-sea clay facies to regressive sandy beaches. Major subglacial meltwater pathways formed tunnel channels and eskers, which commonly fed outwash deltas as they reached the sea. The marine regression was marked by a major relative sea level (RSL) oscillation during which the sea level fell several meters below present for one to two thousand years and then rose back to about 12 m ASL at about 6500 ^{14}C years BP (Dionne, 1988, 1997). This event was recorded at several locations along the south shore of the St. Lawrence Estuary and referred to it as the Laurentian Transgression. For a more extensive recent review of the deglaciation of the St. Lawrence Valley, the reader is referred to Occhietti *et al.* (2011).

While a wide range of surficial units were mapped in the region, the marine basinal and littoral sediments constitute the dominant and most common units. Poorly drained areas are occupied by

large peatlands covering fairly thin silty clay basinal units. In the Appalachian foothills, littoral and sub-littoral sediments commonly grade laterally into deltaic sand bodies emplaced at the mouth of the main rivers emerging in the sea, notably at Saint-Lambert-de-Lauzon (Chaudière River) and Saint-Raphaël (Rivière du Sud). In valleys where terraced deltaic bodies are not present, the glacial sediment deposited earlier (generally till) are incised by streams flowing north towards the St. Lawrence River. Above the marine limit, fluvial patterns tend to be more orthogonal, as the drainage networks are mainly controlled by regional bedrock structures. The sediment thickness over the Appalachian bedrock is marked by abrupt variations associated with the presence of strike ridges.

2.4.1 Bedrock structural landforms

The study area is underlain by two geological provinces, the St. Lawrence Platform and the Appalachians. The subhorizontal sedimentary rocks of the Platform are Cambrian and Ordovician in age and rest unconformably over the Grenville Precambrian basement (Globensky, 1987). The Appalachians consists mainly of sedimentary rocks (sandstone, quartzite and shale, commonly metamorphosed to slates) as well as some volcanic rocks, weakly metamorphosed and deformed during the Taconic and Acadian orogeny. Logan's Line, a regionally significant thrust fault, separates the autochthonous rocks of the Platform from the Appalachian allochthonous (St. Julien & Hubert, 1975). A typical Appalachian quartzite outcrop is shown in Figure 2.4.

Figure 2.4 : A quartzite outcrop surrounded by farmlands in Saint-Germain-de-Kamouraska (Lat/long coord.: 47.6880, -69.7119).

Bedrock units (R) are undifferentiated on the map. Outcrops with a surface area of less than 500 m^2 have not been digitized nor mapped as units (polygons) in order to avoid producing an overcrowded map; isolated bedrock outcrops are thus reported as cross marks on the map, and can be expected in areas mapped as till veneer.

2.4.2 Glacigenic sediments

The regional till (T) was emplaced by successive glacial movements advancing from three main directions (LaSalle *et al.*, 1985; Rappol, 1993; Veillette *et al.*, 2017): (1) from the north-west towards the south-east (main LIS flow), (2) from the south toward the north (Appalachian ice cap/ice-flow reversal) and (3) by ice advancing northeastward along the St. Lawrence Valley (SLIS phase). The till unit forms a blanket (Tc) over a considerable part of the study area, and usually thins out (Tm) around major bedrock outcrops. Elongated, parallel till ridges associated with the St. Lawrence Ice Stream (SLIS) are also present in the area (see Figure 2.5).

Figure 2.5 : Typical surficial till landscape with elongated, convex hills associated with the St. Lawrence Ice Stream (SLIS), St-Alexandre-de-Kamouraska (Lat/long coord.: 47.6658, -69.5983).

Below the upper limit of the Goldthwait Sea, series of beach ridges made of extensively reworked, wave-washed till with high sand and pebbles content (Tr) can be observed and mapped on moderately sloping hillsides. This common transition is illustrated at Figure 2.6. Such wave-washed facies are often characterized by the presence of isolated metric boulders near the level of

maximum submergence. Melt-out facies (Tf) occur sporadically above marine limit in places where buried ice masses were covered by glacial debris during melting.

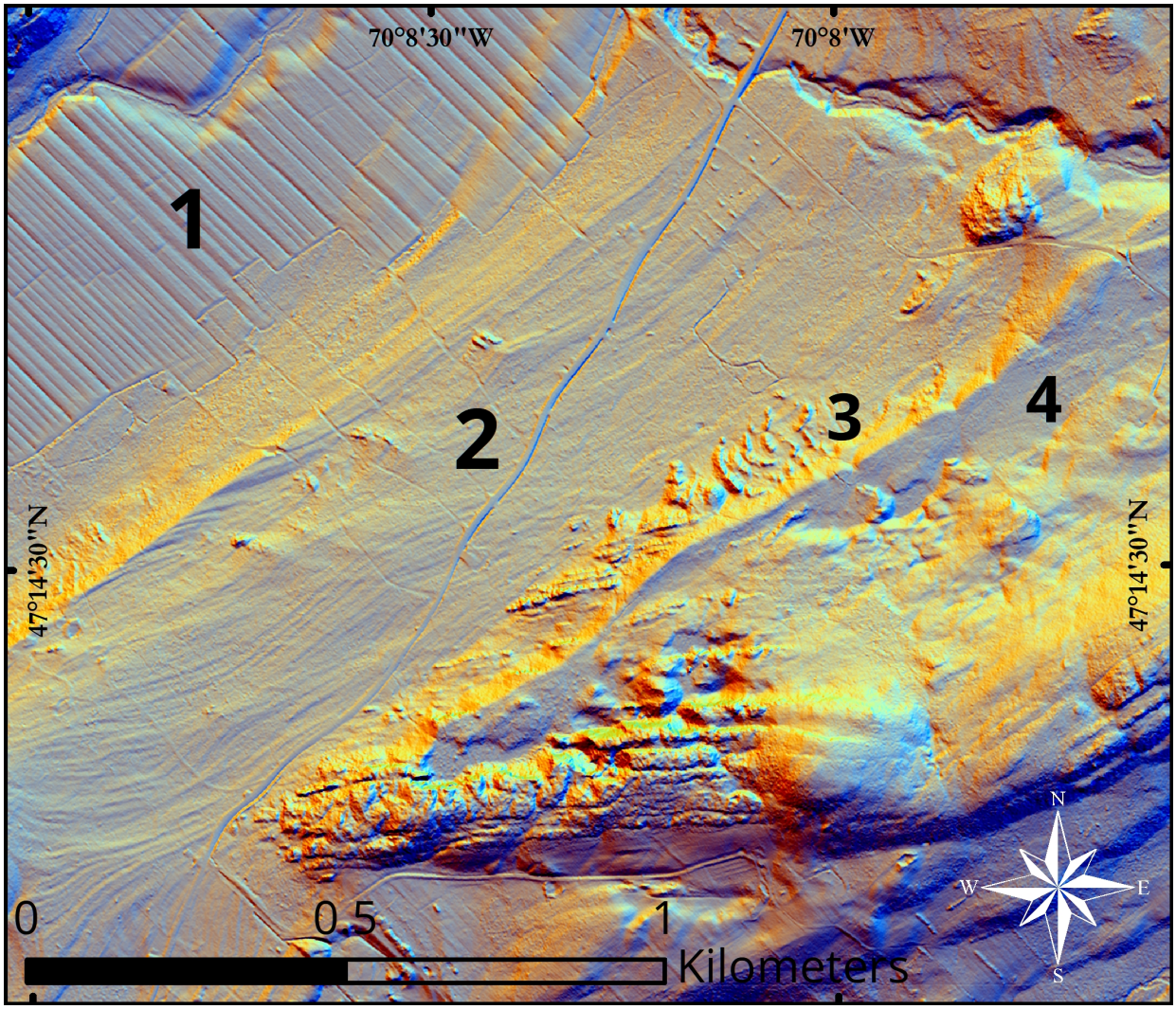

Figure 2.6 : Multishaded color DTM showing the transition between marine offshore facies (1), marine littoral (2), reworked and gullied till (3), and non-reworked till (4) near a bedrock outcrop in Ste-Louise. The maximum submersion limit can be clearly **seen between zones 3 and 4, at around 158 mASL locally.**

2.4.3 Marine and glaciomarine sediments

Marine and glaciomarine sediments (M) are associated with the Goldthwait Sea and Champlain Sea episodes. Massive grey clays and clayey silts (GMa) were mainly deposited in relatively deep water and are usually sparsely fossiliferous, containing several species typical of the actual Arctic Sea conditions (mainly *Macoma calcarea*, *Portlandia arctica* as well as other washed-in species such as *Hiatella arctica* and *Macoma balthica*; see Lortie & Guilbault (1984)). Littoral and pre-

littoral marine deposits (GMb) locally overlie the basinal fine-grained facies and are very abundant, especially between l'Islet and Sainte-Anne-de-la-Pocatière. Littoral features are organized as myriads of small regressive beach ridges (Figure 2.7), tombolos and coastal terraces of variable amplitude, generally parallel to each other. Prodeltaic and deltaic marine sediments (GMd) form perched sandy deltas that were emplaced at the mouth of sediment-laden, high discharge rivers flowing into the Goldthwait Sea. The most notable ones are located near St-Raphaël (Rivière du Sud) and south of l'Islet (Bras St-Nicolas River). Intertidal terraces (GMi) created during the Laurentian Transgression event are present at Saint-Michel-de-Bellechasse (Boyer River), Saint-Vallier (Rivière des Mères), and Montmagny (Rivière à Lacaille and Rivière du Sud). These intertidal units consist of organic-rich muds deposited in intertidal or subtidal zones in sheltered embayments. Marine sediments of the Champlain Sea (Md, Mb, Ma), upstream of Québec City, were mapped in similar fashion.

A precise and continuous cartography of the submergence limit of the Goldthwait and Champlain seas was carried out by identifying raised beaches, barren boulders, and various other littoral features near the washing limits. Field verification was carried out systematically to confirm the interpretation. On a few rare occasions, the submergence limit was mapped slightly outside the available LiDAR coverage using high-resolution aerial imagery. Beaches and other near-shore features can be found at elevations as high as 180 m ASL in the southwest part of the study area (Lotbinière), while the maximum elevation decreases almost linearly northeastward to reach a maximum elevation of 158 m ASL near Rivière-Ouelle.

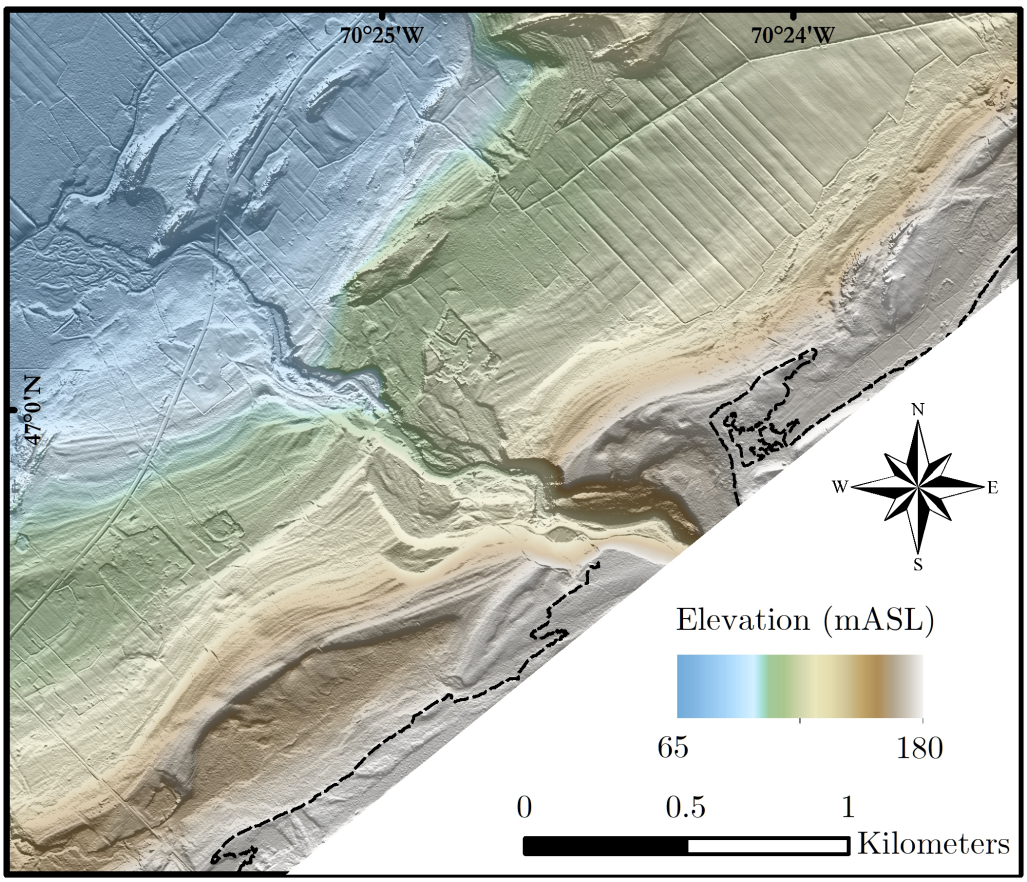

Figure 2.7 : Beach ridges built up against a bedrock ledge near the maximum submersion limit, south-east of Cap St-Ignace Station. The maximum submersion limit is shown as a dashed black line. The white area in the bottom right corner of the map is outside the LiDAR coverage zone.

2.4.4 Glaciofluvial sediments

Glaciofluvial sediments (G) were deposited by meltwater in various settings during the last deglaciation, and are mostly found at higher elevations in the Appalachian Piedmont zone, most notably near the outlets of the Bras St-Nicolas River in l'Islet, Morigeau River (a Rivière du Sud affluent) in St-Pierre-de-la-Rivière-du-Sud, and upstream of the St-Raphaël delta, on Rivière du Sud. In the Piedmont zone, where the bedrock topography is highly variable, subaqueous (Gs) and subaerial (Go) outwash sediments often occupy valley bottoms and can be locally covered by glaciomarine (sometimes diamictic) sediments. Ice-contact deposits (Gx), deposited above or next to the ice margin, can be found all along the Appalachian Piedmont zone.

2.4.5 Alluvial and aeolian sediments, peatlands and landslide deposits

Peatbogs (Ot) and swamps (Om) are the two kinds of peatlands (O) that occupy poorly drained areas in the study area. In areas where drainage is more efficient, alluvial deposits (A) can be found as terraces (At), modern floodplains (Ap), and ancient estuarine sediments (Ae). Large sandy dunes (Ed), locally forming spectacular longitudinal ridges, can be found in the Lotbinière area. In areas of slope instability, scree or talus deposits (Ce) can be found, as well as landslide deposits (Cg) or other mass-wasting deposits (C). Two large, previously unmapped, landslides have been identified in St-Philippe-de-Néri. Both extend over a quasi-circular area of about 0.2 km^2, with the crown and toe of the landslide separated by about 400 m.

2.5 Discussion and conclusion

An area of about 4 305 km^2 was mapped using a hillshaded LiDAR DTM as a base map. The results of this surficial geology mapping are presented on an A0 format map. As the surficial geology maps are generally published at a scale of 1:50,000 in regions of southern Canada, and also due to journal limitations, the map is presented at this reference scale. However, the actual delineation and interpretation of the mapped units and features were carried out at scales ranging from 1:1,000 to 1:10,000. Therefore, for detailed applications, the authors suggest referring to the included polygon shapefiles and a view scale of 1:20,000, at which the map is very reliable. A considerable emphasis was placed on accurately identify bedrock outcrops, as it adds constraints in our depth-to-bedrock map, an important component in any regional hydrogeological survey. This cartography effort produced a highly detailed and reliable surficial geology map of a precision level that was hitherto impossible to reach by traditional air photo interpretation techniques. It can be used for land use planning, potential geo-hazard zones identification, and resource management.

There are considerable differences between this new map and older maps of the same area. While there are very few fundamental differences in interpretation between this map and older maps of the Cotes-du-Sud and Kamouraska areas (Lee, 1962; LaSalle *et al.,* 1977, 1980b; Martineau, 1977; LaSalle, 1978), the differences stem mostly from the level of detail. The new map makes many new distinctions between units of the same broad origin, particularly regarding units of glacial

and marine nature. New landslides are identified thorough the region, particularly in the vicinity of the Boyer River. The newer "PACES" maps (Daigneault *et al.,* 2014) covering the Lotbinière region are overall quite similar to our work for the overlapping areas. The main exception to this is the fluvioglacial deposits (moraines) that we interpret in the areas of Lyster, as well as around the Du Chêne River. These ridges are interpreted as raised beaches in the PACES maps. While we acknowledge most surficial cover in the Lotbinière area indeed show signs of marine reworking near the surface, auger holes drilled during the field validation campaign confirmed the glacial origin of at least some of these ridges.

A major advantage of the LiDAR-based method resides in the fact that it allows the mapper to depict more accurately the surficial geology of heavily wooded areas, a common situation in eastern Canada. In areas of dense forest cover, the proportion of laser reflections penetrating the canopy and hitting the ground is effectively much lower than in deforested areas. Nonetheless, it is generally enough to reconstruct a satisfying model of the surface, allowing the visualization of microtopographic features that would have been completely invisible on conventional aerial photographs, especially when these are taken during the spring or the summer at the time of full-canopy development. Another advantage of using a LiDAR-derived DTM over aerial photography for this task is in the digital nature of the data itself. The creation of a regional LiDAR-based DTM and other derivatives allows the mapper to create a spatially continuous grid that can be investigated readily at multiple scales, exported and shared to other formats, and reviewed directly by other experts who may be less accustomed to stereoscopic analysis.

The rationale for interpreting a high resolution DTM is that the geologist can interpret the geology in real time using a single medium, with both the relative topographical position of morphological features (as with photo-interpretation) and the ground texture (in terms of smoothness, roughness, or patterns) being displayed at the same time. In glaciated terrains, the surface texture is a function of both the nature of the surficial material itself and the characteristics of the depositional process. In this study area, zones covered by till show a rough, irregular texture largely due to the presence of metric to sub-metric boulders while surfaces underlain by marine clays appear as smooth and continuous flat surfaces. The major assumption while doing the actual cartography is that neighboring cells on the raster grid showing the same texture most likely belong to the same

ensemble, and that changes in texture and elevation break lines most likely correspond to unit boundaries. A few points should, however, be taken into account with regards to this most basic assumption. Several factors can influence terrain texture to a certain degree. Anthropogenic activities like intensive agriculture (including tillage, land leveling, irrigation, etc.) on low-relief littoral terrains have the effect of smoothing out subtle relief elements like small beach ridges and littoral spits, making them difficult to distinguish from basinal facies. In addition to these morphological considerations, the variable density of ground returns in a LiDAR dataset has a significant effect on terrain texture of the derived DTM. An insufficient amount of ground returns, or even a local area where the ground return density is significantly lower than the regional average, can create an exaggerated roughness in the DTM that could be wrongly interpreted as a 'rough' surficial geology. In order to assess the impact of the locally varying density of ground returns, it is useful to compute a ground return density grid that can identify areas where a low density may be problematic.

Finally, special care should be exerted when processing the raw laser point cloud data. Numerous airborne LiDAR classification algorithms are available, both in open-source and commercial environments. Several commercial "black box" type software suites are pre-programmed to smooth out and filter out noise in the data. In surficial geology applications, terrain texture and patterns are of great importance. Special care should be taken around the generation of the working rasters, including the DTM and its derivatives. The smoothing of the DTM surface can create undesirable results, as "noise" interpreted the LiDAR data sometimes correspond to real world terrain roughness. In the present study, it was noted that small to medium-size erratic boulders were often classified as "near ground" objects in the original classification of the LiDAR datasets that were made available to us. Since these returns were classified as "non-ground", they were excluded from the creation of the DTM. Thus, the texture associated with those particular features would not have been included in the subsequently generated DTM and would have been replaced by smoothed out zones. Considering the technical complexity associated with the processing of laser point-cloud data, the best practice is to compare the results of different classification algorithms and their associated parameters, test them on a well-known (ground truthed) terrain and then use the most appropriate settings and algorithms to produce a DTM.

Over the last few years, geologists have been using NASA Shuttle Radar Topography Mission (SRTM; NASA JPL (2013)) to map the geology of regions either semi-automatically – by using morphometric filters, object-recognition algorithms, machine learning or other classification methods - or manually by an interpretive process. While the recent Global 1 arc second dataset (SRTMGL1, 30 m ground cell size) is a considerable upgrade over previously available datasets, it is still too noisy to be used as a base DTM for geologic interpretation at scale below 1:100,000 in a geologically complex region such as the St. Lawrence Valley. This is convincingly illustrated in Figure 2.8, which provides a visual comparison of the St-Raphael delta by the following four datasets: (1) SRTMGL1-derived 30-meter shaded relief raster, (2) LiDAR-derived 1-meter shaded relief raster, (3) the previously available 1: 50 000 Quaternary map and (4) the new map prepared for the current publication.

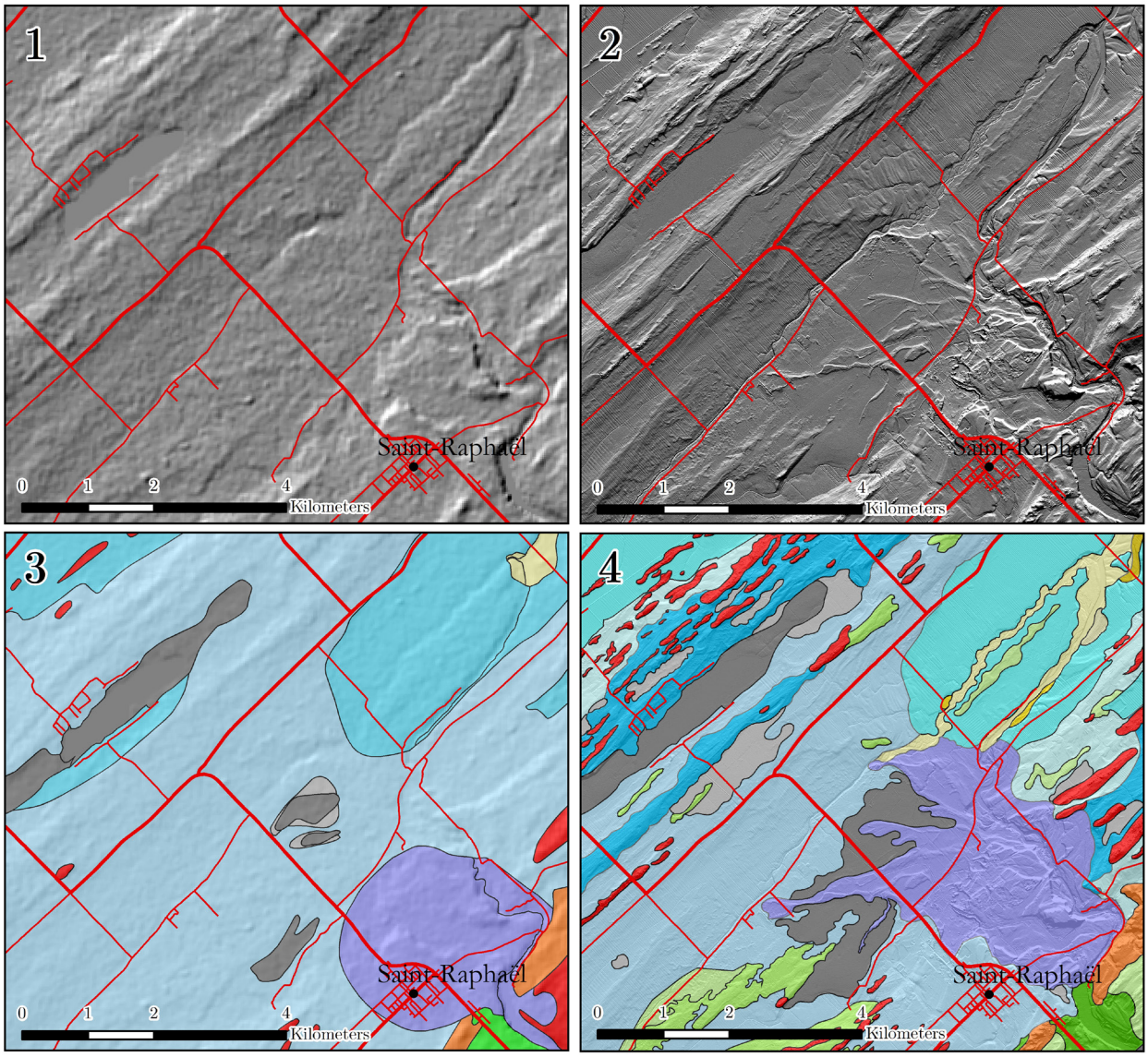

Figure 2.8 : Comparison of a traditional 1:50,000 scale surficial geology map versus the new map presented here, using the St-Raphael delta as an example: (1) Shaded relief image derived from NASA SRTM 1 arc-sec DSM (30 m). Some ridges are visible, but the topography appears smooth and uniform; (2) Shaded relief image derived from LiDAR (1 m). The image shows contrasting textures, structures and complex morphology for the same area; (3) Superficial geology map done by traditional aerial photographic interpretation (LaSalle *et al.*, 1980) ;(4) Superficial geology map interpreted with LiDAR-derived shaded relief image.

The Québec Ministry of Fauna, Forests and Parks (MFFP) has recently undertaken an effort to make basic derivatives of their LiDAR point cloud dataset public. It is expected that more Quaternary geology maps of southern Québec will be produced, revisited and revised using these datasets in the near future as Quaternary researchers become familiar with its potential. A LiDAR-derived DTM of this area, similar to the one produced for this study, is to be made publicly

available by the MFFP by 2022. Since this map was completed, the Québec Ministry of Fauna, Forests and Parks has released an elaborate guide to help a mapper identify typical southern Québec surficial deposits on LiDAR-derived hillshaded relief (Dupuis *et al.,* 2017).

2.6 Acknowledgements

This research was supported by the Fonds de recherche du Québec - Nature et technologies (FRQNT) doctoral scholarship of Guillaume Légaré-Couture and by funds from the Projet Chaudières-Appalaches of the PACES program of the Ministère du Développement durable, de l'Environnement et de la Lutte contre le changement climatique, led by Dr. René Lefebvre (INRS-ETE). We thank the Ministère who provided us with the LiDAR dataset used in this study.

3 Article 2: 3D geological model and regional hydrostratigraphy of the south shore of the St. Lawrence Mid-estuary, Québec, Canada

Modèle géologique 3D et hydrostratigraphie régionale de la rive sud de l'estuaire moyen du fleuve Saint-Laurent, Québec, Canada

Auteurs :

Guillaume Légaré-Couture[1], Michel Parent[2] & René Lefebvre[1]

[1] Institut national de la recherche scientifique – Centre Eau Terre Environnement (INRS-ETE), Québec, Canada

[2] Commission géologique du Canada, Ressources naturelles Canada, Québec, Canada.

Titre de la revue ou de l'ouvrage :

Canadian Water Resources Journal

À soumettre en 2021

Contribution des auteurs :

Le premier auteur est responsable du développement de la méthodologie, de l'analyse, la création du modèle géologique 3D, ainsi que de la rédaction de l'article.

Les deuxièmes et troisièmes auteurs ont contribué à la planification du travail, aux travaux sur le terrain ainsi qu'à la révision du manuscrit.

Lien entre l'article ou les articles précédents et le suivant :

Dans le premier article, la géologie de surface est étudiée et cartographiée avec détail. Le deuxième article propose d'intégrer ces nouvelles informations à des observations terrain, des forages et des travaux de géophysique afin de créer un modèle géologique 3D précis respectant la géologie cartographiée au premier article.

Résumé :

Dans l'étroit corridor de la rive sud de la vallée du Saint-Laurent, entre Lotbinière et Rivière-du-Loup, les événements glaciaires et post-glaciaires du Wisconsinien supérieur ont favorisé le développement d'une séquence géologique complexe dont l'architecture est largement tributaire de la topographie du substratum rocheux et de l'espace d'accommodation. L'objectif de cette étude était de développer un modèle 3D des dépôts du Quaternaire afin de définir la séquence géologique et de modéliser la relation géométrique entre chaque unité afin de créer un modèle "*common earth*" cohérent et sans discontinuités pouvant être utilisé dans d'autres applications comme l'hydrogéologie régionale et la modélisation de l'écoulement des eaux souterraines. Pour ce faire, nous compilons les données géologiques, géophysiques, hydrogéologiques et paléofauniques existantes et nouvelles à partir d'une approche géomatique pour construire le modèle et le contraindre en utilisant des règles topologiques dérivées d'une carte des dépôts meubles à haute résolution basée sur un levé LiDAR. Le modèle 3D final est composé de 12 couches, de la surface du substratum rocheux jusqu'à la surface naturelle du terrain, qui sont illustrées par des cartes d'épaisseur, des coupes géologiques et une méta- coupe conceptuelle présentant les relations lithostratigraphiques régionales, les contextes hydrogéologiques ainsi que l'interprétation génétique de chaque formation. L'évaluation de l'architecture sédimentaire du secteur et l'élaboration du modèle 3D ont permis de mettre en évidence plusieurs caractéristiques géologiques insoupçonnées, notamment d'importantes unités d'argile situées au-dessus de la limite de la mer postglaciaire ainsi que des unités sableuses locales à potentiel aquifère associées à la transgression Laurentienne et/ou à des événements transgressifs mineurs ultérieurs. Bien qu'ils aient une extension latérale limitée, ces nouveaux aquifères trouvés dans cette étroite zone côtière à vocation agricole

pourraient avoir des retombées positives pour les communautés locales puisque les puits forés dans le substrat rocheux contiennent souvent des eaux saumâtres.

Abstract :

In the narrow corridor of the south shore of the Lower St. Lawrence River valley, between Lotbinière and Rivière-du-Loup, glacial and post-glacial marine events during the Late Wisconsinan led to the formation of a complex geological sequence whose architecture is largely controlled by the bedrock topography and by accommodation space. The objective of this study was to develop a 3D model of the Quaternary deposits in order to define the geological sequence and model the geometric relationship between each unit in order to create a seamless "common earth" model to be used in other applications such as regional hydrogeology and groundwater flow modeling. We do this by compiling existing and new geological, geophysical, hydrogeological and paleofaunal data in a GIS-based approach to build the model and constrain it by using topological rules inferred from a high-resolution surficial geology map available for this area. The final 3D model consists of 12 layers, from the bedrock surface to the ground surface, which are illustrated as thickness maps, cross-sections and on a conceptual meta- cross-section reviewing the regional lithostratigraphic relationships, sequence stratigraphy, hydrogeological contexts as well as the genetic interpretation of each formation. The assessment of the depositional architecture in the area and the development of the 3D model helped highlight several unsuspected geological features, including significant clay units located above the maximum limit of submergence by the post-glacial sea as well as potential local sandy aquifer units associated with the Laurentian Transgression and/or subsequent minor transgressive events in the coastal zone. Although of limited lateral extent, new aquifers found in this narrow, agricultural coastal zone could provide several benefits to local communities since wells are drilled into the bedrock often produce brackish groundwater.

3.1 Introduction

While the main geomorphological features of the St. Lawrence Valley are largely inherited from pre-Quaternary erosion, Pleistocene glaciations played a key role in the development of many secondary landscape features. The scarcity of sediments preceding the last glaciation (LaSalle,

1984; Lamothe *et al.*, 1992) is a clear indication that the last glacial cycle was a particularly erosive one. This last regional advance of the Laurentian Ice Sheet (LIS) was followed by a warmer period during which the ice sheet thinned considerably, leading to the formation of a major northeastward flowing ice stream, called the St. Lawrence Ice Stream (SLIS; Parent & Occhietti , 1999). While the onset zone of the SLIS migrated towards the interior of the LIS, a calving bay in which the ice stream discharged formed in the St. Lawrence Estuary, a reentrant of the Atlantic Ocean known as the Goldthwait Sea. The timing of the SLIS development and of the coeval marine incursion remains somewhat imprecise, notably because of uncertainties concerning the marine reservoir effect on radiocarbon dates from marine shells (Occhietti & Richard, 2003; Dyke, 2004). As the crust recovered from its isostatically depressed state, relative sea level (RSL) continued to fall and terrestrial conditions replaced the glaciomarine and marine conditions in the Lower St. Lawrence Valley.

Over the last century, Quaternary deposits of the northern U.S. and Canada have been used for an increasing number of human activities, such as sand and gravel extraction, waste disposal sites and water production infrastructure, all of which are known for their potential impact on groundwater resources. The regional groundwater characterization research program taking place in southern Québec in the last few years has highlighted the fact that understanding the complex 3D architecture of the Quaternary deposits as well as the topography of the underlying bedrock is an essential part of any regional groundwater characterization project (Ross *et al.*, 2005; Larocque *et al.*, 2018). As the medium between the surface and subsurface, Quaternary deposits exercise a major control on confining conditions, recharge and vulnerability of the underlying aquifers, whether they are made up of granular material or fractured rock. At a regional scale, in complex post-glacial terrains like the St. Lawrence Valley, precise maps of the surficial geological and bedrock topography are usually sufficient to model regional flow. However, at smaller scales, local flow and transport processes cannot be accurately modeled without a 3D model of the surficial and bedrock substrate. Accurately representing the extent, limits and transition zones of subsurface aquifers and aquitards remains a considerable challenge, even with recent technological advances. The main obstacles in building a seamless, regional 3D geological/hydrogeological model in the context of a regional hydrogeological characterization project can be classified in three (3)

categories: 1) access to quality geological data; 2) storage and interoperability so that the geological data is accessible and usable by all team members; 3) time constraints.

The objective of this study is to build a seamless 3D geological model of the Quaternary deposits of the region to improve our understanding of the spatial relationship between geological units, and contribute to a common earth model useful in a variety of different applications, including regional hydrogeology.

This paper presents a part of the effort made towards that goal as part of the hydrogeological characterization project of the Chaudière-Appalaches region conducted by the Institut national de la recherche scientifique – Centre Eau Terre Environnement between 2012 and 2015 (Lefebvre *et al.*, 2015), as a part the Groundwater Knowledge Acquisition Program (PACES) of the Québec Ministère de l'Environnement et de la Lutte contre les changements climatiques (MELCC).

3.2 Study area

The study area is located in southern Québec, Canada. It covers an area of 5689 square kilometers on the south shore the St. Lawrence River valley between the cities of Plessisville (Centre-du-Québec region) and Rivière-du-Loup (Bas-Saint-Laurent region) along a SW-NE axis. Its core region is the Appalachian piedmont or foothills, between the St. Lawrence River and the edge of the Appalachian uplands, up to an elevation of about 200 meters. The regional setting of the study area is shown at Figure 3.1. The total population (2016) is 359 805 inhabitants, distributed into three urban centers (Lévis, Plessisville and Rivière-du-Loup) and multiple sparsely populated towns and villages. The part of the study area closest to the St. Lawrence River is mostly occupied by farmlands, whereas the areas closer to the Appalachian uplands are more forested. From a physiographic point of view, the area of interest lies mainly in the Appalachians foothills, except for the Lotbinière area (south-western part of the map) which is located in the St. Lawrence Lowlands. The main rivers (Chaudière, Etchemin, du Sud, Ouelle, du Loup) flow generally from south to north but their orientation turns to northeast as they approach the St. Lawrence Estuary.

The Appalachian foothills are underlain by of an extensively deformed nappes consisting of sedimentary (sandstone, shale), volcanic and metamorphic (schist and quartzite) rocks, while the

St. Lawrence Lowlands are characterized by flat-lying sedimentary Paleozoic rocks. The bedrock in both regions is overlain by variable thickness of Quaternary deposits.

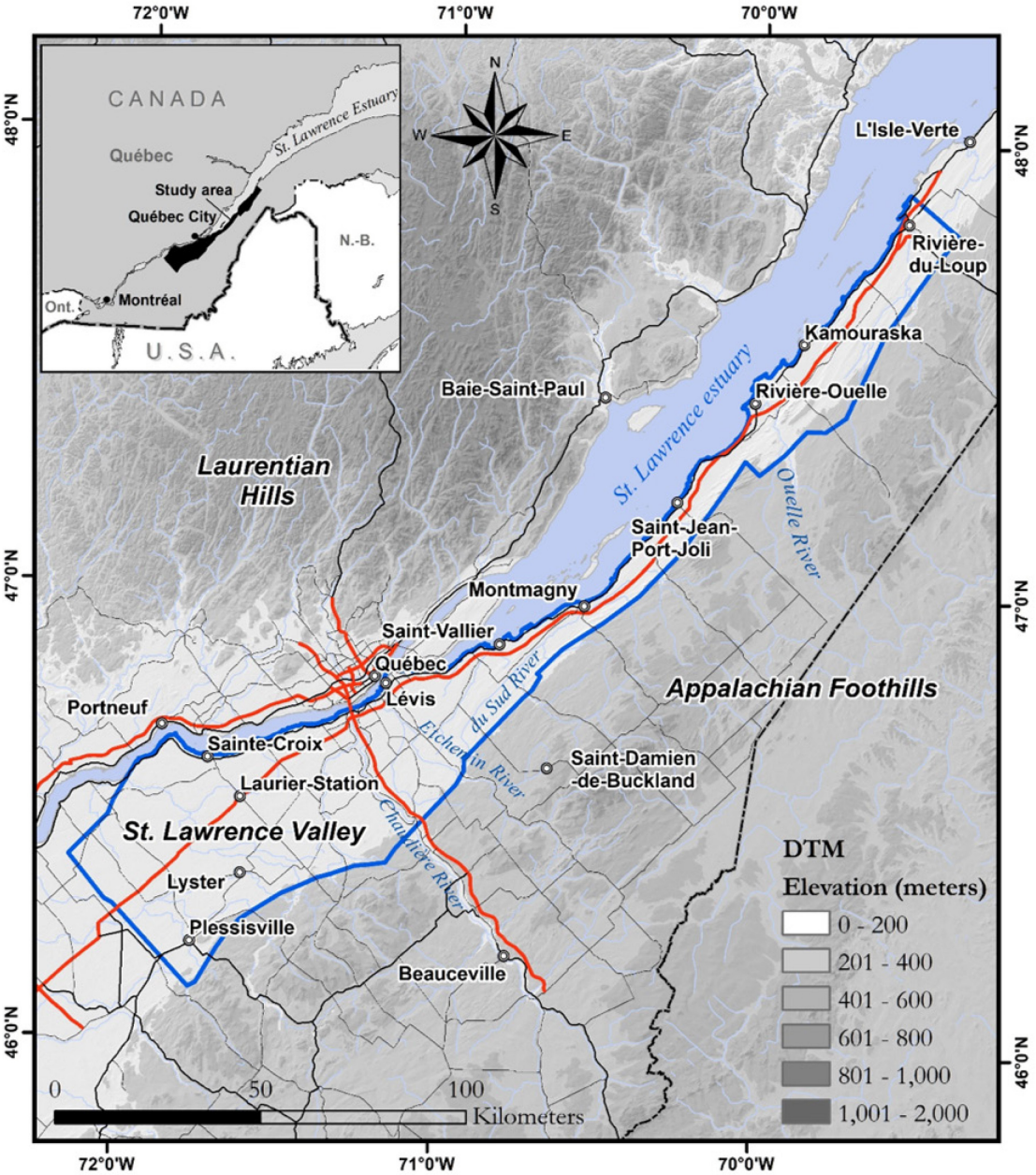

Figure 3.1 : Location of the study area in the Appalachian Foothills.

3.3 Paleogeography and stratigraphy of the St. Lawrence Valley and Estuary

The area of interest has a complex Quaternary stratigraphy. The Late Quaternary events are summarized in Table 3.1 and detailed in the following section.

Table 3.1 : Quaternary chronology, associated events and simplified regional stratigraphic synthesis.

<table>
<tr><th rowspan="2">Epoch</th><th rowspan="2">Stage</th><th rowspan="2">Events</th><th rowspan="2">Age (ka)</th><th rowspan="2">Marine Isotope Stage</th><th>St. Lawrence River Middle-Estuary</th><th>Central St. Lawrence Valley</th><th>Lower Chaudière Valley</th></tr>
<tr><th>(Dionne & Occhietti, 1996)</th><th>(Lamothe, 1989; Lamothe et al., 1992; Parent & Occhietti, 1999)</th><th>(Gadd, 1971; Normandeau , 2010; Caron, 2013)</th></tr>
<tr><td>Holocene</td><td colspan="2">Aeolian activity
Laurentian Transgression and sea-level fluctuations
Lacustrine and fluvial sedimentation, free drainage period
Marine submergence</td><td rowspan="6">10

23

65

80

125</td><td>1</td><td>Laurentian Transgression silts
Goldthwait Sea clay, silt and sand</td><td colspan="2">Post-glacial sediments
Champlain Sea clay, silt and sand</td></tr>
<tr><td rowspan="4">Late Pleistocene</td><td>Late Wisconsinan</td><td>Glaciolacustrine phase (deglaciation)
Gentilly/Lennoxville glaciation</td><td>2</td><td>Glaciomarine stony clay
Younger till
St-Antonin Moraine
Gentilly Till</td><td>Gentilly Till</td><td>Lennoxville Till</td></tr>
<tr><td>Middle Wisconsinan</td><td>Glaciolacustrine phase (partial deglaciation)</td><td>3</td><td rowspan="3">Ile aux Coudres formation</td><td rowspan="2">St-Pierre sediments
La Pérade Clay
Lévrard Till
Deschaillons Varves</td><td>Gayhurst Formation</td></tr>
<tr><td>Early Wisconsinan</td><td>Laurentide glaciation</td><td>4</td><td>Chaudière Till</td></tr>
<tr><td>Sangamonian</td><td>Free drainage, lacustrine and fluvial sedimentation</td><td>5</td><td>Lotbinière Sands</td><td>Massawippi formation</td></tr>
<tr><td>Middle Pleistocene</td><td>Illinoian</td><td>Glaciation</td><td></td><td>Bécancour Till</td><td>Johnville Till</td></tr>
</table>

3.3.1 Pre-Wisconsinan (1.8 Ma BP – 80 ka BP)

Observable geological units in the St. Lawrence Valley predating the Wisconsinan glaciation are scarce and of limited lateral extent, which suggests that the previous Illinoian glacial stage (191 ka - 130 ka) was very erosive. The first recorded evidence of glacial activity in the sector is now assumed to date back to the Illinoian and is represented by the characteristic brick-red Bécancour Till (Fulton *et al.,* 1986). This till contains both igneous and metamorphic elements characteristic of Canadian Shield provenance. The main ice flow direction from this event is recorded as NNW to SSE (Lamothe, 1985).

The Chaudière River valley region contains traces of three major glacial advances: the Johnville (Illinoian), the Chaudière and Lennoxville glaciations, both Wisconsinan in age. Johnville Till is rarely exposed in cross-section. It is a compact and clast-rich diamicton seemingly deposited by ice advancing from the northwest. The Johnville Till is overlain by the Massawippi alluvial sediments, which were deposited in a context of free drainage possibly similar to the current St. Lawrence system. Pollen found in organic sediments dated $>$ 55 ka BP obtained by McDonald & Shilts (1971) suggests a boreal forest climate. The lower part of the Massawippi was possibly deposited in a climate as warm as the current one and may thus record a truly interglacial episode (McDonald, 1969; Matthews, 1987).

The Sangamonian Stage (130 ka - 80 ka), equivalent to Marine Isotope Stage 5 (MIS 5), is an interglacial stage characterized by a climate similar to the current one (Occhietti & Clet, 1989). There is evidence that a system of pro- and post-glacial lakes developed in the valley during the deglaciation; and not unlike during the ensuing Wisconsinan Stage, the isostatically depressed continental platform allowed marine waters to invade the valley (Guettard Sea, Occhietti *et al.* (1995)), leaving behind the Rivières-aux-Vaches silts. A post-glacial fluvial system developed in the St. Lawrence Valley as a result of continental uplift; this is recorded by deposition of the Lotbinière Sands in the Mauricie/Portneuf and Lower Chaudière regions, as well as the Île-aux-Coudres Formation in the St. Lawrence Estuary (LaSalle, 1984).

3.3.2 Lower and Middle Wisconsinan (80 ka BP – 23 ka BP)

During the Lower Wisconsinan, the onset of glaciation is marked by deposition of a succession beginning with the Deschaillons Varves (associated with Lake Deschaillons), the Lévrard Till (Nicolet Stade), the La Pérade clays (Cartier Sea) and the Saint-Pierre Sediments (Gadd, 1971; Hillaire-Marcel & Page, 1981; Lamothe, 1985, 1989; Occhietti *et al.,* 1996). The second till of the regional sequence is Chaudière Till, produced by an ice cap formed in the Appalachians. This maritime ice cap may have developed in Maine or New Brunswick independently from the Laurentide Ice Sheet. The measured flow directions point towards the west-southwest in general, and sometimes full south, probably as a result of a coalescence with Laurentide ice or a variation in the center of the outflow. This compact clay till occurs very commonly in Appalachian valleys. The end of the Chaudière glaciation is marked by a short warmer period when a significant portion of the southern Appalachians became ice free (McDonald & Shilts, 1971). The Middle Wisconsinan was marked by climatic fluctuations that induced changes in the spatial configuration of the ice margins, as shown in the Chaudière and Saint-François Rivers valleys, where proglacial lake sediments (Gayhurst formation) are observed (Shilts, 1981; Caron, 2013). During this period, an ice lobe presumably remained in the central St. Lawrence Valley, blocking the Appalachian drainage system and creating glacial lake Gayhurst. The exact duration of this episode is unknown, but a varve count by Shilts (1981) suggests a minimum duration of 4 ka.

The most recent and surface till of the Chaudière Valley is Lennoxville Till. This grey-brown to buff matrix-dominated glacial diamicton generally forms a thin cover and contains a considerable amount of flattened and angular local clasts typical of Appalachian rocks, but clasts of Shield provenance are also found. The presence of gneiss in the till generally indicates the proximity or presence of the Laurentians, while the occurrence of ultramafic rocks is indicative of Appalachian provenance (Thetford-Mines ophiolitic belt). McDonald & Shilts (1971) correlated the Chaudière Till / Gayhurst Formation / Lennoxville Till sequence with a single till in the St. Lawrence Lowlands, the Gentilly Till.

3.3.3 Late Wisconsinan (23 ka BP – 10 ka BP)

The deglaciation of southern Québec may be divided into three major phases: (1) the St. Lawrence Ice Stream phase (16.0 to 13.0 cal. ka BP), 2) the Younger Dryas (YD) (12.9-11.7 cal. ka BP; ca. 11-10 ^{14}C ka BP) and (3) the early Holocene deglaciation (Occhietti *et al.*, 2011).

In the Appalachians, ice marginal recession began around 18 ka and the rate of retreat was on the order of about 200 m/year (Parent & Occhietti, 1999). As the LIS thickness decreased in the gulf and estuary of the St. Lawrence, a major ice stream formed in the valley where the ice-flow direction shifted abruptly toward NE. As this ice stream discharged at a formidable rate (much like the present-day ice streams in Greenland and Antarctica; (Joughin *et al.,* 2018)) in this rapid ice flow corridor, the onset zone of the stream migrated quickly from north of the Gaspésie Peninsula and deeply into the LIS along the St. Lawrence Valley. As the onset zone of the ice stream migrated southwestward, the Goldthwait Sea incursion also progressed quickly in the valley. During this major ice flow event, ice thickness in the valley likely decreased to less than 1000 meters and may have been less than 500 meters at the time of the Champlain Sea incursion. (Parent and Occhietti, 1999).

Concomitantly, in the Appalachian foothills, major glaciofluvial systems were actively draining meltwater from the ice remaining over the Appalachian uplands. In Kamouraska, these drainage routes can be observed between St-Pacôme and Rivière-du-Loup, about 5 kilometers inland from the estuary. Near St-Antonin, a major morainic system, previously identified by Lee (1962) was emplaced as a depositional system built on the margin of a glacial lobe that readvanced and deposited a 'young till' in the Goldthwait Sea in a few localities, such as near L'lsle-Verte where stony marine clays were observed (Lee, 1962). Gadd (1964) connected the St-Antonin moraine with his "Highland Front Moraine", a much debated conceptual system thought to have controlled the invasion of the St. Lawrence Valley by the Champlain Sea and the drainage of the late glacial lakes (Parent and Occhietti, 1988, 1999. LaSalle *et al.* (1977a) and Rappol (1993) interpret the St-Antonin moraine as a series of time-transgressive feature emplaced successively along the margin of the calving bay of a dynamic ice front.

The coalescence of glacial lakes Memphrémagog, Vermont and Iroquois in the middle and upper St. Lawrence valley formed a large glacial lake, Lake Candona, named after the characteristic freshwater ostracod, *Candona subtriangulata*, present in its sediments (Parent & Occhietti, 1988, 1999; Vernal *et al.*, 1989; Rodrigues, 1992). The deglaciation of the Strait of Québec around 12.0 ka ^{14}C BP allowed the incursion of marine waters in the Central St. Lawrence Lowlands; this structural feature spatially separated the Goldthwait Sea (northeast of the Strait) from the Champlain Sea (Elson, 1970). This marine episode lasted about 2000 years. Marine deltas on the south shore of the St. Lawrence River can be observed up to 185 meters near Plessisville. There are three major phases in the history of the Goldthwait Sea. First, a glaciomarine phase extending between 12.0 ka ^{14}C BP and 11.6 ka ^{14}C BP, where the freshwater fauna of Lake Candona is replaced rapidly by fauna of very cold and saline water (Parent & Occhietti, 1999; Cronin *et al.*, 2012). The full marine phase is the second one and is usually recognized by the presence of bivalve mollusks like the *Hiatella Arctica* in its associated sediments. Marine conditions during this fully marine phase share many characteristics with the contemporary Arctic Sea, with a salinity around 30-33 ‰.

The cooling effect of the Younger Dryas (associated with the St-Narcisse Moraine on the north shore of the St. Lawrence River) does not seem to have had a notable influence in the salinity content of the Goldthwait Sea. By 10,9 ka ^{14}C BP, the St. Lawrence Valley is believed to be essentially free of ice (Richard & Occhietti, 2004). The Saint-Nicolas drift, a poorly sorted clayey diamicton containing shells of *Balanus hameri* dated 11,200 ± 170 BP (GSC-1476; LaSalle *et al.* (1977a)) can be observed in several sections around Québec City. This grey, compact and calcareous glaciomarine-type diamicton was reportedly deposited by a glacial re-advance in the Champlain Sea during a cold climate episode correlated to the Younger Dryas (LaSalle & Shilts, 1993). Thrust planes observed in the sediments suggest that ice was advancing from the north. LaSalle & Shilts (1993) also believed that these sediments were deposited in a deep marine environment and that the ice sheet still had to be anchored to the mainland during deposition of the Saint-Nicolas drift.

In the St. Lawrence Estuary, and only in a narrow coastal zone, Lee (1962) observed a sequence of two overlying tills ("older till" and "younger till") at Rivière-du-Loup, followed by the typical

marine sequence. Rappol (1993) found the same till sequence in an excavation site near Rivière-du-Loup, but here the two tills are separated by a marine clay unit. The authors consider the lower unit, a grey, texturally inhomogeneous till, to be associated with the SLIS. The scarcity of Precambrian pebbles suggests that the ice had been flowing over mostly Appalachian rocks during its deposition, but the source of ice was most likely located much further upstream in the valley. The upper till is considered to represent a post-SLIS readvance of Laurentide ice over early Champlain Sea and Goldthwait Sea sediments.

The latest paleogeographic phase of the post-glacial sea starts around 10.6 ka ^{14}C BP and is marked by the appearance of more temperate faunas, notably *Mya arenaria*.

3.3.4 Holocene (10 ka - present)

Lake Lampsilis is the freshwater water plane that followed the Champlain Sea when isostatic uplift from the deglaciation event drove saltwater out of the St. Lawrence Lowlands. Several levels of Lake Lampsilis have been identified in the St. Lawrence Lowlands (Macpherson, 1966; Lamarche, 2005, 2011), and are also associated with equivalents in the St. Lawrence Estuary. However, since their sediments share most of the characteristics of Champlain Sea sediments, stratigraphic boundaries are not easily determined. The Proto-St. Lawrence phase began after the drainage of the Lake Lampsilis and the building of its last terrace (Saint-Barthélémy) previously established at 8 ka ^{14}C BP (Lamarche, 2011).

Three major fluctuations have been observed in the middle St. Lawrence Valley by Lamarche (2005) and in the St. Lawrence Estuary by Dionne & Pfalzgraf (2001): sea level drops are suggested around 6000-7000 years, 4000 years and 1500 years, while high levels are identified around 5000 years, 3000 years and 1000 years. In the Cap-Rouge watershed, located on the north shore of the St. Lawrence Estuary (Québec), a low Holocene sea level is identified through a series of terraces and dated around 6300-6200 cal. BP (Verville, 2010). This low sea level was followed by the Laurentian Transgression event, where water level rose by several meters, filling with estuarine silts and sands the accommodation space created during the erosion phase of the previous low sea level. This combination of events created a series of very recognizable terraces at various locations along the St. Lawrence middle estuary.

3.4 Methodology

3.4.1 Data compilation

It is common knowledge that a 3D geological model is only as good as the data used to build it. Reliable and detailed stratigraphic information is needed in order to construct an accurate representation of the substratum. The compilation of existing information is an important step as it forms the basis of hydrogeological and geological knowledge of the area studied as part of a regional study. The collected data includes well groundwater depth values, stratigraphy data, rock depth values, groundwater geochemical data, hydraulic conductivity (K) and transmissivity (T) values. In some cases, compilation and processing work involved data reformatting, document and data digitization and other operations necessary to assemble usable datasets. The MDDELCC provided or facilitated the acquisition of the following databases for the study area:

- Hydrogeological Information System (SIH), owned by the MDDELCC

- Geotechnical database of the Ministère des Transports (MTQ) of Québec (including FORLOG, BDG and GEOTECH databases)

- Québec geomining information system (SIGEOM) of the Ministère des Ressources naturelles (MRN) du Québec

Other smaller sources were compiled in the database and are listed in Table 2.1. A total of 13806 boreholes were compiled for the entire study area.

Table 3.2 : Borehole data sources and statistics for the study area

Database	Data owner	Number of observations	Linear length of stratigraphic information (m)
Hydrogeological Information System (SIH)	Ministère de l'Environnement et de la Lutte contre les changements climatiques (MDDELCC)	12 915	97 216
FORLOG, BDG and GEOTECH	Ministère des Transports du Québec (MTQ)	76	1114
Québec geomining information system (SIGEOM)	Ministère des Ressources naturelles (MRN)	24	56.80
SIGPEG	Ministère des Ressources naturelles (MRN)	35	496
Borehole database	Canadian Geoexchange Coalition	60	462
New field data	Geological Survey of Canada	16	121
Various	Consultant reports	268	2 494
New field data	INRS-ETE	32	488
Various	Other public reports	121	459
Québec Groundwater Monitoring Network	Ministère de l'Environnement et de la Lutte contre les changements climatiques (MDDELCC)	6	60
Regional groundwater characterization project of the Communauté métropolitaine de Québec (PACES-CMQ)	Laval University	253	2 206

As this 3D geological modeling project was part of a greater groundwater characterization project, a network-accessible database common to all project members was created and used to store all the historical data as well as newly acquired field data. This reduces the risk of inconsistencies and redundancy of data that would be otherwise stored and shared on multiple disconnected mediums and helps keeping a master up-to-date version of the databases (Mallet, 2002; Ross *et al.,* 2005b).

3.4.2 Quality control and standardization of archival data

In a first step, all wells were systematically compiled, regardless of duplicates, which were fairly common in the compiled databases. One of the greatest difficulties encountered in compiling wells and boreholes was mainly related to the geographical location of some elements. Several reports dating back more than twenty years, before the more widespread use of GPS, did not include an exact location or presented imprecise handwritten plans. In those cases, the location of the elements of interest had to be inferred or estimated. As the compilation progressed, each data entry or observation was assigned a reliability rating to distinguish accurate data from loosely estimated data, and thus facilitate decision-making in the case of inconsistencies later in the modeling process. The identification of duplicates is difficult because of the inaccuracy of geographical coordinates, especially for older wells, but sometimes also because of imprecise stratigraphic descriptions. To solve most duplicate entry problems, the geographic locations of all boreholes were compared, and duplicate entries were flagged. Every borehole flagged this way was manually reviewed.

Borehole descriptions compiled this way from multiple databases using different data entry standards are most time-consuming and are too disparate to be integrated directly in any software used for the construction of a model. It is therefore necessary to simplify and standardize the geological nomenclature, and thus to associate an abbreviation code associated to grain size to each different material description encountered. Here we used the abbreviated code of the Québec Geoscience Centre (Parent *et al.*, 2008). It is often necessary during the model building and interpretation phases to go back to the original drilling report of a borehole (if available) in order to confirm or change the abbreviated geology code in areas of complex stratigraphy.

3.4.3 Strategy, software and constrains

Recently, regional 3D geological models have been built using a myriad of strategies, software and tools. The modeling tools used depend mostly of three (3) factors: the projected end use of the model, the time constraints, and the budget. In the present case study, we opted for a strict GIS-based approach instead of a 3D geological modeling environment. The drawbacks are obvious: general-purpose GIS software simply does not have the modeling, 3D visualization and editing

capabilities that proprietary geomodelling software like gOcad has (Mallet, 2002). However, using a proprietary software is costly, somewhat more time consuming, and more importantly requires a disconnection from the work team common network-accessible database. For this study, a hybrid strategy similar to those used by Ross *et al.* (2005a) and Lin *et al.* (2017) was used. 2D regional cross-sections were built perpendicular to the bedrock strike as well as the depositional setting of the majority of the Quaternary units as this allows to cut across most of the geological contexts as well as the most reliable boreholes. However, as is the case with most regional-scale studies, boreholes tend to be heavily clustered while other areas are almost blank. One of the solutions to this problem resides in the use of the surficial geology map. A high-resolution surficial geology map contains geometric, topological, semantic and stratigraphic data that are essential to a well-built 3D model, and that can be very effectively integrated to a GIS-based approach to 3D modeling. Here, we used the high-resolution surficial geology map of the same area to topologically constrain the 3D model in order to exercise stratigraphic control and to regulate the maximum thickness of some units in areas where fewer boreholes are available.

3.4.4 Foraminifera dating

Samples from various boreholes were examined in the laboratory for microfaunal (Foraminifera and ostracods) contents by Dr. Jean-Pierre Guilbault. The cores from both boreholes were subsampled to establish a microfaunal record of the complete marine sequence. The samples were covered with water in an Erlenmeyer and then disaggregated by agitation on a rotating plate, without prior drying. They were then sieved to isolate the 63-1000 µm fraction. The 1000 µm sieve is used to remove coarse residues such as stones or organic debris. The material retained in the 63 µm sieve is then poured onto a filter paper and oven-dried at 60 °C for one hour (or until the sample is well dried). This material is then passed through a low-density liquor (density 1.9, Lithium polytungstate) to extract a concentrate of foraminifera, while separating the floating and sinking portion of the sample. The samples are then dried again.

3.5 Quaternary geology and stratigraphy of the Lower-Chaudière area

The surficial geology of the study area was investigated thoroughly during this study. Figure 3.2 shows a map of the study area with important locations (field observations, drillings and very reliable boreholes).

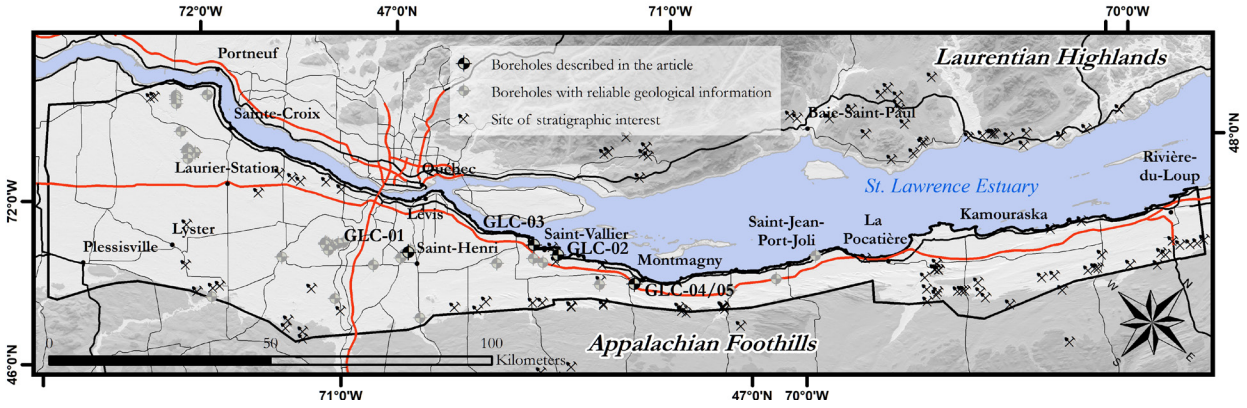

Figure 3.2 : Location of Quaternary investigations and boreholes with highly reliable data

3.5.1 Surficial geology

The basis for the 3D geological model resides mostly in the new, high-resolution Quaternary geology map of the same area, which was produced between 2013 and 2015 as part of a regional hydrogeological study (Lefebvre *et al.,* 2015). This part of the St. Lawrence Valley has a particularly complex surficial geology predominantly inherited from the Last Glacial Maximum (LGM) and deglaciation processes that took place thereafter. Low relief contrast and high vegetation cover have made the region difficult to map using photointerpretation. Therefore, geological units were identified and interpreted based on various derivatives of a digital terrain model (DTM) produced using Light Detection and Ranging (LiDAR) point cloud data (see chapter 2 of this thesis). A generalized version of this map of the area is shown in Figure 3.3.

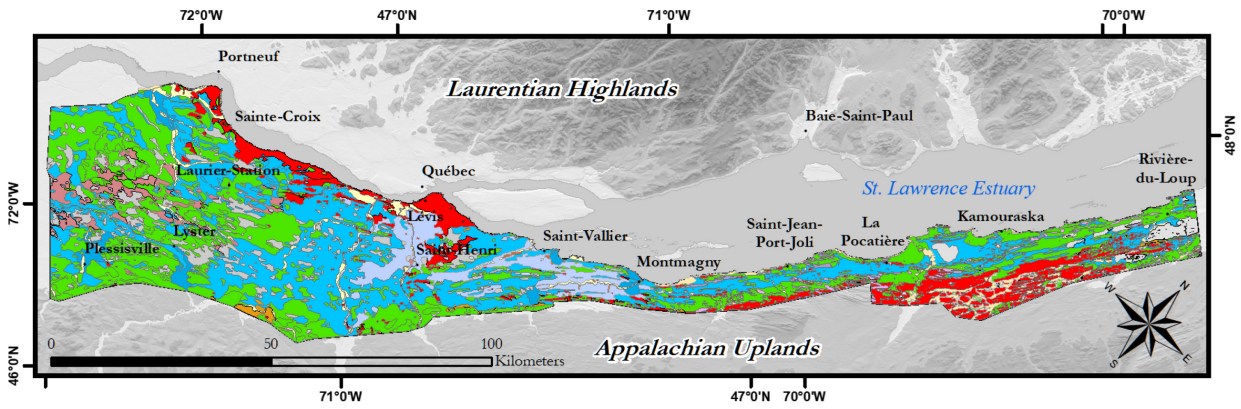

Figure 3.3 : Generalized 1 : 1 000 000 scale surficial geology map of the study area. Bedrock is shown in red, glacial deposits in green tints, glaciofluvial deposits in orange tints, glaciomarine deposits in blue tints, alluvial deposits in yellow tints and organic deposits in grey tints.

3.5.2 Stratigraphy and geological units

The Quaternary stratigraphic record of the study area mainly consists of post-LGM units. While some pre-LGM units outcrops were found, they are uncommon. Lasalle *et al.* (1976) only found sediments associated with the Late Wisconsinan glaciation when investigating and mapping the St-Jean-Port-Joli and La Pocatière regions. Their reported stratigraphic sequence is essentially the same as ours: from bottom to the top, regional till, glaciofluvial sediments, glaciomarine and marine sediments, fluvial sediments and organic deposits.

3.5.2.1 Bedrock and structure

Two geological provinces underlie the St. Lawrence mid-estuary region: the St. Lawrence Platform and the Appalachians. The study area lies almost entirely in the Appalachians, except for the Lotbinière area, where part of the platform outcrops north of Logan's Line (St-Julien & Hubert, 1975). The Cambro-Ordovician sedimentary rocks of the Platform are almost not deformed and rest unconformably on the igneous and metamorphic Grenville basement. The Appalachians consists of low-grade metasedimentary rocks, mainly shales, slates, sandstones and quartzites, that were deformed during the Taconian and Acadian orogenies. Logan's Line, a continental-scale thrust fault separates the autochthonous rocks of the Platform from the allochthonous Appalachian nappes.

In the lower Chaudière region, bedrock outcrops are mostly found in three major areas: along the shore of the St. Lawrence River (Figure 3.4), in the central part of the region (external Appalachian nappes – sandstone and quartzite), and the foothills of the Notre-Dame Mountains (internal Appalachian nappes). Between Beaumont and Berthier-sur-Mer (western part of the study area), a series of SSO – NNE trending normal faults exercise control over the topography and guide the greater part of the Boyer River watershed into the estuary (Lebel & Hubert, 1995). Major faults are mostly absent northeast of Berthier-sur-Mer, Northeast of Berthier-sur-Mer, the landscape becomes mostly controlled by the alternating strike ridges and troughs caused by the lithological contrasts imparted by alternating quartzite and shale strata.

Figure 3.4 : A shale outcrop exposed in the upper intertidal zone near St-Vallier (Lat/long coord.: 46.8862, -70.8554)

3.5.2.2 Pre-LGM Quaternary sediments

Pre-LGM Quaternary sediments and lower tills deposits predating the Late Wisconsinan are very rarely exposed in the study area. In fact, over the 140 sites investigated in the area, only one

showed a formation predating the last glacial maximum (Chaudière Till, see Figure 3.5). Deposits from the Early Wisconsinan and Illinoian glaciations (Chaudière Till and Johnville Till respectively (McDonald & Shilts, 1971; Shilts, 1981; Parent, 1987; Shilts and Caron, 2018)) can be found occasionally in deeply entrenched valleys a few kilometers south of the study area (Normandeau, 2010; Caron, 2013), but are rarely seen in outcrops over the study area. In the vicinity of St-Raphaël (route Tadoussac, northeast of the Rivière du Sud), two till units separated by thin rhythmites were observed in a freshly cleaned roadside ditch. At this location, the upper till consists of compact silty sand diamicton typical of the regional surface till, while the lower till unit is more clayey, compact, and displays a series of listric faults. This succession is characteristic of pre-LGM units, and is thus interpreted as a Chaudière Till-Gayhurst Formation-Lennoxville Till succession.

Figure 3.5 : Chaudière Till outcrop near St-Raphaël (Lat/long coord.: 46.813743, -70.717422)

The Pointe St-Nicolas site described in Occhietti *et al.* (2001) has since been heavily reworked by pit operations and fresh cross sections could not be found. Several boreholes show possible occurrences of isolated sand units below the surface till. As these units do not contain datable

material, they cannot be correlated with any specific pre-LGM unit on the sole basis of the stratigraphic position, and have been simply grouped under a single unit, pre-LGM sands.

3.5.2.3 Wisconsinan glacial sequence

The surface till found in the study area and is known as the Lennoxville Till. It covers most parts of the Estrie-Beauce region. It consists of gray-brown diamict with a sand/silt matrix and its clast content is usually dominated by oblate to bladed particles, typical of Appalachian rocks, but also containing sparse clasts of Grenvillian provenance. This till is generally compact in the Lotbinière/Bellechasse area, and more clayey and deformable in the Kamouraska area. Figure 3.6 shows two typical facies of the Lennoxville Till found in a road ditch in St-Alexandre-de-Kamouraska.

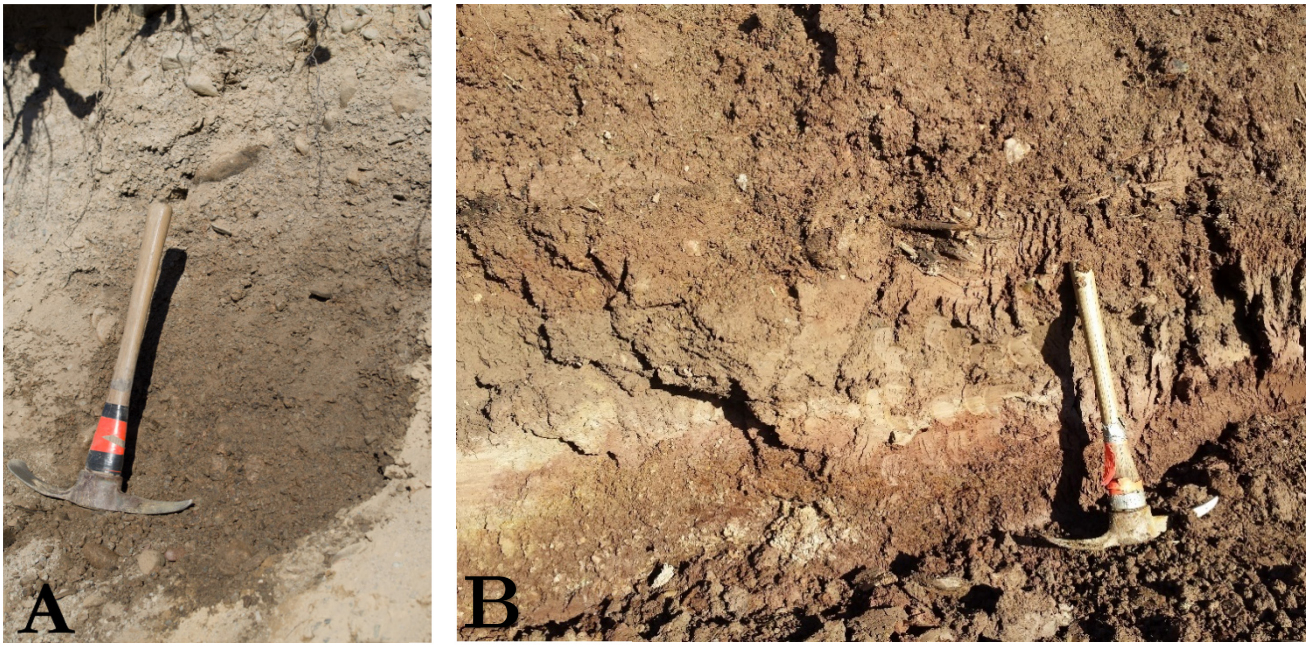

Figure 3.6 : A) Typical surface till (Lennoxville Till) near Saint-Alexandre-de-Kamouraska (Lat/long coord.: 47.6411, -69.5783); B) Intertidal silts overlying a compact reddish till, found in a quarry near St-Appolinaire (Lat/long coord.: 46.6410, -71.5059).

Under the submergence limit of the Goldthwait Sea, the reworking of till by waves and currents is significant and somewhat more considerable than what is observed in the Québec City area and in the Chaudière River watershed, where only the first 50 cm of sediments is usually affected (Lamarche, 2011; Caron, 2013). At most sites downstream of Montmagny, the surficial till is

washed out in its upper 60 – 90 cm. South-west of Montmagny, a small section shows major reworking in over 90 cm of surficial till. This reworked glaciomarine unit is expectedly much more permeable than the regional till unit, as its matrix is winnowed of fine particles. In high energy settings such as meltwater corridors, the underlying till unit can be partially or completely eroded by fluvioglacial streams.

3.5.2.4 Glaciofluvial sequence

The fluvioglacial sequence includes all facies of proglacial outwash sediments (subaerial, subaquatic and ice-contact) deposited by meltwater. While these three facies can be readily distinguished in well-exposed sections on the basis of primary structure assemblages, they cannot be recognized on the sole basis of the grain size information typically provided in well drillers' log. All three facies were grouped together during 3D geological modeling. Ice-contact fluvioglacial sediments are composed of heterogeneous sets of sand and gravel beds with occasional silt layers and sometimes diamictic beds. Below the limit of marine submergence, these units were also reworked by waves and currents. Even though they locally form major sediment bodies, these units occupy a relatively small portion of the study area. The main ice-contact complexes are located in St-Bruno-de-Kamouraska, St-Joseph-de-Kamouraska, St-Antonin and St-Modeste, but smaller, isolated bodies of glaciofluvial sediments can be found sporadically all over the region.

Glaciofluvial deposits are mostly absent from the region extending between Lévis and Kamouraska, except a few mounds near the St-Raphael delta. No complete section exposing glaciomarine deltaic sediments overlying glaciofluvial units could be found. Ice-contact sediments consisting of glaciotectonically deformed fine to medium sands showing fluidization structures were observed in a gravel pit near the base of the glaciomarine delta. The sequence is topped by typical proximal ice-contact bouldery gravels showing paleocurrents toward the northeast. In St-Bruno-de-Kamouraska, the geological context is significantly different from that found in the southwestern end of the study area. Here glaciofluvial deposits mostly occur in a well-developed outwash plain formed above the marine limit on the Appalachians Piedmont, and beyond a first series of major bedrock outcrops. Subaerial and subaquatic fluvioglacial sediments are quite abundant in this sector of the piedmont particularly near St-Bruno-de-Kamouraska and around

the St-Antonin Moraine. Figure 3.7 shows a section found in a gravel pit in St-Bruno-de-Kamouraska, where 5 meters of cross-stratified sand and gravel beds dipping toward the northwest are topped by a bed of coarse gravel.

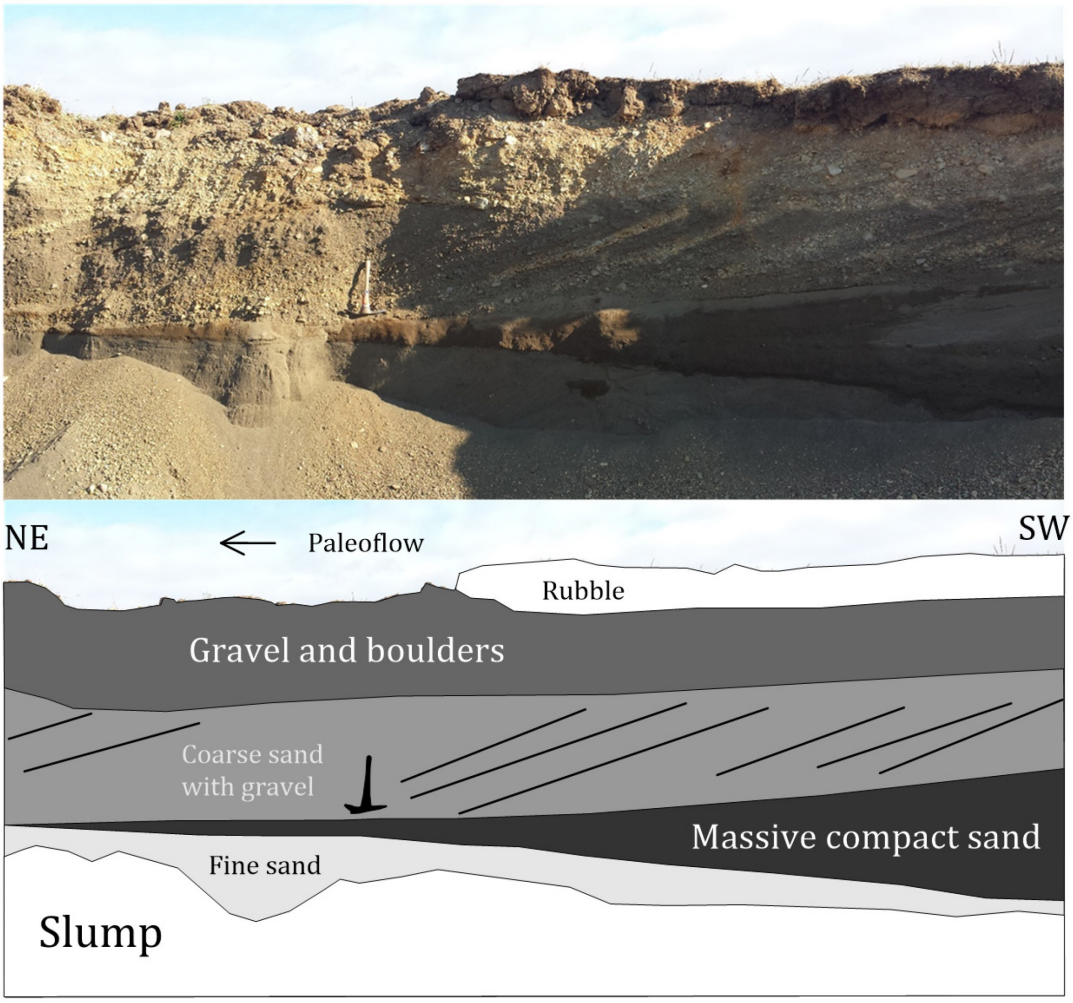

Figure 3.7 : A typical St-Antonin Moraine ice-contact facies in St-Bruno-de-Kamouraska with cross-stratified beds generally inclined toward the northeast and locally toward northwest. They overlie massive fine sands presumably deposited as subaqueous outwash (Lat/long coord.: 47.4418, -69.7894).

Three gravels pits in the St-Antonin Moraine show bottom, middle and top sequences typical of the morainic complex. The bottom sequence is well exposed in a gravel pit in St-Antonin. This pit exposes a 6 m thick fine sand unit showing a coarsening upward sequence with ripple-drift cross-laminated rythmites and paleocurrent toward the northeast (Figure 3.8). In St-Arsène, near the St-Antonin exposure, ice-contact sediments in the core area of the moraine consist of a 3 m thick sequence of plane-bedded coarse sand overlain by cross-bedded gravels with paleocurrents

toward the northeast (Figure 3.9). There the top of the sequence again consists of cobbly gravel. In St-Épiphane, the same cross-stratified coarse gravels, with sparse boulders, are locally topped by a diamicton. The dark grey, fossil-bearing, clayey till dips strongly toward the South.

Figure 3.8 : Subaqueous outwash faciès of the St-Antonin Moraine near the municipality of St-Antonin : exposure shows a 6 m thick sequence of ripple-drift cross-laminated rhythmites (Lat/long coord.: 47.7507, -69.4707).

Figure 3.9 : Ice-contact sand and gravel exposed in pit near St-Arsène, near the northeastern limit of the study area. Note the presence E-W oriented normal faults (Lat/long coord.: 47.9179, -69.3872).

As part of the Portrait des ressources en eau souterraine en Chaudière-Appalaches (Lefebvre *et al.*, 2015), seismic reflection seismic work was carried out on suspected old paleochannels of the Chaudière and Etchemin rivers near Saint-Henri, which are visible on the first derivative grid of the regional aeromagnetic survey (Figure 3.10).

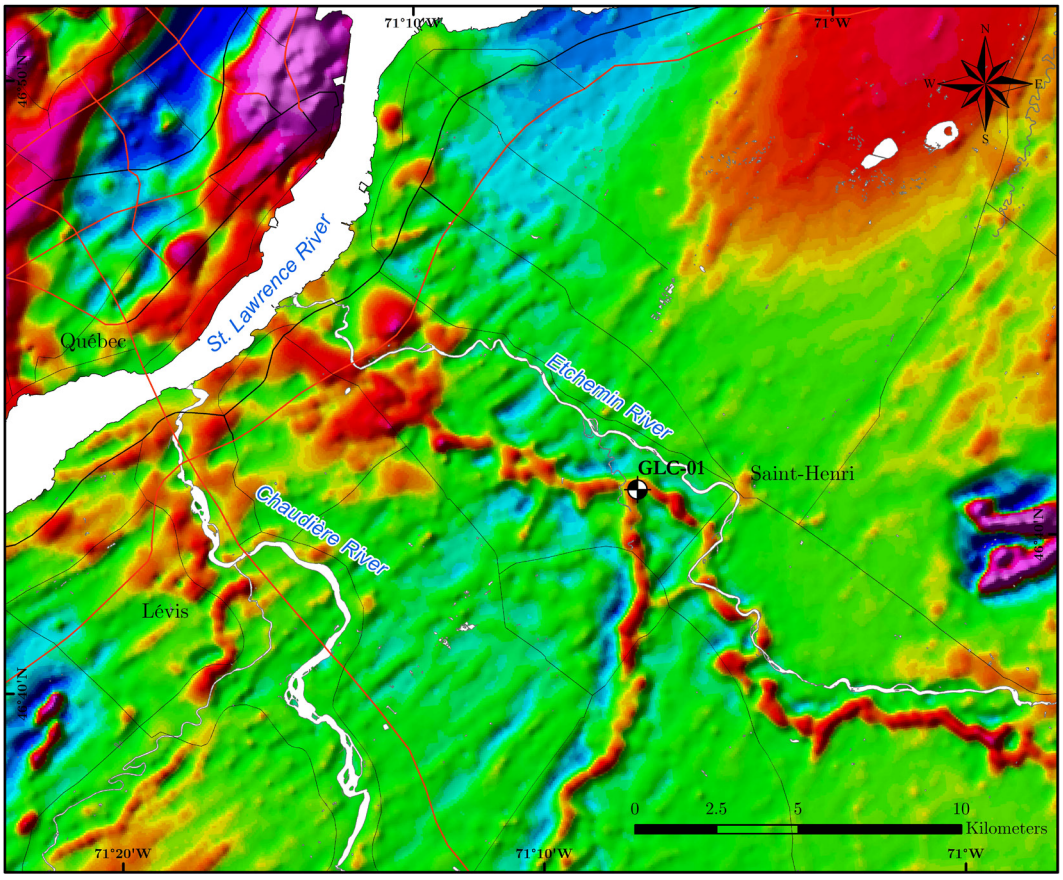

Figure 3.10 : Location of the Saint-Henri magnetic anomaly. The first derivative of the regional aeromagnetic survey is displayed in the background map in a color scale ranging from blue (low) to purple (high). The paleo-Etchemin River in the right portion of the image can be traced by following the red coloured mounds, which show a very similar configuration to the present river. The Chaudière River now seems to flow further east of its former course. The location of the new borehole (GLC-01) drilled in the axis of the magnetic anomaly is also illustrated.

The seismic results did not show any significant lateral variation of the signal between the low and high anomaly zones, but still established that the depth to bedrock varied from 10 to 20 metres. The geological data contained in the public driller's logs (Système d'Information Hydrogéologique – SIH) for the magnetic anomaly zone are erratic and very irregular, but appear to show a thin layer of gravel under the clayey silts found at surface. A CPT hole and an RPSS hole (GLC-01) were drilled along the main axis of the magnetic anomaly. The CPT drill hole

stopped after about 20 meters in a clayey silt (the log of this drill hole is presented in appendix of this thesis). On the other hand, the RPSS drill hole determined the presence of a thin zone of grey sand, then red slate schist pebbles capping a diamictic layer that was also gravelly at first, then more sandy-silty towards the base. Although rather localized and partially disconnected from one another, these zones could potentially be exploited as aquifers.

3.5.2.5 Glaciomarine sequence

While glaciomarine sediments underlie about 50 % of the study area, they are seldom observed in sections. The marine units consist of offshore basal silt and clay, littoral and sublittoral sands and gravels, as well as deltaic and prodeltaic sands or silty sands. Offshore marine sediments were deposited during the marine submergence phase, typically filling topographic depressions between bedrock ridges. They are mainly composed of massive clayey silt or of silty clay, medium to dark grey, sparsely fossiliferous (mainly *Portlandia arctica*), laminated, locally rhythmically in the vicinity of large deltaic complexes such as in the St-Raphael delta. With a thickness of up to 51.2 m in boreholes, these clays form a regional aquitard whose extent is controlled by bedrock ridges. Isostatic uplift prompted by ice sheet melting led to the deposition of : offlap sequences of sand, silt and gravelly sands forming beaches, coastal ridges, tombolos and terraces. While the thickness of these sediments ranges from 0.5 to 20 m, they generally form a thin cover over basinal clayey silts. They occur between the maximum submergence limit (from 190 m in the Lotbinière area down to about 155 m in Rivière-du-Loup) and the lower terraces of the Proto-St. Lawrence terraces in the Lotbinière area or Laurentian Transgression terraces in the Lower St. Lawrence. During deglaciation, the melting of the ice sheet delivered substantial amounts of water and sediments to the proglacial systems, creating vast deltaic complexes at the mouth of major rivers flowing into the Champlain and Goldthwait seas. Such glaciomarine deltas in the study area consist of up to 30 m (in boreholes) of well-sorted sand and gravel, showing occasional glaciotectonic deformations and water escape structures.

Boreholes (roto-percussion and rotosonic methods) and cone penetrometer soundings (CPT, Geotech GEORIG 605D drill rig) were recovered in 4 key locations inside the study area: St-

Henri-de-Lévis, St-Vallier, St-Michel-de-Bellechasse, and Montmagny, and allowed the characterization of the glaciomarine/marine units and their transition to littoral units.

Borehole GLC-01 (St-Henri-de-Lévis) shows a sequence somewhat typical of littoral sediments underlain by basinal glaciomarine silts. Boreholes GLC-02 (St-Vallier) and GLC-03 (St-Michel-de-Bellechasse) show that rapid lateral facies changes may occur in the littoral/basinal transition units. The upper sequence of the GLC-02 borehole shows a rapid transition from littoral/sublittoral with 2 successive fine sand units intercalated between silt units at elevations of about 8 and 6.75 m ASL, to a typical basinal silty clay facies from + 6 m to -15 m, below which a silty diamicton (till) was intersected. While borehole GLC-03 is essentially at the same elevation as GLC-02, the nature of the top units differs radically. A complex sequence of alternating silts, sands and gravelly beds lie between the surface (5 m ASL) and the top of the basinal silty clay at -5 m ASL. The small clasts or rock fragments usually consist of red shale or grey sandstone and are occasionally accompanied by marine fossils. The transition between the littoral and basinal units is not well defined, being separated by silt and sand rhythmites containing a noticeable amount of plant organic debris. The undisturbed clayey silt basinal unit is about 5 m thick and overlies another set of grey, sandy silt rhythmites unit. This silt unit is 4 m thick and rests on a heterogeneous glaciomarine diamicton, at least 6 m thick, that could not be sampled all the way to bedrock. This till is a very stony diamicton, with a sandy silt -calcareous matrix and a diverse clast lithology.

As part of the Geological Survey of Canada's seismic risk program, a rotosonic borehole was drilled during the spring of 2016. Located in an area of large overburden thickness in Montmagny, borehole GLC-04 provides the most complete and detailed stratigraphic information of the study area. The geological description is presented in Figure 3.11, while the associated geophysical data are compiled in Appendix B. The Quaternary sequence rests on Appalachian bedrock at a depth of 32 m. At the base is a 4 m-thick diamicton identified as a lower till. This grey to dark grey compact diamicton has a compact calcareous silty matrix and contains typically faceted glacial clast. This diamicton is overlain by a 4 m thick, gravelly and sandy beds, in turn overlain by another till unit. The basinal marine silts are about 18 m thick and directly overlie the upper till. Throughout the marine sequence, the grey clayey silt is marked by slightly calcareous reddish

levels of sand with abundant dropstones. The basinal sequence is overlain by a 1.5 m-thick fluvial sand unit.

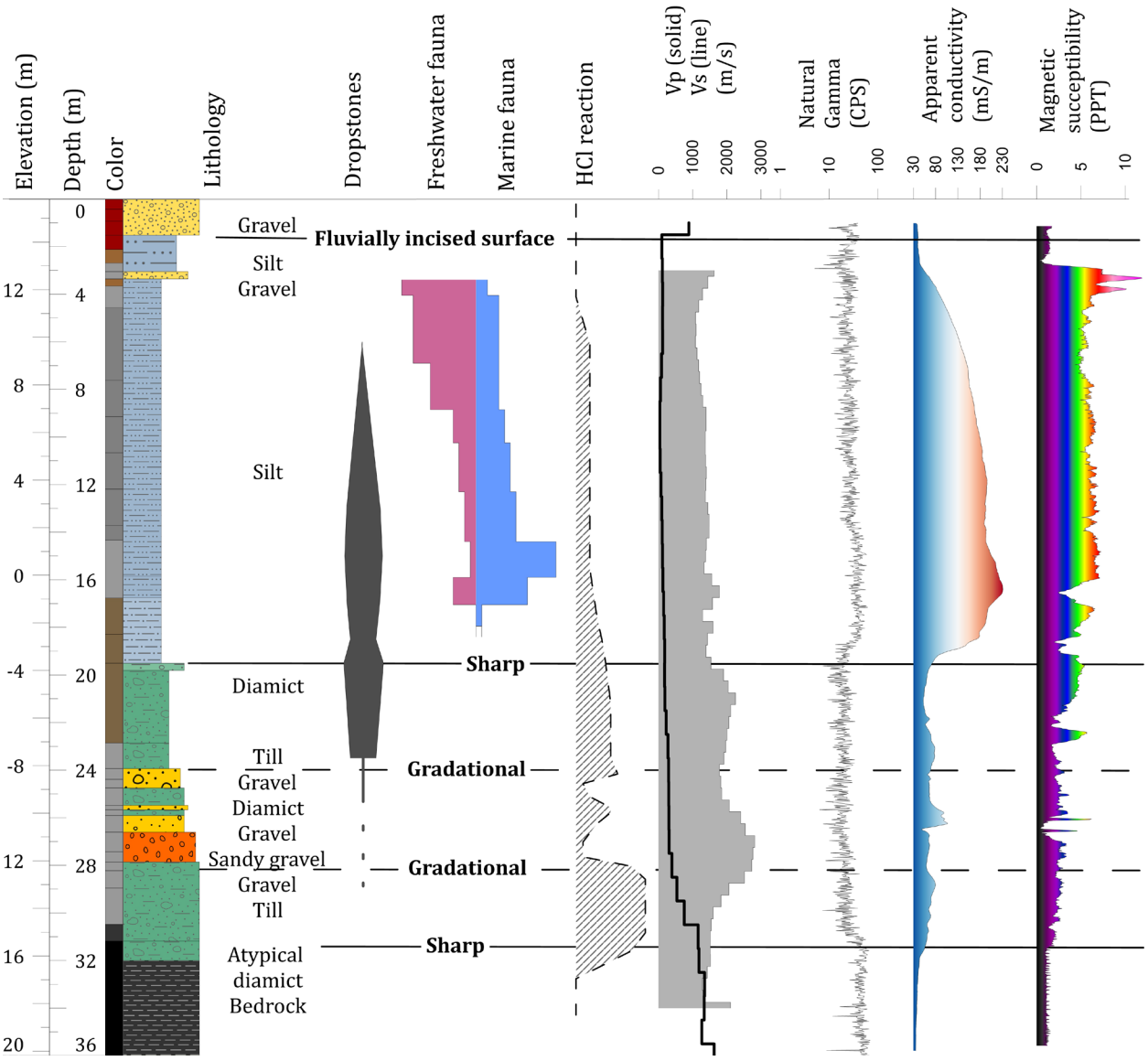

Figure 3.11 : Lithological, biological and geophysical attributes of borehole GLC-04, which is typical of the Quaternary strata encountered in the Lower St. Lawrence Valley near Montmagny.

In St-Nicolas, the glaciofluvial sequence exposed at a sand pit on Route Lagueux shows a base of very fossiliferous trought-bedded stratified medium to fine sand (Figure 3.12). The thanatocoenotic assemblage includes *Hiatella arctica, Macoma balthica, Mytilus edulis, Balanus spongicola,* and *Mya truncata*. This sequence is at least 3 meters thick and is topped by a finer sand unit of a meter thick. A few cobbles are present in each of the two subunits.

Figure 3.12 : Thick beds of shelly sands and gravels (mostly *Hiatella Arctica* and *Macoma balthica)* overlaid by a fine sand unit in a small active St-Nicholas sandpit (Lat/long coord.: 46.694985, - 71.378389).

3.5.2.6 Alluvial deposits

The oldest dated alluvial deposits in the area lie unconformably over the underlying sediments or bedrock and were deposited in tidal basins during transgressive episodes (Laurentian Transgression) in the maritime estuary. Consisting of silt, sandy silt, and sand generally containing fragments of terrestrial and aquatic plants, this unit was initially described by Dionne (1988); it is characterized by a massive, weakly laminated or rhythmic structure and is rarely thicker than 5 m. The younger sequences are associated with contemporary fluvial systems which commonly cut through antecedent Quaternary formations. Alluvial terraces consist of a variable mixture of sand, sandy silt, gravelly sand and gravel, and frequently contains plant fragments.

3.5.2.7 Peat deposits

Peat bogs and swamps occupy the poorly drained areas in the region. While most of these organic units are generally less than 5 meters thick, a few actually exceed 10 meters in thickness, notably near Rivière-du-Loup where commercial peat extraction has been active for years. They usually lie conformably on littoral silty sands or on fluvial terraces along the St. Lawrence.

3.5.2.8 Aeolian deposits

Linear dunes of more than 15 m of relief and consisting of fine laminated sands are especially prominent in the Lotbinière region and are mostly oriented SW-NE (e.g. Figure 3.13). They usually overlie littoral sands or marine silts where they constitute readily distinguishable geomorphic features; in boreholes however, these aeolian sands are undistinguishable from other fine sand units.

Figure 3.13 : Section across a 10 m high linear dune trending toward the SW in the Lotbinière region (Lat/long coord.: 46.5710, -71.5466).

3.5.3 Geochronology and dating

A group of 32 samples from boreholes GLC-01 (Saint-Henri) and GLC-04 (Montmagny; see figure Figure 3.2 for locations) were examined in the laboratory for microfaunal (foraminifers and ostracods) contents.

The GLC-01 assemblages contain few specimens and species diversity is low. In total, there are 6 taxa of foraminifers, only 2 of which are present in significant quantity: *Elphidium excavatum forma clavata* and *Cassidulina reniforme*. These are the two most common species in glaciomarine sediments. Similarly, there are only 2 species of ostracods (except for a few fragments), one represented by a bivalve species (*Cytheropteron arcuatum*) in samples throughout the core. The other species, *Cytheropteron pseudomontrosiense*, is represented by a few valves in 15 of the 20 samples. However, in the 20.41 m (depth) sample, there are 56 valves and no foraminifera. Both species are marine and *C. arcuatum* prefers deeper waters (>20 m). *C. pseudmontrosiense*'s preferences are less obvious, but is still known to prefer glacial environments (Guilbault, 1993). As the total number of foraminifera was so low, it is not possible to determine the type of depositional environment more precisely than a glacial marine environment.

Table 3.3 : Foraminifera found in the marine sequence of borehole GLC-01. "Fg" and "Fgs" refer to a fragment or several fragments of shells that were found in samples. "√" means « present », while "-" means present but in very small quantities.

	Foraminifera									Ostracodes												Other fossils											
Depth	*Cassidulina reniforme*	*Islandiella helenae*	*Elphidium excavatum*	*Elphidium* sp.	*Haynesina orbiculare*	Glandulinidés indifférenciés	Polymorphinidés indifférenciés	Miliole indéterminée	Foram calcareux indéterminés	*Cytheropteron pseudomontrosiense*	*Cytheropteron nodosum*	*Cytheropteron* sp. juvénile	*Cytheropteron* cf. *arcuatum*	*Cytheropteron* aff. *nodosum*		*Cytheropteron* sp. B in Cronin (1988)	Ostracodes indéterminés	Total number of forams and ostracodes	Identified forams per 100 g of sediment	**Identified** forams	Number of species	Echinoderms fragments	Gastropod (juvenile)	Periostraca	Sponge spicules	Pyrite framboïde	Insect fragments	Megaspore	Coniferous pollen	Gyttja with coniferous pollen	Non-fibrous organic matter	More or less degraded plant material	Wood charcoal	Identified forams per 100 g of sediment
1.64	34		8		1				1	6				1				45	38.2	40	4	√			√							√√		0 50 100
2.69	5		1			1				0								7	6.11	7	3							√					.
4.67	1		1						fg	0								2	2.09	2	2		√						.			.	
5.77	2		1							0								3	2.97	3	2								.			.	
7.72	21		5							7							2 fgs	26	20	23	3	√											
8.82	13		1					1		1	1						fg	15	11.5	15	3	√			√						√	√	√	
10.87	12		8		1					5								24	19.2	21	4											√	
11.87	28	1	18				fg?			9								49	41.1	42	4	√			√		√					√	
13.77	22		8							6						fg	fg	28	19.6	27	4			.					.			√	
14.42	16		4				2			3								20	17.4	19	4	√			√						√	√	
15.34	23		12							9			1				fg	35	20.2	27	4											.	
16.44	33		21						1	9		1	1					59	37.1	53	4								.			.	√	
17.01	41		13	1						6								54	53.1	49	3	√		√					.			.	
18.49	22		8	1						7								36	22.5	30	3	√		√								√	√
19.49	23	1	11	1			1			5							1	36	18	33	4	√				.			.			√	√
20.41	0		0							61								56	0	0	1												
21.49	12		6	1						5	1							19	21.6	15	3			√					.			.	
21.89	16		5				fgs			7	1							22	21.6	18	4	√					√					.	
22.09	16		5	1						3								24	25.4	20	3											.	
22.19	2		0			1												2	2.4	2	2											√	

Salt water indicators | Freshwater indicators

The GLC-04 foraminiferal assemblage is much richer than in GLC-01. 14 foraminifer taxa are present, most of the population formed by 3 species: *Elphidium excavatum forma clavata*, *Cassidulina reniforme*, and *Islandiella helenae*. The upper portion of the core (0 to 3 m) consists of Holocene sediments in which freshwater diatoms are abundant, but no foraminifers or ostracods were found. The microfauna of the late marine and post-glacial unit below this first horizon can be subdivided into 2 groups:

- Biofacies A (3.4 m to 16.6 m): *Elphidium excavatum* is dominant in the upper few meters of the borehole. In this biofacies, the occurrence of *Elphidium excavatum* lowers downward as this species is progressively replaced by an equivalent increase of *Cassidulina reniforme* and *Islandiella helenae*. Diatoms of *Coscinodiscaceae* family are also present in this biofacies.

- Biofacies pre-A (from 16.6 m to 18.4 m): Only a very limited number of common glaciomarine foraminifers is observed. The composition of the assemblage is fairly uniform, and the number of specimens is on the order of a few tens, which is very little even for the Champlain/Goldthwait

Sea assemblages. The ostracod *Cytheropteron pseudomontrosiense* is present but in low numbers, as only 11 ostracod specimens were found in the entire biofacies. With such a low number of specimens, paleoecological interpretation of this facies is somewhat tenuous, but it is assumed to be associated with proximal glaciomarine conditions.

The microfauna composition of Biofacies A is similar to zone A in the Champlain Sea (Guilbault, 1989), and the glaciomarine to freshwater transition. The assemblage of *Elphidium excavatum*, *Cassidulina reniforme*, and *Islandiella helenae* is very typical in glaciomarine proximal environments. *Nonionellina labradorica* grows in very similar environments than *Islandiella helenae* but is notably absent from this particular assemblage. In ice marginal conditions, the front of a rapidly melting glacier will produce fine sediment that prevents light penetration into the water column, and thus limit algae productivity. As a result, only the species that are less demanding in terms of food can survive in them. The least demanding are, in order: *Elphidium excavatum*, *Cassidulina reniforme*, and *Islandiella helenae* (Korsun & Hald, 1998, 2000). That principle results in a zonation from the glacier front towards the deep sea that reproduces exactly this succession. However, in this case, the sequence seems inverted. Water salinity most likely exercised a greater control on the community structure than food supply. The minimum salinity for *C. reniforme* is around 26‰, while that of *E. excavatum* is at the freshwater limit (Polyak *et al.*, 2002). The transition towards a less saline environment is seen through the community structure. Very close to the glacier, no foraminifera are found. As the ice gets more distant, a few *E. excavatum* appear, then *C. reniforme* in addition to *E. excavatum* and finally, *I. helenae* join in the community, all under normal salinity conditions (32‰ or more). When water salinity reaches a threshold at 15.2 m of depth, *E. excavatum* is replaced progressively by *C. reniforme* and *I. helenae* (beginning of Guilbault's (1989) zone A). At 8.2 m of depth, water salinity begins to drop again, as *E. excavatum* regains more representation in the community structure.

The presence of the *Cytheropteron pseudomontrosiense* ostracode in the base of the core (Biofacies pre-A) also suggests the presence of a glacial environment, but its preferences are less obvious. The total number of foraminifera being low in this portion, it is not possible to determine the type of depositional environment more precisely than a glacial marine environment.

Table 3.4 : Foraminifera found in the marine sequence of borehole GLC-04

Depth	Foraminifera														Total number of forams and ostracodes	Identified forams per 100 g of sediment	Number of species	Shannon diversity index	Other fossils: Interpretation	Identified forams per 100 g of sediment
	Spiroplectammina biformis	*Buliminella hensoni*	*Stainforthia feyling*	*Stainforthia concava*	*Cassidulina reniforme*	*Islandiella helenae*	*Islandiella norcrossi*	*Eoeponidella pulchella*	*Astrononion gallowayi*	*Nonion labradoricum*	*Elphidium excavatum*	*Elphidium incertum*	*Elphidium hallandense*	*Haynesina orbiculare*						0 1000 2000
1.95																			Freshwater	
2.3																				
3.4					I	III	I	II		I	IIIIIII	I	I	II	391	122	12	1.23		
4.7	II		III		III	II		I			IIIIII		I	I	428	2299	10	1.22		
5.6	II	I	III		II	II	I	II	I		IIIIII		I		324	356	14	1.47	Open marine	
8.2	II	I	III		III	II	I	I			IIIII		I	I	404	822	12	1.61	environment	
9.5	I	II	IIIII		IIIII	III	II		I		IIII				397	1038	12	1.62	(Champlain	
11	I	I	II	I	IIIII	IIIII	I		I		III				347	596	16	1.45	Sea Zone A)	
13.6	I		I	I	IIII	IIIII					II			I	356	917	8	1.11		
15.2				I	IIIII	IIIII	I		I		III				278	306	11	1.23		
16.6					IIIIIII						IIII				73	82	2	0.64	Marginal	
17.5					29	11					4				45	52	4		marine	
18.4					6	3					1				10	12	3		environement	

No shells large enough for radiocarbon dating were found in the marine units of GLC-04, but organic plant material found in the thin gravel unit near the top of the core was dated 7720 +/- 30 BP (Beta – 460128). Considering the age and elevation of the gravel unit (13 mASL), it is likely that this unit is associated with lateral migration of a river bar deposited sometime during the Goldthwait Sea regression. The laminated silt unit directly underneath contains some organic debris and shell fragments. It is worthy to note that the identified age corresponds to the first phase of Laurentian Transgression phase as identified by Bélanger (1993), who's relative sea level curve for the south shore of the middle St. Lawrence estuary area differs from Dionne's (2002). According to this alternative curve, the regression of the Goldthwait Sea to the current level would have occurred around 9000 BP and would have been followed by a first phase of the Laurentian Transgression at 7850 BP, which would have reached a relative maximum elevation of about 7 mASL. This older relative sea level curve and the events it relates to are, however, poorly documented and have not received considerable attention.

3.6 Regional 3D geological model

The three-dimensional geological model of the study area consists of 12 stratigraphic units identifiable either at the surface or in boreholes, from the base upward: bedrock, pre-LGM units, LGM regional till, glaciofluvial deposits, glaciolacustrine deposits, glaciomarine clays, glaciomarine littoral sands, glaciomarine deltas, marine transgression sands, alluvial sediments, organic sediments and aeolian sediments.

3.6.1 Thickness grids

The following figures present excerpts of the 3D geological model in a 2D plan view. The first panel shows the bedrock topography, while the second one shows the total sediment thickness. For each subsequent modeled unit, the extension of the geological unit and its thickness are shown in a single panel.

Located at the contact between two subcontinental geological provinces, the region is characterized by a rugged bedrock topography (Figure 3.14, first panel). The relief of the Appalachian foothills is much more rugged than that of the subhorizontal sedimentary rocks of the St. Lawrence Platform. In a few isolated locations, two tills can unequivocally be differentiated in borehole logs. This older sequence consists of pre-Last Glacial Maximum (pre-LGM) deposits and are shown in Figure 3.14, third panel. This surface of the bedrock is largely covered by the LGM till (Figure 3.14, fourth panel) which consists of a sandy silt diamicton with an average thickness of 6 m and a maximum thickness of 20 m. Below the maximum marine submergence limit, this diamicton has been winnowed and reworked by the action of currents and waves.

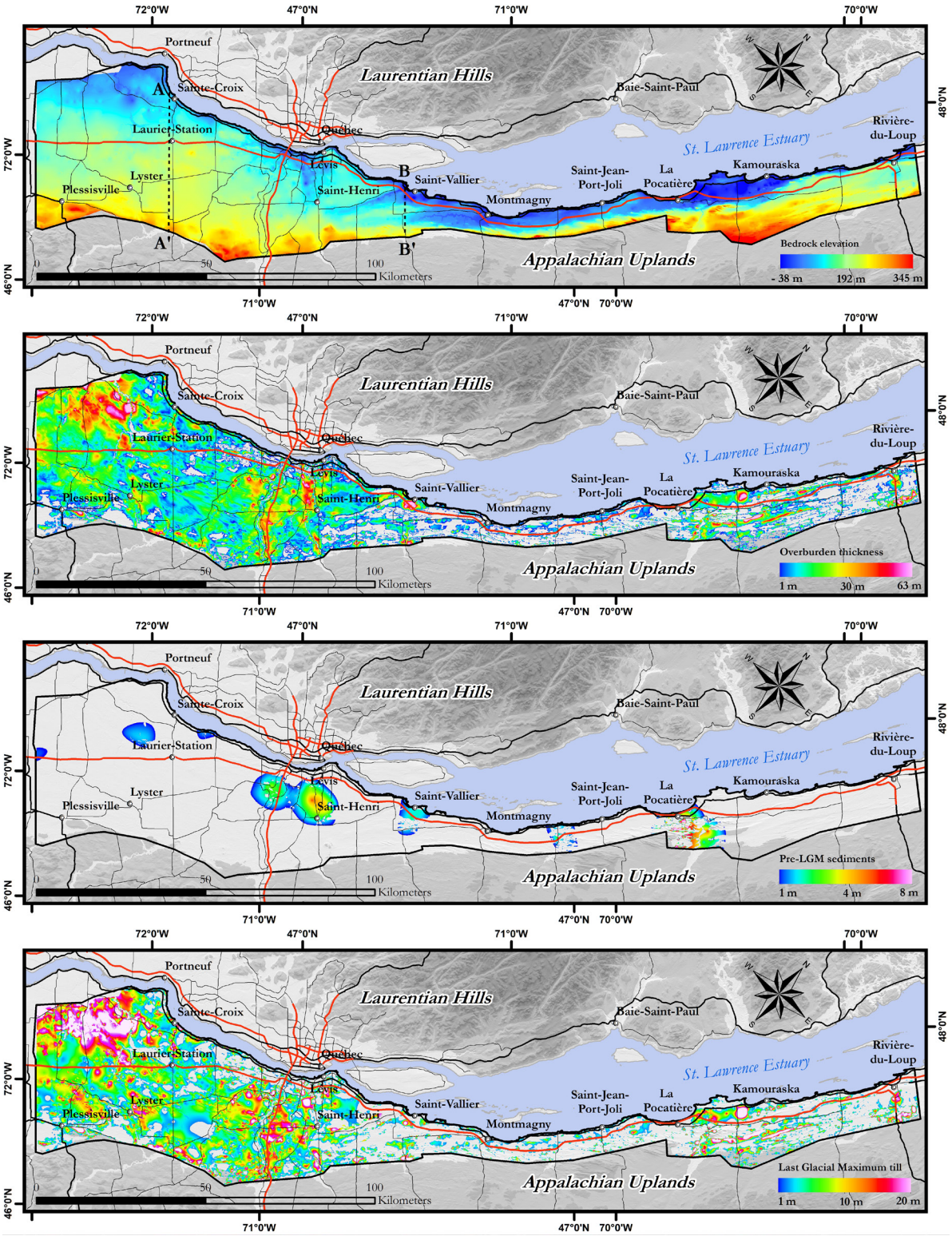

Figure 3.14 : 3D geological model. From top to bottom: Elevation of the bedrock, total sediment thickness, Pre-Last Glacial Maximum (LGM) deposits thickness, Last Glacial Maximum till thickness. The location of cross-sections A-A' and B-B' (see Figure 3.18 and Figure 3.19) is also shown in the first frame.

The regional extent and thickness (42 m maximum) of the very heterogeneous glaciofluvial sands and gravels are shown in Figure 3.15 (first panel). During the early stages of deglaciation, ice-dammed lakes formed in the Chaudière Valley, and probably in other main valleys as well. Several boreholes show clayey silt and clay units above the maximum submergence limit in the Appalachian foothills. Although those deposits have not been observed in any cross-sections or in recent boreholes, this unit is represented in a considerable amount of older boreholes and cannot be neglected. They are associated with a glaciolacustrine phase where sediments derived from the melting of Appalachian ice accumulated in one or several lakes that had formed between the mountains and the ice front. Those deposits reach up to 20 meters in thickness.

Following deglaciation, the Champlain and Goldthwait marine episodes left 4 main types of sediments in the region: (1) clayey, sometimes sandy silts associated with offshore environments (2) deltaic sands and gravels, (3) sandy silty sediments associated with intertidal environments and (4) sands and gravels deposited in littoral settings. The offshore marine unit fills depressions between bedrock ridges as well as most of the valley bottoms in the study area. This unit can reach a thickness of 45 m in boreholes. Littoral sediments, deposited mainly as raised beaches and marine terraces during land emergence, have thicknesses ranging from 0.5 to 15 m. Deltaic sediments were deposited at the mouth of the main tributaries (Chaudière River, Rivière du Sud, Etchemin River and Rivière des Mères) as they entered the sea, and reach a maximum of 24 m.

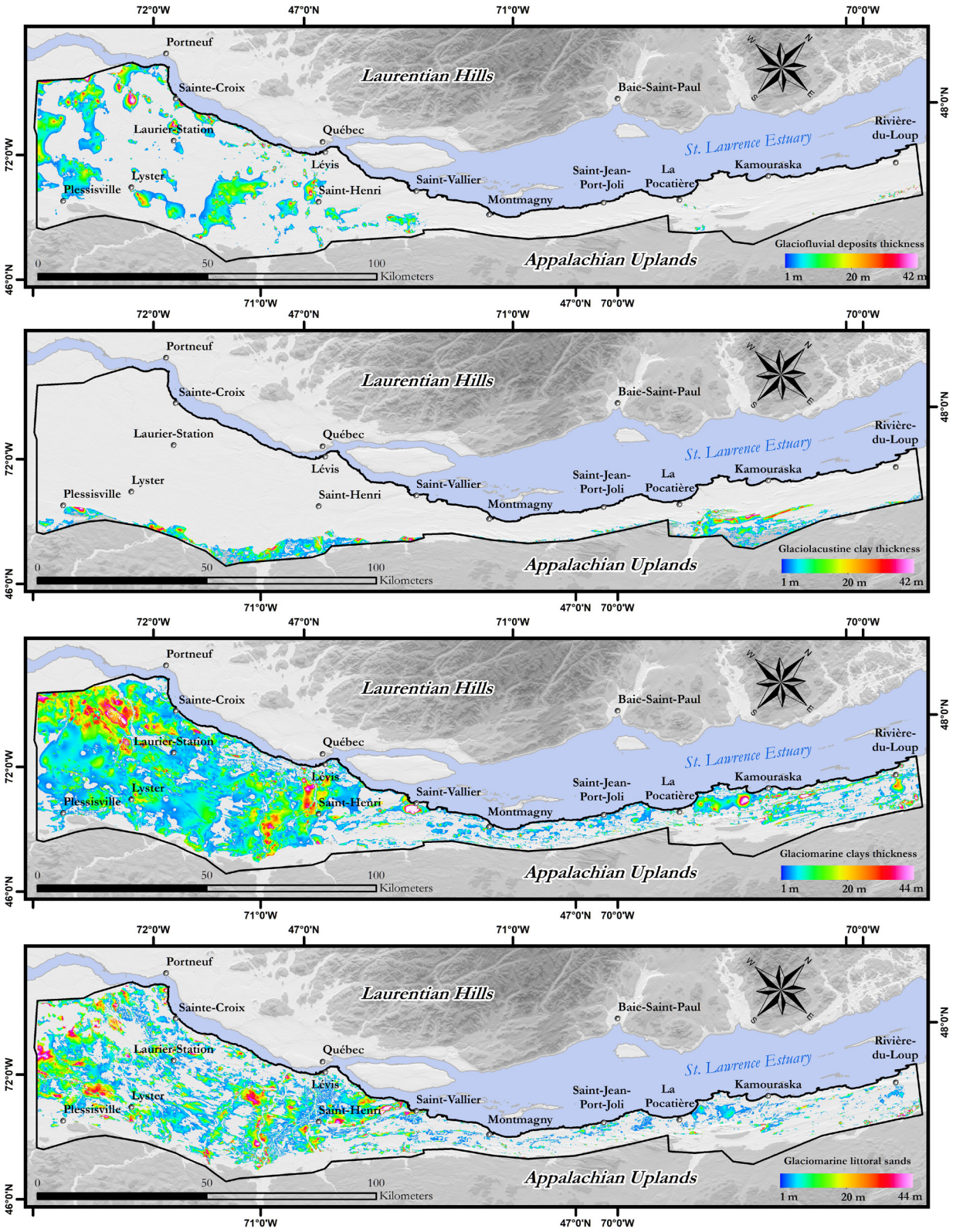

Figure 3.15 : 3D geological model. From top to bottom: Glaciofluvial deposits thickness (including the St-Antonin Moraine), glaciolacustrine clays thickness, glaciomarine silts and clays thickness, and glaciomarine littoral sands and gravels

Sea-level fluctuations over the past 6000 years, most importantly the Laurentian Transgression, led to deposition of a transgressive sand unit in various embayments in the study area. The unit commonly forms a low terrace truncating the typical marine sequence and is sometimes overlain by another unit of littoral marine sediments (Figure 3.16). The thickness of this sandy unit ranges from 1 to 12 m. The alluvial sediments, organic deposits and aeolian deposits occupy the top of the regional stratigraphy and generally form thin local units (Figure 3.17).

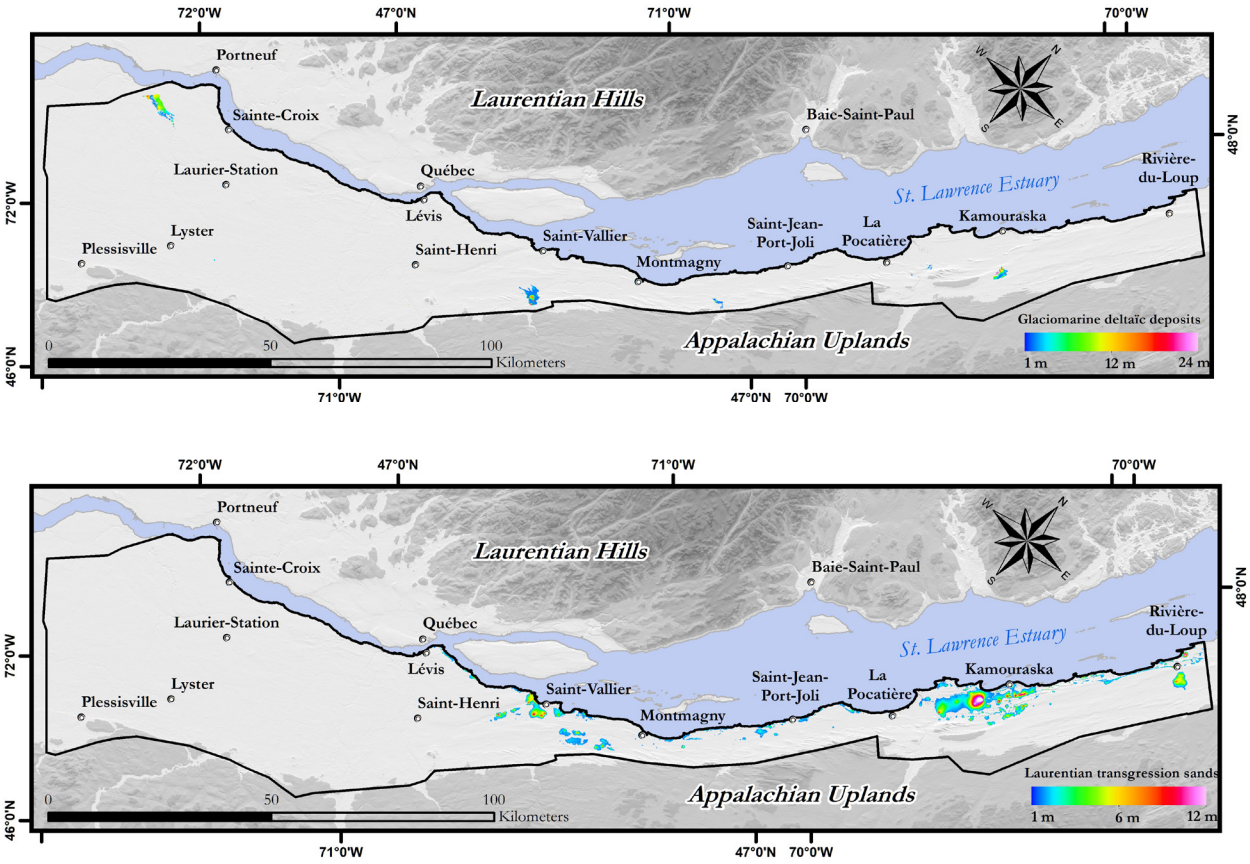

Figure 3.16 : 3D geological model. From top to bottom: Glaciomarine deltaic deposits, Laurentian Transgression sands.

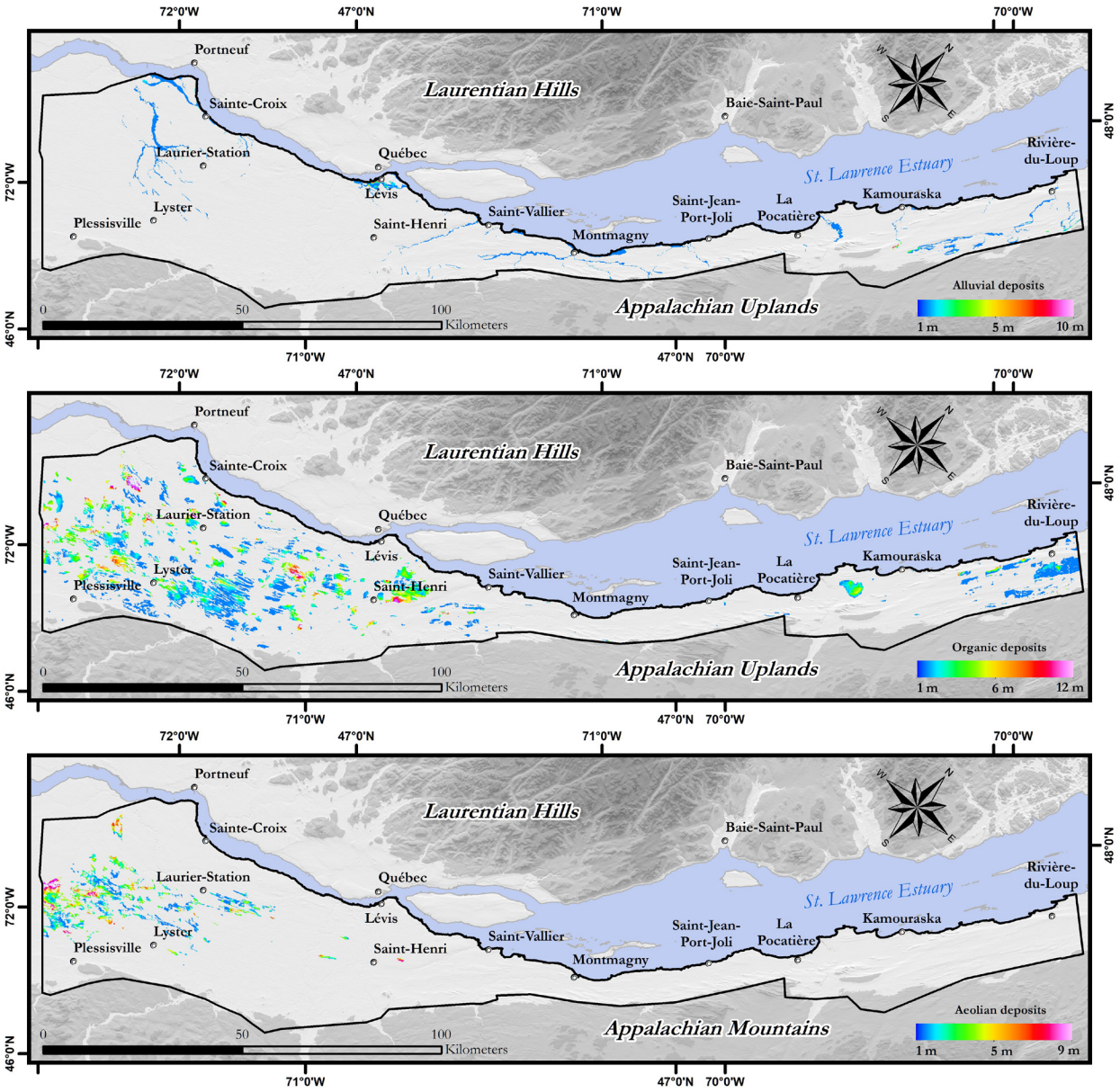

Figure 3.17 : 3D geological model. From top to bottom: Alluvial deposits, organic deposits, and aeolian deposits.

3.6.2 3D geological model cross-sections

The stratigraphy and architecture of surficial deposits provide significant hydraulic control over groundwater flow, vulnerability, recharge and potential of buried granular aquifers, making it crucial to properly define a conceptual hydrogeological model.

The typical sequence of Quaternary sediments in the east-central St. Lawrence Lowlands sector is represented by cross-section A – A' (Figure 3.18). It follows approximately an NW-SE axis and extends about 35 km inland so as to cross the main tributary valleys. In Lotbinière, the stratigraphy is simple, consisting of a thin layer of till showing signs of reworking overlying the rock. The thickness of unconsolidated deposits becomes greater at Laurier-Station, where more than 20 m of coastal and pre-coastal marine sediments typically composed of sandy silt are intersected. Bedrock depressions are very local, and the basins thus created are generally filled with glacial or fluvioglacial sediments. Towards the southeast, the thickness of the till increases considerably (more than 10 m in some areas), then the rock rises southward in a series of steps. Organic sediments are present in the less well-drained areas, and small-scale marine deltas are intersected at the Rivière du Chêne, where just under 10 m of sandy deposits are observed. Dunes are present locally but are not visible on the cross-section at this scale.

The subsurface geology typical of the context observed below the marine limit in the Lower St. Lawrence Valley is illustrated in cross-section B – B' (Figure 3.19). It begins in St-Michel-de-Bellechasse, on the south shore of the St. Lawrence River (left side of the cross-section), and ends at the marine limit in St-Raphaël. The marine clay units underlying the marine plains are about 20 meters thick. While many bedrock depressions are filled with marine clay, others are generally filled by till and others, very locally, by sandy deposits.

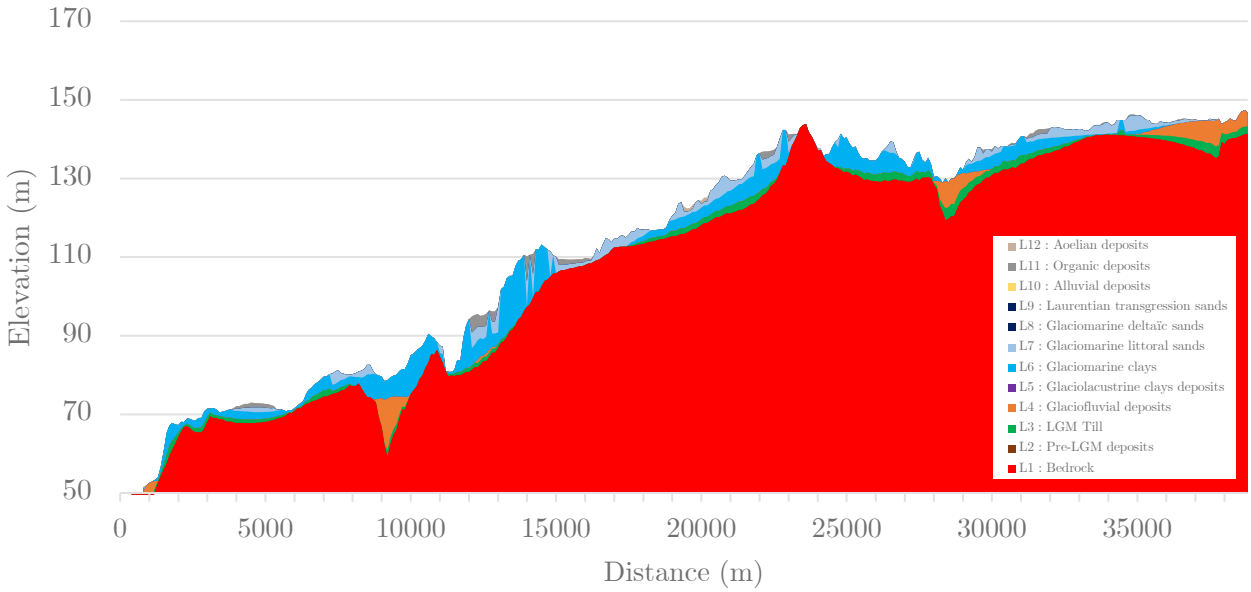

Figure 3.18 : Surficial geology cross-section A – A' across the Lotbinière area between the St. Lawrence River near St-Edouard, through Laurier-Station, and onto the Appalachian foothills. Vertical exaggeration: 125x.

As the bedrock gradually rises in elevation, surface clays are progressively replaced by thinner coastal silts and sands. On the south side of the bedrock ridge at the center of the section, offshore marine facies are rare. Instead, they are replaced by nearshore marine sediments, then by the coarser deltaic sediments emplaced by Rivière du Sud at St-Raphaël. Higher up in the foothills, the steep rise of the bedrock surface results in landscapes that are not favorable to the accumulation of unconsolidated sediment, and the bedrock surface thus remains very close to the surface. There is a relatively continuous till blanket covering the bedrock depressions. Discontinuous glaciofluvial sediments are locally interposed between the till and glaciomarine deposits, which form the rest of the stratigraphic column. Rather exceptionally, in the axis of some valleys where bedrock is particularly incised, sediments associated with an older configuration of the valley system can be found. The bottoms of rocky valleys can then be filled with several meters of fluvial sediments. Occasionally, sandy units interpreted as proximal glaciomarine deposits may be observed within the main body of clayey marine unit but are too local to be modeled regionally and are thus not illustrated.

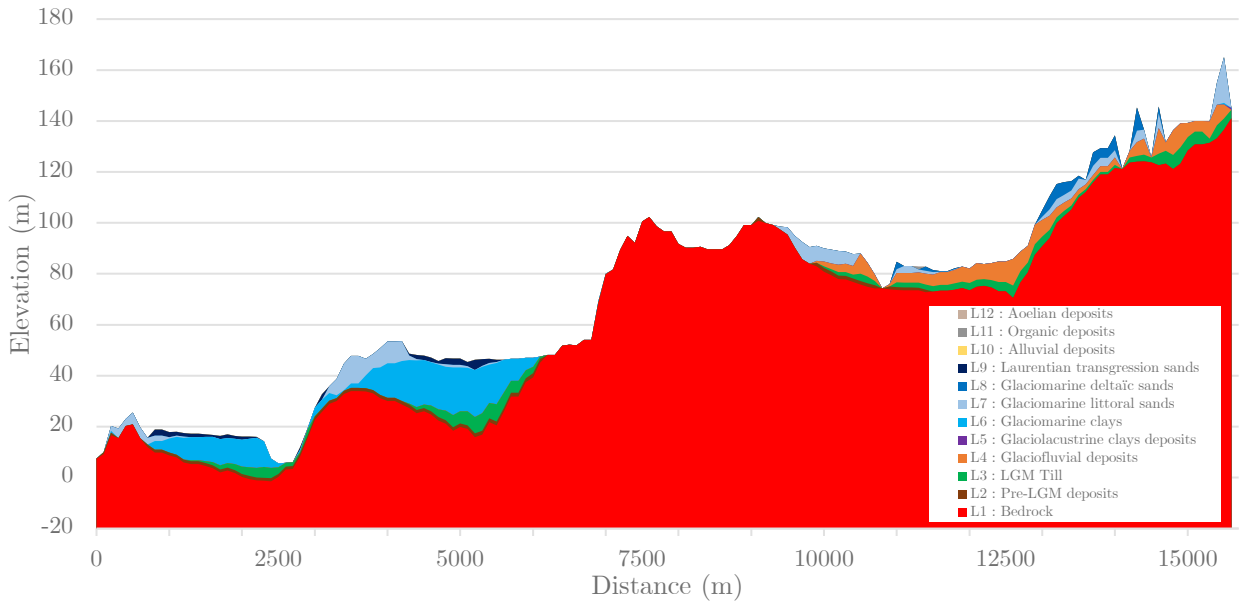

Figure 3.19 : Surficial geology cross-section B – B' between St-Michel-de-Bellechasse and the St-Raphael delta. Vertical exaggeration: 40x.

3.6.3 Conceptual cross-sections and hydrogeological contexts

As the bedrock topography of the study area is very rugged and the relative thickness of surficial units is generally low but still highly variable, it can be challenging to illustrate the typical geological sequence in a meaningful way in a single cross-section. A conceptual composite geological cross-section is presented at Figure 3.20 and includes a simplified version of most of the geological contexts present in the area. The section shows that the bedrock is mostly depressed near the coast (left), and gradually rises inland (towards the right). Outcrops in the coast zone are common, and bedrock depressions farther inland create contexts where sedimentary basins are partly isolated and laterally disconnected. Complex but usually thinner arrangements are encountered in the Appalachian foothills at elevations higher than the maximum submersion limit of the post-glacial sea. A typical transgressive unit, mostly composed of fine sand and silt, located between near-shore sediments and fluviatile sands is illustrated in the left part of the cross-section. The sequence of events is exposed in the "B" part (sequence stratigraphy) part of Figure 3.20. The regional geology makes for a relatively simple hydrogeological setting that, however, varies greatly laterally. Aquifer formations are mostly at the top of the sequence, with the exception of buried

valley aquifers and "intra-Goldthwait" sandy strata. The lateral extent of both are highly controlled by the bedrock topography.

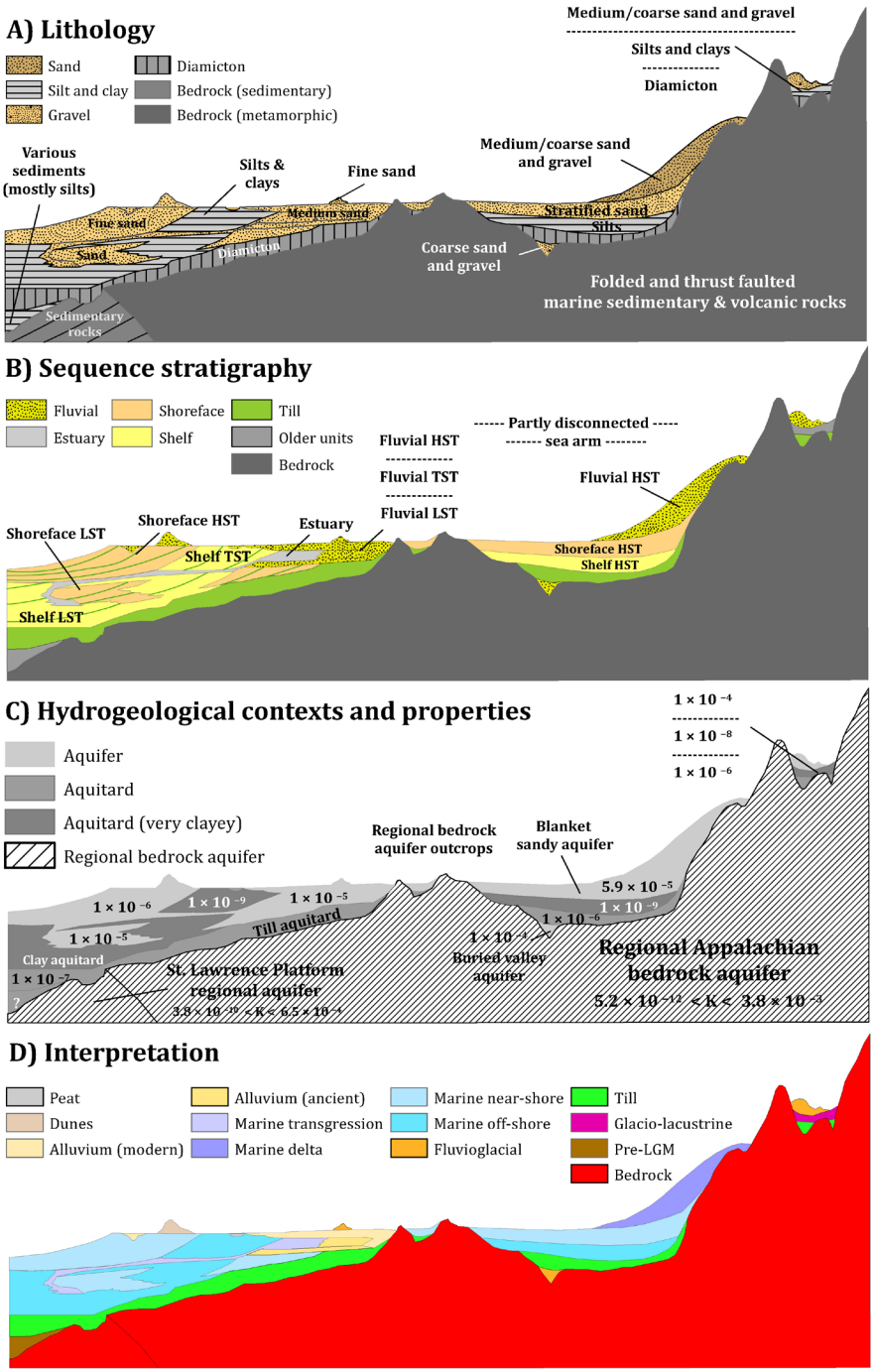

Figure 3.20 : Conceptual geological and hydrogeological cross-section of the study area (NW-SE, from left to right): A) Lithostratigraphy; B) Sequential stratigraphy; C) Hydrogeology; D) Genetic interpretation. Hydraulic conductivities (K; m/s) are from Tecsult (2008), Ladevèze (2017) and Janos *et al.* (2018). Sequence stratigraphy abbreviations are as follows: HST: Highstand system tract; TST: Transgressive system tract; LST: Lowstand system tract.

3.7 Discussion

The 3D geological model was developed over a period of three years as part of a regional hydrogeological characterization program (Lefebvre *et al.*, 2015) and was later extended both towards the north-east to Rivière-du-Loup, and the southwest to Plessisville (Lotbinière) in order to include key areas. However, a geological model is only as reliable as the input data used to build it. Considering that more than half of the observations used to build this model come from the public driller's logs (Système d'Information Hydrogéologique – SIH), there are some uncertainties a clear uncertainty about the model in several areas. Nevertheless, as the model was built using a detailed, high-resolution surficial geology map as both a hard constraint and a conceptual model, the modeling results can be viewed as relatively reliable. A notable gap in boreholes distribution (associated with a lack infrastructure and occupation) in the axis of St-Pascal, St-Alexandre and St-Antonin villages (north-eastern part of the study area) greatly impacts the representation of this zone in the 3D model. The occurrence of glaciofluvial deposits in the area is clear from the surficial geology map, but the rugged bedrock topography and lack of boreholes in this vast post-glacial drainage system make it impossible to model accurately using the available data. Instead of representing these deposits conceptually, they were omitted from the model and only the surface till is represented in this area. This drainage system is oriented northeast toward the St-Antonin Moraine, which is accurately depicted in the model as several boreholes are available in its vicinity as well as directly on this surficial feature.

3.8 Conclusion

The objective of this study was to develop a 3D model of the Quaternary deposits in order to define the geological sequence and to model the geometric relationship between each unit in order to create a coherent and seamless "common earth" model that can be used in other applications such as regional hydrogeology and groundwater flow modeling. To do so, we compiled existing and new geological, geophysical, hydrogeological and paleofaunal data in a GIS approach to build the model and constrain it using topological rules derived from a high-resolution surficial deposit map based on an available LiDAR survey for the same region. The stratigraphic succession observed in the study area presents a challenge in understanding the events that followed the last

deglaciation. The assessment of the depositional architecture in the area and the development of a three-dimensional geological model have revealed a few unsuspected geological features, including considerable clay thickness above the maximum marine submergence as well as a potential sandy aquifer unit associated with the Laurentian Transgression and/or subsequent minor transgressive/regressive events. In this narrow coastal zone where most land is intensively used for agricultural activity, water demand will not decrease any time soon. Several wells are drilled into deep formations bearing brackish water. An in-depth study of those units would provide an opportunity to define the industrial potential of groundwater resources.

3.9 Acknowledgements

This research was supported by the Fonds de recherche du Québec - Nature et technologies (FRQNT) doctoral scholarship of Guillaume Légaré-Couture and by funds from the Projet Chaudière-Appalaches of the PACES program of the Ministère du Développement durable, de l'Environnement et de la Lutte contre le changement climatique, led by Dr. René Lefebvre (INRS-ETE). This project also benefited from funds coming from the Research Affiliate Program (RAP) of the federal government of Canada via the Geological Survey of Canada (GSC). The Geological Survey of Canada (GSC) funded the rotosonic drilling via the Public Safety Geoscience Program of Natural Resources Canada. Heather Crow (GSC) is thanked for the borehole geophysics analysis. Jean-Pierre Guilbault (Musée de la paléontologie et de l'évolution) was responsible for the marine microfaunal analysis. We would also like to express our gratitude to the entire research team of the PACES Chaudière-Appalaches project, this small piece being part of the larger project. We would like to thank to Jean-Marc Ballard (INRS-ETE) for running the CPT drilling rig and dealing with all the complications that come with drilling boreholes in unknown terrain. Thanks also to Miroslav Nastev (GSC) who also helped with the field work.

4 Article 3: Paleo-ice streams in the St. Lawrence valley – New evidence of fast ice flow activity in the Québec-Labrador sector of the Laurentide ice sheet based on airborne LiDAR surveys and field surveys

Paléo-courants glaciaires dans la vallée du Saint-Laurent - Nouvelles preuves d'écoulement rapide de glace dans le secteur Québec-Labrador de l'Inlandsis Laurentidien sur la base de levés LiDAR aéroportés et de travaux de terrain

Auteurs :

Guillaume Légaré-Couture[1], Michel Parent[2] & René Lefebvre[1]

[1] Institut national de la recherche scientifique – Centre Eau Terre Environnement (INRS-ETE), Québec, Canada

[2] Commission géologique du Canada, Ressources naturelles Canada, Québec, Canada.

Titre de la revue ou de l'ouvrage :

Geomorphology

À soumettre en 2021

Contribution des auteurs :

Le premier auteur est responsable du développement de la méthodologie, de l'analyse, de la cartographie ainsi que de la rédaction de l'article. Les deuxièmes et troisièmes auteurs ont

contribué à la planification du travail, aux travaux sur le terrain ainsi qu'à la révision du manuscrit.

Lien entre l'article ou les articles précédents et le suivant :

La méthodologie présentée dans le deuxième chapitre est ici utilisée afin de cartographier les méga-linéations glaciaires présentes dans la vallée du Saint-Laurent.

Résumé :

Dans la basse et moyenne vallée du Saint-Laurent, entre la région de Québec et l'estuaire moyen du fleuve Saint-Laurent, un vaste système géomorphologique de terrain profilé est ici reconnu comme faisant partie de l'empreinte du Courant glaciaire du Saint-Laurent (*Saint-Lawrence Ice Stream, SLIS*), un paléo-courant glaciaire qui aurait opéré il y a environ 18 000 à 13 000 ans. Des milliers de méga-linéations glaciaires (*Mega-scale glacial lineations, MSGL*) convergentes ainsi que des éléments de marge de cisaillement ont été identifiés, cartographiés et interprétés en utilisant des modèles numériques de terrain dérivés de levés LiDAR aéroportés disponibles pour certains secteurs de la vallée. Les linéations situées au-dessus de la limite de submersion des mers postglaciaires de Goldthwait et Champlain sont remarquablement bien préservées. Ces travaux permettent de proposer une nouvelle carte régionale des lignes d'écoulement pour cet événement, basée sur un assemblage d'affleurements rocheux érodés et profilés, de méga-fossés glaciaires, de méga-rainures et de traînées morainiques derrière abri. Divers secteurs problématiques sont identifiés pour les perspectives de recherche future. Une reconstitution paléogéographique suprarégionale des événements est proposée et soulève des questions quant à la chronologie des événements glaciaires tardifs.

Mots-clés : Courant glaciaire du Saint-Laurent, courants glaciaires, LiDAR, écoulement glaciaire rapide, méga-linéations glaciaires, géologie du Quaternaire, Dryas récent

Abstract :

In the Mid- and Lower St. Lawrence Valley, between the Québec City area and the St. Lawrence mid-estuary, a large land system of glacially streamlined terrain is here recognized as part of the footprint of the St. Lawrence Ice Stream (SLIS), a paleo-ice stream which operated between around c. 18 - 13 ka cal BP. Thousands of converging mega-scale glacial lineations (MSGLs) as well as shear margin features have been identified, mapped and interpreted using LiDAR-derived digital terrain models available for some parts of the valley. Glacial lineations located above the submergence limit of the post-glacial Goldthwait and Champlain Seas are remarkably well preserved. We propose a new regional flowlines map for this event based on an assemblage of preferentially eroded outcrops, glacial troughs, mega-grooves, mega-ridges and crag-and-tail ridges. Various problematic areas are identified for future research. A supra-regional paleogeographic reconstruction of the events is proposed and raises questions pertaining to the chronology of late glacial events.

Keywords : St. Lawrence Ice Stream, ice stream, LiDAR, fast ice flow, mega-scale glacial lineations, MSGL, Quaternary geology, Younger Dryas

4.1 Introduction

During the last glacial period, much of the North American continent was occupied by a massive ice sheet called the Laurentide Ice Sheet (LIS). The main deglaciation event started around 16 ka BP, when the LIS started to retreat rapidly (Dyke, 2004). In multiple areas of the ice sheet, ice streams, or corridors of rapid ice flow, were responsible for much of LIS mass wasting (Bond *et al.,* 1992). Ice streams are often analogically referred to as the arteries of ice sheets (see Bennett, 2003), capable of discharging massive amounts of ice from an ice sheet. They can be either surrounded by immovable bedrock (topographical forcing) or by zones of sluggish ice movement. The existence of paleo-ice streams in the LIS has been inferred from several types of evidence, including the bedform imprint, topographic constraints or the presence of major offshore sedimentary depo-centers (Stokes *et al.*, 2015). One of the widely accepted geomorphological indicator of fast ice flow is the presence mega-scale glacial lineations (MSGLs; Stokes & Clark, 2002). Although the exact mechanisms leading to the development of these elongated and profiled

bedforms remain a disputed matter, they are unquestionably created by fast-flowing ice. Contemporary ice streams on the West Antartic Ice Sheet (WAIS) have been shown to be very dynamic, slowing down and accelerating often abruptly, and could account for over 90% of all the ice sheet mass loss (Bamber *et al.*, 2000). While the existence of paleo-ice streams has been acknowledged for a long time, this area of research has gained significant traction over the past decades. A better understanding of the drainage regime and subglacial conditions of ice streams is critical to our assessment of current ice sheets around the world. Although the mass of ice streams is incorporated in global sea level, their activity may have led to large delayed impacts on global sea level, given their ability to drain large areas of ice sheets over short periods of time, and in a somewhat unpredictable way (Joughin *et al.,* 2002). A better understanding of the processes governing their activity is therefore vital, especially in the context of anthropogenic global warming.

The existence of a major northeastward flowing ice stream in the St. Lawrence River valley, named the St. Lawrence Ice Stream (SLIS), was recognized a few decades ago (Parent & Occhietti, 1999; Occhietti *et al.,* 2001b; Ross *et al.,* 2006), but has received considerably less attention than the concomitant ice streams that also operated in the northeastern part of the LIS. In the quest for a better cartography of glacial terrain, the growing availability of airborne LiDAR data has led to a paradigm shift in areas of smooth bedrock topography. Recently, LiDAR point clouds or LiDAR-derived digital terrain models (DTMs) have been used to investigate the bedform imprint of paleo-ice stream activity at various scales (Sookhan *et al.*, 2018). With the recent availability of high-resolution LiDAR-derived DTMs for key parts of the St. Lawrence River valley, investigating the SLIS bed footprint is becoming primordial not only to strengthen our understanding of the formation of MSGLs and other ice stream landforms, but also to understand the deglaciation dynamics of the St. Lawrence Valley.

This paper reports newly discovered flow sets of converging mega-scale glacial lineations (MSGLs) present on both the north and south shore of the St. Lawrence River forming a system here recognized as the bed of the St. Lawrence Ice Stream. The main aims of this research are to 1) investigate and map the footprint of SLIS in the St. Lawrence Valley; 2) characterize and classify

MSGLs and other sub-glacial features; and 3) interpret the glacial dynamics associated with the ice stream.

4.2 Study area

The supra-regional study area encompasses the middle to lower St. Lawrence Valley, and includes parts of its major tributary valleys. It is illustrated at Figure 4.1 in the context of the Québec-Labrador sector of the Laurentide Ice Sheet.

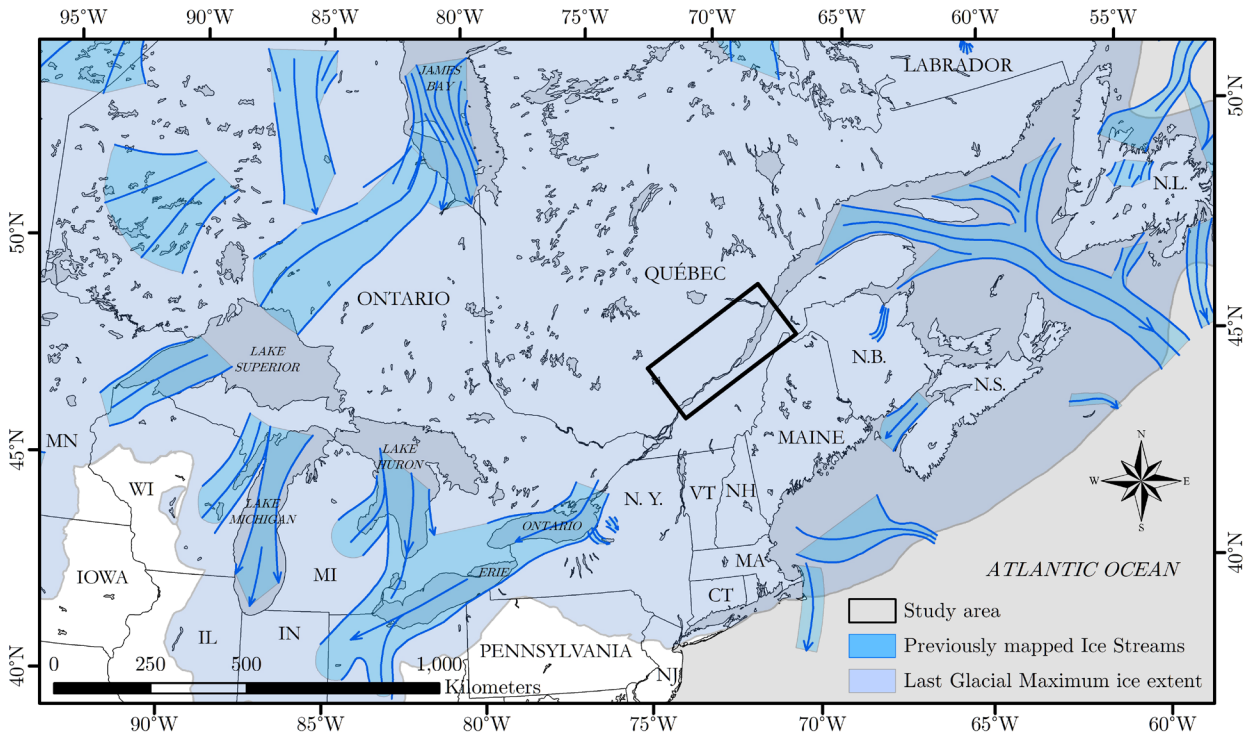

Figure 4.1 : Study area location relative to the northeastern part of the Laurentide Ice Sheet at the LGM (light blue) as well as other known ice streams (adapted from Margold *et al.*, 2015b).

This study area is further subdivided in key regional contexts (1-6) where the footprint of the SLIS varies considerably. These regions are illustrated in Figure 4.2, and are referenced in the following sections. The main SLIS trunk is known to have extended across regions 1, 2 and 3. This area covers a strip of land approximately 300 kilometers in length between Leclercville (Lotbinière) and Rimouski (on the south shore) and extends about 15 kilometers inland onto the Appalachian foothills. Previous studies and mapping efforts helped outline the main surficial geology features and Quaternary evolution of the region (LaSalle *et al.,* 1977; LaSalle, 1978; Normandeau, 2010;

Caron, 2013). Regional contexts 4, 5 and 6 are presented as areas upstream or peripheral to the SLIS and contribute to a better understanding of the main ice stream. As a complete review of the deglacial history of these areas is beyond the scope of present study, the reader is referred to Occhietti *et al.* (2011).

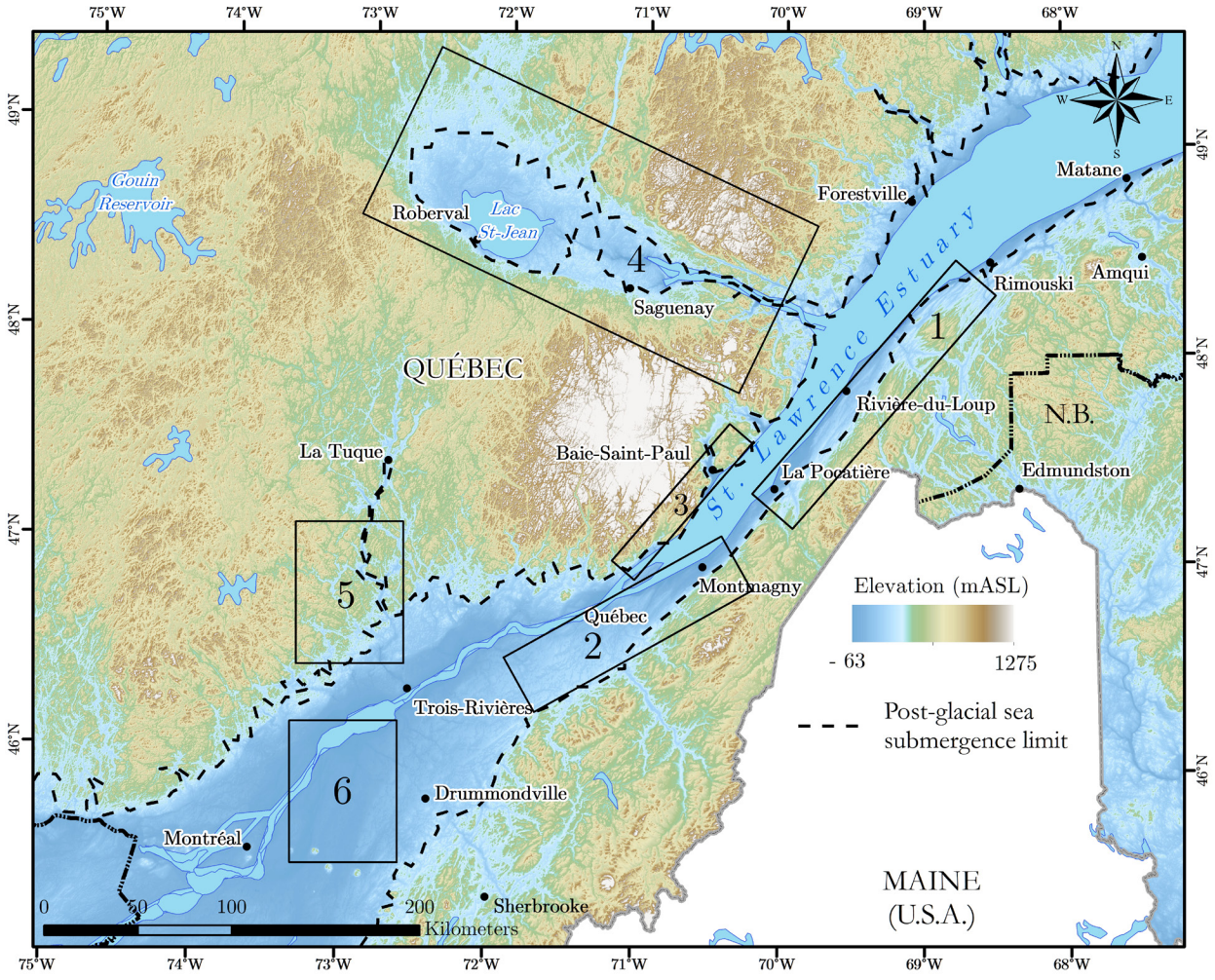

Figure 4.2 : Area of study and location of the regions referenced in the text. The post-glacial sea submergence limit is illustrated as a dashed black line.

4.2.1 Physiographical setting

The St. Lawrence Valley is an important link in the glacial history of North America as it occupies a central position between one of the core regions of the Laurentide Ice Sheet (LIS) and its terminal position at the latitude of New York. The region is marked by several ice flow events. During the Wisconsinan Stage, the lowlands of the St. Lawrence Valley were periodically invaded by marine

or glaciolacustrine water bodies whose history was governed by fluctuations of the ice front, regional glacio-isostatic adjustments and global sea level changes. From a geomorphological perspective, this part of the St. Lawrence Valley can be described as a series of plains and low plateaus superficially modified by coastal processes associated with the regression of post-glacial Goldthwait and Champlain seas in post-LGM time. Although a wide variety of deposits can be observed at the surface, marine sediments are the dominant facies. The ground topography is relatively flat, disrupted only by a series of SW-NE striking Appalachian bedrock ridges. The total overburden thickness varies between 0 and 110 meters (in boreholes) but is generally thin and is mostly controlled by the irregular bedrock topography.

4.2.2 Bedrock geology

The St. Lawrence Valley actually straddles three main geological provinces: the Canadian Shield (Laurentian Highlands) on the north, the St. Lawrence Platform in the middle, and the Appalachians on the south. Logan's line, a major fault that stretches from Lake Champlain to Québec City and beyond, separates the St. Lawrence platform from the Appalachians. The rocks of the St. Lawrence platform are sedimentary in origin, and Cambro-Ordovician in age. They unconformably rest on the igneous and metamorphic rocks of the Precambrian shield basement and are generally arranged in horizontal strata, which were slightly deformed during the Appalachian orogeny (St-Julien & Hubert, 1975).

4.2.3 Glacial history and previous work on the SLIS

We summarize here the glacial history and stratigraphy of the St. Lawrence Valley, with regards to events that took place between the Sangamonian interglacial and the Holocene.

Stratigraphic evidence from the St. Lawrence Valley suggests an erosive Illinoian glaciation that removed almost all traces of prior deposits, except for a few very local units found in cross-sections or boreholes (see Occhietti *et al.* (1995)). The oldest ice movement recorded in the Kamouraska region indicates an ice flow direction toward 120° to 130° (Martineau, 1977), but very few outcrops have preserved evidence of this movement. Pre-Last Glacial Maximum (LGM) deposits can be found locally in some sections (e.g. Occhietti (1977)), but their lateral extent is rarely more than

a few tens of meters, beyond which lateral connections are most of the time ambiguous. While the main ice sheet could have persisted in the Laurentian Highlands at least through MIS 5a, much of the St. Lawrence Valley was deglaciated, as evidence by the deposition of the St. Maurice Rythmites and the Vieilles Forges Sands, both deposited in free drainage conditions (Occhietti, 1982).

The main Wisconsinan glaciation started around the end of Marine Isotope Stage (MIS) 5, between the Sangamonian Stage and the current interglacial stage known as the Holocene. As the LIS expanded over high plateaus of central Québec and flowed southward and southeastward across the Laurentians. Smaller ice caps developed concomitantly in the Appalachians uplands (McDonald & Shilts, 1971; Lamothe *et al.*, 1992) as well as in the Charlevoix Highlands (Govare, 1995). The beginning of MIS 4 is marked by the readvance of Laurentide ice across the valley, with partial deglaciation recorded by glaciolacustrine deposits in the Appalachians (Lake Gayhurst) and marine waters in the Gulf and Estuary of the St. Lawrence (Gratton *et al.,* 1984; Dionne & Occhietti, 1996). The major ice mass formed by the coalescence of Laurentide ice with other ice masses in Atlantic Canada and New England is referred to as the major ice dome of the LIS (Occhietti *et al.*, 2011). At the LGM, the entire St. Lawrence Valley was completely covered by ice.

The deglaciation history of the lower St. Lawrence Valley is complex, as deglaciation modes varied considerably between the three physiographic contexts (the Laurentide Highlands, the St. Lawrence Lowlands and the Appalachian Uplands). The melting of the ice at counter slope in the valley favored the development of proglacial lakes at the southern margins of the ice sheet. Climate forcing and the ensuing negative mass balance of the main ice sheet produced a significant drawdown of the ice surface, and this in turn favored the development of ice streams, as topography progressively exercised more control on ice flow. It had long been thought that ice continued to flow southward during the regional deglaciation of the Appalachians, but subsequent research supported a late northward ice movement (Gauthier, 1975; Lortie, 1976; LaSalle *et al.,* 1977; Lebuis & David, 1977). This led to question the nature and paleogeographic context of the Appalachian "Highland Front" system of Gadd (Gadd, 1964). It was, however, argued that this

model included too many dissimilar and discontinuous elements to be included in a unifying geomorphological framework (LaSalle *et al.,* 1977; Prichonnet, 1977; Occhietti *et al.,* 2001b).

The best-preserved ice movements in the striation record on the south shore of the Lower St. Lawrence Valley are directed towards the north, with directions varying from 320° to 20°. These ice movements were interpreted by Martineau (1977) as the final ice movement of an isolated Appalachian ice cap flowing towards the post-glacial Goldthwait Sea, following the passage of a calving bay that progressed upwards in the St. Lawrence Valley during the deglaciation (LaSalle *et al.*, 1985). Martineau (1977) also identified ice movements towards the NE and the SW, the first direction being approximately parallel the St. Lawrence, and noted that the outcrops showing these striations were only found in the coastal zone. A considerable number of striations with azimuths between those two main orientations were also identified and were associated with deflections due to topography. However, as evidence showed that the northeastward ice movement was a significant one (LaSalle *et al.*, 1977a; Lebuis & David, 1977; Locat, 1977; Martineau, 1979, 1980), it became clear that north and northeastward striations cross-cutting older southeastward striae were indeed part of a large-scale post-LGM ice-flow reorganization and were not simply the result of a local temporary ice flow adjustment. The supra-regional glaciation model of the Maritimes area of Denton & Hugues (1981) required ice coming from the St. Lawrence Valley as well. Rappol (1993) interpreted this system of northeastward flow features in the coastal zone as a major ice flow event representing the convergence of Appalachian and Laurentian ice into a fast-moving ice corridor that developed into the Gulf of St. Lawrence. Surveys on the north shore of the St. Lawrence River revealed an extensive set of cross-cutting glacial striae, suggesting that a major ice-flow reorientation event towards the east and northeast took place after the LGM on the north shore as well (Lanoie, 1995; Dionne & Occhietti, 1996; Cloutier *et al.,* 1997). The St. Lawrence Ice Stream concept was developed a few years later by Parent & Occhietti (1999) as an important process intricately linked to the Appalachian ice-flow reversal event. Occhietti *et al.* (2001b) suggested that it was the combination of ice thinning, accelerated calving in the Gulf of St. Lawrence and climate forcing that increased the topographic control of the ice flow, and thus caused major flow reorientation in the LIS. This positive feedback loop shifted the predominantly southward LGM flow of the ice sheet towards a northeast-trending ice stream which penetrated

deep into the LIS, evacuating ice mass at a rapid flow rate, probably as much as one order of magnitude higher than that of the neighboring ice masses. The progressive thinning of the LIS by the action of the SLIS effectively broke the connection between the Appalachian ice mass (south shore of the St. Lawrence River) from the main Laurentide ice sheet (north shore). The concept of a calving bay in the St. Lawrence estuary during the latest deglaciation to explain the Appalachian ice flow reversal found considerable support in the 1970s and 1980s, but calving bay concept is much less necessary in a model that includes an ice stream (Parent & Occhietti, 1999). Occhietti *et al.* (2011) argued that in a model where ice was thinning fast on the south shore of the St. Lawrence River estuary, calving would in fact have occurred in a way that was parallel to the axis of the valley and the shore.

The timing of this ice stream activity is estimated to have begun between 15,500 and 14,000 BP (Occhietti *et al.*, 2001b, 2011), which would be concomitant with ice stream activity in southwestern Québec and eastern Ontario (Ross *et al.*, 2006), where the footprint of a sudden ice flow regime shift towards the southwest is also recorded. This last event is believed to have occurred around 14,400 BP, and is referred to as the Lake Ontario Ice Stream by Ross *et al.* (2006) and Occhietti *et al.* (2011), and to the Ontario-Erie Ice Stream by Taylor (1913) and Sookhan *et al.* (2018).

4.3 Methodology

The GIS analysis workflow as well as the terminology used to describe the geomorphological elements associated with the St. Lawrence Ice Stream bedform imprint are presented and assessed in the following section.

The identification of terrestrial paleo-ice streams relies largely on the mapping of mega-scale glacial lineations (MSGLs; see Clark, 1994). Most recent efforts to characterize the bedform imprint of paleo-ice streams of the LIS have been done using satellite imagery, airborne radar elevation data, photogrammetric elevation data. Eyles & Putkinen (2014), for example, used an hillshaded relief image of the Canadian Digital Elevation Dataset DTM (Natural Resources Canada, 1995) in order to map broad scale fast ice flow features on Anticosti Island, Québec, which are associated with the Laurentian Channel Ice Stream (Shaw *et al.*, 2006). While the identified features are indeed

clearly visible on their images, the spatial resolution of the CDED (0.75 arc seconds from north to south and 3 arc seconds east to west) generally limits the scale of investigation to broad features. Krabbendam *et al.* (2016) used Landsat 8 satellite images and Shuttle Radar Topography Mission (SRTM) Global 1 Arc, Version 3 with 30 m pixel spacing (NASA JPL, 2013) and stitched CDED raster tiles as their terrain data in order to describe and analyze 'hard-bed' landform systems from former Laurentide and British–Irish ice sheets. We show in Figure 4.3 a comparison between a LiDAR-derived 1-meter resolution hillshaded relief image (left) and an SRTM-derived hillshaded relief image (right) for the same area. The glacial lineations that are clearly visible on the left part of the image are clearly not visible on the lower-resolution DTM, making it impossible to map the continuity of ice flow features.

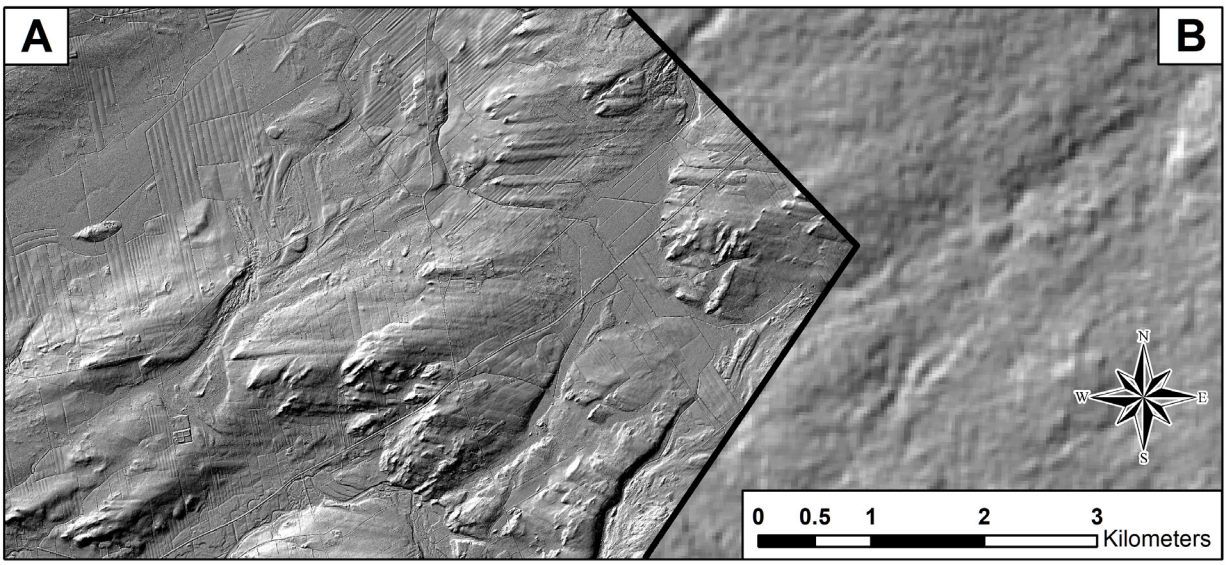

Figure 4.3 : Visual comparison of a continuous area between A) an hillshaded relief image calculated from a LiDAR-derived 1-meter resolution DTM and B) an hillshaded relief image calculated from SRTM 1-arc second DSM (NASA). The two images are separated by a black line. The continuity of the glacial lineations on the left section is completely lost on the right part of the image (area NW of Valley-Jonction, near the Chaudière River).

In the St. Lawrence Valley, the fact that the main alignment of the SLIS features parallels the strike of Appalachian bedrock complicates the interpretation of low-resolution global DTMs, as it is generally not possible to reliably distinguish bedrock lineations from glacial lineations. To further complicate matters, the radar-derived SRTM DEM is essentially a digital surface model (DSM) rather than a digital terrain model (DTM), as radar wavelengths do not penetrate the

canopy which is a patchwork of densely forested lots and open fields in the region. In the St. Lawrence Valley, most well-preserved glaciation lineations are in fact located in densely forested areas with thick canopies, while features located in plains tend to have been smoothed or even leveled out by agricultural activity over time or by the post-glacial marine invasion. Observations and interpretations using low-resolution satellite imagery or DTMs must therefore be made carefully and need to be supported by extensive field surveys.

In the present study, geomorphological elements associated with the SLIS were mapped primarily via the interpretation of several sets of high-resolution ground elevation data obtained from airborne LiDAR (Light Detection and Ranging) surveys. The high refresh rates and large swath angle of most airborne laser sensors allow not only precise elevation measurements, but also a good chance of penetrating the canopy. As metadata were not available for every survey, raw laser files (LAS point cloud format) were reclassified in order to identify ground returns using a standardized method for all surveys so that the derived-DTMs could be fully compatible. The average ground point spacing varied considerably between datasets, from 0.89 to 14.12 m. The Simple Morphological Filter (SMRF) approach (Pingel *et al.*, 2013) was incorporated into a JSON pipeline in the PDAL point cloud library (PDAL Contributors, 2018) in order to reclassify and export 1 m resolution DTMs for each tile. Regional DTMs were then created in SAGA GIS (Conrad *et al.*, 2015) using each region's tiles. Several different first derivative shaded relief rasters were computed for each region following a principal component analysis (PCA) of the DTM in order to determine illumination directions most associated with topographic variations. Subtle terrain morphology, for example, could be hidden in the shade of a large hill, and features whose forms or structures lie parallel to the direction of illumination can be essentially invisible. To solve this problem, multiple shaded relief rasters, or a multiple illumination hillshade (e.g., Webster *et al.* (2006)) were created so that no features are missed. Those analysis were done using Relief Visualization Toolbox (RVT) software (Zakšek *et al.*, 2011). Hillshades and other DTM derivatives such as terrain roughness were calculated in SAGA-GIS and visualized in QGIS, where glaciation lineations and ice margin features were interpreted and digitized directly into shapefiles. The final maps for the figures of this article were prepared in ArcMap 10.5

This cartography effort started in mid-2015, before the start of a national initiative of the Québec provincial government, in a partnership between 6 departments (Ministère des Forêt, de la Faune et des Parcs (MFFP); Ministère de l'Énergie et des Ressources naturelles (MERN); Ministère de l'Agriculture, des Pêcheries et de l'Alimentation du Québec (MAPAQ); Ministère du Développement durable, de l'Environnement et de la Lutte contre les changements climatiques (MDDELCC); Ministère des Transports du Québec (MTQ); Ministère des Affaires municipales et de l'Occupation du territoire (MAMOT)) and Hydro-Québec, to acquire and make available LiDAR-derived DTMs covering all public and private land in southern Québec. Consequently, new datasets from this program were added sporadically during the course of this research project as they became available.

As subglacial bed landforms terminology can still be somewhat contentious, we define here the terms used in this paper to describe ice stream glacial lineations and other associated bedform elements. The term "megascale" glacial lineations has recently been used somehow loosely to describe glacial lineations with lengths ranging for 100 meters to 180 kilometers (see table 1 in Spagnolo *et al.* (2014)). As terrestrial ice streams have been shown to generate shorter glacial lineations than marine ice streams, we opted here to include features of at least 100 m of length and an elongation ratio of at least 1 : 10, which is in line with most of the current literature (see Stokes and Clark, (2002)). Table 4.1 (modified from Krabbendam *et al.* (2016)) presents the glacial forms that are identified and discussed in the following sections.

Table 4.1 : Terminology of ice stream landforms and related features described in this paper (modified from Krabbendam *et al.* (2016)).

Feature	Description	Length	Elongation ratio
Crag-and-tail ridge	Hard bedrock knob followed by a tail of till on the lee side pointing in the local direction of the flow	$>$ 100 m	$>$ 1 : 10
Till fluting	Similar to the crag and tail, but where no specific bedrock knob is observed upstream of the till fluting	$>$ 100 m	$>$ 1 : 10
Glacial trough	U-shaped valley carved into the bedrock where ice flow was channeled	$>$ 1000 m	$>$ 1 : 10
Eroded bedrock with drift bed	Outcrop where the upper part of the rock was seemingly cut clean by ice flow, with associated till fluting on the lee side	$>$ 1000 m	$>$ 1 : 10
Streamlined rock bed	Highly elongated large bedrock outcrops almost wiped clean of sediments	$>$ 1000 m	$>$ 1 : 20
Mega-furrow	A highly elongate negative feature where grooves in soft sediment circumvent a bedrock outcrop	$>$ 1000 m	$>$ 1 : 10
Rock drumlin	A positive streamlined rock feature, less elongate than a megaridge, with the typical convex drumlin forms	$>$ 100 m	$>$ 1 : 10
Mega-ridge/Bedrock fluting	A positive rough bedrock feature more elongate than a rock drumlin,	$>$ 100 m	$>$ 1 : 10
Megalineation	A collective term for highly elongate positive and negative features	$>$ 100 m	$>$ 1 : 10

Fieldwork and geological observations along with detailed surficial geological mapping were conducted in the main trunk area of the SLIS, both on the north and south shore of the valley. While many geological and geomorphological features observed on LiDAR DTMs were obvious in the field, smaller features were often impossible to be ground truthed and confirmed because of poor access, ruggedness or insufficient relief of the features.

4.4 The St. Lawrence Ice Stream bedform imprint

The SLIS bedform imprint includes a series of landforms observed in key terrestrial areas of the St. Lawrence Valley. These areas are outlined in Figure 4.2. All localities referenced in the text are shown in Figure 4.4.

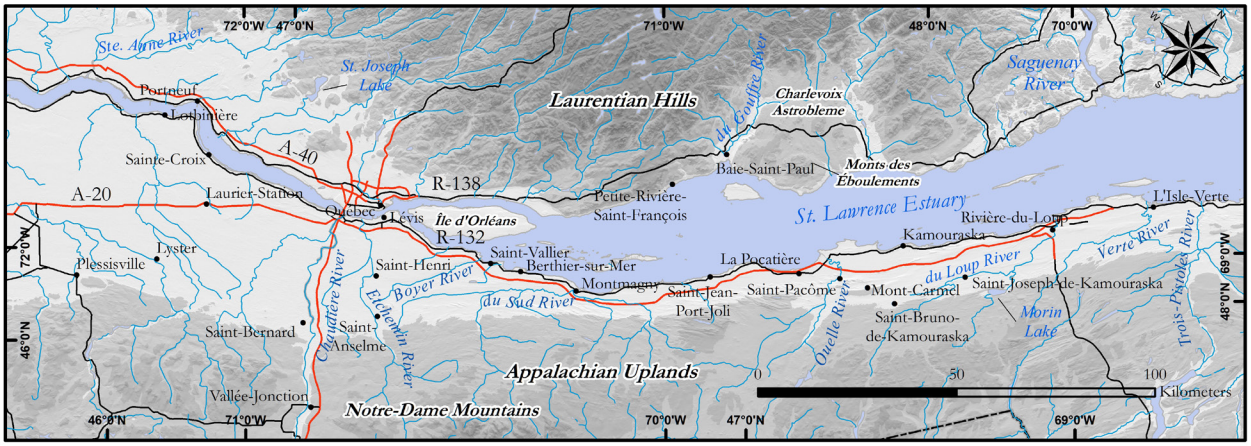

Figure 4.4 : Map of all the locations referred in the next sections.

Some of the figures are illustrated in grey scale shaded relief images instead of color-shaded relief in order to highlight less perceptible features. Elongated glacial landforms associated with fast ice flow were observed in all areas in the lower St. Lawrence Valley, particularly in the Appalachian and Laurentian foothills. Many bedforms located below the post-glacial sea submergence limit have been obliterated as a result of active erosion and reworking during the regression of the post-glacial Goldthwait and Champlain seas. The analysis of the currently available high-resolution DTM data in the St. Lawrence Valley reveals a part of the main trunk of the SLIS, as well as several marginal deposits, secondary ice streams and divergent flows.

4.4.1 Main trunk: South shore, Lower St. Lawrence Valley

The St. Lawrence Ice Stream was the main ice stream that formed in the Lower St. Lawrence Valley (region 1, Figure 4.2). Various features of the ice stream, most notably abrupt shifts in ice-flow direction, had been identified over the years in previous reports (Rappol, 1993; Parent & Occhietti, 1999; Occhietti *et al.,* 2001b), but were never assembled nor fully put into context due to the lack of spatially connected terrain data.

Ice from the SLIS flowed from southwest to northeast in the eastern St. Lawrence Valley. The main trunk is located in regions 1 and 2 of Figure 4.2, where most of the terrain stands between 100 and 120 meters above current mean sea level, which implies that most ice streams features were subject to active marine reworking by littoral and nearshore processes during post-glacial

marine emergence. Given the strong structural control on major bedrock landforms, beaches and raised shorelines tend to be aligned parallel to the St. Lawrence Valley and are thus also aligned with most of the glacial lineations formed by the SLIS main trunk.

Between the Etchemin River and St-Vallier, two 3 km-wide mega-grooves are carved in bedrock and antecedent glacial deposits (Figure 4.5). They are bounded to the west by the Boyer River, which partly filled the depressions with fluvioglacial and fluvial sediments following deglaciation. Both furrows were carved in feldspathic sandstone and wrap around an outcrop area of mudrocks with siltstone interbeds. The mudrocks are also streamlined, particularly in the downstream section of the mega-furrows. It is likely that these were carved during an ice stream phase where the center of the outcrop was a sticky spot as a full-fledged SLIS flowed over the entire area. MSGLs found on the Ile d'Orléans (see following section) at similar elevations support this hypothesis. The west depression disappears under the St. Lawrence River, where it widens to about six kilometers. The east groove can be traced over a distance of 50 kilometers, its downstream end marking the onset of a long corridor of streamlined bedrock MSGLs. This corridor extends over at least 100 km before disappearing under the estuary.

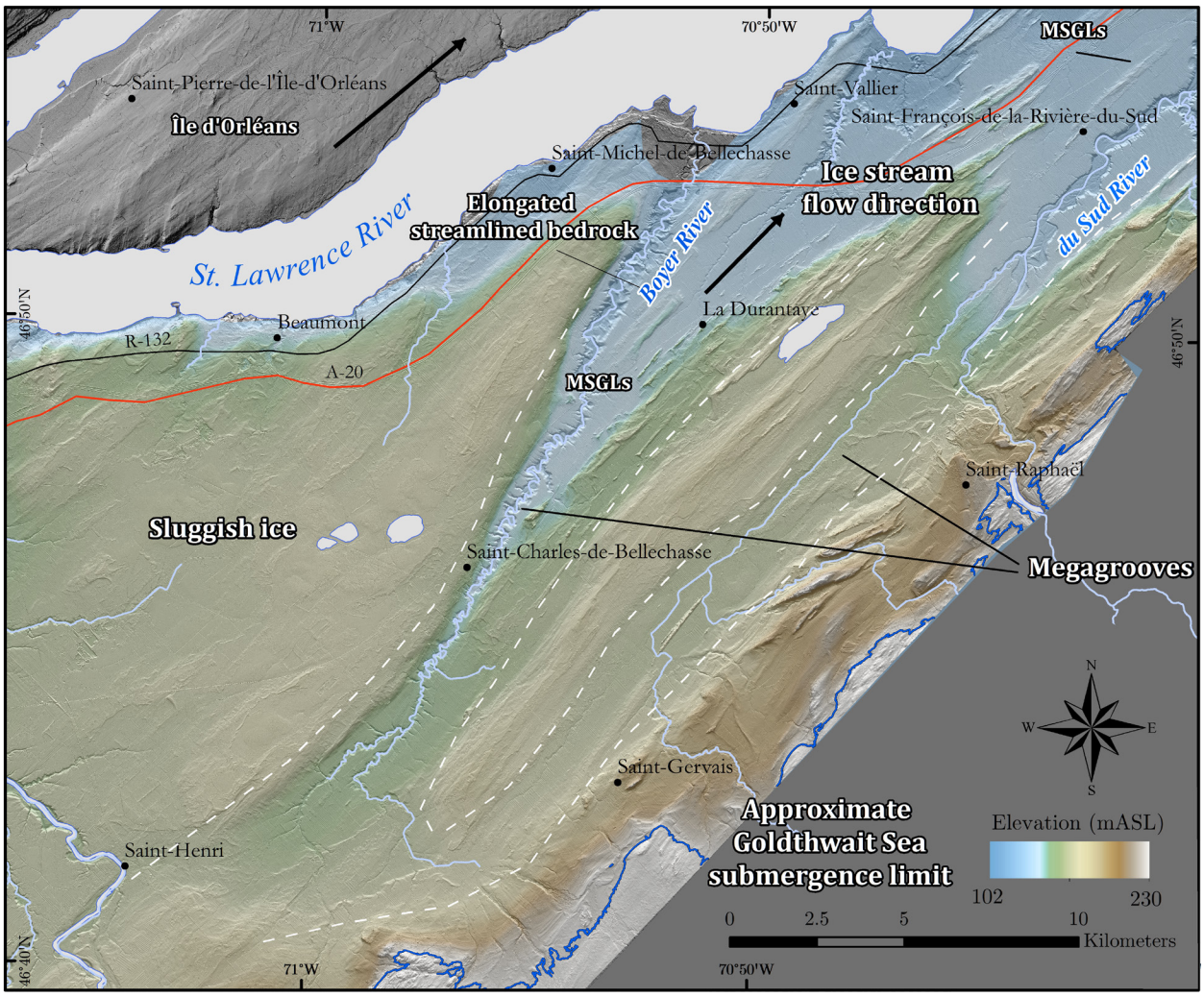

Figure 4.5 : Mega-furrows carved in soft sediments and bedrock in the Bellechasse area. Dashed white lines mark the margin of the mega-furrows.

The main trunk of the SLIS, and its fastest-flowing zone based on elongation ratios of MSGLs, is located in the Kamouraska region on the south shore of the valley. One of the most prominent features of the southern part of the bed is the pattern of curved and elongated streamlined bedrock mega-ridges and mega-furrows striking SW-NE, which are followed by tails of glacial till on the lee side (Figure 4.6). Located about 2.5 km northeast of Saint-Bruno-de-Kamouraska, this set of rock outcrops separates the lower Appalachian foothills (northwestern side, ≈185 mASL) from a plateau sitting at 220 mASL (southeastern side). The ridges are up to 50 meters high, with a width varying from 20 to 200 meters. They are composed of hard feldspathic sandstone knobs and tails consisting of very local, typical Appalachian till. The length of the tails, which average about 1.1 km, is not proportional to the size of the bedrock outcrop. There is a noticeable 3-4 degrees

deviation between the bedrock strike and the ice flow direction inferred from the glacial sediment tail, which suggests that local topography exerted only partial control on ice stream flow.

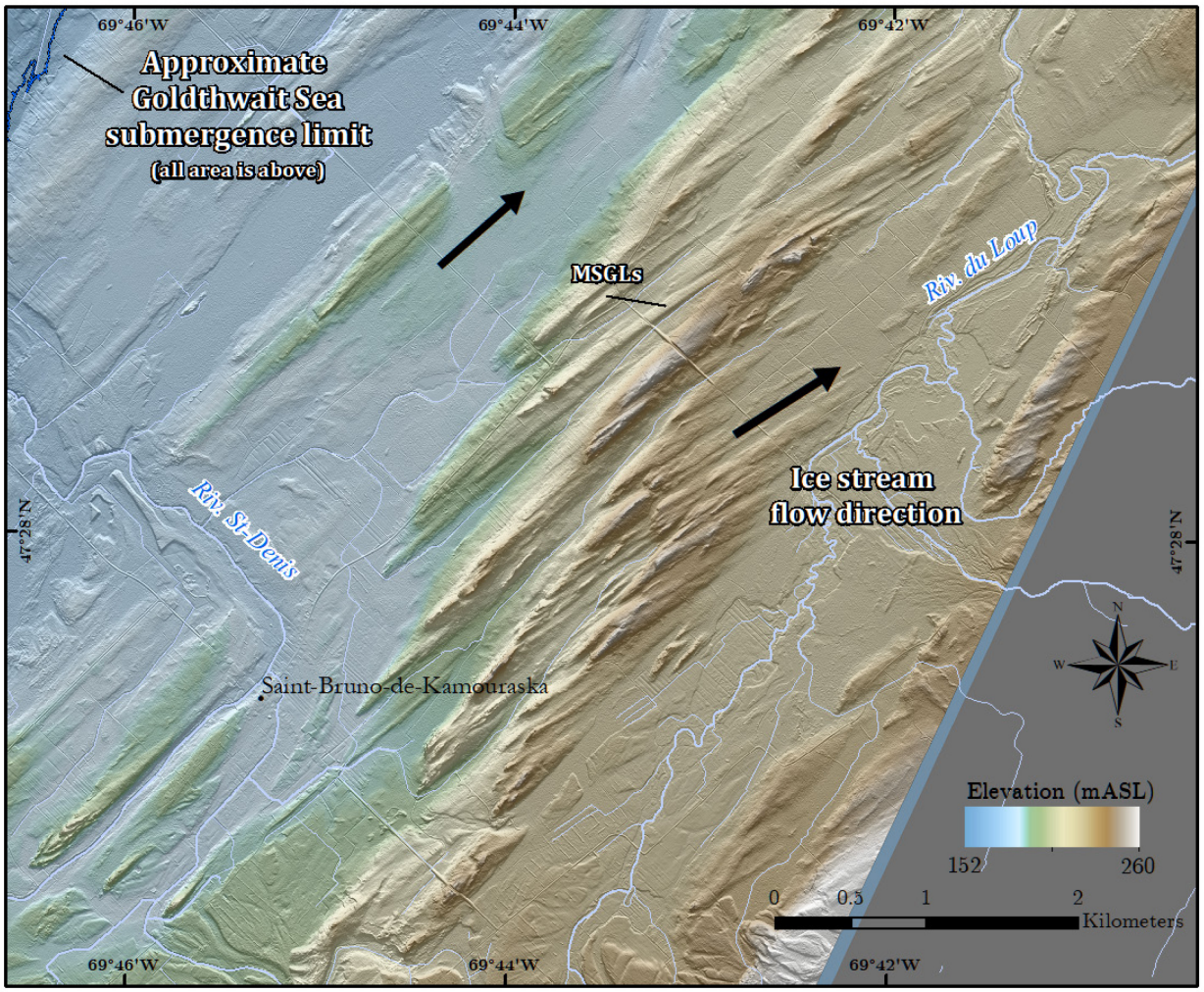

Figure 4.6 : Mega-ridges and till flutings near St-Bruno-de-Kamouraska. The two main ice flow directions are shown as black arrows.

Between Mont-Carmel and St-Pacôme, large over-deepened furrows formed around both sides of prominent orthoquartzite outcrops, creating depressions about 15 meters below the surrounding till plain (Figure 4.7). The bifurcating, sinuous furrows around strike ridges suggest that the basal ice stream was undergoing enhanced plastic flow around large bed obstacles.

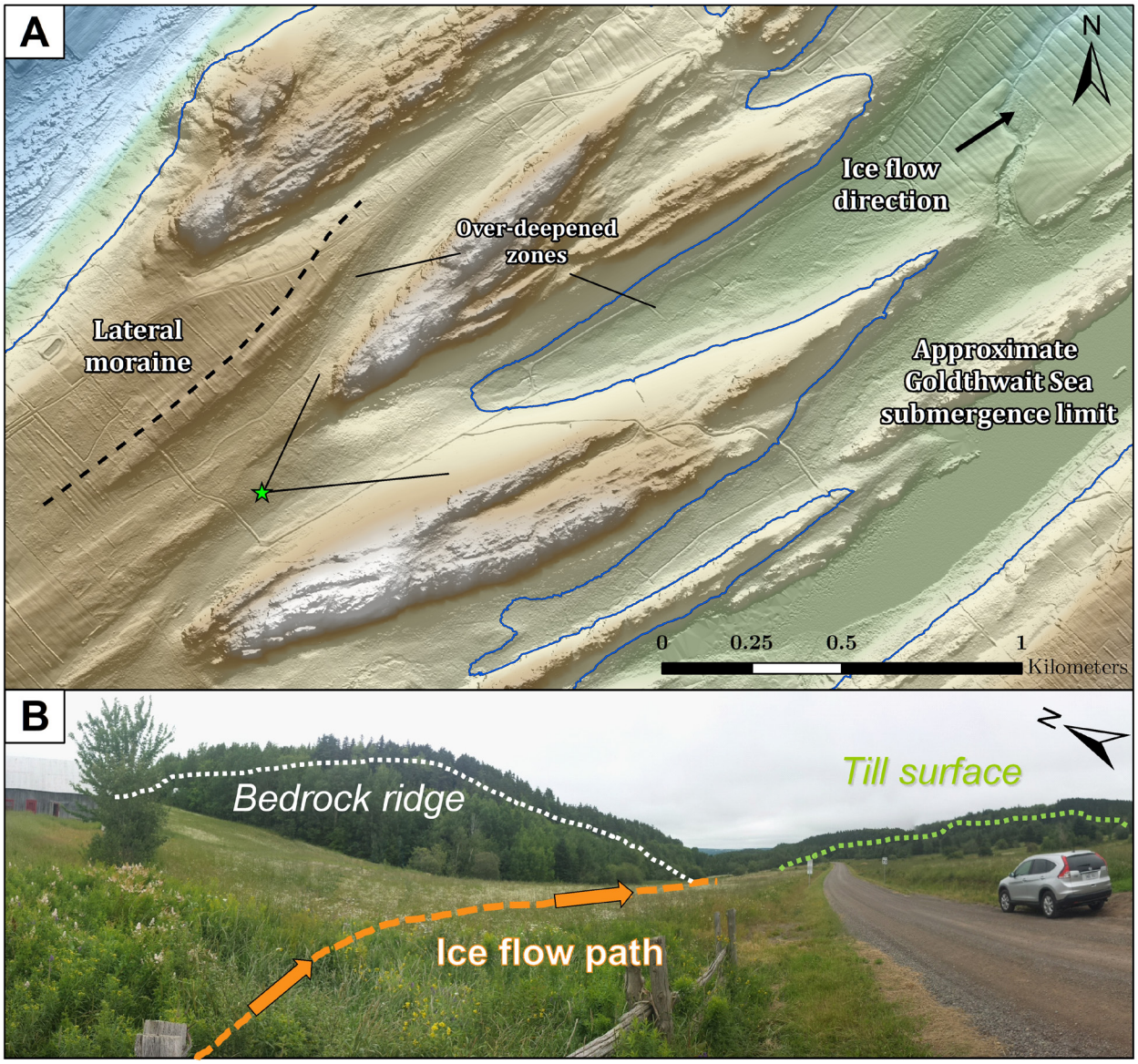

Figure 4.7 : A) A set of bifurcating overdeepened mega-furrows created around Appalachian rock outcrops near St-Pacome. B) Wide angle photograph of the center ridge and grooves set from the ground (Lat/long coord.: 47.4174, -69.9254).

Northeast of St-Joseph-de-Kamouraska (northwest of Lac Morin), a prominent corridor of very thin MSGLs over glacially polished Appalachian feldspathic sandstone is exposed (Figure 4.8). It forms a several km-long strip between two minor streams where the streamlined landforms are cross-cut by the younger drainage system. The corridor is at least 2 kilometers wide, but most likely extends over the boundary of our LiDAR dataset. The smoothed topography shows small bedrock outcrops and associated flutings often stretching over 5 kilometers, with a few sediment tails having elongation ratios of over 1: 50. This smoothed mega-lineated bedrock was formed in

a zone where the bedrock floor is relatively flat, which is the closest geomorphological analog to modern ice streams beds (e.g., Livingstone *et al.*, 2012). It is interpreted as the last fast flow tract of the SLIS. The SW-NE direction of the flutings is strikingly parallel to local bedrock strike, which may indicate that the accelerated flow was in part due to low frictional resistance at the ice stream bed. Characteristically, a thin compact till overlies bedrock outcrops in the area. This till may have been compact enough to have facilitated ice flow over the rock basement. As those large scale elongated bedforms are most likely the result of preferential focused abrasion, a relatively constant sediment supply would have been required to maintain this type of bed (see Spagnolo *et al.*, 2016).

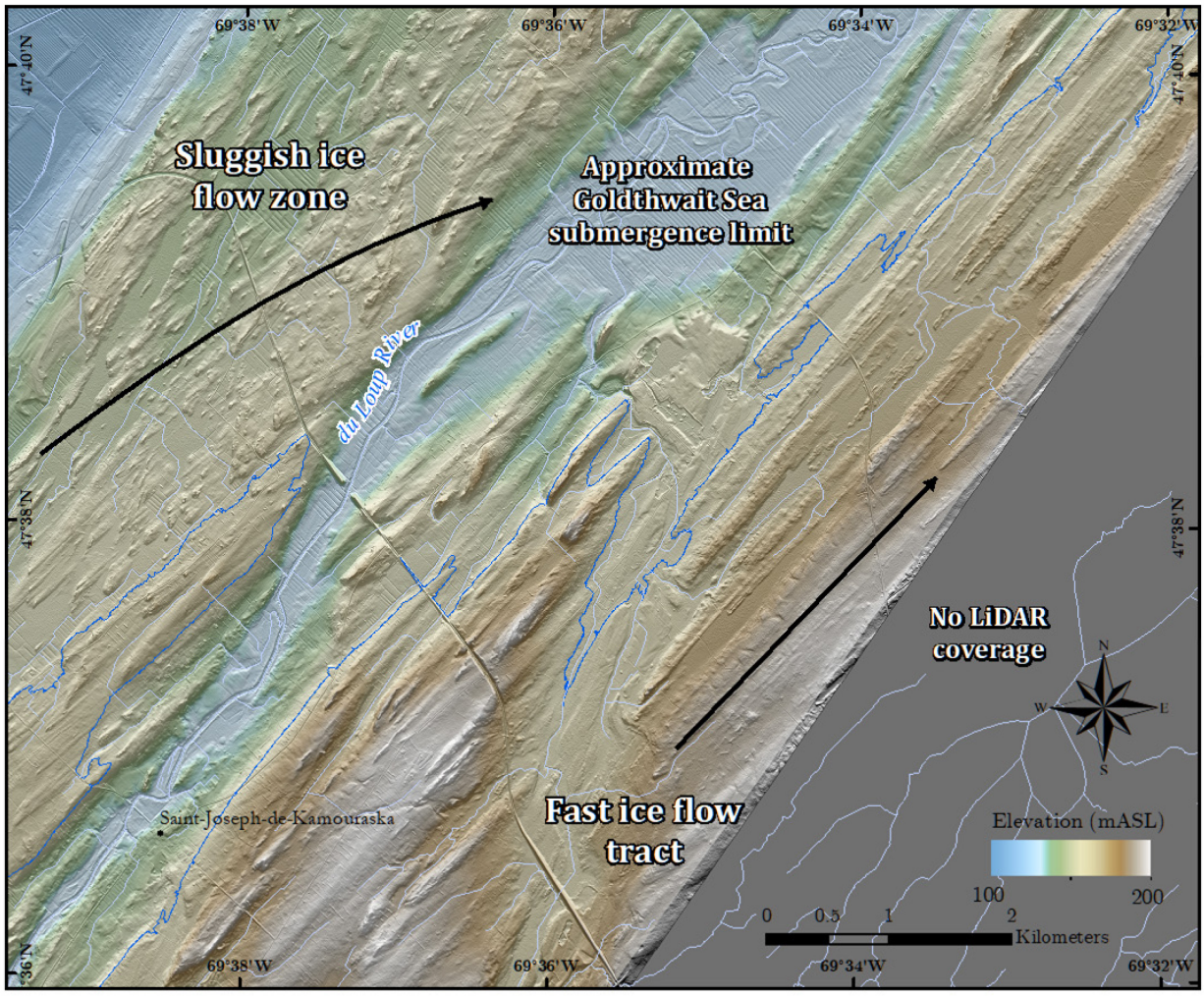

Figure 4.8 : The St. Lawrence Ice Stream main trunk southwest and upstream of the St. Antonin Moraine, near St-Joseph-de-Kamouraska. The Goldthwait Sea submergence limit is shown as a blue strait.

Directly west of the fast ice flow tract, hundreds of small crag-and-tails are observed (the "sluggish ice flow zone" of Figure 4.8). These features, which are the smallest linear bedforms observed in the SLIS imprint, are located on an elongated plateau between two valleys that were fully inundated during the Goldthwait Sea incursion that succeeded ice stream activity. Even though the plateau lies a few meters below the local submergence limit for that area, most bedforms were preserved from erosion and reworking by littoral processes. These small crag-and-tails features cover an area of about 2000 square meters, and their shapes are highly variable. While the bedrock strikes towards the NNE, perhaps parallel to MSGLs formed previously, till flutings show a 30-degree deviation towards the east and exhibit high spatial coherence. This deviation suggests that the zone of slower ice flow converged into the fast track area.

At Rivière-du-Loup, the bedform signature of the main trunk disappears in the axis of the St-Antonin Moraine (Martineau & Corbeil, 1983; Rappol, 1993), which overlies the streamlined bedrock over a distance of about 15 kilometers. The signature of the streamlined bed reappears downstream at the latitude of Ile Verte. Between this location and the Trois-Pistoles River delta, a 20-kilometer-long curved track of somewhat roughly streamlined bedrock consisting of arkose and conglomeratic sandstone is observed (Figure 4.9). In this area individual crag-and-tails are almost non-existent, which suggests that basal conditions must have been different than those which produced the bed found upstream of the St-Antonin Moraine. Elongation ratios of over 1:60 observed on a few outcrops suggests a higher flow velocity than upstream. The arcuate streamlining pattern suggests convergence of ice sourced from the southwest as well as from the southeast, in the Appalachian uplands. Out of the 34 striations reported in the streamlined zone (Lee, 1962; Lortie & Martineau, 1987; Rappol, 1993), none record a northeastern ice flow event, although Rappol (1993) reported northeastward striations associated with the SLIS in the narrow coastal zone closer to the St. Lawrence River.

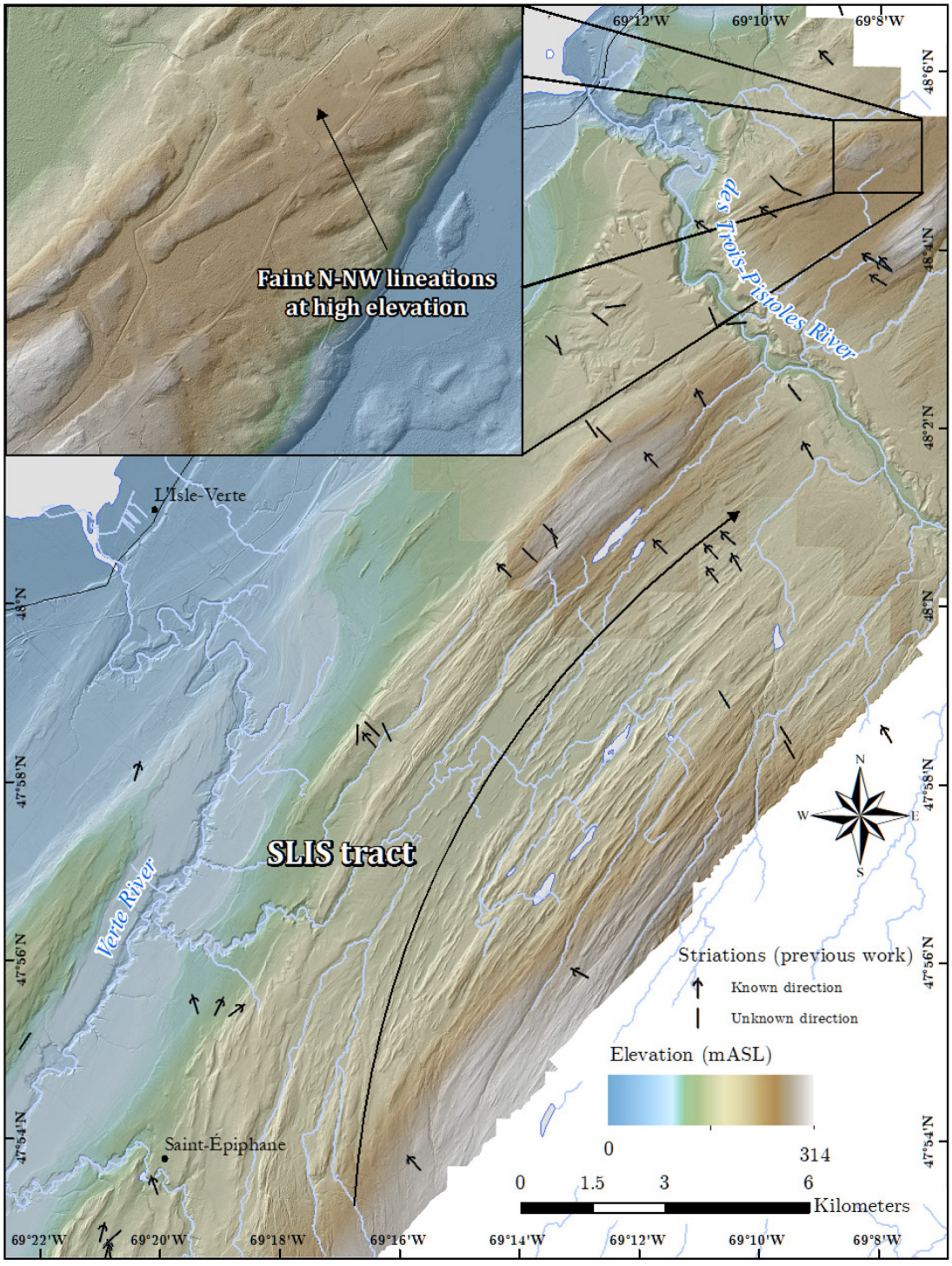

Figure 4.9 : Streamlined hard bed recording a main trunk of the St. Lawrence Ice Stream in the vicinity of Trois-Pistoles. Also shown are striations reported by Lee (1962), Lortie & Martineau, (1987) and Rappol (1993). An older ice movement towards the northwest is recorded in glacial lineations (upper left insert).

Bedrock outcrops streamlined towards the northeast are visible past the Trois-Pistoles River again, but they seem to predate a younger ice movement towards the northwest that is registered as faint till flutings (see insert of Figure 4.9), matching exactly the mean striae direction for this area, which is about 326°. This northwest ice-flow system was traced up the Temiscouata Valley and into New Brunswick. Rappol (1993), who had tentatively associated this late ice movement to a terrestrial ice stream, had noted that the absence of northwestward striae downstream of Trois-Pistoles could be associated with slower or less erosive ice flow. The current lack of LiDAR data for the coastal zone between Trois-Pistoles and Rimouski does not allow us to map the terrestrial extent of the SLIS further to the northeast. However, no MSGLs could be identified from a LiDAR scan of the Rimouski/Neigette area from the coast to about 10 kilometers inland. This implies that the bedform imprint of the SLIS is either locally covered by more recent deposits, that the main trunk was located in the central axis of the estuary or that it was located farther inland.

4.4.2 Ice stream margin and tributaries: North shore, Mid- to Lower St. Lawrence Valley:

Directly northeast of Québec City, the St. Lawrence River splits in two channels and flows around Île d'Orléans on which a very distinctive set of MSGLs can be observed downglacier of bedrock outcrops located at the southwest end of the island (upper left corner of Figure 4.5). The southwestern tip of the Île d'Orléans lies perpendicular to the mega-furrows described in the previous section. It seems likely that the local ice stream flow conditions were comparable to those leading to the formation of mega-furrows on the south shore. Thus, early ice stream activity may also be responsible for the overdeepened mega-furrows wrapping around Ile d'Orléans.

While the area around Québec City does not record much evidence of fast ice flow, a few MSGLs can be observed in the hills southwest of Lake St. Joseph and southeast of Sergent Lake, where they converge towards the central axis of the St. Lawrence Valley. Rapid ice flow over crystalline basement bedrock leaves an imprint that differs from the lineations found on the softer bedrock on the south shore and are reminiscent of the "glacial scour" described by Krabbendam *et al.* (2016) and also encountered by Sookhan *et al.* (2018). Those bedforms are further discussed in the section on the Portneuf – Mauricie region.

Glacial lineations are virtually absent on the north shore of the St. Lawrence River between Québec City and Beaupré. Beyond that location, a few northeast-trending glacial lineations, essentially small crag-and-tails, are observed on low uplands at the southeastern margin of the Laurentian Hill. The orientation of till tails varies considerably locally and tends to be oriented along the valley floors, which suggests a high degree of topographic control. This area forms a corridor about 10 kilometers wide from the coast, where the bedrock is more flattened, soft and uniform. The signature of this northern SLIS margin is lost in the vicinity of Petite-Rivière-Saint-François, where a series of recessional moraines are deposited transversely to the ice flow. In the high uplands directly west of Petite-Rivière-Saint-François, at an altitude above 500 m, a small zone of till flutings aligned northwest/southeast can be observed on the LiDAR DTM, but their orientation is at odds with nearby SLIS features. This is unlikely to be due to a local ice deflection, as the same lineation pattern also occurs on the west flank of the Rivière du Gouffre Valley, between Baie-St-Paul and La Mare.

The Charlevoix astroblem area displays three distinct flowsets featuring at small crag-and-tails whose lengths range between 50 and 2500 m (Figure 4.10). Along the coast, sheltered by the Mont des Éboulements, a flowset toward the northeast is attributed to the SLIS main trunk. Striae found on streamlined paragneiss outcrops along the main road show a direction of 18°. Faint till flutings and crag-and-tails oriented towards the south-southeast in the southwest part of the astrobleme record a seemingly pre-SLIS flow phase. A third, eastward-trending flowset is also observed in the astroblem. It was referred to as the "Jean-Noël ice flow" by Brouard (2016). Features located at the intersection of the second and third flowsets show cross-cutting relationships in the form of "palimpsest" forms in the axis of the Jean-Noël Valley. Brouard (2016) interprets the partial lack of topographic steering of the eastward ice movement either as a consequence of the thinning of the LIS at its southern margins near the St. Lawrence estuary, or as a tributary to the SLIS. The striae compiled by Brouard (2016) have an average direction of 136°, while the striae identified in this study average 115°. Of the three flowsets depicted in Figure 4.10, only flowsets 1 and 2-a show distinct cross-cutting relationships. Flowset 2-b is interpreted as a main trunk feature of the SLIS and may in fact be the youngest one. As palimpsest landforms of flowset 1 can be observed in parts of flowset 2-a, flowset 1 most likely represents glacial features

formed by general ice sheet flow prior to SLIS development, an interpretation which seems consistent with the faint features of flowset 2. The central area between the 3 flowsets, the Mont des Éboulements, bears no glacial lineations and is thus interpreted as a sticky spot during the SLIS episode; it may also have been a sticky spot during earlier ice sheet flow (flowset 1).

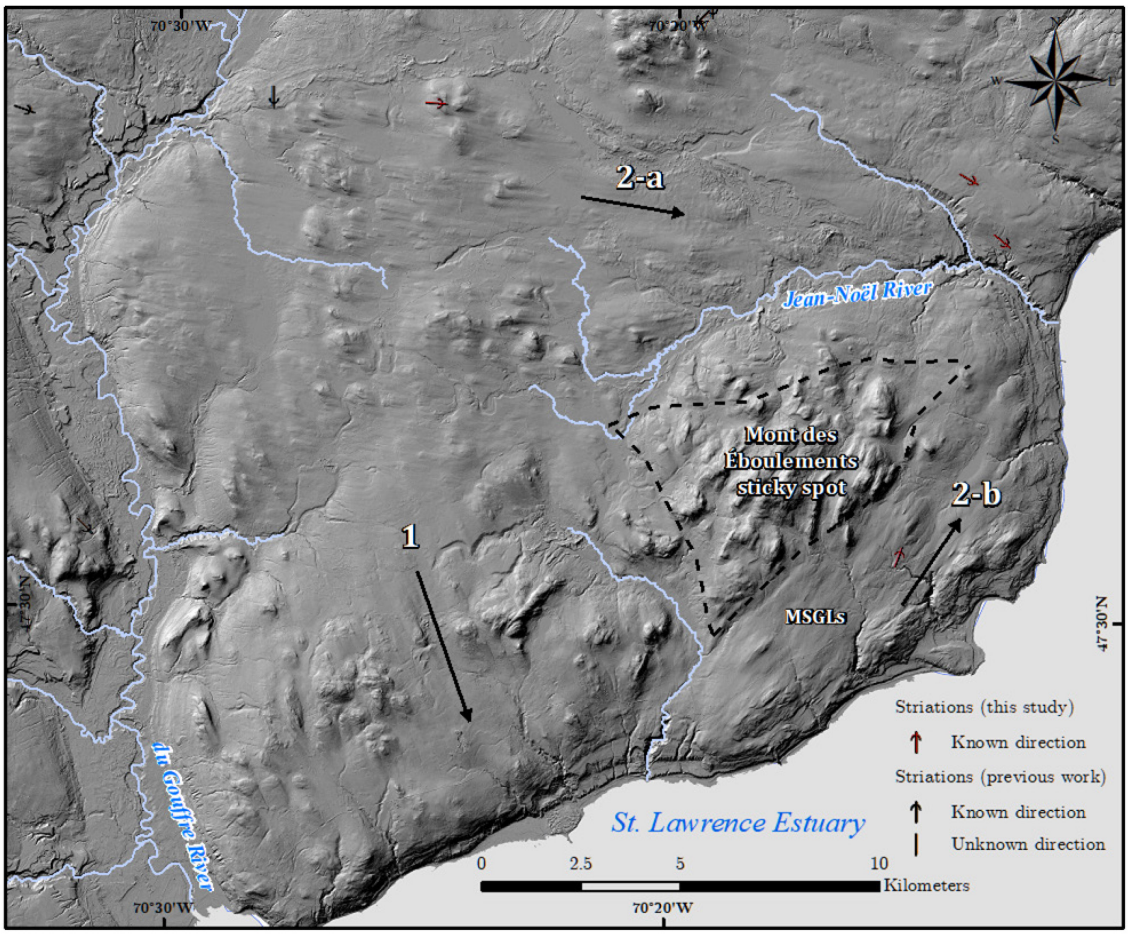

Figure 4.10 : The Charlevoix Astrobleme impact crater zone showing 3 different sets of ice flow directions; 1) An earlier southeast flow towards the St. Lawrence Valley; 2-a) Eastern flow towards the SLIS main trunk; 2-b) Northeastern flow west of the Mont des Éboulements, marked as a sticky spot zone.

4.4.3 Ice stream shear margin indicators and divergence zones

About 5 km southeast further inland from the Mont-Carmel mega-furrows, a spectacular landscape composed of various subglacial features can be observed. The western bank of the Ouelle River Valley locally rests at a higher elevation than the northeast bank, and locally controlled by the bedrock elevation. The plateau is covered by a thick blanket of till overlying bedrock, on which

rest poorly developed, faint small transverse ridges made up of coarse, sandy till. The spacing between these ridges is irregular but averages about 100 meters. No glacial lineations can be observed on the plateau even though it lies entirely above the post-glacial marine submergence limit (Figure 4.11). The eastern flank shows a completely different geomorphology: a hummocky terrain composed of well-developed small till hummocks mostly oriented towards the northeast (parallel to the NE ice flow). They have a mean height of 2.5 meters, contain a typical Appalachian silty sand till core and are covered by a coarser sandy till. This zone is at least 4 kilometers wide perpendicular to the ice stream and extends beyond currently available LiDAR coverage. In the eastern part of this hummocky zone, a distinct series of parallel, linear and continuous till ridges that seem to overly the hummocky terrain can be followed for about 1.5 kilometers.

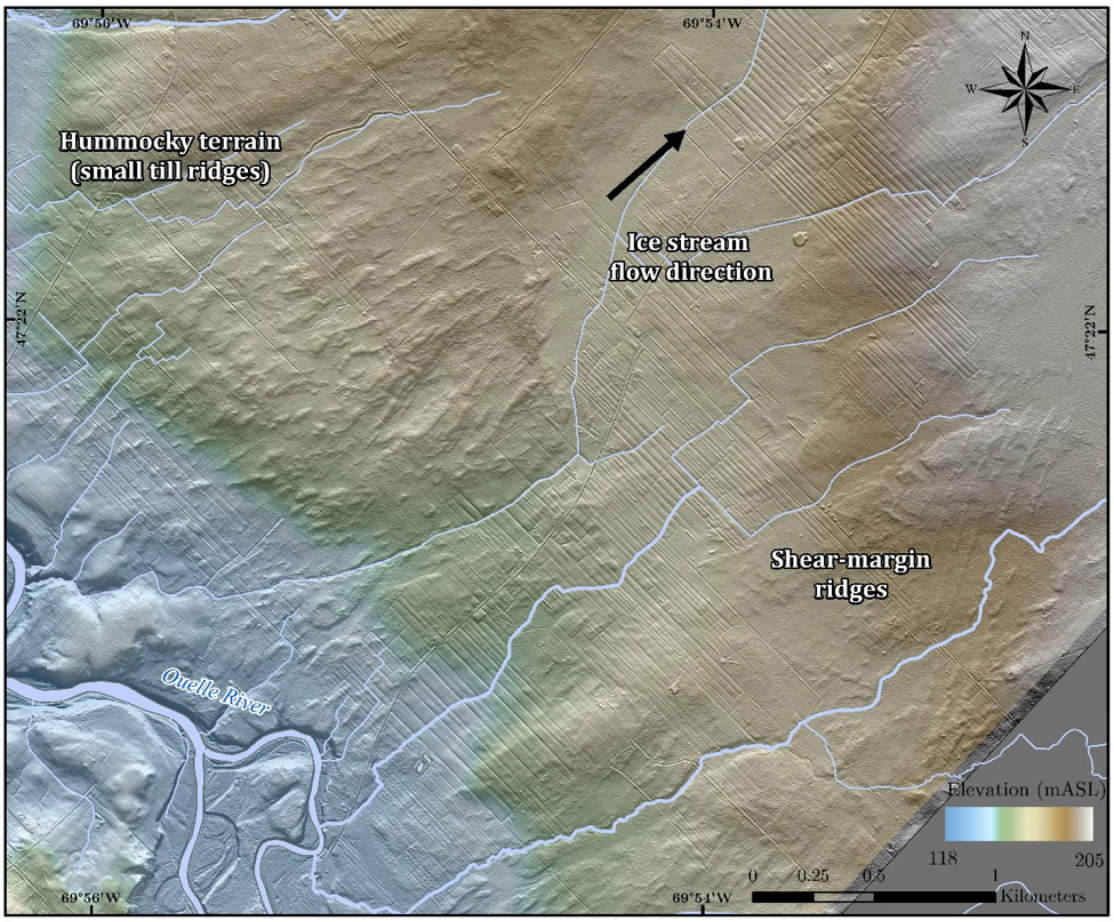

Figure 4.11 : Hummocky terrain featuring small till hummocks west of Mont-Carmel. A much more defined series of till ridges are visible on the right part of the image.

Further down ice, the bottom of the Ouelle River Valley is occupied by the same hummocky terrain that progressively evolves into well-shaped transverse ridges that are analogous to the crevasse-squeeze ridges (CSRs) identified by Evans *et al.* (2016) on the bed of the Maskwa paleo-ice stream (Figure 4.12). Based on field investigations, these ridges are all till-cored, and locally overlain by proglacial outwash sands and gravels containing exclusively Appalachian pebbles. There are two main hypotheses for the formation of this hummocky terrain. This entire zone could be interpreted as the remains of a late stage of the retreating SLIS prior to its shutdown, as it overprints a main corridor of the ice stream. Geomorphological evidence suggests that both the parallel and transverse ridges were deposited nearly simultaneously, and sedimentological analysis confirm that they are comprised of the same diamictic material. This is only compatible with basal till injection into a chaotic, full depth crevasse system. This in turn requires the ice to be relatively thin, as modern ice streams analogues in Antarctica do not appear to be crevassed over their full depth. Another hypothesis would be that this zone corresponds to a shear margin between the main body of the SLIS and a simultaneous eastward-flowing branch that would have created a series of tensile strike-slip fractures between the two trunks moving at different flow speeds. This explanation finds some support in the fact that this area is located exactly at the angle of a divergence in the ice stream just southeast of Mont-Carmel (Figure 4.12). Here, typical northeastward megaridges and till flutings are partly eroded by a major post-ice stream glaciofluvial system that drained northeastward towards the St. Antonin Moraine. This paleo-drainage system was fed by meltwater coming from the nearby Appalachian uplands and discharged through the present-day Ouelle and Kamouraska valleys.

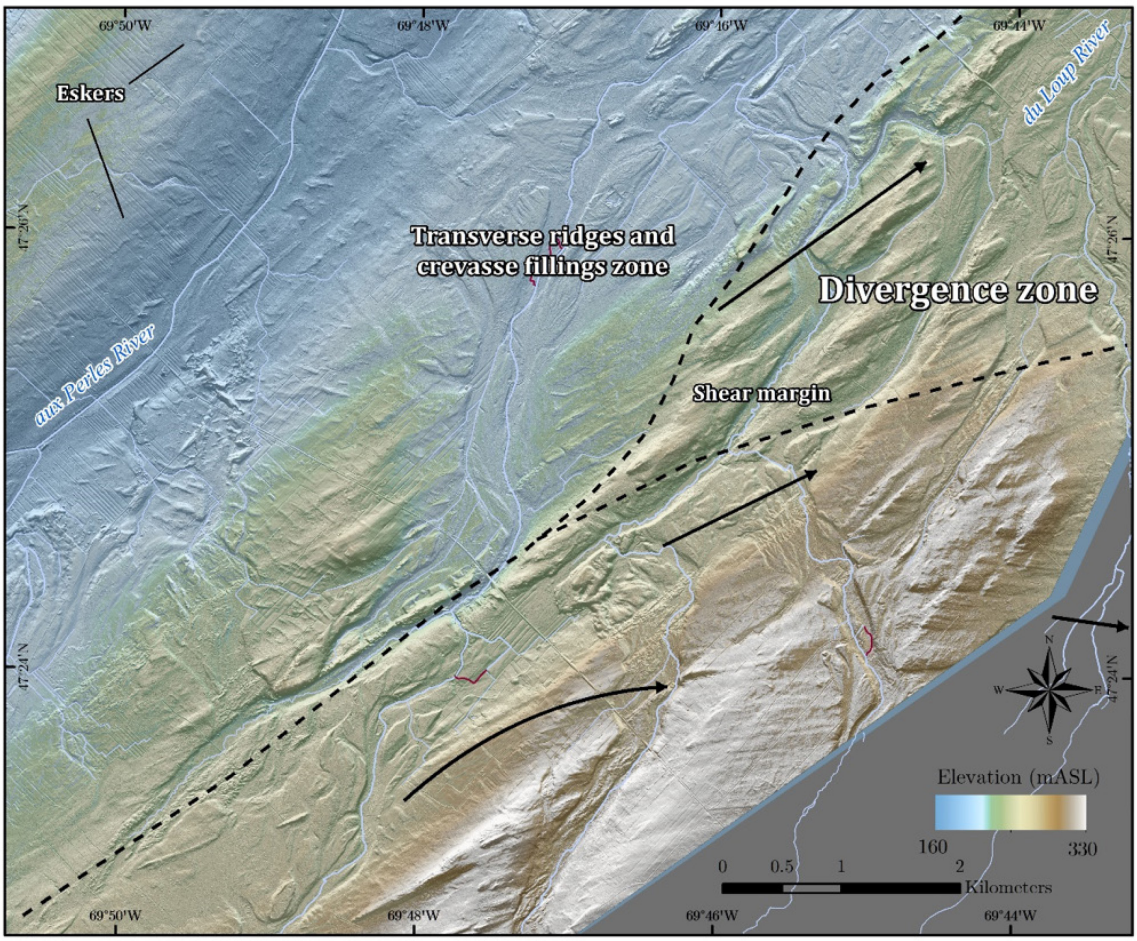

Figure 4.12 : Major divergence zone in the St. Lawrence Ice Stream, 10 kilometers south of Mont-Carmel. The fast ice flow lineations system appears to be splitting into a northeast flow and an eastern bound flow.

Lying parallel to the ice flow, on the northwest flank of the valley, are a set of sinuous eskers made of a grey-brown sandy till with blocks. Although the eskers tend to be located on the margins of the CSRs, there is no clear transition zone between the two sets of features. It is entirely possible that some ridges identified as CSRs might actually be partly overridden eskers that were part of the SLIS subglacial drainage system. In St-Bernard, near the Chaudière River (Figure 4.13), a divergent shift towards the east and even southeast is observed in till flutings and small crag-and-tails lying at a much higher elevation than the main SLIS corridor. This ice movement may also be recorded as east-west and southeast-northwest striae observed about 4 km farther inland in the Notre-Dame Mountains (Lortie & Martineau (1987).

A similar divergence zone is observed near the Chaudière River, just south of St-Bernard, where a large set of crag-and-tails displaying a clockwise shift towards the southeast, into the Chaudière River Valley, developed over a prominent series of schist outcrops (Figure 4.13). Glacial striae in this area also record this flow direction (Lortie & Martineau, 1987) with a mean orientation of 133°. The analysis of incomplete LiDAR data from the Chaudière Valley suggests that this divergence might in fact be only a small deflection of the ice, as the footprint of this flowset seem to vanish. Upstream in the Chaudière River Valley, just south of Vallée-Jonction, a small, isolated set of 600 to 1600 m long faint glacial lineations reflects an ice flow towards the northeast.

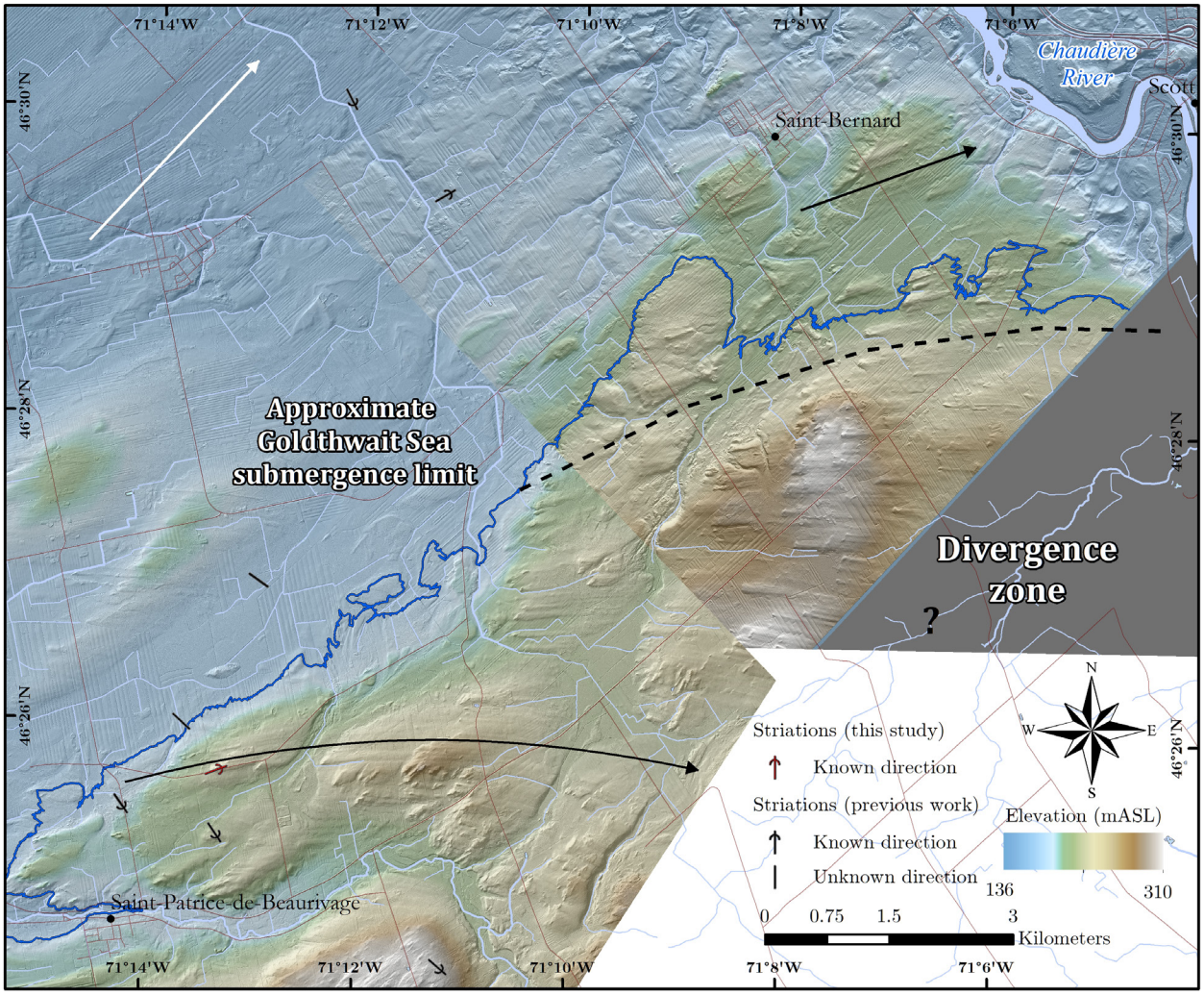

Figure 4.13 : Major divergence zone in the upstream part of the St. Lawrence Ice Stream, a few kilometers south of St-Bernard. The white arrow points toward the general ice stream direction in the valley, while the black arrows mark the divergent flow direction into the Chaudière River Valley. Also shown are striae reported by Lortie & Martineau (1987) as well as by the current study.

Both north (Figure 4.14) and south of Saint-Anselme, on both sides of the Etchemin River, two high plateaus standing above the maximum submergence limit, are marked by northeast-trending MSGLs on which a series of transverse ridges have-developed over a 4 kilometers-wide corridor. While their average length is about 250 m, some are up to 1 km long. Subglacial forms can also be observed at lower elevations but they are extensively reworked or partly buried. The fact that the ridges overlie the MSGLs suggests that they formed after ice flow had slowed significantly or even stagnated. Unlike those observed at Mont-Carmel, these transverse ridges do not seem to have developed as shear margin features in a divergence zone.

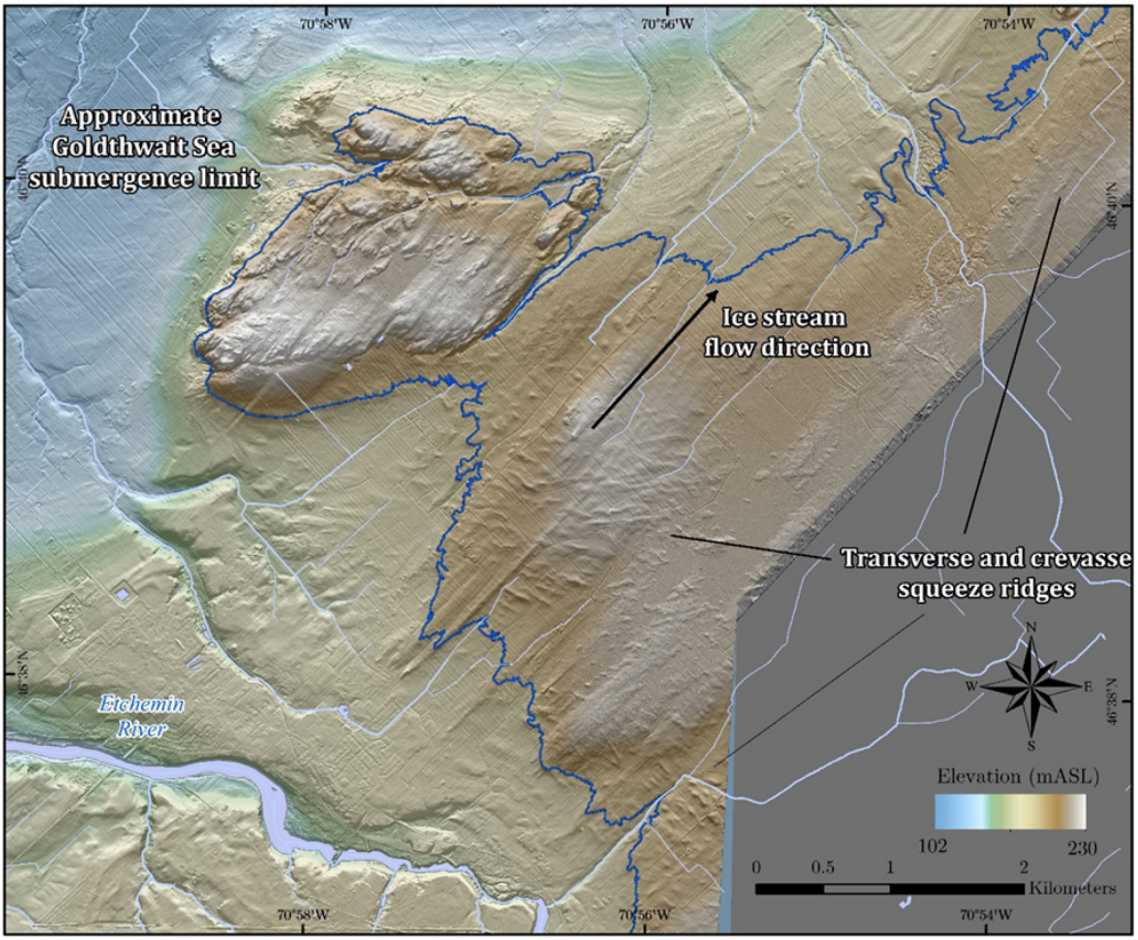

Figure 4.14 : Crevasse-squeeze ridges superimposed on mega-scale glacial lineations north of Saint-Anselme.

4.5 St. Lawrence Ice Stream tributaries and fast ice flow systems in rugged terrains

The St. Lawrence Ice Stream was fed by ice coming from the Laurentian Highlands as well as from the Appalachians Uplands. Upon further investigation, it seems clear that some key parts of the supra-regional catchment area of the SLIS were in fact other zones of fast, converging ice flow. Converging sets of MSGLs can be observed in the Saguenay River and Lac St-Jean area, as well as in the Portneuf-Mauricie and Estrie regions. While a thorough review of each region is beyond the scope of this work, a glance at paleo-ice stream activity in nearby regions allows us to better place the SLIS into its regional context.

4.5.1 Péribonka and Saguenay areas: Major tributaries to the St. Lawrence Ice Stream

A rapid ice flow system, tributary to the SLIS, operated in the axis of the Saguenay River and Péribonka River valleys (region 4 of Figure 4.2), as shown by the MSGLs observed in that area (Figure 4.15). The fast ice flow zone near the Péribonka River is at least 12 kilometers wide, but it is potentially wider as it exceeds the boundaries of available LiDAR surveys (Figure 4.15). Fast ice flow over the very hard crystalline basement rocks of this region streamlined bedrock knolls and produced till ridges up to 20 kilometers in length. The elongation ratio of these bedform lineations averages 1:10, but 1:20 forms are also observed sporadically. The flow direction is mainly southeastward, towards Lake St-Jean, where it merges with ice flowing along the axis of the Saguenay River. Rock drumlins as well as glacial troughs can also be found in this area.

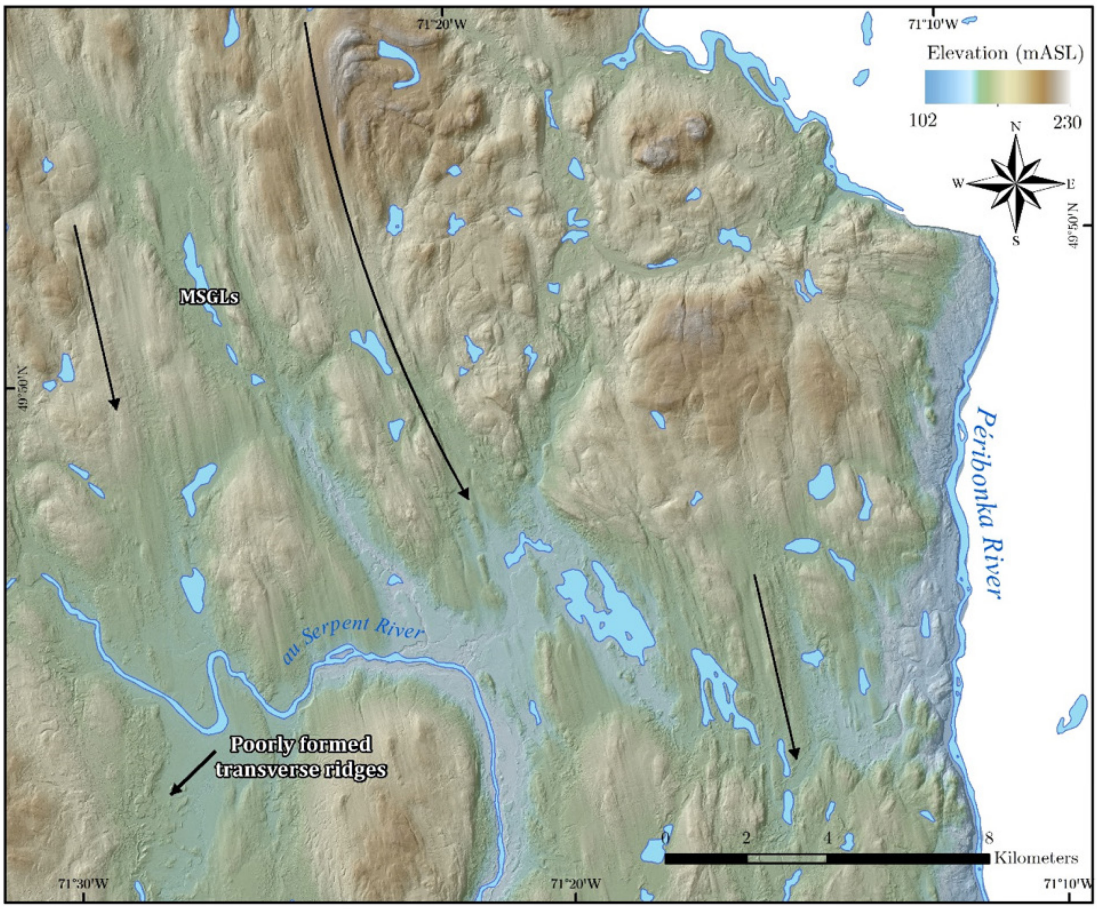

Figure 4.15 : Péribonka River area, northeast of Lac St-Jean, with a characteristic streamlined "hard bed" over crystalline rocks

The distinct arched flow lines recorded in the streamlined bedrock suggest that topographic steering was limited. Transverse ridges are also observed in the same types of context as in the St. Lawrence Valley, but are generally not as well preserved as their counterparts, possibly because of the rugged topography. In the Saguenay River Valley, ice flow was essentially in the same direction as the contemporary river. The valleys of the Mistassibi River and other streams were not investigated during this study, but it is likely that other trunks of fast-flowing ice contributed to glacial streaming in the Saguenay River.

4.5.1 Portneuf – Mauricie region: focused ice flow over rough crystalline bedrock

In the Mauricie region (region 5 in Figure 4.2), areas of focused (fast?) flow are observed on the basis of thick drift zones downglacier of partly eroded bedrock outcrops. A spectacular example is illustrated at Figure 4.16, where enhanced basal flow occurred (in the sense of Boulton (1982)) just south of Sacacomie Lake. In this particular context, the thick till flutings reaches more than 30 m of thickness. Even though these features often lack continuity in either upstream or downstream directions, several have been identified and mapped between the St-Narcisse moraine and the Matawin River. In the case of the Sacacomie Lake, the notable gullying observed on the till flutings suggests a relatively fine till matrix that could be the result of the re-entrainment of pre-Wisconsinan sediments at the base of the glacier. This process is likely to have contributed in some respects to the important till thickness encountered in several valleys of southwestern Mauricie (Légaré-Couture *et al.*, 2018).

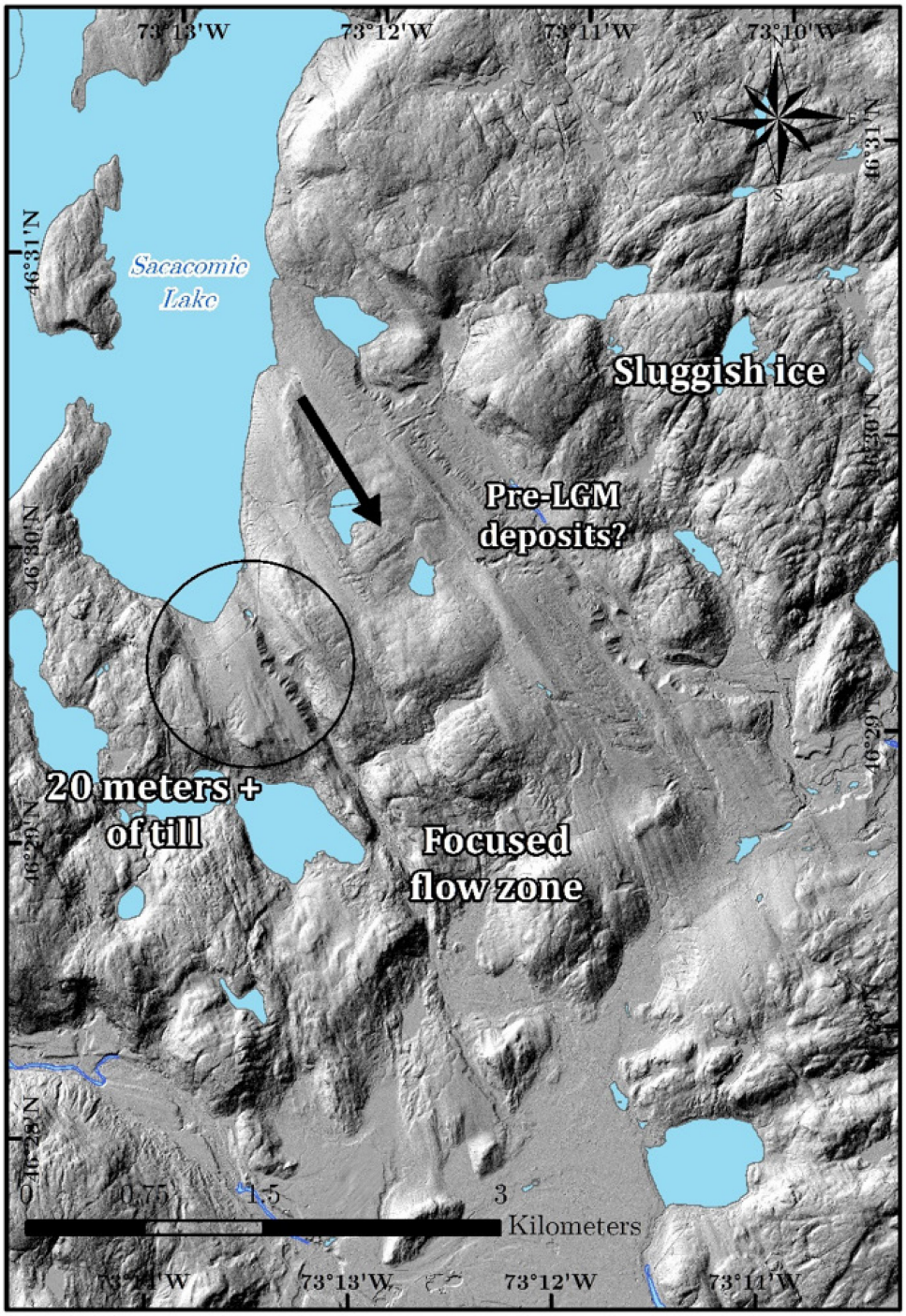

Figure 4.16 : Focused ice flow over rugged crystalline Canadian Shield terrain in Mauricie, south of Sacacomie Lake. The black arrow depicts the ice flow direction. The zone circled in black shows an area where the till blanket is heavily ravined. The difference in elevation between the top of the till surface and the bottom of the ravine is at least 20 m.

As this fast ice flow zone shows no apparent deflection toward the SLIS, it may be inferred to lie beyond its catchment area. Without having to assume that the Ontario-Erie Ice Stream (OEIS; Ross *et al.* 2006; Sookhan *et al.* 2018) and the SLIS were coeval, this indicates that the Mauricie region was beyond the catchment areas of both ice streams. The occurrence of eastward-trending crag-and-tail ridges in the adjacent eastern region of Portneuf (Parent *et al.,* 1998) suggests that the Trois-Rivières region remained in what may be called an inter-ice stream area. Unfortunately, glacial lineations in the Lower Mauricie area were either buried or eroded during the marine submergence that followed the deglaciation. Perhaps surprisingly, the glacial lineations of the Mauricie region find some continuity with an important set of MSGLs in a well-defined ice stream corridor identified on the south side of the St. Lawrence Valley (see next section). Based on the general orientation of the glacial lineations, Laurentide ice coming from the Mauricie region might have been feeding either the Ontario-Erie Ice Stream or the Memphrémagog Ice Stream, depending on the time frame.

4.5.2 Estrie region: The Memphrémagog ice flow zone

In the Eastern Townships region of Québec, east of Mount Orford (region 6 of Figure 4.2), a major south-flowing ice flow system (ice stream?) is identified using a patchwork set of LiDAR data. The main corridor is located between Sherbrooke and Mount Orford, although glacial lineations oriented towards the southeast are also present west of Mount Orford (Figure 4.17). The bed of the main corridor consists of a very smooth till plain showing till flutings and MSGLs with lengths varying from 2 to 10 kilometers. The flow direction is not straight but rather arcuate, deflecting from southeast to south at the latitude of lakes Magog and Memphrémagog. The catchment area of this ice flow can be traced back northwestward to Saint-Germain-de-Grantham on the Appalachian piedmont.

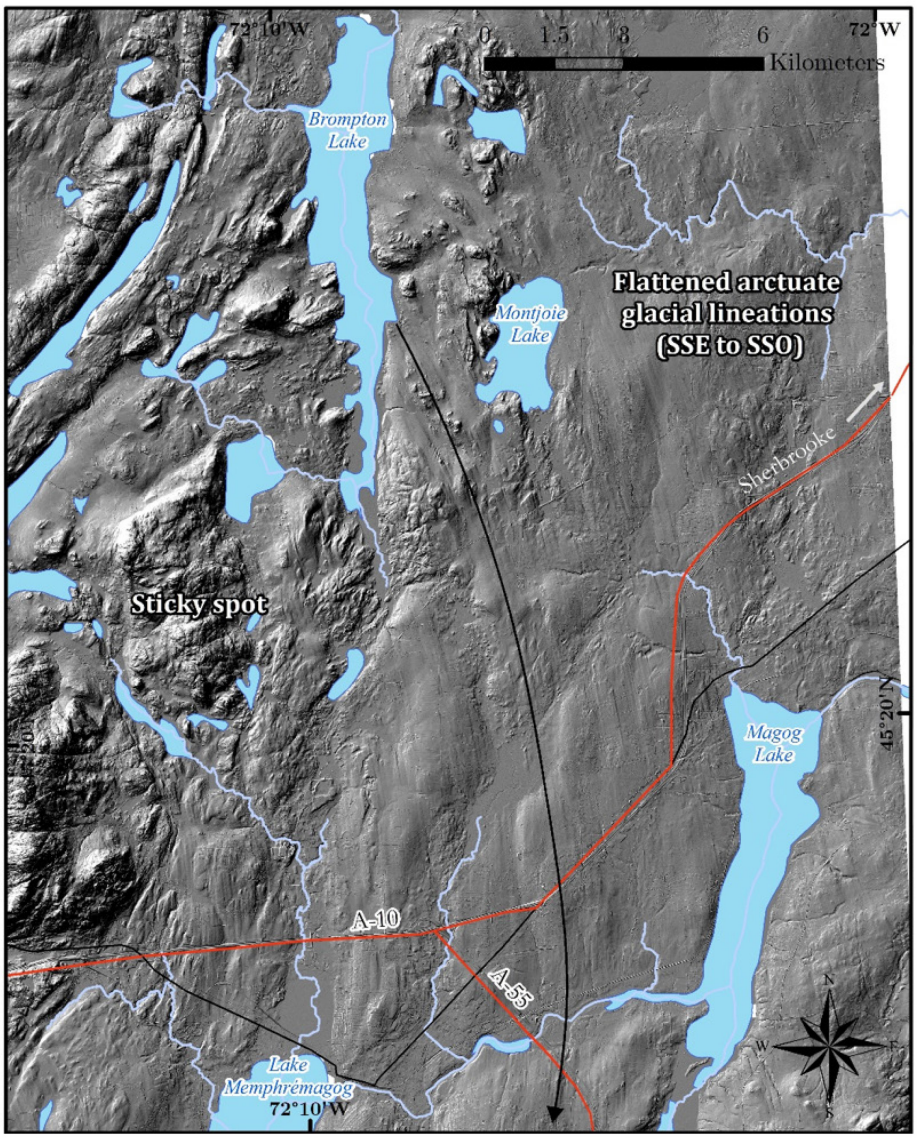

Figure 4.17 : Mega-lineated streamlined hard bed of the Memphrémagog ice flow, flowing southward from across the St. Lawrence Valley and Appalachian ridges and into Vermont (immediately south of LiDAR image)

An impressive transition of subglacial forms occurs between the "onset" area and the streamlined bed (Figure 4.18). From upstream to downstream, the earliest shapes that are encountered are till ridges that appear drumlinized to some degree. Beaches crests often rest directly atop the drumlins, sharing their north-south alignment. These small ridges progressively turn into longer lineations downstream as they are overridden and reworked by faster flowing ice, and the relief eventually turns into full flutings. As the

flow converges towards the fast ice flow zone, glacial lineations increase in length, progressively evolving into till drumlinoids with an elongation ratio of 1:30 further downstream and technically qualifying as MSGLs in terms of lengths and elongation ratios. The local ruggedness of the bedrock, however, probably prevented the construction of a proper drumlins field, as the relief further south changes to outcropping streamlined bedrock with crags-and-tails extending over two kilometers of length.

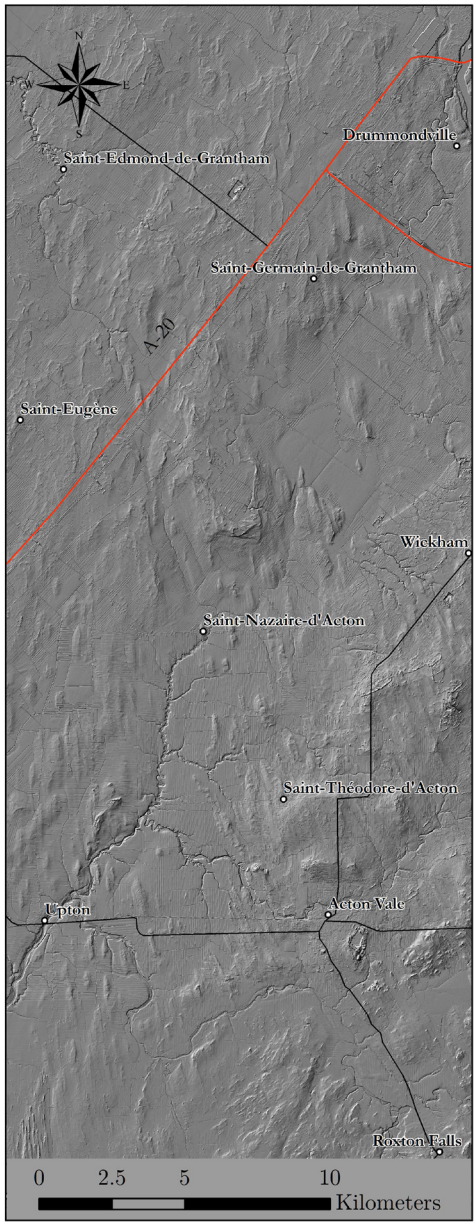

Figure 4.18 : Transition pattern between till drumlinoids (upper part of the image) and MSGLs between Drummondville and Acton Vale constructed by ice flowing southwards.

4.6 Interpretation and discussion

The Lower St. Lawrence River valley shows an evolving ice stream landscape including 1) upglacier catchment areas on the crystalline Canadian Shield basement composed of preferentially eroded outcrops and glacial troughs; 2) hybrid transition zones with mega-furrows mega-ridges and an assemblage of various elongated, convergent glacial lineations and MSGLs; 3) a central main trunk with highly elongated MSGLs mostly covered by a thin till layer. The main trunk of the SLIS occupied the center of the St. Lawrence Valley but likely migrated towards the south shore during its last stages. It was feeding from ice coming from the LIS through a few main corridors, most notably the Saguenay River region as well as the Portneuf/Mauricie area. Hummocky zones are found on the south shore in the vicinity of two divergence zones of yet undefined significance at the mouth of Appalachian river valleys. CSRs are found near the side margins of the ice stream in the Lotbinière and Kamouraska areas. Mapped MSGLs with lengths over 1000 m as well as the main ice margin features of the SLIS in the Lower St. Lawrence Valley are shown at Figure 4.19.

The simplified reconstructed ice flow lines during the SLIS episode are shown in Figure 4.20. During the late stage of the ice stream, the main trunk of the ice stream (flow set 1) was located on the south shore of the St. Lawrence River, where ice was funneled mainly from the north shore through the Saguenay River Valley (flow sets 3 and 4) as well as the main valleys between Mauricie and Charlevoix (flow set 5) shows the supra-regional ice stream flow sets of this part of the St. Lawrence Valley. MSGLs on the Île d'Orléans suggest that the main trunk of the ice stream might have migrated laterally during its activity. The main trunk was most likely located in the central corridor of the valley (presently submerged) during an earlier stage of the ice stream, while it was completely grounded on the south shore during its late stage. Ice coming from the Mauricie area (flow set 6) most likely fed the Memphrémagog ice flow (flow set 7). The normalized ice flow velocity shown at Figure 4.20 was calculated using an index of the normalized elongation ratio as well as the normalized lineament packing. The purple-colored central SLIS channel upstream of Rivière-du-Loup is conceptual; no LiDAR coverage for this area was available at the time of publication.

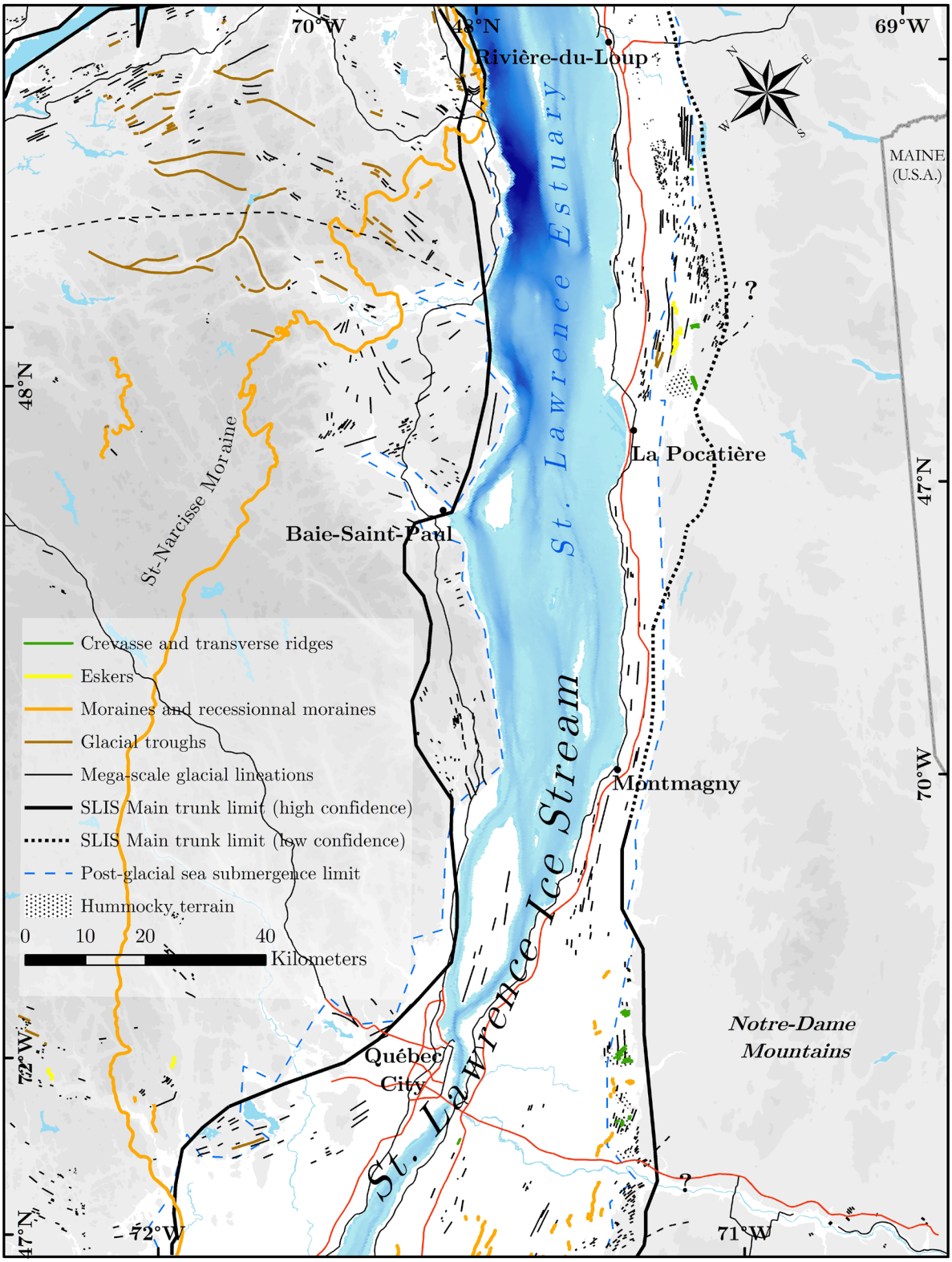

Figure 4.19 : Mega-scale glaciation lineations (lengths are at actual scale) and main ice margin features of the Lower St. Lawrence Valley. Note that the map frame is slightly rotated as the north direction is towards the upper-left corner of the map.

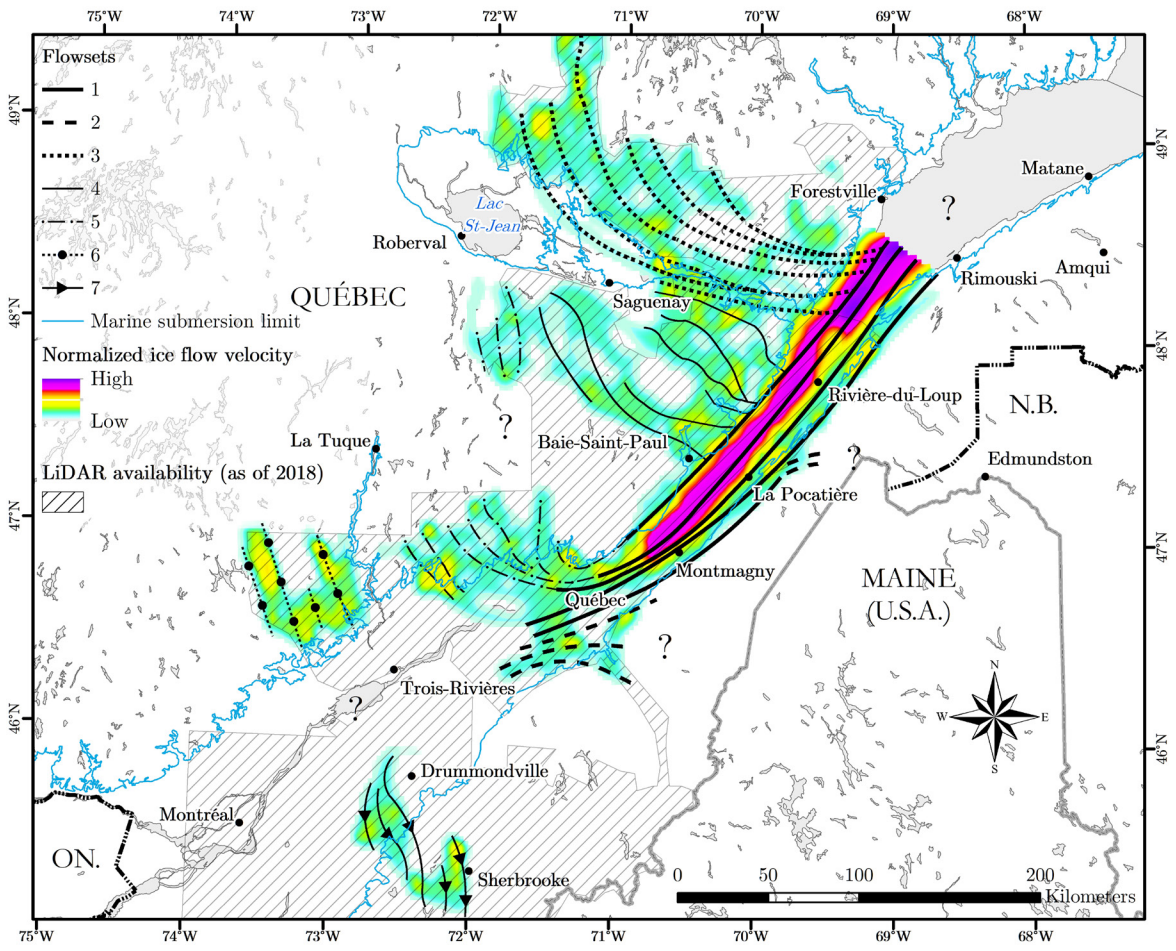

Figure 4.20 : St. Lawrence Ice Stream and tributaries flowsets reconstructed using mega-scale glaciation lineations.

4.6.1 Catchment area and bed characteristics

Parent & Occhietti (1999) suggested a width of about 25 km for the SLIS based on known ice flow patterns at the time. The results of this study show that fast ice flow towards the northeast occurred on both the north and the south shore of the St. Lawrence River. The newly mapped MSGLs and flowsets suggest that while the main fast ice flow trunk likely migrated laterally along the corridor of the valley, it was mostly grounded along the south shore of the river during its last phase. Even though fast ice flow towards the northeast was occurring in the Appalachian Piedmont, the main source of ice was the Laurentide ice sheet, especially during its last phase before the ice stream shutdown. In fact, glacial lineations on the northwestern flanks of Notre-Dame Mountains suggest that prior to the ice stream shutdown, there was no convergence of ice

coming from an Appalachian ice cap, at least not as illustrated in the ice stream conceptual model of Parent & Occhietti (1999).

The bedrock characteristics of each part of the study area are summarized in Table 4.2. Kleman *et al.* (2010) suggest differentiating ice streams (and paleo-ice streams) by their genetic characteristics into five groups: classical, semi-stable, transient, topographic, and rebalancing. The SLIS has specific features that do not fit well in a single category. At both large scales (major valleys) and small scales (Appalachian outcrops with furrows and grooves), topographic effects are evident, but the ice flow is not convergent to the extent that it is restricted into a "funnel". At medium scales (regional), the ice often flowed against the terrain slope, against the bedrock strike or unexpectedly over areas of high rugosity (i.e., divergent flows into the outlets of valleys, flow through crystalline bedrock, etc.). The mapped glacial bedforms do not suggest the presence of a significant amount of meltwater and therefore of an overly lubricated bed. The only exception to this is the Kamouraska area on the SLIS main trunk between Saint-Bruno-de-Kamouraska and Rivière-du-Loup, where a major drainage system is found on the surface. However, this system was most likely active during the penultimate Laurentian deglaciation, long after the ice stream shutdown. The bedrock lithology does not seem to have a significant impact on the localization of the ice stream. The SLIS could represent a transient flow of a rigid base glacier that developed and accelerated as a result of an imbalance in the profile of the ice, caused by a major drawdown near its terminus in the Gulf of St. Lawrence (Hughes *et al.*, 1985).

Table 4.2 : Relationship between fast ice flow and local geology

Area #	Region	Dominant lithology	Relation between ice flow and bedrock structure	Topographic steering
1	Main trunk	Feldspathic sandstone; mudslate, mudrock	Mostly parallel to bedrock strike	Moderate
2	Lower Chaudière	Varied, but mostly feldspathic sandstone; slate shale with siltstone and limestone interbeds	Often parallel to bedrock strike, but sometimes perpendicular	Poor
3	Beaupré/Charlevoix	Charnockitic gneiss and migmatite, anorthositic Gabbro	Mostly parallel to bedrock strike on the Beaupré coast, but flowing against the terrain slope	Poor
4	Péribonka and Saguenay River valleys	Varied, but mostly Anorthosite, leuconorite, gabbro, norite and ultramafic rocks	Mostly perpendicular to bedrock strike	Moderate
5	Portneuf/Mauricie	Charnockitic migmatite with biotite, hornblende	Not controlled by structure	Moderate
6	Estrie	Slate; some siltstone and clay siltstone	Mostly perpendicular to bedrock strike	Poor

4.6.2 Drumlins and MSGLs

Drumlins have been linked to zones of accelerating ice flow towards an ice stream, a fast-fetch zone (Smith *et al.* (2007)). In the upper St. Lawrence Valley, southwest of Montréal, Ross *et al.* (2006) interpreted glacial drumlinoids previously identified as Rogen moraines by Carl (1978) as pre-existing drumlins that were reoriented and partially reshaped as palimpsest forms by the action of an ice stream flowing towards the Ontario Basin. The transition between drumlins and MSGLs is beautifully illustrated by Sookhan *et al.* (2018) in a paper where they present a simple conceptual model for the formation of MSGLs from drumlins in the Great Lakes sector of the

Laurentide Ice Sheet. While no real drumlins are found in the Mid- to Lower St. Lawrence Valley, we identified in the onset zone of the Memphrémagog Ice Stream a convincing hierarchical transition between till ridges and drumlinized lineations. One explanation could be that the fast ice flow trunk of the SLIS was very dynamic and migrated upstream as well as laterally as its calving bay progressed inland, thus overriding any previously deposits soft bedforms. A simpler hypothesis is that the bed characteristics, terrain roughness and general layout of the valley prevented the formation of complete drumlins.

4.7 Conclusion

The mapping of thousands of converging, northeast bearing mega-scale glaciation lineations (MSGLs) in the Mid- and Lower St. Lawrence Valley using LiDAR-derived digital terrain models provides unambiguous evidence that fast ice flow occurred in the valley as part of an early deglaciation phase during the Upper Wisconsinan. This new data is consistent with striations identified on both the north and south shore of the St. Lawrence River. This work highlights that airborne LiDAR land elevation data is an invaluable technology to quaternary geology research overall, and the mapping of paleo-ice streams beds as well as paleogeographic reconstructions. The mapping of the entire SLIS footprint is nevertheless far from complete, as high-resolution DTMs of critical areas are still not available to the public. The inventory, documentation and interpretation of the geomorphological footprints of paleo-ice streams is crucial to the better understanding of the glaciodynamic conditions that prevailed during the first phase of the Upper Wisconsinan deglaciation in the northeast part of the Laurentide Ice Sheet. The Ministère des Forêts, de la Faune et des Parcs (MFFP) of the province of Québec is currently working to make available airborne LiDAR derivative products for the entire southern Québec. This opens a major gateway for future research of the geology of glaciated terrains in this area. As additional datasets become available, more work will be required in order to connect the ice stream features identified here to the glacial lineations found in other parts of the St. Lawrence Valley and fully capture the essence of this critical glacial event.

4.8 Acknowledgements

This research was supported by the Fonds de recherche du Québec - Nature et technologies (FRQNT) doctoral scholarship of Guillaume Légaré-Couture and by funds from the Projet Chaudières-Appalaches of the PACES program of the Ministère du Développement durable, de l'Environnement et de la Lutte contre le changement climatique, led by Dr. René Lefebvre (INRS-ETE). The LiDAR data used in this study were either bought directly from the Ministère de l'Énergie et des Ressources naturelles (MERN) via Géoboutique Québec, acquired from the Bureau de coopération interuniversitaire (BCI) under a research and teaching purposes license, or obtained from the *Forêt Ouverte* Ministère des Forêts, de la Faune et des Parcs website (https://www.foretouverte.gouv.qc.ca/).

5 Article 4: New evidence of a Laurentide ice readvance in the Champlain Sea in the Quebec City region during the early Younger Dryas

Nouvelles preuves d'une réavancée glaciaire Laurentidienne dans la Mer de Champlain dans la région de Québec durant les débuts du Dryas récent

Auteurs :

Guillaume Légaré-Couture[1] & Michel Parent[2]

[1] Institut national de la recherche scientifique – Centre Eau Terre Environnement (INRS-ETE), Québec, Canada

[2] Commission géologique du Canada, Ressources naturelles Canada, Québec, Canada.

Titre de la revue ou de l'ouvrage :

Boreas

À soumettre en 2021

Contribution des auteurs :

Les deux auteurs sont responsables du développement de la méthodologie, de l'analyse, de la cartographie ainsi que de la rédaction de l'article.

Lien entre l'article ou les articles précédents et le suivant :

Cet article fait le point sur la découverte d'un nouvel ensemble de crêtes morainiques cartographiées dans la région de Lotbinière. Il s'agit d'un des résultats de la cartographie des formations superficielles discutée dans le cadre du premier article et de la cartographie de

l'empreinte du Courant glaciaire du Saint-Laurent discutée dans le troisième article. Il requiert le développement d'un cadre conceptuel et chronologique détaillé pour bien le mettre en contexte dans le cadre de la déglaciation du Québec méridional.

Résumé :

Cet article présente un nouvel ensemble de crêtes morainiques cartographiées sur la rive sud du Saint-Laurent dans la région de Lotbinière, identifiées sur la base de données de terrain et d'un levé LiDAR à haute résolution. Ces moraines représentent les positions récessionnelles d'un front glaciaire laurentidien à la suite d'une réavancée dans un bassin précoce de la Mer de Champlain. Leur découverte soutient et renforce l'hypothèse de la réavancée glaciaire de Saint-Nicolas, en même temps qu'il en modifie considérablement la portée sur le schéma de déglaciation régionale.

Abstract :

This paper presents a hitherto unmapped set of moraine ridges on the south shore of the St. Lawrence River in the Lotbinière region. These ridges were identified on the basis of new fieldwork and high-resolution LiDAR data. They are interpreted as recessional moraines emplaced in the aftermath of a readvance of the Laurentide ice front in an early basin or arm of the Champlain Sea. While their discovery supports and strengthens the Saint-Nicolas readvance hypothesis, it considerably modifies its significance in the regional deglaciation scheme.

5.1 Introduction

Some aspects of Late Wisconsinan deglaciation events in the Quebec City region are complex, notably the deglaciation patterns and chronology (Parent and Occhietti, 1988, 1999; LaSalle and Chapdeleine, 1990)). Global warming following the Last Glacial Maximum (LGM) was responsible for the gradual thinning and retreat of the Laurentide Ice Sheet (LIS). By 18 ka BP, a major ice stream, the St. Lawrence Ice Stream (SLIS) had developed in the eastern sector of the LIS and discharged massive amounts of ice through calving in the St. Lawrence Gulf and Estuary (Parent and Occhietti, 1999), causing a reversal of flow in the Appalachian uplands (Shilts, 1981). Around the same time, the Ontario-Erie Ice Stream (OEIS) operated in a similar fashion as it funneled ice towards the Lake Ontario basin (Taylor, 1913; Ross *et al.,* 2006; Sookhan *et al.,* 2018). While

the retreat of the LIS operated generally from south to north, starting in the Appalachian uplands and piedmont before the St. Lawrence Valley and the Laurentian Hills, the massive transport of ice by the SLIS disrupted this general pattern and contributed to considerable thinning of the LIS along the axis of the SLIS. Rapid thinning and retreat of the SLIS allowed early penetration of marine waters up in the St. Lawrence Estuary, an event that preceded the main phase of the Champlain Sea and been labeled the Charlesbourg Phase by Parent & Occhietti (1988). Several hundreds of kilometers upstream, the northeastward retreat of the OEIS resulted in the coalescence of glacial lakes Iroquois, Vermont and Memphrémagog into a single freshwater body, named Glacial Lake Candona on the basis of the key presence of a freshwater ostracod *Candona subtriangulata* (Parent & Occhietti, 1988, 1999; de Vernal *et al.,* 1989; Ross *et al.,* 2006). Lake Candona is equivalent to the expanded Fort Ann phase of Lake Vermont (Franzi et al.2007; Rayburn *et al.,* 2005, 2007, 2011) and to Lake St. Lawrence (Rodrigues, 1992), but the name Lake Candona has temporal precedence and furthermore, it is based on well-defined shorelines and sediments (Parent & Occhietti, 1988, 1999). Sedimentological and geomorphological evidence of the drainage route of Glacial Lake Candona towards the Goldthwait Sea is still lacking to this day.

At the scale of the St. Lawrence Valley, the chronology of deglacial events is difficult to reconstruct because of challenges associated with marine shell radiocarbon dating, and also because many deglacial features were covered by marine clays or extensively reworked by the wave action and currents in shallower parts of the marine basin. Significant morpho-sedimentological markers are thus difficult to secure, and the deglaciation chronology has long relied on the radiocarbon ages obtained from marine shells. While marine shells in both thanatocoenotic and biocoenotic assemblages have been abundantly observed in excavations and riverbank exposures below the limit of marine submergence, radiocarbon (^{14}C) ages on Champlain Sea shells usually yield ages 350 - 1800 years older than ages from contemporary terrestrial material (Occhietti *et al.,* 2001b; Occhietti & Richard, 2003; Richard & Occhietti, 2005; Cronin *et al.,* 2008). This age difference was first noted and discussed by Lasalle (1966) as well as by Karrow *et al.* (1975), and was frequently reported in the following decades of research as many ages well over 12,000 ^{14}C BP were obtained on marine shells from the western Champlain Sea basin. Hillaire-Marcel *et al.*(1979)

and Karrow (1981) attributed these anomalous ages to ^{14}C depletion in marine carbonates induced by the addition of inorganic carbon from glacial meltwater. The additional aging has also been associated with salinity effects (Rodrigues, 1988), old carbon reservoir effects (Hillaire-Marcel, 1981, 1988), vital effects for different species as well as other unknown factors (Anderson, 1988; Rodrigues, 1992). An additional potential effect was also recently proposed by Laurencelle *et al.* (2018) who showed that the resurgence of old subglacial groundwater in the marine basin may account for a significant influx of old CO^2 into Champlain Sea waters. The reliability and meaningfulness of ^{14}C ages obtained from marine shells in the Champlain-Goldthwait Seas have been discussed extensively over the past decades (Hillaire-Marcel *et al.,* 1979; Hillaire-Marcel & Vincent, 1980; Hillaire-Marcel, 1981; Rodrigues, 1992; Rodrigues & Vilks, 1994; Parent & Occhietti, 1999; Dyke *et al.,* 2003). Because it is difficult to evaluate the local reservoir effect affecting marine shells, the early ages cited in the literature were often expressed as "shell ages" (marine) or as "cold sea shell ages" by several authors (Occhietti & Hillaire-Marcel, 1977; Parent & Occhietti, 1988, 1999) that could not be reliably used to establish the chronology of deglaciation without the support of terrestrial material dating.

Recently, the timing of the drainage of Glacial Lake Candona and the early Champlain Sea incursion in the St. Lawrence Valley were established more reliably at around 11 100 ± 100 ^{14}C yr BP (12 950 – 13 050 cal ka BP) based on basal Accelerator Mass Spectrometry (AMS) ages from terrestrial plant macrofossils coupled with the pollen content of postglacial lake sediments at the Hemlock Carr site on Mont Saint-Hillaire (Occhietti & Richard, 2003; Richard & Occhietti, 2005). Despite this new evidence, the chronology of regional events surrounding the early Younger Dryas (YD) remains tentative because of the variability, complexity and abruptness of these changes. The strong dilatation of ^{14}C ages in relation to calibrated or calendar ages, observed at the end of the Allerød, and the subsequent contraction in the early YD adds to this complexity (see Occhietti, 2007). These uncertainties have made it hard to establish a consistent chronology of events in the Quebec City narrow, a key sector that controlled the early marine incursion in the St. Lawrence Valley during deglaciation and later controlled the exchange of marine waters between the Champlain Sea and Goldthwait Sea basins. On the south shore of the St. Lawrence River near Quebec City (the Lotbinière area), LaSalle & Shilts (1993) identified isolated small

moraine segments containing shell-bearing glaciomarine diamicton, and attributed their occurrence to a LIS readvance into the early Champlain Sea. The climatic importance of this episode, informally referred to as the St-Nicolas readvance, was however never demonstrated, and since the moraine associated with the readvance (St-Edouard moraine) stood as an isolated feature, the regional significance of this event was never assessed regionally following the paper of LaSalle & Shilts (1993).

The objectives of this article are to (1) provide a review of glacial and deglacial patterns observed in the Quebec City area, (2) describe a set of newly mapped moraines in the Lotbinière area, (3) review the relevant ^{14}C ages (marine and terrestrial) available for this time period, and (4) propose an updated regional deglaciation model integrating all the available information from the Quebec City area.

5.2 Quaternary geology overview and paleogeography

The Lotbinière region is located on the south shore of the St. Lawrence River, just southwest of Quebec City and Lévis. The physiography of this part of the St. Lawrence Valley is characterized by a flat and low plateau, with elevations ranging between 40 and 80 m ASL and surface slopes generally not exceeding 2%. The upper limit of marine submergence in this region reaches approximately 185 m ASL. This region has significant paleogeographical interest as it was the gateway to marine invasion of the middle and upper St. Lawrence Valley during the last deglaciation.

The surficial geology of this area was first mapped in part by Dubé (1971) at a 1 : 63 360 scale (National Topographic System – NTS - sheet 21L/05 (Lyster)) and in part by LaSalle *et al.* (1980a; NTS sheet 21L/12 (Portneuf)). Deglacial features were compiled by Chauvin *et al.*(1985). Both map sheets were recently updated during the course of a regional mapping effort as part of regional groundwater characterization studies (Daigneault *et al.,* 2014; Lefebvre *et al.,* 2015; Godbout, 2013; Thiery, 2016). The surficial deposits of this region are relatively thin in comparison to the central part of the St. Lawrence Valley. The stratigraphic record is generally quite simple, consisting of a fairly thin till layer resting on bedrock, and overlain by generally thin marine sediments, ranging from glaciomarine lithofacies to littoral and deltaic lithofacies. Offshore marine

clays are also noticeably thin and uncommon in this region. Very few glaciofluvial sediments or ice marginal features were identified on either of these map sheets in earlier publications, with the exception of a localized glaciofluvial unit identified from LiDAR data interpretation and interpreted as a possible esker by Thiery (2016) as well as a series of very small discontinuous moraines west of Laurierville that were mapped by Godbout *et al.* (2011)

A conceptual model of Late Wisconsinan deglaciation events in the St. Lawrence Valley between 20 cal ka BP and 12.9 cal ka BP is presented at Figure 5.1. In this model, the regional ice flow lines of 20 cal ka BP (Figure 5.1 insert 1) are disrupted by the development of the St. Lawrence Ice Stream (SLIS) and by rapid ice mass loss, presumably by calving, at the downstream end of the SLIS (northeastward flow; Parent and Occhietti, 1999; Figure 5.1, insert 2) and of the Ontario-Erie Ice Stream (southwestward flow, Ross *et al.*, 2006). The action of the SLIS resulted in major thinning of the ice sheet margin, which in turn accelerated surface melting and increased the topographic control of ice flow in the St-Lawrence Valley. As a consequence of ice stream development (Parent and Occhietti, 1999), ice flow was reoriented northward in the Appalachian uplands, an event labeled the Appalachian ice flow reversal by Shilts (1981, and references therein). This event is recorded by abundant striations over much of the Appalachian uplands and piedmont (Lamarche, 1971, 1974; Lortie & Martineau, 1987; Rappol, 1993) and also as far as the north shore of the St. Lawrence River in the Charlevoix and Quebec City regions (Lanoie, 1995; Paradis & Bolduc, 1999). By 14.4 cal ka BP (around 13.5 ^{14}C ka BP), the ice stream had retreated up to Rivière-du-Loup and continued to progress inland (Rappol, 1993), and beyond Québec City around 13.3 cal ka BP (12.5 ^{14}C ka BP; LaSalle (1987); Figure 5.1, insert 3). This process quickly isolated Appalachian ice from Laurentide ice (Thomas, 1977), with a complete disconnection possibly happening before 13.1 cal ka BP (Figure 5.1, insert 4). The deglaciation of most Appalachian valleys would have allowed the drainage of Glacial Lake Candona at about the same time (Figure 5.1, insert 5), as well as the initial invasion of marine waters in the St. Lawrence Valley (Occhietti & Richard, 2003), but the exact timing of those events in the Quebec City area remains uncertain.

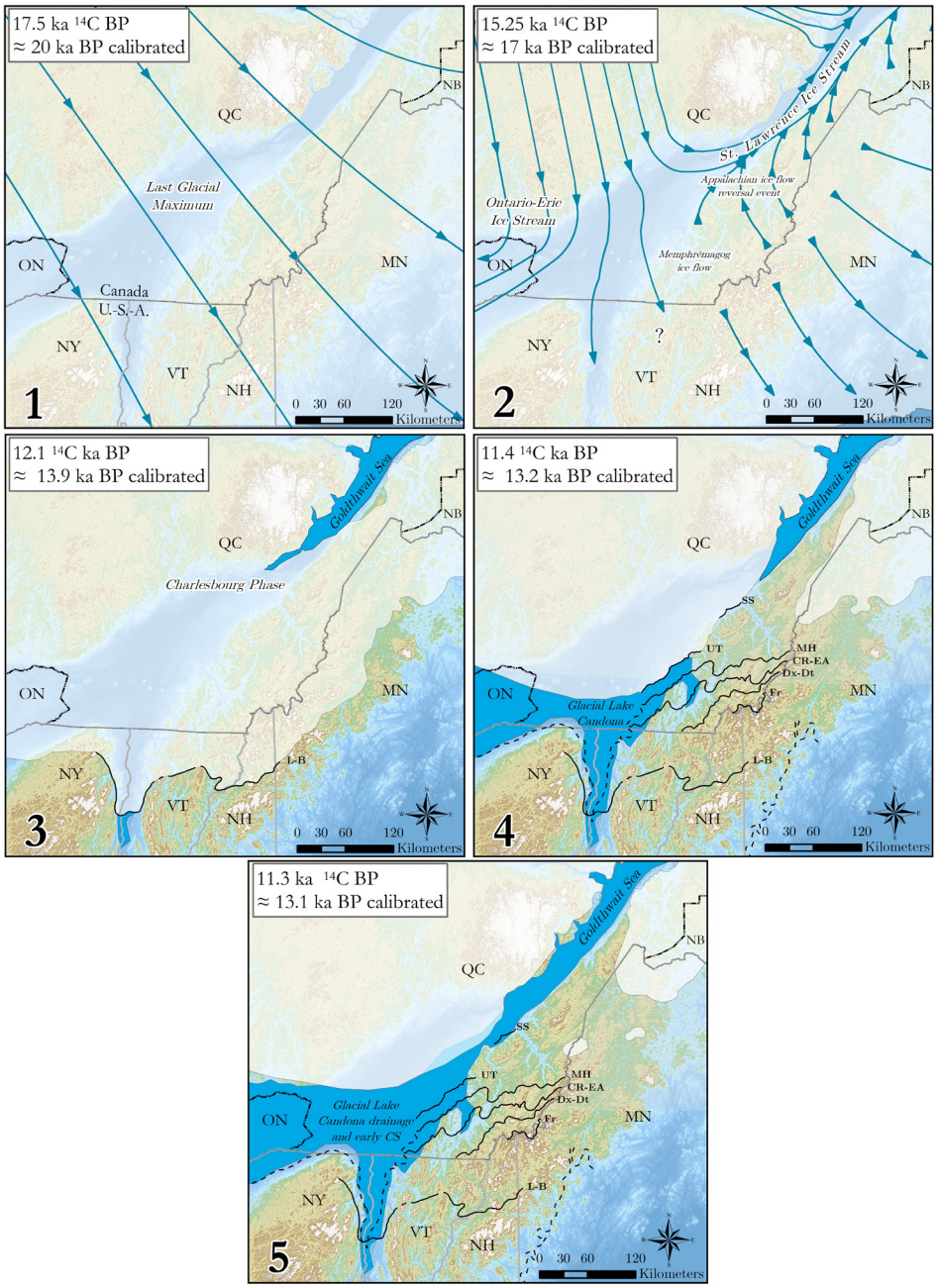

Figure 5.1 : Conceptual model of the Late Wisconsinan ice margins (black lines) in the central and lower St. Lawrence Valley during the stages preceding and following the St. Lawrence Ice Stream. Blue lines depict the generalized ice flow lines, while blue areas depict the surface occupied by post-glacial seas and lakes. Approximate Appalachian ice margins are from Richard et al. (2007). Ice retreat patterns and chronology (conventional 14C years BP) for the south-central Québec and adjacent New England are from Richard and Occhietti (2005). The outline of the Ulverton-Tingwick (UT), Mont Ham (MH), Cherry River-East-Angus (CR-EA) and Dixville-Ditchfield (Dx-Dt) moraines are after Parent (1987). The Frontier Moraine (Ft) is after Shilts (1981) while the Littleton-Bethlehem Moraine is after Ridge et al. (1999). 1: Development of ice streams (SLIS and OEIS) changing ice flow lines; 2: Development of ice streams (SLIS and OEIS) changing ice flow lines; 3: SLIS retreat and Goldtwait Sea early incursion; 4: Glacial Lake Candona development and disconnection of LIS from Appalacian ice; 5: Drainage of Glacial Lake Candona and early Champlain Sea.

The marine incursion in the valley was followed closely by the first cold pulse of the Younger Dryas, and was associated by LaSalle & Shilts (1993) with a Laurentide ice readvance over the marine basin based on the presence of a shell-bearing glaciomarine diamicton underlying the main marine sequence at several localities in Lotbinière. In the absence of a well-defined regional context, the regional significance of this event has since remained somewhat contested (see Occhietti *et al.,* 2011).

5.3 Methodology

5.3.1 Moraine mapping

Moraines were mapped primarily through the interpretation of a high-resolution digital terrain model (DTM) derived from airborne LiDAR point-cloud data in the entire study area (see Figure 5.3). Multiple illumination shaded relief grids were created and interpreted, and moraine ridges were mapped in QGIS 2.8 Wien (QGIS Development Team, 2014). The full methodology to create these grids can be found in Webster *et al.* (2006). Moraines were digitized at a cartographic scale varying between 1: 500 and 1: 2 000, depending on their size. Fieldwork was conducted primarily to verify and validate the geomorphic interpretation of the LiDAR data.

5.3.2 Chronology

As only one radiocarbon date pertaining to deglacial or early Champlain Sea events was obtained in the course of this research, we have to rely on radiocarbon dates drawn from the literature. Ages are either reported as conventional ($\partial\,^{13}C$ = -25 ‰) ^{14}C years before present (^{14}C BP), or as calibrated (calendar) years before present (cal BP). Calibrated ages examined in the discussion section were calibrated using IntCal13 for terrestrial material (Reimer *et al.,* 2013). All radiocarbon dates discussed in this paper are referenced either in Table 5.1 (Quebec City area) or Table 5.2 (outside the Quebec City area).

As the radiocarbon ages obtained on Champlain Sea and Goldthwait Sea shells are generally affected by a multitude of effects, including global and local reservoir effects (Occhietti & Richard, 2003; Richard & Occhietti, 2005), they may differ from terrestrial material of equivalent age by 350 to 1800 years and are often considered unreliable, except in terms of relative chronology for a

given area or for selected mono-specific assemblages, such as *Hiatella arctica* assemblages. Thus, the chronologic framework of Cronin *et al.* (2012) for the Champlain Sea invasion of the St. Lawrence Valley is used here as a regional reference, as their chronology was established from radiocarbon dates obtained on terrestrial plant material, or extracted from varve counting, pollen stratigraphic record and ice-marginal retreat data.

Occhietti and Richard (2003) established the total reservoir effect affecting *Macoma* sp. shells at 1780 ^{14}C years from the AMS cross-dating of plant debris (10 510 ± 40 ^{14}C yr BP) trapped in a lake basin on Mount St. Hilaire about 500 ^{14}C years after the inception of Champlain Sea. In the easternmost part of the basin, a total reservoir effect of 1300 ^{14}C years was estimated by Lamarche (2011) by cross-dating *Hiatella arctica* shells and *Salix sp.* twigs in deltaic sands deposited in the Champlain Sea. Lamarche (2011) showed that it was not possible to build a reliable relative sea-level curve without limiting the selection of ages to monospecific assemblages, in this case *Hiatella arctica.* Tremblay (2008) obtained a mean reservoir age of 1060 ± 220 ^{14}C for a colony of *Balanus crenatus* found near Hemmingford, and 1210 ± 200 for *Hiatella arctica.* Austin *et al.* (1995) observed a 700 - 800 ^{14}C years reservoir effect by comparing ^{14}C ages of shallow marine mollusks from the Hebridean Shelf of northwest Scotland to the apparent ages of the Icelandic Vedde ash from various regions in the North Atlantic. Here, we chose to subtract a marine reservoir value of 1000 ^{14}C years to all conventional ages reported for shells in an attempt to build a chronology that is both compatible with the terrestrial ^{14}C record of the St. Lawrence Valley and with the deglaciation chronology of New England (Thompson *et al.,* 2011).

5.4 Results, chronology and interpretation

5.4.1 Early Champlain Sea in the St. Lawrence Valley

Evidence for the earliest incursion of the Champlain Sea in the St. Lawrence Valley is recorded sparsely in the eastern part of the basin by radiocarbon-dated marine shells or shell fragments contained in silts overlying glacial or fluvioglacial sediments. They provide a minimum age for local ice retreat between the Appalachian piedmont and the Saint-Narcisse moraine. In the southwestern part of the study area, S. Occhietti collected *Hiatella arctica* shells dated 11 900 ^{14}C BP ± 100 (GSC-5854; McNeely (2006)) enclosed in silty sands overlying ice-proximal sands. At

Rivière du Chêne in Lotbinière, an age of 11 700 ± 100 ^{14}C BP was obtained on *Balanus hameri* shells contained in a pavement overlying ice-proximal sands and overlain by marine silts (GSC-5927 ; Occhietti *et al.,* 2001b; McNeely, 2006).

In Charlesbourg (St. Lawrence River north shore), *Portlandia arctica* shells collected by P. LaSalle in a marine sandy silt unit were dated at 12 900 ± 110 ^{14}C BP (GSC-1533; (Lowdon & Blake, 1973; LaSalle *et al.,* 1977). Although this age may appear as inconsistent with the two previous dates because of its much older apparent ^{14}C age, it should be noted that the dated unit at the Charlesbourg site underlies a compact till unit (LaSalle *et al.,* 1977a, p. 26). This till unit may actually record a glacial readvance in an earlier phase (Charlesbourg) of the Champlain Sea (Parent and Occhietti, 1988). The large age discrepancy between GSC-1533 and GSC-5854 might be explained simply by the fact that they do not record the same marine phase: GSC-1533 refers to a relatively narrow marine embayment developed right after the SLIS while GSC-5854 refers to the later invasion of the main Champlain Sea basin.

5.4.2 St. Lawrence River south shore

In the Lotbinière area, LaSalle & Shilts (1993) associated the St-Edouard moraine to a Laurentide ice readvance into the early Champlain Sea on the basis of the discovery of a shell-bearing glaciomarine diamicton at several nearby locations, including the sites of Issoudun II (GSC-4998, 11 810 ± 90 ^{14}C, *Balanus hameri* shell) and Saint-Nicholas IV (GSC-1476, 11 600 ± 170 ^{14}C, *Balanus hameri* shell). LaSalle & Shilts (1993) refer to this event as the St-Nicolas readvance and correlate it with the Younger Dryas events of northwestern Europe.

The Ruisseau Bourret site adds a minimum age for the St-Nicolas readvance in the Lotbinière area, with *Mya arenaria* shells dated at 10 600 ± 100 ^{14}C (GSC-4996) contained in a shallow water littoral facies directly above the typical *Balanus hameri* bearing diamicton (LaSalle & Shilts, 1993). The Issoudun I site (GSC-4997, 10 700 ± 90 ^{14}C Y BP, *Hiatella arctica*) also confirms the minimum age of the event, with an age notably similar to GSC-4996. In fact, GSC-4996, GSC-4997 & GSC-4998 constrain this part of the glacial readvance event in time. Just south of the St-Edouard moraine, at Les Trois Fourches (GSC-4769), marine silts contain *Balanus hameri* shells dated 10 900 ± 120 ^{14}C Y BP. This site is not described nor interpreted in LaSalle & Shilts (1993),

but notes by the first author in McNeely & Brennan (2005) suggest that the initial interpretation was that the *Balanus hameri* fauna developed near an advancing ice front which emplaced the St. Edouard moraine. Since the silt unit in which the shells were found is not overlain by the typical glaciomarine diamicton unit, it probably represents conditions similar to the settings of GSC-4996 and GSC-4997 (i.e. habitat re-establishment following the glacial readvance and retreat) and be interpreted as a minimum age for the ice readvance. The Saint-Edouard site near Rivière du Chêne (GSC-4752) shows a similar context, with *Portlandia arctica* shells dated at 10 800 ± 90 ^{14}C (LaSalle & Shilts, 1993).

The St-Edouard Moraine identified by LaSalle and Shilts (1993) does not, however, stand as an isolated ice marginal feature; two other moraine ridges can be mapped on the south shore of the St. Lawrence River between the St-Edouard moraine and the Appalachian Uplands. One is the Les Trois-Fourches Moraine, named after the Les Trois-Fourches site of LaSalle & Shilts (1993) where *Balanus hameri* shells were found in Champlain Sea sediments. This almost continuous moraine lies about 3 kilometers south of the St-Edouard Moraine segments mapped by these authors. However, the longest and most prominent moraine ridge of this area (identified in the context of this work) was mapped 15 kilometers further south, and is herein referred to as the Lyster Moraine (Figure 5.2 and Figure 5.3). The narrow ridge extends southwestward from St-Agapit to Notre-Dame-de-Lourdes in a characteristic arcuate outline, common to numerous other ice-marginal features identified in this region.

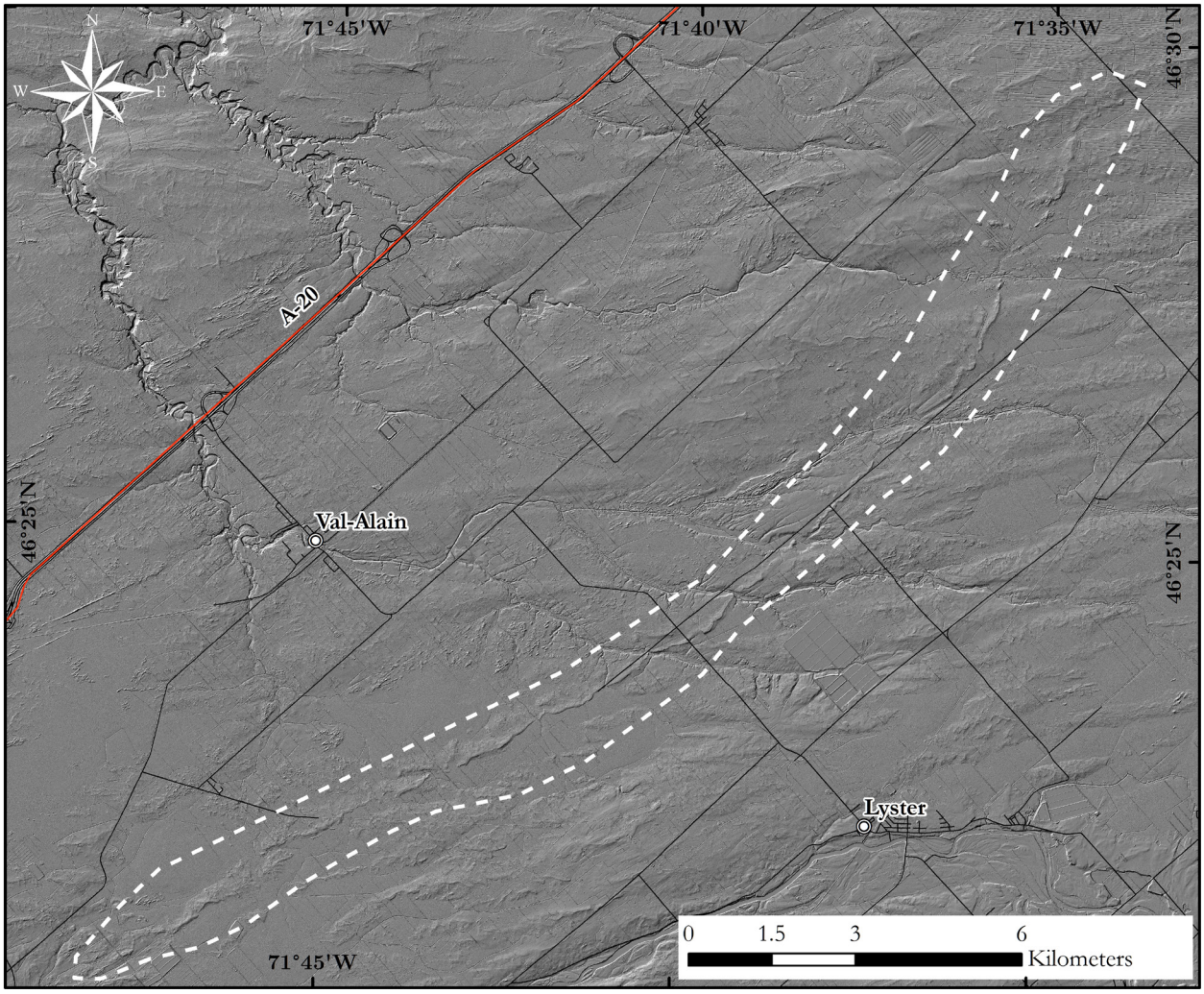

Figure 5.2 : LiDAR-derived hillshaded relief map showing the Lyster Moraine extending from the southwest to the northeast of the map frame.

Minor, less developed and discontinuous moraines are ubiquitous in Lotbinière County between the Appalachian Uplands and the St. Lawrence River, but most are relatively faint due to heavy reworking by Champlain Sea waves and currents (Figure 5.3). The location of the Issoudun I site (GSC-4997) of LaSalle & Shilts (1993), south of both the St-Edouard and Les Trois Fourches moraines but north of the Lyster Moraine, suggests that the latter may in fact represent the outermost position of the early YD readvance in the Lotbinière region. While its continuity is clearly visible on a LiDAR-derived hill-shaded relief map, it is faint and hardly noticeable in the field, which could explain why only Dubé (1971) had mentioned the presence of a morainic ridge at that location. A shallow auger borehole in the moraine revealed the surface material to be

composed of compact stony diamicton with a sandy matrix and subangular to subrounded stones. Dubé (1971) reported a section exposing about 4.5 meters of fossiliferous till.

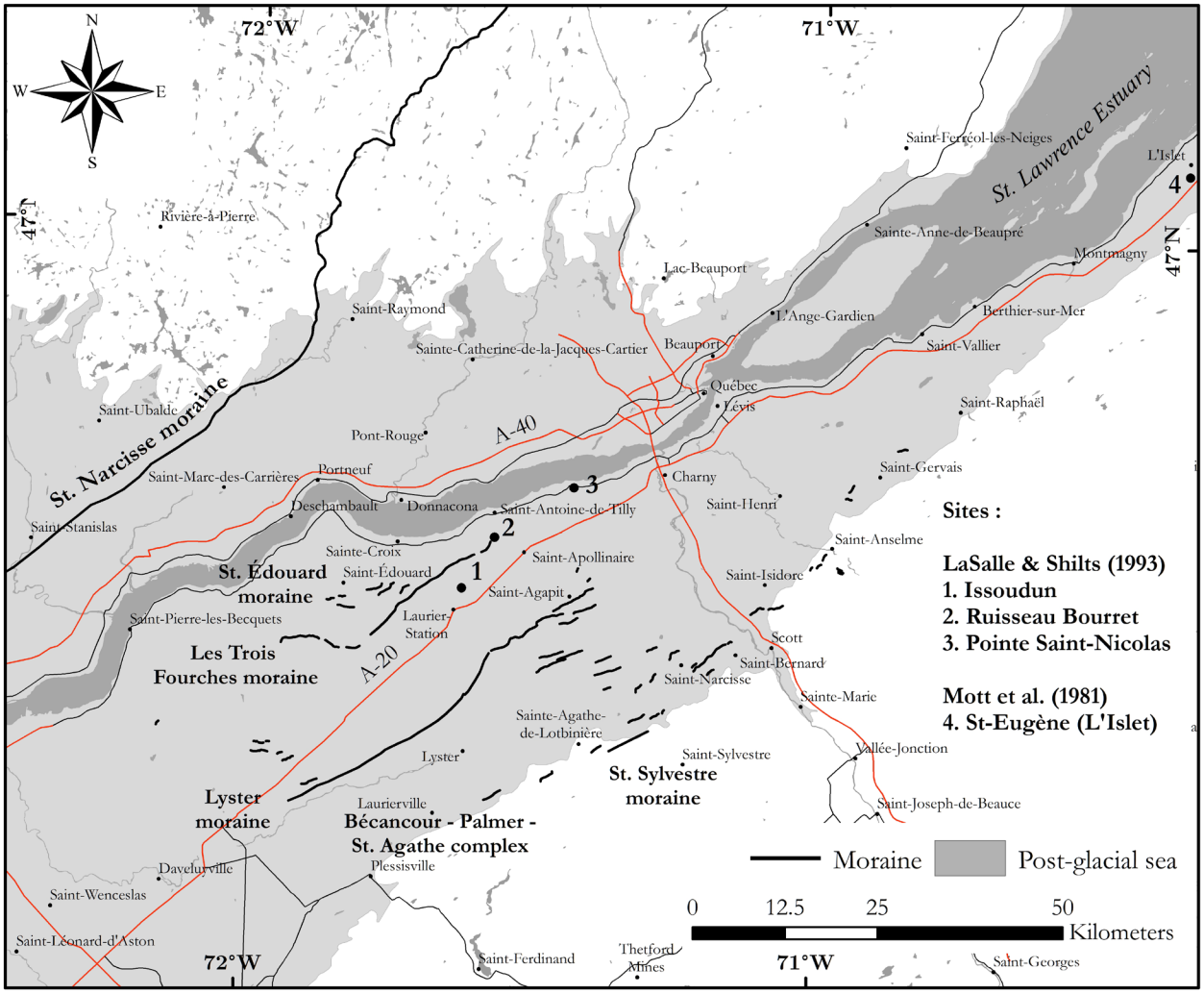

Figure 5.3 : Newly mapped Laurentide ice moraines in the Lotbinière area.

As suggested by LaSalle & Shilts (1993), there is evidence that the ice front was very close to L'Islet (St-Eugene site) northeast of Montmagny on the south shore of the St. Lawrence River around 11 050 ± 130 ^{14}C BP (QU-448; δ^{13}C assumed to be -27‰). This age was obtained on an organic layer interstratified with Champlain Sea deltaic sediments (LaSalle *et al.,* 1977; Mott & Anderson, 1981) and characterized by an arctic beetle fauna and flora, which points towards the presence of a nearby ice front (Morgan, 1987). This dating on terrestrial material was interpreted by LaSalle & Shilts (1993) to be too young to represent the early YD Laurentide ice readvance

event in the Champlain Sea, but we now know that shell dates are not directly comparable to terrestrial material because of marine radiocarbon reservoir effects. At 12 709 – 13 125 cal BP, an interval that includes Lake Candona drainage, the Champlain Sea invasion as well as the freshening of the CS basin, QU-448 is in agreement with the chronology of Cronin *et al.* (2012).

In the western part of the study area, in a Gentilly River section, A. Bolduc (reported in McNeely (2002)) associated a glacio-marine diamicton containing *Balanus hameri* (11 600 ± 100 ^{14}C Y BP, GSC-5394) with the Saint-Narcisse episode, even though the ice front position at that time lies at least 30 km further north. A microfaunal analysis by J.P. Guilbeault (pers. comm.) indicates that the foraminiferal assemblage is very similar to that present in the vicinity of the Saint-Narcisse moraine. It is unlikely that similar glaciomarine conditions existed that far from the ice front during the Saint-Narcisse episode. A glacial readvance with a frontal position close to Gentilly would better fit the paleoecological setting of GSC-5394.

5.4.3 St. Lawrence River north shore

Post-LGM glaciomarine diamictons and moraines have also been observed on the north shore of the St. Lawrence River in the Quebec City area.

LaSalle (1970) initially interpreted the Lake Saint-Charles moraine as part of the Saint-Narcisse moraine system, but subsequent mapping by LaSalle et al. (1972) traced the St-Narcisse Moraine as a continuous feature in the Laurentian Highlands between Saint-Léonard-de-Portneuf and Saint-Siméon near the Saguenay fjord. This work thus showed that the Saint-Narcisse Moraine lies several tens of kilometers north of the Lake Saint-Charles moraine. The Lac Saint-Charles moraine thus has to represent an event older than the St-Narcisse Moraine. In the conceptual deglaciation model proposed here, the Lac Saint-Charles moraine is construed as a lateral moraine emplaced on the north side of a Laurentide outlet glacier re-advancing into the Champlain Sea.

Table 5.1 : List of selected published radiocarbon dates pertaining to the early Younger Dryas in the Quebec City area. All these observations are illustrated on the map in Figure 5.4. Dated materials are *Balanus hameri* shells unless otherwise stated. CS: Champlain Sea, GM: Glaciomarine, FG: Fluvioglacial. Calibrated age 1-σ cal BP age ranges for shells are calculated by applying a total reservoir effect of 1000 ^{14}C years (i.e. by subtracting 1000 ^{14}C to the conventional ages) and calibrating using the IntCal13 (terrestrial) curve.

Site name	Lab number	Position or deposit	Elevation (mASL)	Conventional ^{14}C BP age	Calibrated age 1-σ cal BP*	Reference
Charlesbourg	GSC-1533	Marine clays: early CS (Portlandia arctica)	110	12 900 ± 110	13565 - 13838	Lowdon and Blake, 1973; LaSalle *et al.*, 1977; McNeely and Brennan, 2005
St-Henri de Lévis	QU-93	Hiatella arctica in ice-contact seds, Interstratified layered clay and gravel in ice-contact ridge	104	12 640 ± 160 BP	13292 - 13695	Samso*n et al.* 1977
Chutes Jean-Larose	TO-10929	Shells	?	12 300 ± 90	13082 - 13240	Occhietti *et al.* 2007
Notre Dame des Laurentides	GSC-1235	GM diamicton (Mya truncata)	176	12 000 ± 160	12741 - 13007	Lowdon and Blake, 1976; LaSalle and Elson, 1975; McNeely and Brennan, 2005
St. Sylvere	GSC-5854	Silty sand: early CS (Hiatella arctica)	79	11 900 ± 110	12700 - 12897	McNeely, 2006; McNeely and Brennan, 2005
Issoudun II	GSC-4998	GM diamicton	90	11 800 ± 90	12649 - 12772	McNeely and Jorgensen, 1993; LaSalle and Shilts, 1993; McNeely and Brennan, 2005
Rivière du Chêne	GSC-5927	Pavement between deglaciation sands and marine silts: early CS	60	11 700 ± 100	12572 - 12711	Occhietti et al.2001a; McNeely, 2006; McNeely and Brennan, 2005
Deschambault	GSC-6051	GM diamicton	10	11 700 ± 100	12572 - 12711	McNeely, 2006; McNeely and Brennan, 2005
Pointe Saint-Nicolas	QU-20	GM ice-contact Drift (Mya truncata)	70	11 660 ± 290	12085 - 12825	Samson et al.1977
Gentilly River (II)	GSC-5394	GM diamicton	65	11 600 ± 100	12428 - 12684	McNeely, 2002; McNeely and Brennan, 2005
Lapointe	GSC-1295	GM diamicton	67	11 600 ± 160	12381 - 12713	Lowdon and Blake, 1976; LaSalle and Elson, 1975; McNeely and Brennan, 2005
Saint-Nicholas IV	GSC-1476	GM diamicton	61	11 600 ± 170	12378 - 12715	Lowdon and Blake, 1979; LaSalle and Elson, 1975; McNeely and Brennan, 2005
Chevalier	GSC-1232	Ice rafted GM diamicton	106	11 500 ± 160	12158 - 12629	Lowdon and Blake, 1976; LaSalle and Elson, 1975; McNeely and Brennan, 2005
Valcartier	Beta-242524	Hiatella arctica	160	11 450 ± 60	12175 - 12528	Unpublished
Les Grands Déserts	GSC-6283	GM diamicton	75	11 300 ± 110	11950 - 12385	McNeely, 2006; McNeely and Brennan, 2005
Issoudun III	GSC-5957	Sands underlying GM diamicton	90	11 300 ± 130	11935 - 12390	Occhietti et al.2001a; McNeely, 2006; McNeely and Brennan, 2005,
Place Notre-Dame	GSC-6292	Sand overlying diamicton (Mya calcarea)	85	11 100 ± 120	11404 - 11943	McNeely, 2006; McNeely and Brennan, 2005

Table 5.1 (cont.) : List of selected published radiocarbon dates pertaining to the early Younger Dryas in the Quebec City area. All these observations are illustrated on the map in Figure 5.4. Dated materials are *Balanus hameri* shells unless otherwise stated. CS: Champlain Sea, GM: Glaciomarine, FG: Fluvioglacial. Calibrated age 1-σ cal BP age ranges for shells are calculated by applying a total reservoir effect of 1000 ^{14}C years (i.e. by subtracting 1000 ^{14}C to the conventional ages) and calibrating using the IntCal13 (terrestrial) curve.

Site name	Lab number	Position or deposit	Elevation (mASL)	Conventional ^{14}C BP age	Calibrated age 1-σ cal BP*	Reference
St-Henri de Lévis	Beta-11587	Hiatella arctica in ice-contact sediments, Interstratified layered clay and gravel in ice-contact ridge	?	11 080 ± 80	11404 - 11803	Occhietti *et al.* 2001
St-Eugene	QU-448	Organic matter in stratified sands	145	11 050 ± 130	12797 - 13039	Lortie & Guilbault (1984)
Les Trois Fourches	GSC-4769	GM silts	60	10 900 ± 120	11204 - 11415	McNeely and Jorgensen, 1992; LaSalle and Shilts, 1993; McNeely and Brennan, 2005
Saint-Edouard	GSC-4752	GM clays (Portlandia arctica)	38	10 800 ± 90	11122 - 11323	McNeely and Jorgensen, 1992; LaSalle and Shilts, 1993; McNeely and Brennan, 2005
Issoudun I	GSC-4997	Sands above GM diamicton (Hiatella arctica)	90	10 700 ± 90	10867 - 11228	McNeely and Jorgensen, 1993; LaSalle and Shilts, 1993; McNeely and Brennan, 2005
Sainte-Christine II	GSC-5529	GM diamicton (Hiatella arctica)	115	10 700 ± 100	10866 - 11230	McNeely, 2005; McNeely and Brennan, 2005
Ruisseau Bourret	GSC-4996	Sands above GM diamicton (Mya arenaria)	68	10 600 ± 100	10782 - 11124	McNeely and Jorgensen, 1993; LaSalle and Shilts, 1993

Table 5.2 List of selected published radiocarbon dates pertaining to the early Younger Dryas outside of the Quebec City area. CS: Champlain Sea, GM: Glaciomarine, FG: Fluvioglacial. Calibrated age 1-σ cal BP age ranges for shells are calculated by applying a total reservoir effect of 1000 ^{14}C years (i.e. by subtracting 1000 ^{14}C to the conventional ages) and calibrating using the IntCal13 (terrestrial) curve.

Site name	Lab number	Position or deposit	Elevation (mASL)	Conventional ^{14}C BP age	Calibrated age 1-σ cal BP*	Reference
Trois-Pistoles	GSC-102	Portlandia a in clays under a till	?	13 130 ± 170	13 748 - 14248	Lee, 1963
Saint-Modeste	TO-948	Portlandia a in clays under a till	?	12 860 ± 160	13 477 - 13 840	Rappol, 1993
Les Éboulements II	UL-2174	Shell fragments	140	12 580 ± 110	13295 - 13538	Occhietti et al., 2001; FOP
Les Éboulements I	Beta-143295	Shell fragments	140	12 310 ± 100 BP	13085 - 13258	Occhietti et al., 2001; FOP
Rivière-du-Loup	TO-947	Portlandia a in fossiliferous till	?	12 130 ± 160	12 807 - 13 112	Rappol, 1993
Mont-Carmel I	Beta-343392	Portlandia a	53	11 870 ± 40	12708 - 12763	Unpublished
Mont-Carmel II	Beta-375090	Portlandia a	73	10 930 ± 40	11255 - 11388	Unpublished
Charette	Beta-343391	Shell	?	10 770 ± 40	11179 - 11234	Unpublished

In close proximity and in a somewhat similar geomorphological and ice dynamics context, glaciolacustrine sediments were observed by Lamarche (2011) to overlie ice-proximal sands in the Montmorency River Valley. These sediments were deposited in an ice-dammed lake in which perched deltas were emplaced in both the main river valley and in several adjacent minor valleys up to a maximum elevation of 335 m. The ice-dammed lake used a series of outlets as the ice margin retreated southward, namely a 335 m stage at Sainte-Brigitte-de-Laval, a 295 m stage at Lac Beauport, and minor stages at the Lac de la Retenue before reaching its main delta in the Goldthwait Sea. As these glaciolacustrine deposits rest conformably on a glaciofluvial succession and reach up to 20 m of thickness, it is clear that a major part of the Montmorency watershed was already deglaciated when the outlet glacier readvanced in the St. Lawrence Valley and blocked, at least partly, the main connection between the Champlain and Goldthwait seas.

While those glaciolacustrine units are lacking dateable material, glaciomarine diamictons have been dated at key locations in this area. In Notre-Dame-des-Laurentides, whole valves of *Mya truncata* enclosed in a glaciomarine diamicton observed at an elevation of 176 mASL were dated at 12 000 ± 160 ^{14}C yr BP (GSC-1235; Lasalle & Elson (1975), Blake Jr. & Lowdon (1976)). Fragments of *Balanus hameri* present in a glaciomarine diamicton near Sainte-Anne-de-Beaupré were dated at 11 600 ± 160 ^{14}C yr BP (Lapointe site of LaSalle and Elson, 1975, GSC-1295). Fragments of *Balanus hameri* were also found in a glaciomarine diamicton overlying an unidentified sand unit and overlain by 0.9 m of fossiliferous sand at the Chevalier site in Beauport (GSC-1232). These specimens were dated at 11 500 ± 160 ^{14}C yr BP. Both the Lapointe and Chevalier diamictons were interpreted by LaSalle & Shilts (1993) as most likely deposited by icebergs floating into shoals.

On the banks of the St. Lawrence River, near Deschambault, a glaciomarine diamicton containing *Balanus hameri* shells in growth position and dated at 11 700 ± 100 ^{14}C yr BP, (GSC-6051) provides another record of the outlet glacier re-advance. The Deschambeault assemblage is essentially identical to that of the Pointe Saint-Nicolas site (*Balanus hameri* shells, 11 600 ± 170 ^{14}C yr BP, GSC-1476, LaSalle & Shilts (1993); *Mya truncata* shells, 11 660 ± 290 ^{14}C yr BP , QU-20, (Samson *et al.,* 1977)), and their ages are remarkably similar. A similar *Balanus hameri* bearing diamicton was also observed at the Les Grands Déserts site, near Ancienne-Lorette, and was dated

at 11 300 ± 110 ^{14}C yr BP (GSC-6283; (McNeely, 2005, 2006). A few kilometers to the northeast, a section at the Place Notre-Dame site (GSC-6292) exposes a fossil-bearing sand overlying till. *Macoma calcarea* shells collected at the interface were dated at 11 100 ± 120 ^{14}C yr BP (McNeely, 2006; McNeely and Brennan, 2005) which can be considered as a minimum age for retreat of the outlet glacier margin from this part of the valley.

Up-ice from the postulated readvance, a glaciomarine diamicton containing *Hiatella arctica* was observed by A. Bolduc south of Sainte-Christine in the Portneuf region, very close to the position of the Saint-Narcisse moraine. Bolduc reports in McNeely and Brennan (2005) that their age of 10 700 ± 100 ^{14}C yr BP (GSC-5529; Sainte-Christine II) cannot be used to assess the age of the glacial readvance but that it provides a minimum age for the readvance.

5.4.4 Proposed deglaciation model

We propose a revised deglaciation model for the time interval between 11 200 and 10 400 ^{14}C yr BP based on the newly mapped moraines as well as a reinterpretation of published radiocarbon dates obtained on shells collected in Champlain Sea sediments (Figure 5.4). We show the St-Narcisse Moraine at 10 400 ^{14}C yr BP, but it is known that the main ridge often overlies marine clays (Gadd & Karrow, 1960; Occhietti, 2007; Légaré-Couture *et al.,* 2018), which implies that the ice front had retreated at least a few kilometers north of the main morainic ridge before its emplacement.

The proposed ice margins for 11 000 and 10 800 ^{14}C yr BP are fairly similar to those drawn by LaSalle & Shilts (1993), but the 11 200 ^{14}C yr BP margin is entirely new. The readvance is here viewed as a 25 kilometer-wide outlet glacier that occupied the valley several hundred years prior to the emplacement of the St-Narcisse Moraine. This outlet glacier, here referred to as the Sainte-Foy Outlet Glacier, developed in the aftermath of ice flow reorientations and streaming that had marked the development of the SLIS.

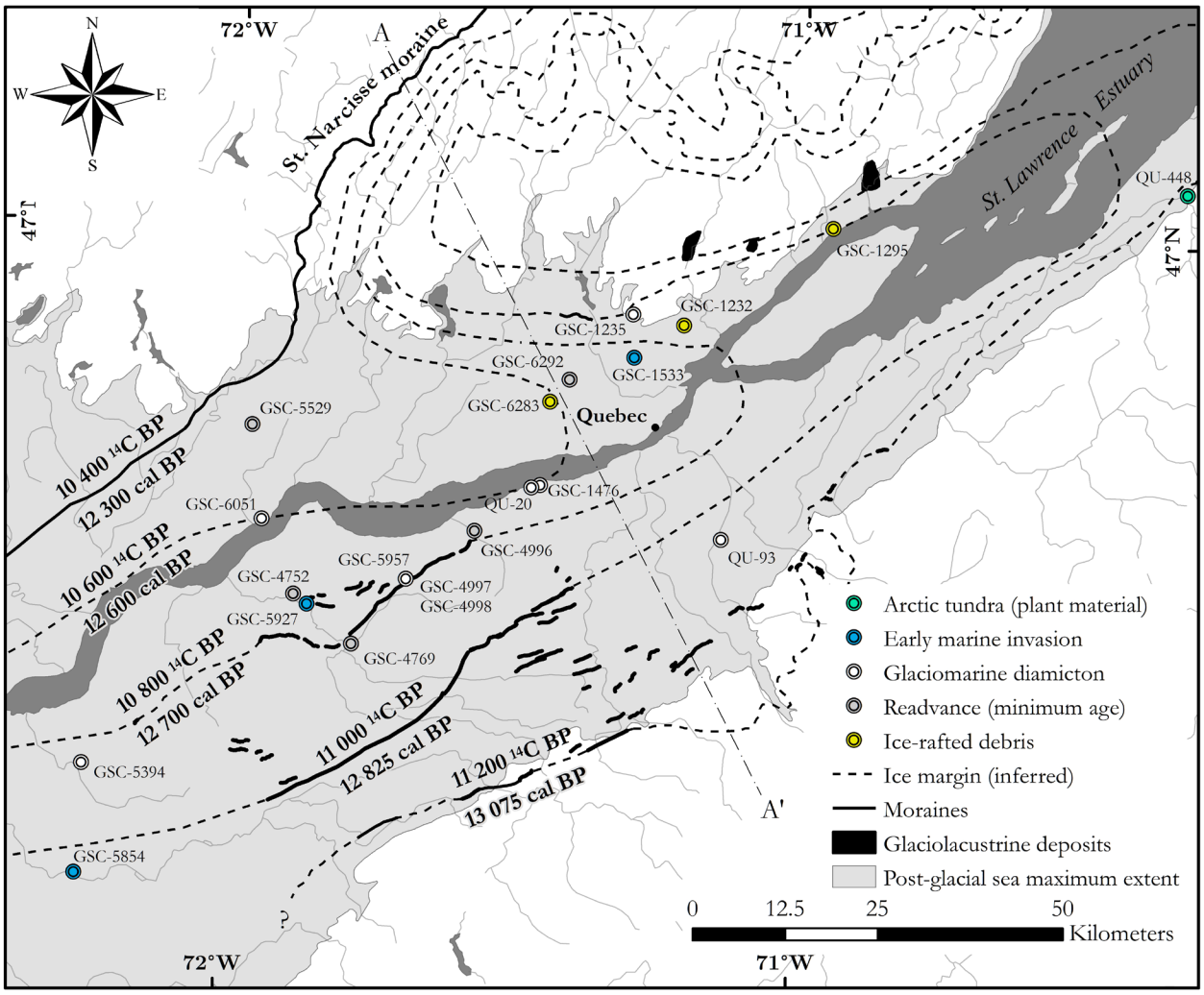

Figure 5.4 : Proposed ice margins between 11 200 and 10 400 ^{14}C BP and relevant published radiocarbon dates (see Table 5.1 for details). The A – A' cross-section across the St. Lawrence River refers to Figure 5.6.

This configuration, in relation to the early Champlain Sea in the St. Lawrence Valley, can account for various Quaternary events and features in the Quebec City area: 1) the presence of a series of arcuate end moraines on the south shore often containing a glaciomarine diamicton; 2) the geometry of the Lac Saint-Charles moraine (visible on Figure 5.4, east of the location of the GSC-1235 sample) and other moraine ridges near Mont Ste-Anne and in the St-Tite basin ; 3) ice-dammed lakes recognized at high levels in Laurentian valleys along the Côte-de-Beaupré area, as well as northward trending paleocurrents in ice-contact sediments in the Montmorency Valley; 4) the arctic tundra vegetation found at the St-Eugène site; 5) the co-occurrence of marine and freshwater ostracods in sediments of the early Champlain Sea basin (Cronin *et al.,* 2012).

The presence of an outlet glacier in this part of the St. Lawrence Valley also accounts for the ice contact stratified sediments (including the Valley-Jonction delta) identified by Blais & Shilts (1989) in the Chaudière and Etchemin river valleys that were interpreted as deposited by a southward-flowing glacier. Glaciolacustrine sediments present in this area were described in detail by Normandeau (2010). The interpretation of a LiDAR-derived digital terrain model of the Chaudière River delta reveal a set of well defined, arcuate, southeastward oriented glacial lineations (Figure 5.5). At Saint-Patrice-de-Beaurivage, no glacial lineations are visible south of the Saint-Sylvestre moraine. While the moraine becomes discontinuous in the axis of the Chaudière River, glacial lineations are not present south of the Saint-Elzéar - Sainte-Marie axis. This assemblage suggests that during the last ice movement in this part of the valley, a deflection of the outlet glacier flowed into the Chaudière River Valley, stopping its advance just north of Valley Jonction. This configuration could explain the presence of a clayey till lying on heavily deformed lacustrine sediments resting directly on the Lennoxville till (LGM) in the same valleys (McDonald & Shilts, 1971; Blais & Shilts, 1989).

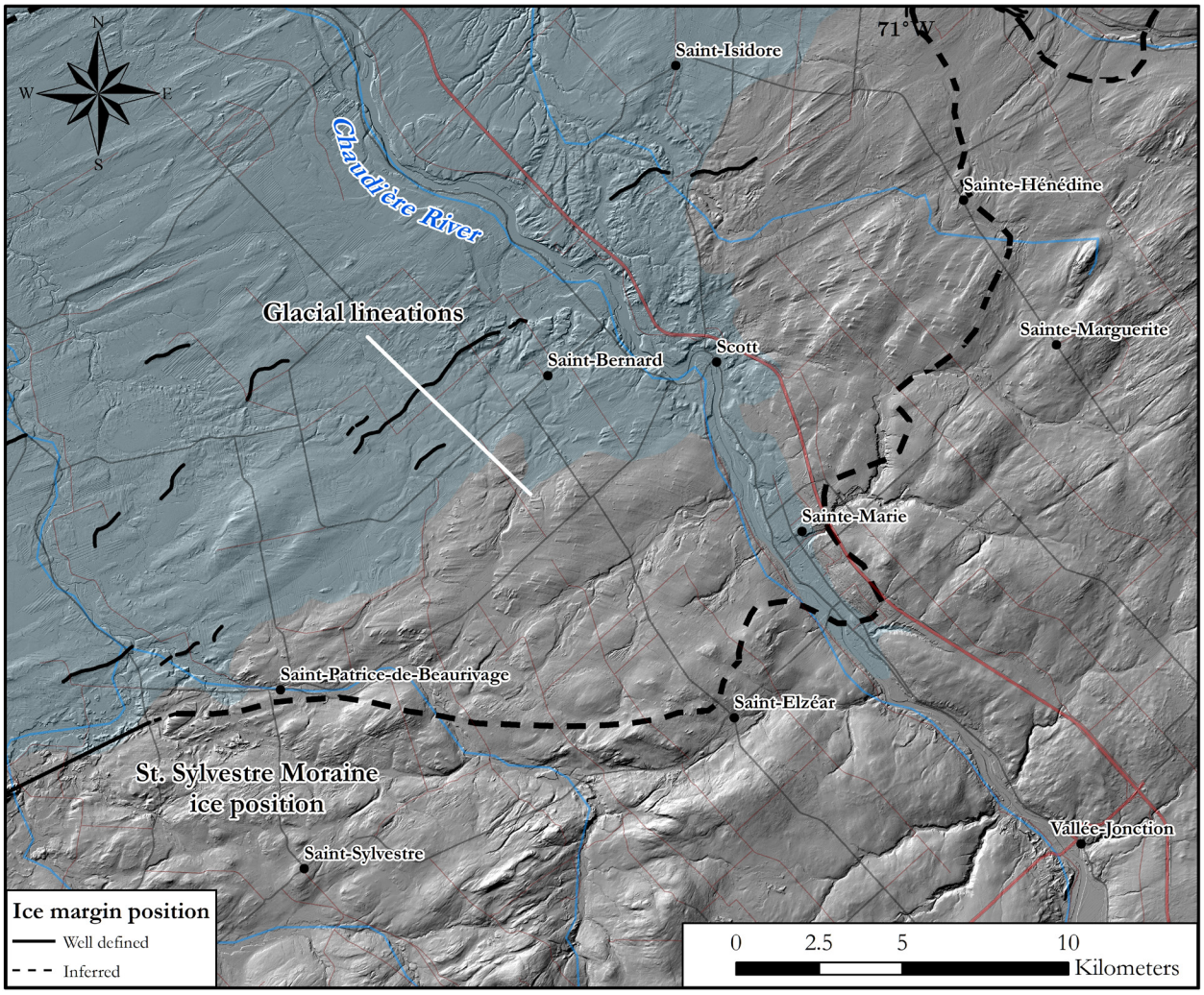

Figure 5.5 : Chaudière River delta in the Sainte-Marie area. Glacial lineations oriented towards the east and southeast, suggesting ice flow into the Chaudière River, are omnipresent north of the St. Sylvestre Moraine, and notably absent south of it. The blue shade indicates the maximum extension of the Champlain Sea.

5.5 Interpretation and discussion

Cronin *et al.* (2012) identified rapidly fluctuating salinity levels in the Champlain Sea during the first centuries of its existence (zone Pre-A) on the basis of the improbable cohabitation of the ostracode *Candona subtriangulata* with marine foraminifera, as observed in several cores in the Lake Champlain sub-basin. The sequence of events recorded in those cores includes complete freshening of the basin and a quick return to marine conditions within a few hundred years at the most. They attributed this major change in salinity to a freshwater influx from proglacial Lake Agassiz (Broecker *et al.,* 1989; Teller *et al.,* 2002) based on faunal and oxygen isotope ($\delta^{18}O$) data.

Stratigraphic evidence of this proglacial lake drainage event through the St. Lawrence Valley is, however, lacking. The discovery of new LIS moraines in the Lotbinière sector leads to a reappraisal of the hypothesis of a glacial readvance near Quebec City, as discussed briefly but dismissed by Cronin *et al.* (2012) on the basis of the lack of geological evidence at that time. A readvancing Laurentide ice front across the early Champlain Sea embayment likely blocked temporarily the incursion of Goldthwait Sea waters in the main Champlain Sea basin and went on to control the incursion of marine waters in the central valley. As LaSalle & Shilts (1993) point out, the shell-bearing diamicton observed at many sites suggests that the ice margin was at least partially grounded during the readvance as it incorporated shells of the deep-water barnacle (*Balanus hameri*) living attached to stones on the seafloor (Hillaire-Marcel, 1980). Furthermore, the abundance of stones on the seafloor indicates that swift bottom currents were maintained as the readvancing ice margin blocked part of the connection between the Goldthwait Sea and Champlain Sea basins.

Our review and analysis lead us to the sequence of events illustrated on a spatiotemporal diagram (Figure 5.6) representing the location of the ice margin on a cross-section across the St. Lawrence River valley at the height of Quebec City. Ice streaming in the St. Lawrence River contributed to the thinning of this part of the glacier up until it allowed the penetration of marine waters up the estuary (*Charlesbourg Phase,* Parent & Occhietti (1988)) and eventually led to the isolation of Appalachian ice from the LIS. Following these events, a first cold pulse is recorded and is referred to as the *Beauce Event* (Occhietti *et al.,* 2001b).

Prior to this study, the last morainic belts of the northwestward retreating Laurentide ice sheet in this sector of the Appalachian piedmont were the Ulverton–Tingwick Moraine and the Saint-Sylvestre Moraine (see Figure 5.1), neither of which have been dated directly. We correlate the emplacement of the former with the maximum extension of the ice during the *Beauce Event*. The ice likely retreated from the position of the Ulverton-Tingwick Moraine around 11 250 ^{14}C BP, as established from a varve count at the Rivière Landry section (Parent, 1987; Parent & Occhietti, 1999)

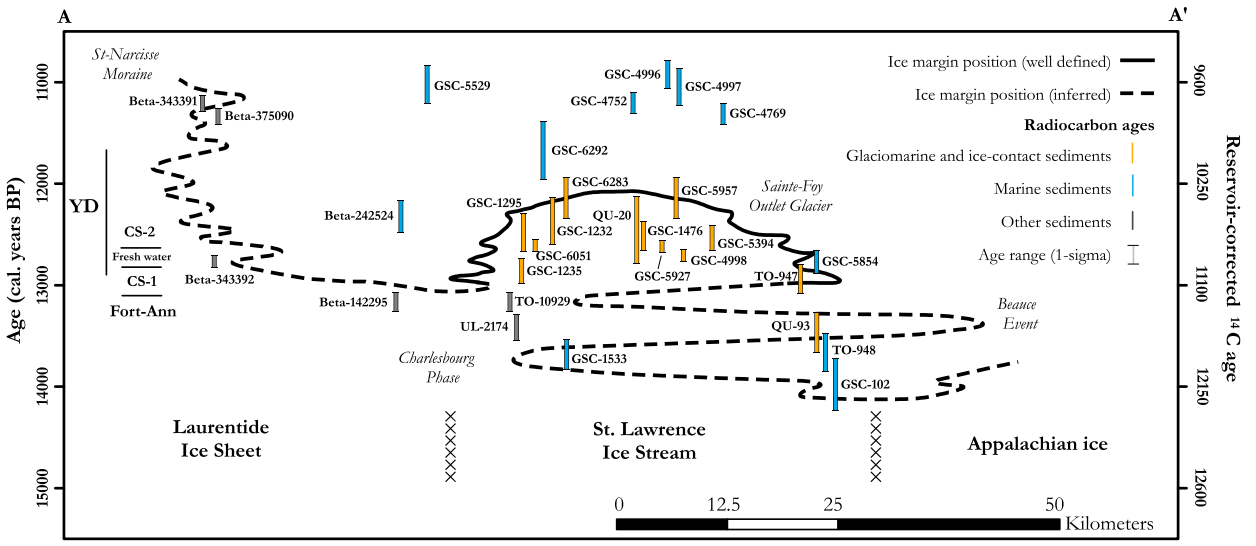

Figure 5.6 : Conceptual time-distance diagram of the position of the Laurentide ice front projected on a cross-section across the St. Lawrence Valley in the Quebec City area (left is towards the north, right is towards the south) during the last deglaciation. Published radiocarbon ages related to this period are projected as colored bars of varying lengths representing their respective 1-σ calibration range.

The *Beauce Event* was shortly followed by a warmer climate interval, which we associate with the drainage of Glacial Lake Candona and the inception of the Champlain Sea. The timing of the drainage of Glacial Lake Candona and the early Champlain Sea incursion in the St. Lawrence Valley has been established at around 11 100 ± 100 ^{14}C yr BP on the basis of basal AMS-dates of terrestrial plant macrofossils coupled with pollen content of underlying postglacial lake sediments at the Hemlock Carr site on Mont Saint-Hilaire (Occhietti & Richard, 2003; Richard & Occhietti, 2005). This short interval was quickly followed by another cold pulse, which we associate with the Laurentide ice readvance (St-Nicolas flow) postulated by LaSalle & Shilts (1993). We refer to this outlet glacier as the *Sainte-Foy Outlet Glacier*. We tentatively associate the deposition of the "Younger" till (i.e. post LGM) in the Rivière-du-Loup area (Lee, 1962) as well as the northwest flank of the St-Antonin Moraine with this readvance event and outlet glacier (Figure 5.7). Rappol (1993) dated shells contained in this till at 12 130 ± 160 ^{14}C yr BP (TO-947). A glacier advancing eastward deposited this till which is clearly a glaciomarine diamicton as it contains marine shells. While Occhietti & Richard (2003) suggested that this age could not be used to assess the mode of retreat nor the deglaciation duration of this region because of the unknown local reservoir effect in this part of the Goldthwait Sea, our paleogeographic

reconstruction is compatible with those ages when corrected with the same total reservoir effect of 1000 ^{14}C yr.

Following the end of this short cold pulse, the outlet glacier progressively retreated towards the St-Narcisse position, building the newly mapped moraines presented earlier at several intermediate positions.

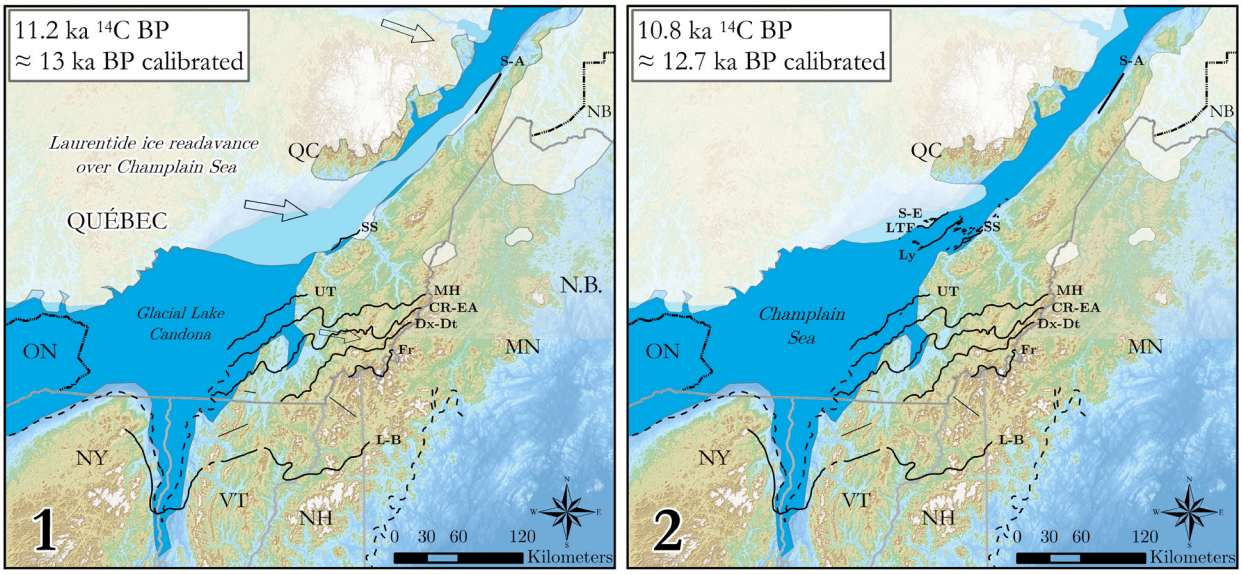

Figure 5.7 : Paleogeographic reconstruction of the proposed late Wisconsinan ice margins in the central and lower St. Lawrence Valley during the early Younger Dryas Laurentide ice between 11.2 ka ^{14}C BP (1) and 10.8 ka ^{14}C BP (2) (continuation of Figure 5.1).

5.6 Conclusion

New Laurentide ice end moraines were discovered and mapped in the Lotbinière area using high-resolution LiDAR-derived digital terrain models. This finding suggests a surging Laurentide ice front in the Quebec City area, followed by an outlet glacier advancing into the marine embayment a short time after the initial marine invasion and acting as a barrier between the early Champlain Sea and the Goldthwait Sea. While the supra-regional significance of the St-Nicolas readvance has yet to be demonstrated, this event may explain the rapid salinity oscillations recorded in the Lake Champlain cores (Cronin *et al.,* 2012). This new evidence does not invalidate the possibility that the drainage events of Lake Agassiz may have been responsible for the abrupt salinity fluctuations. The swift drainage of Lake Agassiz could have had a considerable impact on the salinity levels of

the Champlain Sea basin, but it no longer stands alone as the sole process potentially responsible for a rapid and temporary salinity drop and $\delta^{18}O$ depletion. If the ages used in our paleogeographic reconstruction, as well as their associated local reservoir effect, are in fact correct, the incursion of the Champlain Sea in the St. Lawrence Valley, the drainage of Glacial Lake Candona and the St-Nicolas readvance all occurred in a time span of about 150 ^{14}C years. This interval is quite narrow to be properly captured by radiocarbon dating on molluscs, in part because of the unknown local radiocarbon reservoir effects. This reconstruction thus highlights the need for additional research that could perhaps include different dating methods in order to better define this crucial time period.

6 DISCUSSION GÉNÉRALE ET CONCLUSION

Cette thèse de doctorat propose un cadre de la géologie du Quaternaire renouvelé pour le secteur de la Basse-Chaudière et de la rive sud de l'estuaire moyen du fleuve Saint-Laurent. Une cartographie de précision des dépôts meubles a été effectuée à l'aide de données LiDAR aéroportées. Celle-ci a ensuite été utilisée afin de construire et contraindre un modèle géologique 3D des dépôts meubles à l'échelle régionale. La paléogéographie du Wisconsinien Supérieur a ensuite été étudiée, avec un accent particulier sur deux phénomènes clés de cette période : le Courant glaciaire du Saint-Laurent, et la réavancée glaciaire dite de Saint-Nicolas dans la Mer de Champlain.

6.1 Cartographie des dépôts meubles par LiDAR

Les travaux réalisés dans le cadre du premier article ont permis de cartographier la géologie de surface d'une superficie d'environ 4 305 km^2 à l'aide d'un MNT LiDAR à relief ombragé comme carte de base. Les résultats montrent que cette méthode a permis de cartographier la zone d'intérêt avec précision et une grande confiance, dans un temps comparable ou plus rapide que les méthodes de photo-interprétation traditionnelles. Un total de 35 unités géologiques ont été différenciées sur la zone à l'étude, en plus des divers éléments linéaires qui ont été tracés (plages, limite de submersion marine, etc.), contrairement aux cartographies précédentes qui n'identifiaient qu'une quinzaine d'unités par secteur. La cartographie précise de la limite marine permettra de mieux estimer le gradient de gauchissement glacioisostatique en présence lors de l'épisode de la Mer de Champlain/Goldthwait.

Cette cartographie a été réalisée dans un contexte de projet d'acquisition de connaissances en eaux souterraines, le PACES Chaudières-Appalaches : quelques objectifs particuliers étaient donc de mise. La différenciation des unités de till remaniées et non remaniées est cruciale dans l'estimation de la recharge. Un accent particulier a été mis sur l'identification précise des affleurements rocheux, car elle ajoute des contraintes à notre carte de profondeur au substratum rocheux, un élément important dans toute étude hydrogéologique régionale. Des glissements de terrain non répertoriés auparavant situés en zone boisée, comme celui de Saint-Philippe-de-Néri

(Figure 6.1), ont également été identifiés dans des zones de sables littoraux perchés sur des affleurements rocheux alignés sud-ouest – nord-est. Ce contexte n'étant pas typique des glissements de terrain du sud du Québec, il serait intéressant d'étudier la source de l'événement et les propriétés mécaniques des sols environnants. Plusieurs autres questions restent en suspens, notamment l'origine du système fluvioglaciaire majeur identifié dans la région de Kamouraska, dans les terres et au-delà des premières séries d'affleurements rocheux. La disponibilité d'un levé LiDAR allant au-delà de la zone côtière est cruciale à la résolution de ce problème.

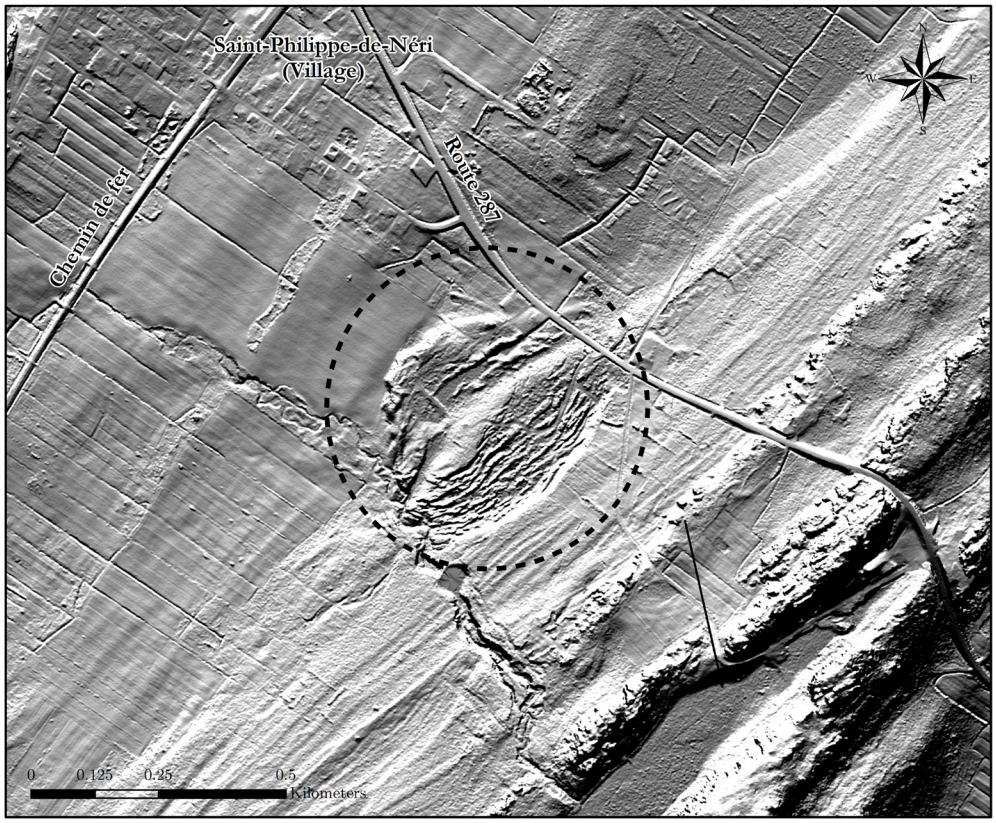

Figure 6.1 : Glissement de terrain à Saint-Philippe-de-Néri dans une zone de sables littoraux accrochés à une barre d'affleurements rocheux

L'un des principaux avantages de la méthode LiDAR réside dans le fait qu'elle permet au cartographe de représenter avec plus de précision la géologie de surface des zones fortement boisées, un phénomène courant dans l'est du Canada. Dans les zones de couvert forestier dense, la proportion de retours laser pénétrant dans la canopée et frappant le sol est beaucoup plus faible que dans les zones déboisées, mais néanmoins généralement suffisante pour reconstruire un modèle acceptable de la surface du sol. Un autre avantage de l'utilisation d'un MNT dérivé du LiDAR

plutôt que de la photographie aérienne pour interpréter et identifier la géologie de surface et les caractéristiques géomorphologiques réside dans la nature numérique des données elles-mêmes. La création d'un MNT régional basé sur LiDAR et d'autres dérivés permet au cartographe de créer une grille spatialement continue qui peut être étudiée facilement à plusieurs échelles, exportée et partagée vers d'autres formats, et examinée directement par d'autres experts sans avoir recours à des méthodes stéréoscopiques.

Il faut toutefois considérer le temps requis pour le prétraitement et le traitement des nuages de points LiDAR afin de créer les dérivées. Cette étape de la méthodologie peut toutefois être grandement restreinte dans certains cas considérant les récents efforts du ministère de la Faune, des Forêts et des Parcs du Québec (MFFP), qui a entrepris de rendre publics les dérivés de leurs jeux de données LiDAR. Il convient d'être particulièrement prudent lors du traitement des données brutes du nuage de points laser. En effet, de nombreux algorithmes de classification de nuage de points provenant du LiDAR aéroporté sont disponibles, autant dans des environnements à code ouvert que des logiciels commerciaux. Plusieurs logiciels commerciaux de type "boîte noire" sont préprogrammés pour lisser et filtrer le bruit dans les données. Dans des applications typiques d'hydrologie, il convient d'avoir un modèle numérique de terrain lissé où toutes les mailles s'écoulent vers un exutoire. Cependant, dans les applications en géologie de surface, la texture et le relief du terrain étant très importants, le lissage de la surface du MNT peut créer des résultats indésirables : ce qui pourrait être considéré comme du bruit pour certains utilisateurs peut en fait correspondre à la véritable rugosité de la surface. Dans la présente étude, il a été noté que les blocs erratiques de petite à moyenne taille étaient souvent classés comme des objets "près du sol" dans la classification originale des ensembles de données LiDAR qui nous ont été fournis. Ces retours laser étant classés comme "non sol", elles avaient été exclues de la création du MNT. Ainsi, la texture associée à ces éléments particuliers n'aurait pas été incluse dans le MNT généré par la suite et aurait été remplacée par des zones lisses. Compte tenu de la complexité technique associée au traitement des données des nuages de points laser, la meilleure pratique consiste à comparer les résultats des différents algorithmes de classification et leurs paramètres associés et à les tester sur un terrain connu, puis à utiliser le MNT le plus approprié pour le terrain étudié.

Cette démocratisation des données LiDAR amène un vent nouveau au domaine de la géologie du Quaternaire. Il faut s'attendre à ce qu'un plus grand nombre de cartes géologiques du Quaternaire du sud du Québec soient produites, revisitées et révisées à l'aide de ces ensembles de données dans un proche avenir, à mesure que les chercheurs du Quaternaire se familiariseront avec son potentiel. Des interrogations importantes concernant la chronologie de la déglaciation du sud du Québec resté en suspens depuis des décennies pourront être revisitées à la lumière de ces nouvelles données.

Il est important de noter que bien que cette approche reste innovante, elle n'est désormais plus très exclusive. En effet, pendant les travaux réalisés dans le cadre de cette thèse, le Ministère de la Faune, des Forêts et des Parcs du Québec (MFFP) a publié un guide élaboré pour aider un cartographe à identifier les dépôts superficiels typiques du sud du Québec sur un relief ombragé dérivé du LiDAR (Dupuis *et al.,* 2017). Bien que cet ouvrage n'aborde pas le thème de la géologie de surface sous l'aspect de la génétique des formes, une excellente description morphologique des éléments typique des terrains glaciaires du sud du Québec y est faite. Il se doit de noter que la morphologie et la texture de la géomorphologie de surface sont fonction non seulement de la nature du matériel lui-même, mais aussi des particularités associées aux processus de mise en place.

La géomorphométrie, qui fait référence à l'analyse numérique des paramètres ou des attributs du terrain, est née de l'avènement des modèles numériques et elle découle directement de l'analyse de ceux-ci (Evans, 1972). La résolution des MNT contrôle largement les possibilités de visualisation et d'analyse. Un MNT à l'échelle du Canada doté d'un maillage de 10 kilomètres, par exemple, rend possible l'extraction des formes associées aux Rocheuses canadiennes, aux grandes plaines centrales et aux zones côtières. Un MNT d'un maillage de 100 mètres permet d'analyser et d'extraire du modèle les formes du terrain à une échelle de « mesorelief », donc à moyenne échelle ; les vallées peuvent être différenciées des hauts plateaux, et les réseaux de drainages peuvent être identifiés. La récente disponibilité de relevés LiDAR aéroportés pour plusieurs régions autour du globe a donné un souffle nouveau à la discipline. La haute résolution des données d'élévation LiDAR permet d'investiguer les formes du terrain à l'échelle du « micro » ou « nano » relief. Avec un MNT d'un maillage de 1 m ou moins, des éléments subtils comme des lignes de plages, des zones de till remanié par les vagues ou encore de petits affleurements rocheux deviennent évidents et facilement identifiables.

Les attributs du terrain (convexité, concavité, pente, exposition topographique, index plus complexes, etc.) peuvent être calculés, différenciés et regroupés en classes. Plusieurs méthodes semi-automatisées et automatisées de classification de terrain mettant à profit les modèles numériques d'élévation et les attributs du terrain ont été récemment développées (Anders *et al.*, 2011). La science numérique des terrains n'échappera sans doute pas à l'engouement et l'enthousiasme récent pour l'apprentissage statistique (*machine learning).* L'information associée à l'essentiel des paramètres et attributs du terrain est en fait contenu dans une seule et même couche mère, le modèle numérique de terrain, alors que les paramètres sont seulement des dérivés. Il s'agit d'un excellent cas de figure et opportunité de recherche pour une application d'apprentissage profond (*deep learning*).

Dans un futur rapproché, il est très probable que le Québec municipalisé entier soit couvert par des levés d'élévation LiDAR de haute précision. L'exercice décrit précédemment nous permettrait d'élaborer une méthode afin de classifier ou d'identifier rapidement des éléments géomorphologiques recherchés sur d'autres données LiDAR du sud du Québec. Par exemple, il serait possible d'identifier les formations superficielles accumulées dans les fonds ou les flancs d'une vallée, où la végétation dense n'aurait pas permis leur identification autrement, ou encore d'identifier des zones à risque de glissement de terrain. Dans cette optique, le contexte géologique de la vallée du Saint-Laurent est particulièrement intéressant en raison de la grande diversité des éléments topographiques retrouvés et du défi que cette particularité impose.

6.2 Modélisation géologique 3D du piémont Appalachien dans le Bas Saint-Laurent

La complexité de la succession stratigraphique du secteur à l'étude présente un défi à la compréhension des événements ayant suivi le dernier cycle glaciaire. L'évaluation de l'architecture sédimentaire du secteur et l'élaboration d'un modèle géologique tridimensionnel ont mis en évidence diverses caractéristiques géologiques insoupçonnées, dont une épaisseur d'argile considérable au-dessus de la limite maximale de submersion de la mer postglaciaire qui pourrait être associée à des dépôts glaciolacustres, une hypothèse qui reste encore à vérifier. Une unité aquifère sableuse potentielle associée à la transgression Laurentienne et/ou aux événements

transgressifs/régressifs subséquents a été identifiée à plusieurs endroits dans la zone côtière. Les travaux réalisés dans le cadre de ce volet de recherche ont permis d'identifier d'importants dépôts fluvioglaciaires qui pourraient être des aquifères potentiels dans une zone où les résidents rencontrent souvent de l'eau saumâtre dans leurs puits forés au roc ou très profondément dans les dépôts meubles.

Le forage GLC-04 de Montmagny amène plusieurs éléments nouveaux à la paléogéographie de cette région de l'estuaire moyen, en particulier à ce qui a trait à la transition entre la déglaciation et l'invasion de la Mer de Goldthwait. La présence de cailloux délestés sur près de 50% de la séquence marine témoigne de la proximité de la glace pendant une période plutôt étendue. Il a permis la découverte d'une unité glaciomarine intra-till de gravier sableux gris associé à des fluctuations des conditions paléo environnementales et des marges glaciaires. Les assemblages fauniques du forage GLC-04 montrent une transition d'un environnement de marge glaciaire vers la séquence typique de la Mer de Goldthwait.

Le modèle géologique 3D a été développé sur une période de trois ans dans le cadre d'un programme régional de caractérisation hydrogéologique (Lefebvre *et al.*, 2015) et a ensuite été étendu vers le nord-est jusqu'à Rivière-du-Loup et vers le sud-ouest jusqu'à Plessisville (Lotbinière) afin d'inclure des secteurs clés cartographiés en surface dans le cadre du premier article de cette thèse. Cependant, le temps à lui seul ne rend pas nécessairement un modèle meilleur : la qualité d'un modèle géologique est tributaire des données utilisées pour sa construction, en plus de l'exactitude du modèle conceptuel. Comme plus de la moitié des observations utilisées pour construire ce modèle proviennent de la base de données du Système d'Information Hydrogéologique (SIH), il est évident qu'une incertitude existe, et que celle-ci reste difficile à quantifier. Néanmoins, puisque le modèle a été construit en considérant les contraintes strictes associées à la carte des dépôts meubles à haute résolution aussi produite dans le cadre de cette thèse, nous sommes confiants des résultats de la modélisation.

Cependant, l'absence notable de forages dans certains secteurs, comme dans l'axe des villages de St-Pascal, St-Alexandre et St-Antonin (partie nord-est de la zone d'étude) a un impact important sur la représentation de cette zone dans le modèle 3D. La présence de dépôts fluvioglaciaires dans

la région de Kamouraska en amont de la première zone d'affleurements rocheux est évidente d'après la carte géologique des dépôts superficiels, mais la topographie accidentée du substratum rocheux et l'absence de forages dans ce vaste système de drainage postglaciaire rendent impossible la modélisation précise de ces formations à partir des données disponibles. Faute de moyens supplémentaires pour réaliser des forages exploratoires additionnels dans cette zone déjà plutôt inaccessible, ces dépôts ont pour l'instant été omis du modèle 3D ; seul le till de surface est représenté dans cette zone. Ces dépôts sont toutefois clairement identifiés sur la carte des dépôts de surface réalisée dans le cadre du premier article. Ce système de drainage est orienté vers le nord-est et est parallèle à la Moraine de St-Antonin, qui elle est bien représentée dans le modèle 3D étant donné la disponibilité de données de forage à proximité et même directement dans la formation.

6.3 Cartographie de l'empreinte du Courant glaciaire du Saint-Laurent

La cartographie de milliers de méga-linéations glaciaires (MSGLs) convergentes vers le nord-est dans la vallée moyenne et l'estuaire moyen du fleuve Saint-Laurent à l'aide de modèles numériques de terrain dérivés du LiDAR fournit des preuves incontestables qu'un écoulement glaciaire rapide s'est produit dans la vallée durant le Wisconsinien Supérieur. Cette partie de la vallée du Saint-Laurent présente un relief de courant glaciaire en évolution, comprenant : 1) des zones d'alimentation en amont sur le socle cristallin du Bouclier canadien composées d'affleurements et de méga-fossés glaciaires érodés préférentiellement ; 2) des zones de transition hybrides avec méga-crêtes, méga-dépressions et diverses linéations et méga-linéations glaciaires qui convergent vers une direction principale d'écoulement; 3) un lit principal sur roche paléozoïque superposé par une mince couche de till. Le tronc principal du Courant glaciaire du Saint-Laurent devait occuper le centre de la vallée du Saint-Laurent, mais a probablement migré vers la rive sud lors de ses dernières phases. Il s'alimentait principalement de glace provenant de la rive nord par quelques corridors principaux, notamment la région du Saguenay, de Portneuf et de la Mauricie. Des zones « hummocky » se trouvent sur la rive sud, à proximité de deux zones de divergence. Des crêtes de tills interprétés comme du remplissage de crevasse peuvent être trouvées près des marges latérales du courant glaciaire dans les régions de Lotbinière et de Kamouraska.

Ces nouvelles analyses concordent plutôt bien avec les propositions passées au niveau du Courant glaciaire du Saint-Laurent (Parent & Occhietti, 1999), et peuvent expliquer plusieurs assemblages de stries identifiées précédemment autant sur la rive nord que la rive sud du fleuve. Ces travaux soulignent une fois de plus que les données d'élévation du terrain dérivée de levés LiDAR aéroportés sont inestimables en support à la recherche en géologie quaternaire, et peuvent faciliter autant la cartographie des lits de courants glaciaires anciens que les reconstructions paléogéographiques.

La cartographie des linéations associées au SLIS a permis de préciser le cadre chronologique des événements associés au courant glaciaire. La compilation des données de stries glaciaires pour le secteur à l'étude montre bien l'ampleur de l'inversion de l'écoulement des glaces Appalachiennes s'effectuant pendant le développement du Courant glaciaire dans la vallée. Des stries témoignent de cette réorientation partout dans la partie est des Appalaches et aussi loin que sur la rive nord du fleuve Saint-Laurent, dans des vallées des Laurentides. Ce mouvement de glace n'étant pas enregistré dans les linéations glaciaires visibles sur les données LiDAR confirme qu'il a dû se produire dans une phase plutôt précoce, où l'appel de glace créer par le SLIS a pu progressivement isoler les glaces Appalachiennes de l'Inlandsis Laurentidien.

Quelques questions restent cependant en suspens. Des divergences importantes du Courant glaciaire montrant un écoulement vers les Monts Notre-Dame à l'est restent pour l'instant inexpliquées. Alors que l'écoulement glaciaire rapide dans le centre de la vallée du Saint-Laurent peut être expliqué par plusieurs facteurs incluant la présence d'un lit relativement lubrifié, des eaux souterraines pressurisées, un gradient topographique important et la présence de roches sédimentaires offrant peu de résistance et/ou la présence de dépôts meubles anciens, les bifurcations observées vers l'intérieur du piedmont Appalachien sont plus difficilement explicables. Il pourrait s'agir des embranchements d'un réseau d'écoulement glaciaire dendritique, ou encore d'un phénomène plus complexe. Aussi, nous montrons que certains « lits de till » associés à un écoulement concentré (rapide ?) dans certaines zones des Laurentides sont remarquablement bien préservés, même en amont glaciaire de la position de la Moraine de St-Narcisse, qui a été déposée lors d'une réavancée de l'Inlandsis Laurentidien pendant le Dryas récent. Non seulement les processus en causes ici ne sont-ils pas bien compris, mais certaines de ces zones de linéations de

till se trouvent à des endroits qui devaient pourtant contribuer aux réavancées glaciaires subséquentes. Cela implique que les réavancées glaciaires Laurentidiennes ayant suivi l'épisode du courant glaciaire aient été relativement peu érosives, ou encore que la marge du glacier Laurentidien ait eu une configuration qui diffère des modèles proposés.

La cartographie de l'ensemble de l'empreinte du SLIS est néanmoins loin d'être complète, car des MNT haute résolution dérivés de données LiDAR aéroportées de plusieurs zones critiques ne sont toujours pas disponibles pour le public. L'inventaire, la documentation et l'interprétation de l'empreinte géomorphologique des paléo-courants glaciaires sont essentiels à une meilleure compréhension des conditions glaciodynamiques ayant prévalu durant le Wisconsinien supérieur dans le secteur nord-est de l'Inlandsis Laurentidien, et aussi pour développer nos connaissances sur les processus menant à l'activation ou l'arrêt des courants glaciaires. Au fur et à mesure que d'autres ensembles de données deviendront disponibles, d'autres travaux seront nécessaires pour relier les éléments identifiés ici à ceux que l'on pourrait retrouver dans d'autres parties de la vallée du Saint-Laurent et ainsi saisir pleinement l'essence de cet événement glaciaire critique.

6.4 Cadre chronologique des événements glaciaires

La cartographie des formations superficielles du secteur à l'étude à l'aide de données de terrain à haute résolution, présentée dans le premier article de cette thèse, a permis l'identification de nouvelles moraines dans le secteur de Lotbinière. Certaines sections de ces moraines avaient été correctement esquissées par LaSalle & Shilts (1993) alors que d'autres ont été plus effacées du relief par l'action subséquente du littoral de la Mer de Champlain, tout en demeurant bien visibles dans les données LiDAR. Ces moraines représentent vraisemblablement les positions de stabilisation et de retrait d'un front de glace laurentidien en réavancée dans le bassin d'une Mer de Champlain précoce au Dryas récent. Leur découverte soutient et renforce l'hypothèse de la phase d'écoulement glaciaire dite de Saint-Nicolas, qui serait corrélée à un court épisode de détérioration climatique au début du Dryas récent, et qui pourrait être associée une série de dépôts marginaux localisés entre Québec et Rivière-du-Loup, notamment le till de Saint-Nicolas, la moraine de St-Édouard (LaSalle & Shilts, 1993) et le "Younger till" (Lee, 1962 ; Rappol, 1993) présent en surface dans la région de Kamouraska et Rivière-du-Loup.

Une reconstitution paléogéographique de cet épisode clé du développement de la Mer de Champlain est présentée sur la base d'une revue des datations radiocarbones effectuées sur des mollusques vivant dans la mer post-glaciaire publiées jusqu'à maintenant dans la littérature. Les marges de glace proposées pour 11 000 ^{14}C BP sont somme toute similaires à celles estimées par LaSalle & Shilts (1993). La réavancée est ici considérée comme un lobe de glace ou un glacier émissaire qui s'est développé à partir de la marge glaciaire principale des Laurentides aux alentours de Québec dans un patron d'écoulement dynamique qui aurait pu être similaire à celui de la phase de courant glaciaire qui s'est produite précédemment dans cette région. La reconstitution est appuyée par une combinaison de preuves géologiques, stratigraphiques et microfauniques, et a l'avantage de réconcilier plusieurs éléments paléographiques: 1) la présence d'une série de moraines arquées sur la rive sud de Québec contenant souvent un diamicton glaciomarin ; 2) la végétation de toundra arctique que l'on trouve sur le site de Saint-Eugène (Mott & Anderson, 1981; Morgan, 1987) ; 3) la géométrie de la moraine du lac Saint-Charles ainsi que les grandes structures d'effondrement observables qui suggèrent qu'au moins une partie de ces sédiments ont été déposés sur la glace (Blais *et al.,* 1989); 4) les dépôts glacio-lacustres isolés dans certaines vallées de la région de Beauport, ainsi que les paléocourants vers le nord dans la vallée de la rivière Montmorency ; 5) la cooccurrence d'ostracodes marins et d'eau douce dans les sédiments du début du bassin de la Mer de Champlain (Cronin *et al.,* 2012) ; 6) les variations microfauniques observées par C. G. Rodrigues dans les sédiments marins de la région de Saint-Lambert-de-Lauzon (Blais *et al.,* 1989) ; 7) les sédiments stratifiés en contact avec la glace déposés par les glaciers s'écoulant vers le sud dans les vallées des rivières Chaudière et Etchemin, y compris le delta de Vallée-Jonction (Blais & Shilts, 1989); 8) des dépôts de till argileux reposant sur des sédiments lacustres fortement déformés et reposant directement sur le till Lennoxville dans les mêmes vallées (McDonald & Shilts, 1971; Blais & Shilts, 1989). Ce modèle de réavancée glaciaire propose aussi une explication aux conditions de drainage du Lac Candona et à la variation rapide de la salinité entre les épisodes lacustres et glaciaires au début de la Mer de Champlain en raison du blocage de glace dans Mer de Goldthwait au niveau de Québec.

Beaucoup de travail reste encore à faire afin de préciser le cadre chronologique de cet événement clé de la chronologie glaciaire de la vallée du Saint-Laurent. Bien que l'analyse détaillée des âges

radiocarbones de la littérature permet de dresser un portrait plausible de la séquence d'événements, elle met également en évidence encore une fois les limites des datations radiocarbone sur des mollusques et de la problématique de l'effet réservoir. La découverte de nouvelles coupes plus complètes ou de macrorestes végétaux en combinaison avec des coquilles de sédiments marins contribuerait à réduire l'incertitude associée à ces facteurs, en permettant notamment de mieux estimer l'effet réservoir local affectant les coquilles marines de la Mer de Champlain durant la période du Dryas récent.

7 BIBLIOGRAPHIE

Anders NS, Seijmonsbergen AC, Bouten W (2011) Segmentation optimization and stratified object-based analysis for semi-automated geomorphological mapping. *Remote Sensing of Environment* **115**: 2976–2985, doi:10.1016/j.rse.2011.05.007.

Anderson TW (1988) Late Quaternary pollen stratigraphy of the Ottawa Valley-Lake Ontario region and its application in dating the Champlain sea. Dans In Gadd, N.R., Ed., 1988, The Late Quaternary Development of the Champlain Sea Basin: Geological Association of Canada, Special Paper 35, pp. 207–224.

Austin WEN, Bard E, Hunt JB, Kroon D, Peacock JD (1995) The 14 C Age of the Icelandic Vedde Ash: Implications for Younger Dryas Marine Reservoir Age Corrections. *Radiocarbon* **37**: 53–62, doi:10.1017/S0033822200014788.

Bamber JL, Vaughan DG, Joughin I (2000) Widespread Complex Flow in the Interior of the Antarctic Ice Sheet. *Science* **287**: 1248 LP – 1250.

Bélanger C (1993) Étude géomorphologique des basses terrasses marines sur la côte sud de l'estuaire laurentien. Thèse de doctorat, Université Laval, Québec, 222 p.

Bennett MR (2003) Ice streams as the arteries of an ice sheet: Their mechanics, stability and significance. *Earth-Science Reviews* **61**: 309–339, doi:10.1016/S0012-8252(02)00130-7.

Bernier F, Occhietti S (1991) Nouvelle séquence glaciaire antérieure aux Sédiments de Saint-Pierre, Sainte-Anne-de-la-Perade, Québec. *Géographie physique et Quaternaire* **45**: 101–110.

Blais A, Demers D, Lamothe M, Shilts WW, Lasalle P (1989) Friends of the Pleistocene 52nd Annual Reunion, May 19-20-21 1989.

Blais A, Shilts WW (1989) Surficial geology of Saint-Joseph-de-Beauce map area, Chaudiere River valley, Quebec. *Current Research* **89–1**: 137–142.

Blake W, Lowdon JA (1976) Geological Survey of Canada Radiocarbon Dates XVI. Geological

Society of Canada. 1–21 p. doi:10.4095/102617.

Bolduc AM (2003) Géologie des formations superficielles, Charny, Québec. Commission géologique du Canada, Dossier public 1776, échelle 1/50 000.

Bond G, Heinrich H, Broecker W, Labeyrie L, McManus J, Andrews J, Huon S, Jantschik R, Clasen S, Simet C, Tedesco K, Klas M, Bonani G, Ivy-Ochs S (1992) Evidence for massive discharges of icebergs into the North-Atlantic ocean during the Last Glacial Period. *Nature* **360**: 245–249, doi:10.1038/360245a0.

Boulton GS (1982) Processes and Patterns of Glacial Erosion. Dans Glacial Geomorphology, D.R. Coates, ed. (Dordrecht: Springer Netherlands), pp. 41–87.

Broecker WS, Kennett JP, Flower BP, Teller JT, Trumbore S, Bonani G, Wolfli W (1989) Routing of meltwater from the Laurentide Ice Sheet during the Younger Dryas cold episode. *Nature* **341**: 318.

Brouard E, Lajeunesse P, Cousineau PA, Govare É, Locat J (2016) Late Wisconsinan deglaciation and proglacial lakes development in the Charlevoix region, southeastern Québec, Canada. *Boreas* **45**: 754–772, doi:10.1111/bor.12187.

Carl JD (1978) Ribbed moraine–drumlin transition belt, St. Lawrence Valley, New York. *Geology* **6**: 562, doi:10.1130/0091-7613(1978)6<562:RMTBSL>2.0.CO;2.

Caron O (2013) Synthèse et modèle cartographique 3D des formations quaternaires pour les bassins-versants des rivières Chaudière et Saint-François : Géochronologie, stratigraphie et paléogéographie Wisconsinienne du sud du Québec. Thèse de doctorat, Université du Québec à Montréal, 358 p.

Caron O, Lamothe M, Shilts WW (2013) Midwisconsinan history of the southeastern sector of the Laurentide ice sheet and the late Quaternary stratigraphic record of southeastern Quebec. Dans Abstracts with Programs, Geological Society of America, ed. (Boulder, Colorado), p. 413.

Chauvin L, Martineau G, LaSalle P (1985) Deglaciation of the Lower St. Lawrence Region, Quebec. Dans Late Pleistocene History of Northeastern New England and Adjacent Quebec, H.W.

Boms Jr., P. LaSalle, and W.B. Thompson, eds. (Geological Society of America), pp. 111–124.

Clark CD (1994) Large-scale ice-moulding: a discussion of genesis and glaciological significance. *Sedimentary Geology* **91**: 253–268, doi:10.1016/0037-0738(94)90133-3.

Clet M, Occhietti S (1994) Palynologie et paléoenvironnements des épisodes du Sable de Lotbinière et des Varves de Deschaillons (Pléistocène supérieur) de la vallée du Saint-Laurent. *Canadian Journal of Earth Sciences* **31**: 1474–1485, doi:10.1139/e94-130.

Cloutier M, Parent M, Bolduc AM (1997) Géologie des formations superficielles [document cartographique] : région de Saint-Marc-des-Carrières, Québec. Ressources naturelles Canada, Centre géoscientifique de Québec & Commission géologique du Canada. (Ottawa: Commission géologique du Canada).

Conrad O, Bechtel B, Bock M, Dietrich H, Fischer E, Gerlitz L, Wehberg J, Wichmann V, Böhner J (2015) System for Automated Geoscientific Analyses (SAGA) v. 2.1.4. *Geoscientific Model Development* **8**: 1991–2007, doi:10.5194/gmd-8-1991-2015.

Cronin TM, Manley PL, Brachfeld S, Manley TO, Willard DA, Guilbault J-P, Rayburn JA, Thunell R, Berke M (2008) Impacts of post-glacial lake drainage events and revised chronology of the Champlain Sea episode 13–9 ka. *Palaeogeography, Palaeoclimatology, Palaeoecology* **262**: 46–60, doi:https://doi.org/10.1016/j.palaeo.2008.02.001.

Cronin TM, Rayburn JA, Guilbault J-P, Thunell R, Franzi DA (2012) Stable isotope evidence for glacial lake drainage through the St. Lawrence Estuary, eastern Canada, ~13.1-12.9 ka. *Quaternary International* **260**: 55–65, doi:10.1016/j.quaint.2011.08.041.

Cuffey KM, Paterson WSB (2010) The Physics of Glaciers (Amsterdam: Academic Press).

Daigneault RA, Roy M, Milette S, Hurtubise MA, Leduc E, Thiery G, Horth N, Dubois-Verret M (2014) Cartographie des formations superficielles de la partie sud du projet PACES Chaudière Appalaches. UQAM, Rapport présenté au Ministère des Ressources Naturelles du Québec. 51 p.

Davis JC (1986) Statistics and Data Analysis in Geology (New York: John Wiley & Sons Inc.).

Denton GH, Hugues T (1981) The Last Great Ice Sheets (New York: Wiley-Interscience).

Dionne J-C (1988) Holocene relative sea-level fluctuations in the St. Lawrence estuary, Québec, Canada. *Quaternary Research, Volume 29, Issue 3, p 233-244* **29**: 233–244, doi:10.1016/0033-5894(88)90032-4.

Dionne J-C (1997) Nouvelles données sur la transgression Laurentienne, côte sud du moyen estuaire du Saint-Laurent, Québec. *Géographie physique et Quaternaire* **51**: 201, doi:10.7202/033118ar.

Dionne J-C (2002) Une nouvelle courbe du niveau marin relatif pour la région de Rivière-du-Loup (Québec). *Géographie physique et Quaternaire* **56**: 33–44, doi:10.7202/008603ar.

Dionne J-C, Occhietti S (1996) Apercu du quaternaire a l'embouchure du Saguenay, Quebec. *Géographie physique et Quaternaire* **50**: 5-34., doi:10.7202/033072ar.

Dionne J-C, Pfalzgraf F (2001) Fluctuations holocènes du niveau marin relatif à Rivière-Ouelle, côte sud du moyen estuaire du Saint-Laurent : données complémentaires. *Géographie physique et Quaternaire* **55**: 289, doi:10.7202/006856ar.

Dowdeswell JA, Canals M, Jakobsson M, Todd BJ, Dowdeswell EK, Hogan KA (2016a) The variety and distribution of submarine glacial landforms and implications for ice-sheet reconstruction. *Geological Society, London, Memoirs* **46**: 519 LP – 552, doi:10.1144/M46.183.

Dowdeswell JA, Ottesen D, Rise L (2016b) Landforms characteristic of inter-ice stream settings on the Norwegian and Svalbard continental margins. *Geological Society, London, Memoirs* **46**: 437 LP – 444, doi:10.1144/M46.164.

Dubé JC (1971) Géologie des dépôts meubles, région de Lyster. Ministère des Richesses naturelles du Québec. R.P. 596, carte 1762. 12 p.

Dupuis M, Leboeuf A, Vaillancourt E, Lachance D (2017) Guide d'utilisation du LIDAR pour l'identification des dépôts de surface et des bancs d'emprunt. Ministère des Forêts, de la Faune et des Parcs Forêts, Secteur des Direction des inventaires forestiers. 107 p.

Dyke A, Prest V (1987) Late Wisconsinan and Holocene History of the Laurentide Ice Sheet. *Géographie physique et Quaternaire* **41**: 237–263, doi:https://doi.org/10.7202/032681ar.

Dyke AS (2004) An outline of North American deglaciation with emphasis on central and northern Canada. Dans Ehlers, J. and Gibbard, P.L. (Eds.), Quaternary Glaciations – Extent and Chronology, Part II., (Amsterdam), pp. 373–424.

Dyke AS, McNeely R, Southon J, Andrews JT, Peltier WR, Clague JJ, England JH, Gagnon JM, Baldinger A (2003) Preliminary assessment of Canadian marine reservoir ages. Dans Joint Annual Meeting of the Canadian Quarternary Association and the Canadian Geomorphology Research Group. Halifax, NS, pp. 8–12.

Elson J (1970) Late Quaternary marine submergence of Québec. *Revue de géographie de Montréal* **23**: 247–258.

Evans DJA, Storrar RD, Rea BR (2016) Crevasse-squeeze ridge corridors: Diagnostic features of late-stage palaeo-ice stream activity. *Geomorphology* **258**: 40–50, doi:10.1016/j.geomorph.2016.01.017.

Evans IS (1972) General geomorphometry, derivatives of altitude, and descriptive statistics. Dans Spatial Analysis in Geomorphology, R.J. Chorley, ed. (Harper & Row), pp. 17–90.

Eyles N, Putkinen N (2014) Glacially-megalineated limestone terrain of Anticosti Island, Gulf of St. Lawrence, Canada; onset zone of the Laurentian Channel Ice Stream. *Quaternary Science Reviews* **88**: 125–134, doi:10.1016/j.quascirev.2014.01.015.

Fagnan N, Bourque E, Michaud Y, Lefebvre R, Boisvert E, Parent M, Martel R (1999) Hydrogéologie des complexes deltaiques sur la marge nord de la Mer de Champlain. *Hydrogéologie* **4**: 9–22.

Fagnan N, Michaud Y, Lefebvre R, Boisvert E, Parent M, Martel R, Paradis D, Larose-Charette D (1998) Cartographie hydrogéologique régionale du piémont laurentien dans la MRC de Portneuf : hydrostratigraphie et piézométrie des aquifères granulaires de surface. Commission géologique du Canada. Dossier public 3664b, 1 feuille. 5 p. doi:10.4095/210071.

Ferland P, Occhietti S (1990) Révision du stratotype des Sédiments de Saint-Pierre et implications stratigraphiques, vallée du Saint-Laurent, Québec. *Géographie physique et Quaternaire* **44**: 147–158, doi:10.7202/032814ar.

Fulton RJ, Karrow PF, LaSalle P, Grant DR (1986) Summary of Quaternary stratigraphy and history, Eastern Canada. *Quaternary Science Reviews* **5**: 211–228.

Gadd NR (1964) Géologie de la région de Beauceville, Québec (dépôts meubles). Commission géologique du Canada. Études 64-12,1 feuille. 3 p. doi:10.4095/101009.

Gadd NR (1971) Surficial geology, central St.Lawrence Lowland, Quebec / Géologie des dépôts meubles, la partie centrale des Basses-Terres du St-Laurent, Québec. Commission géologique du Canada. Carte série 'A' 1197A, 1 feuille. doi:10.4095/108939.

Gadd NR, Goldthwait JW (1971) Pleistocene geology of the central St. Lawrence lowland : with selected passages from an unpublished manuscript the St. Lawrence lowland. Commission géologique du Canada. 153 p.

Gadd NR, Karrow PF (1960) Surficial geology, Trois-Rivières, St-Maurice, Champlain, Maskinonge and Nicolet Counties, Québec. Commission géologique du Canada. Cartes préliminaires 54-1959, 1 feuille, échelle 1. doi:10.4095/108651.

Gauthier CR (1975) Deglaciation d'un secteur des rivieres Chaudiere et Etchemin. Thèse de doctorat, McGill University, Montréal, Québec, 180 p.

Globensky Y (1987) Géologie des Basses-Terres du Saint-Laurent. Ministère de l'Énergie et des Ressources du Québec. Rapport MM 85-02. 63 p.

Godbout P-M (2013) Géologie du Quaternaire et hydrostratigraphie des dépôts meubles du bassin versant de la rivière Bécancour des zones avoisinantes, Québec. Mémoire de maîtrise, Université du Québec à Montréal, Montréal, Québec, 218 p.

Govare É (1995) Géomorphologie et paléoenvironnements de la région de Charlevoix, Québec, Canada. Thèse de doctorat non publiée, Université de Montréal, Montréal, Québec, 425 p.

Gratton D, Gwyn QHJ, M. Dubois JM (1984) Les paléoenvironnements sédimentaires au Wisconsinien moyen et supérieur, île d'Anticosti, golfe du Saint-Laurent, Québec. *Géographie physique et Quaternaire* **38**: 229, doi:10.7202/032565ar.

Guilbault J-P (1989) Foraminiferal Distribution in the Central and Western Parts of the Late Pleistocene Champlain Sea Basin, Eastern Canada. *Géographie physique et Quaternaire* **43**: 3–26, doi:https://doi.org/10.7202/032750ar.

Guilbault JP (1993) Quaternary Foraminiferal Stratigraphy in Sediments of the Eastern Champlain Sea Basin, Quebec. *Geographie Physique Et Quaternaire* **47**: 43–68.

Hillaire-Marcel C (1981) Paleo-oceanographie isotopique des mers post-glaciaires du Quebec. *Palaeogeography, Palaeoclimatology, Palaeoecology* **35**: 63–119, doi:https://doi.org/10.1016/0031-0182(81)90094-8.

Hillaire-Marcel C (1988) Isotopic composition (18O, 13C, 14C) of biogenic carbonates in Champlain Sea sediments. Dans The Late Quaternary Development of the Champlain Sea Basin, N.R. Gadd, ed. (Geological Association of Canada, Special Paper 35), pp. 177–194.

Hillaire-Marcel C, Causse C (1989) Chronologie Th/U des concrétions calcaires des varves du lac glaciaire de Deschaillons (Wisconsinien inférieur). *Canadian Journal of Earth Sciences* **26**: 1041–1052, doi:10.1139/e89-085.

Hillaire-Marcel C, Page P (1981) Isotopic paleotemperatures of glacial lake Deschaillons. Dans Quaternary Paleoclimate, W.C. Mahaney, ed. (Norwich: Geo Books), pp. 273–298.

Hillaire-Marcel C, Soucy J-M, Cailleux A (1979) Analyse isotopique de concrétions sous-glaciaires de l'inlandsis laurentidien et teneur en oxygène 18 de la glace. *Canadian Journal of Earth Sciences* **16**: 1494–1498, doi:10.1139/e79-132.

Hillaire-Marcel C, Vincent J-S (1980) Rencontre géologique de la baie d'Hudson Juin 1979 : livret-guide, stratigraphie de l'holocene et evolution des lignes de rivage au sud-est de la baie d'Hudson, Canada (Montréal, Québec: Universite du Québec a Montréal, Laboratoire d'archéologie).

Hughes T, Borns Jr. HW, Fastook JL, Hyland MR, Kite JS, Lowell T V (1985) Models of glacial

reconstruction and deglaciation applied to Maritime Canada and New England. *Late Pleistocene History of Northeastern New England and Adjacent Quebec* **197**: 139–150, doi:10.1130/SPE197-p139.

Hutchinson MF (1989) A new procedure for gridding elevation and stream line data with automatic removal of spurious pits. *Journal of Hydrology* **106**: 211–232, doi:10.1016/0022-1694(89)90073-5.

Hutchinson MF (2004) ANUDEM version 5.3, user guide.

Janos D, Molson J, Lefebvre R (2018) Regional groundwater flow dynamics and residence times in Chaudière-Appalaches, Québec, Canada: Insights from numerical simulations. *Canadian Water Resources Journal* **43**: 214–239, doi:10.1080/07011784.2018.1437370.

Joughin I, Smith BE, Howat I (2018) Greenland Ice Mapping Project: ice flow velocity variation at sub-monthly to decadal timescales. *The Cryosphere* **12**: 2211–2227, doi:10.5194/tc-12-2211-2018.

Joughin I, Tulaczyk S, Bindschadler R, Price SF (2002) Changes in west Antarctic ice stream velocities: Observation and analysis. *Journal of Geophysical Research: Solid Earth* **107**: EPM 3-1-EPM 3-22, doi:10.1029/2001JB001029.

St. Julien P, Hubert C (1975) Evolution of the Taconian Orogen in the Quebec Appalachians. *American Journal of Science* **275A**: 337–362.

Karrow PF (1981) Late-glacial regional ice-flow patterns in eastern Ontario: Discussion. *Canadian Journal of Earth Sciences* **18**: 1386–1390.

Karrow PF, Anderson TW, Clarke AH, Delorme LD, Sreenivasa MR (1975) Stratigraphy, paleontology, and age of Lake Algonquin sediments in southwestern Ontario, Canada. *Quaternary Research* **5**: 49–87.

Kleman J, de Angelis H, Greenwood S (2010) Paleo-ice stream types. Dans AGU Fall Meeting Abstracts, p. B1.

Korsun S, Hald M (1998) Modern Benthic Foraminifera off Novaya Zemlya Tidewater Glaciers, Russian Arctic. *Arctic and Alpine Research* **30**: 61–77, doi:10.2307/1551746.

Korsun S, Hald M (2000) Seasonal dynamics of benthic foraminifera in a glacially fed fjord of Svalbard, European Arctic. *Journal of Foraminiferal Research* **30**: 251–271, doi:10.2113/0300251.

Krabbendam M, Eyles N, Putkinen N, Bradwell T, Arbelaez-Moreno L (2016) Streamlined hard beds formed by palaeo-ice streams: A review. *Sedimentary Geology* **338**: 24–50, doi:10.1016/j.sedgeo.2015.12.007.

Kumarapeli PS, Saull VA (1966) The St. Lawrence Valley system : A North American equivalent of the East African rift valley system. *Canadian Journal of Earth Sciences* **3**: 639–658, doi:10.1139/e66-045.

Ladevèze P (2017) Aquifères superficiels et ressources profondes : le rôle des failles et des réseaux de fractures naturelles sur la circulation des fluides. Thèse de doctorat, Institut national de la recherche scientifique, Centre Eau Terre Environnement, Québec, Québec, 245 p.

Lamarche L (2005) Histoire géologique Holocène du lac Saint-Pierre et de ses ancêtres. Mémoire de maîtrise, Université du Québec à Montréal, Montréal, Québec, 225 p.

Lamarche L (2011) Évolution paléoenvironnementale de la dynamique quaternaire dans la région de Québec : Application en modélisation tridimensionelle et hydrogéologie. Thèse de doctorat, Institut national de la recherche scientifique, Centre Eau Terre Environnement, Québec, Québec, 222 p.

Lamarche RY (1971) Northward moving ice in the Thetford Mines area of Southern Quebec. *American Journal of Science* **271**: 383–388.

Lamarche RY (1974) Southeastward, northward, and westward ice movement in the Asbestos area of southern Quebec. *Geological Society of America Bulletin* **85**: 465–470.

Lamothe M (1985) Lithostratigraphy and geochronology of the Quaternary deposits of the Pierreville and St-Pierre les Becquets areas, Quebec. Thèse de doctorat, University of Western Ontario, London, Ontario, 249 p.

Lamothe M (1989) A New Framework for the Pleistocene Stratigraphy of the Central St. Lawrence Lowland, Southern Québec. *Géographie physique et Quaternaire* **43**: 119, doi:10.7202/032764ar.

Lamothe M, Huntley DJ (1988) Thermoluminescence Dating of Late Pleistocene Sediments, St. Lawrence Lowland, Québec. *Géographie physique et Quaternaire* **42**: 33, doi:10.7202/032707ar.

Lamothe M, Parent M, Shilts WW (1992) Sangamonian and early Wisconsinan events in the St. Lawrence Lowland and Appalachians of southern Quebec, Canada. Dans The Last Interglacial-Glacial Transition in North America, P.U. Clark, and P.D. Lea, eds. (Boulder, Colorado: Geological Society of America), pp. 171–184.

Lanoie J (1995) Les écoulements glaciaires du Wisconsinien supérieur en Charlevoix occidental. Mémoire de maîtrise, Université du Québec à Montréal, Montréal, Québec, 83 p.

Larocque M, Cloutier V, Levison J, Rosa E (2018) Results from the Quebec Groundwater Knowledge Acquisition Program. *Canadian Water Resources Journal / Revue canadienne des ressources hydriques* **43**: 69–74, doi:10.1080/07011784.2018.1472040.

LaSalle P (1966) Late Quaternary vegetation and glacial history in the St. Lawrence Lowlands, Canada. *Leidse Geologische Mededelingen* **38**: 91–128.

LaSalle P (1970) Notes on the St-Narcisse morainic system north of Quebec City. *Canadian Journal of Earth Sciences* **7**: 516–521.

LaSalle P (1978) Géologie des sédiments de surface de la région de Québec. Ministère des Richesses Naturelles. Rapport DPV-565, échelle 1:50 000. 3 p.

LaSalle P (1984) Quaternary stratigraphy of Quebec: A review. Dans Quaternary Stratigraphy of Canada - A Canadian Contribution to IGCP Project 24. R.J. Fulton (Ed.) Paper 84-10, (Geological Survey of Canada), pp. 155–171.

LaSalle P (1987) The Quebec City area. Dans Pleistocene Stratigraphy in the St. Lawrence Lowland and the Appalachians of Southern Quebec: A Field Guide, M. Lamothe, ed. (Université du Québec à Montréal), pp. 52–71.

LaSalle P, Chapdelaine C (1990) Review of late-glacial and Holocene events in the Champlain and Goldthwait Seas areas and arrival of man in eastern Canada. Dans Archaeological Geology of North America, N.P. Lasca, and J. Donahue, eds. (Boulder, Colorado: Geological Society of America), pp. 1–19.

LaSalle P, David P., Chauvin L (1985) Ice limits during the last glacial maximum in Gaspesie, Quebec, Canada Abstracts with Programs. Dans Abstracts with Programs : Geological Society of America, p. 30.

Lasalle P, Elson JA (1975) Emplacement of the St. Narcisse moraine as a climatic event in Eastern Canada. *Quaternary Research* **5**: 621–625, doi:https://doi.org/10.1016/0033-5894(75)90018-6.

LaSalle P, Hardy L, Poulin P (1972) Une position du front glaciaire au nord et au nord-est de la ville de Québec. Ministère des Richesses naturelles du Québec. Rapport S-135. 8 p.

LaSalle P, Martineau G, Chauvin L (1976) Géologie des sédiments meubles d'une partie de la Beauce et du Bas Saint-Laurent. Ministère de l'Énergie et des Ressources du Québec. Rapport DPV-438. 13 p.

LaSalle P, Martineau G, Chauvin L (1977) Dépôts morainiques et stries glaciaires dans la région de Beauce - Monts - Notre-Dame - Parc des Laurentides/ Morainic deposits and glacial striae in Beauce - Notre-Dame Mountains - Laurentide Park area. Ministère des Richesses naturelles du Québec. Rapport DPV-516. 74 p.

LaSalle P, Shilts WW (1993) Younger Dryas-age readvance of Laurentide ice into the Champlain Sea. *Boreas* **22**: 25–37.

LaSalle P, Thibaut L, Charbonneau L (1980a) Géologie des sédiments meubles de la région de Portneuf. Ministère des Richesses Naturelles du Québec. Rapport DPV-741, 1 carte à 1/50 000. 1 p.

LaSalle P, Thibaut L, Charbonneau L (1980b) Géologie des sédiments meubles de la région de Saint-Raphaël. Ministère des Richesses naturelles du Québec. Rapport DPV-742, 1 carte à 1/50 000. 1 p.

Laurencelle M, Lefebvre R, Parent M, Molson J (2018) Paleo-hydrogeological evolution of a fractured-rock aquifer since the Champlain Sea incursion in the St. Lawrence Valley (Quebec, Canada). Dans EGU General Assembly 2018, Vienna, Austria, p. 1.

Lebel D, Hubert C (1995) Géologie de la région de Saint-Raphael (Chaudière - Appalaches). Travaux réalisés dans le cadre de l'Entente auxiliaire Canada-Québec sur le développement minéral. Ministère de l'Énergie et des Ressources naturelles, Québec. Rapport ET 93-02.

Lebuis J, David PP (1977) La stratigraphie et les événements du Quaternaire de la partie occidentale de la Gaspésie, Québec. *Géographie physique et Quaternaire* **31**: 275, doi:10.7202/1000278ar.

Lee HA (1962) Surficial geology of Riviere-du-Loup - Trois-Pistoles areas, Quebec. *Geological Survey of Canada, Paper* **61–32**: 1–2, doi:10.4095/247881.

Lefebvre R, Ballard J-M, Carrier M-A, Vigneault H, Beaudry C, Berthot L, Légaré-Couture G, Parent M, Laurencelle M, Malet X, Therrien A, Michaud A, Desjardins J, Drouin A, Cloutier MH, Grenier J, Bourgault M-A, Larocque M, Pellerin S, Graveline M-H, Janos D, Molson J (2015) Portrait des ressources en eau souterraine en Chaudière-Appalaches, Québec, Canada Projet réalisé conjointement par l'Institut national de la recherche scientifique (INRS), l'Institut de recherche et développement en agroenvironnement (IRDA) et le Regroupement des organismes de bassins versants de la Chaudière-Appalaches (OBV-CA) dans le cadre du Programme d'acquisition de connaissances sur les eaux souterraines (PACES), Rapport final INRS R-1580, soumis au MDDELCC en mars 2015.

Légaré-Couture G, Leblanc Y, Parent M, Lacasse K, Campeau S (2018) Three-dimensional hydrostratigraphical modelling of the regional aquifer system of the St. Maurice Delta Complex (St. Lawrence Lowlands, Canada). *Canadian Water Resources Journal* **43**: 92–112, doi:10.1080/07011784.2017.1316215.

Lin B, Zhou L, Lv G, Zhu AX (2017) 3D geological modelling based on 2D geological map. *Annals of GIS* **23**: 117–129, doi:10.1080/19475683.2017.1304450.

Lisiecki LE, Raymo ME (2005) A Pliocene-Pleistocene stack of 57 globally distributed benthic

δ18O records. *Paleoceanography* **20**: doi:10.1029/2004PA001071.

Locat J (1977) L'émersion des terres dans la région de Baie-des-Sables/Trois-Pistoles, Québec. *Géographie physique et Quaternaire* **31**: 297, doi:10.7202/1000279ar.

Lortie G (1976) Les écoulements glaciaires Wisconsiens dans des cantons de l'Est et la Beauce, Québec. Mémoire de maîtrise non publié, McGill University, Montréal, Québec, 200 p.

Lortie G, Guilbault J-P (1984) Les diatomées et les foraminifères de sédiments marins post-glaciaires du Bas-Saint-Laurent (Québec): une analyse comparée des assemblages. *Naturaliste canadien* **111**: 297–310.

Lortie G, Martineau G (1987) Les systèmes de stries glaciaires dans les Appalaches du Québec. Ministère de l'Énergie et des Ressources. Rapport DV 85-10. 46 p.

Lowdon JA, Blake W (1973) Geological Survey of Canada, Radiocarbon dates XIII. Études no. 73-7. 61 p. doi:10.4095/103332.

Macpherson JC (1966) The post-Champlain evolution of the drainage pattern of the Montreal lowland. Mémoire de maîtrise, McGill University, Montréal, Québec, 265 p.

Mallet J-LL (2002) Geomodeling: Applied Geostatistics Series (Oxford ; New York : Oxford University Press).

Margold M, Stokes CR, Clark CD (2015a) Ice streams in the Laurentide Ice Sheet: Identification, characteristics and comparison to modern ice sheets. *Earth-Science Reviews* **143**: 117–146, doi:10.1016/j.earscirev.2015.01.011.

Margold M, Stokes CR, Clark CD, Kleman J (2015b) Ice streams in the Laurentide Ice Sheet: a new mapping inventory. *Journal of Maps* **11**: 380–395, doi:10.1080/17445647.2014.912036.

Martineau G (1977) Géologie des dépôts meubles de la région de Kamouraska/Rivière-du-Loup. Mnistère des Richesses Naturelles, Direction Générale des Mines. Service de l'exploitation géologique, division du Quaternaire. Rapport DPV-545. 18 p.

Martineau G (1979) Géologie des dépôts meubles de la région du Lac Témiscouata. Ministere des

richesses naturelles, Direction generale de la recherche geologique et minerale. Rapport DPV-618. 18 p.

Martineau G (1980) Dépôts meubles de la région de Rimouski - Trois-Pistoles. Ministère des Richesses naturelles du Québec. Rapport DPV-717. 10 p.

Martineau G, Corbeil P (1983) Réinterprétation d'un Segment de la Moraine de Saint-Antonin, Québec. *Géographie physique et Quaternaire* **37**: 217–221.

Matthews JVJ (1987) Macrofossils ofinsects and plants from Southern Québec. Dans Pleistocene Stratigraphy in the St. Lawrence Lowland and the Appalachians of Southern Québec: A Field Guide, M. Lamothe, ed. (Montréal, Québec: Université de Montréal), pp. 166–181.

McDonald BC (1969) Surficial geology of La Patrie-Sherbrooke area, Québec, including Eaton River watershed. Geological Survey of Canada. Dossier 67-52. 21 p.

McDonald BC, Shilts WW (1971) Quaternary Stratigraphy and Events in Southeastern Quebec. *Geological Society of America Bulletin* **82**: 683–698.

McNeely R (2002) Geological Survey of Canada radiocarbon dates XXXIII. *Geological Survey of Canada, Current Research* **2001**: 1–51, doi:10.4095/213319.

McNeely R (2005) Geological Survey of Canada radiocarbon dates XXXIV. *Current Research* 1–117, doi:10.4095/221464.

McNeely R (2006) Geological Survey of Canada radiocarbon dates XXXV. *Geological Survey of Canada, Current Research* **2006-G**: 1–151, doi:10.4095/223025.

McNeely R, Brennan J (2005) Geological Survey of Canada revised shell dates. Commission géologique du Canada. Dossier public 5019. 530 p. doi:10.4095/221215.

Morgan A V (1987) Late Wisconsin and early Holocene paleoenvironments of east-central North America based on assemblages of fossil Coleoptera. *North America and Adjacent Oceans During the Last Deglaciation* **K-3**: 0, doi:10.1130/DNAG-GNA-K3.353.

Mott RJ, Anderson TW (1981) Late-glacial paleoenvironments of sites bordering the Champlain

Sea based on pollen and macrofossil evidence. Dans Quaternary Paleoclimate. Geo Abstracts, Norwich, 464 P., W.C. Mahaney, ed. pp. 129–172.

Murat V, Martel R, Michaud Y, Fagnan N, Beaudoin F, Therrien R (2000) Cartographie hydrogéologique régionale du piémont laurentien dans la MRC de Portneuf : comparaison des méthodes d'évaluation de la vulnérabilité intrinsèque. Commission géologique du Canada. Dossier publique 3664d, 1 carte. doi:10.4095/211790.

NASA JPL (2013) NASA Shuttle Radar Topography Mission Global 1 arc second. Distributed by NASA EOSDIS Land Processes DAAC. doi:https://doi.org/10.5067/MEaSUREs/SRTM/SRTMGL1.003.

Normandeau P-X (2010) Histoire du drainage tardiglaciaire de la vallée de la rivière Chaudière et des régions avoisinantes, Québec. Mémoire de maîtrise, Université du Québec à Montréal, 154 p.

Occhietti S (1977) Stratigraphie du Wisconsinien de la région de Trois-Rivières-Shawinigan, Québec. *Géographie physique et Quaternaire* **31**: 307–322.

Occhietti S (1982) Synthèse lithostratigraphique et paléoenvironnements du Quaternaire au Québec méridional. *Géographie Physique et Quaternaire* **36**: 15–49.

Occhietti S (1990) The Quaternary lithostratigraphy of the St. Lawrence Valley: method, conceptual framework and sedimentary sequences. *Géographie Physique et Quaternaire* **44**: 137–145.

Occhietti S (2007) The Saint-Narcisse morainic complex and early Younger Dryas events on the southeastern margin of the Laurentide Ice Sheet. *Géographie Physique et Quaternaire* **61**: 89–117.

Occhietti S, Balescu S, Lamothe M, Clet M, Cronin T, Ferland P, Pichet P (1996) Late Stage 5 Glacio-isostatic Sea in the St. Lawrence Valley, Canada and United States. *Quaternary Research* **45**: 128–137, doi:DOI: 10.1006/qres.1996.0015.

Occhietti S, Chartier M, Hillaire-Marcel C, Cournoyer M, Cumbaa SL, Harington CR (2001a) Champlain sea paleoenvironments in the Québec City area, 11 300-9750 BP: The Saint-Nicolas site (Québec). *Géographie physique et Quaternaire* **55**: 23–46.

Occhietti S, Clet M (1989) The last interglacial/glacial group of sediments in the St Lawrence Valley, Quebec, Canada. *Quaternary International* **3–4**: 123–129.

Occhietti S, Hillaire-Marcel C (1977) Chronologie 14C des événements paléogéographiques du Québec depuis 14 000 ans. *Géographie physique et Quaternaire* **31**: 123–133, doi:https://doi.org/10.7202/1000058ar.

Occhietti S, Long B, Clet M, Boespflug X, Sabeur N (1995) Séquence de la transition Illinoien–Sangamonien : forage IAC-91 de l'île aux Coudres, estuaire moyen du Saint-Laurent, Québec. *Canadian Journal of Earth Sciences* **32**: 1950–1964, doi:10.1139/e95-149.

Occhietti S, Parent M, Lajeunesse P, Robert F, Govare E, Govare É, Govare E (2011) Late pleistocene-early holocene decay of the laurentide ice sheet in québec-labrador. Dans Developments in Quaternary Science, (Elsevier), pp. 601–630.

Occhietti S, Parent M, Shilts WW, Dionne J-C, Govare É, Harmand D (2001b) Late Winconsinan glacial dynamics, deglaciation, and marine invasion in southern Quebec. *Geological Society of America Special Papers* **351**: 243–270, doi:10.1130/0-8137-2351-5.243.

Occhietti S, Richard PJH (2003) Effet réservoir sur les âges C de la Mer de Champlain à la transition Pléistocène-Holocène : révision de la chronologie de la déglaciation au Québec méridional. *Géographie physique et Quaternaire* **57**: 115, doi:10.7202/011308ar.

Paradis. SJ, Bolduc AM (1999) Mouvement glaciaire vers le nord sur le piémont laurentien dans la région de Québec. Geological Survey of Canada. Current Research 1999-D. 1–7 p.

Paradis D, Martel R, Michaud Y, Lefebvre R, Beaudoin F (2000) Cartographie hydrogéologique régionale du piémont laurentien dans la MRC de Portneuf : détermination des périmètres de protection en milieu. Commission géologique du Canada. Dossier public 3664e, 1 feuille. doi:10.4095/211791.

Parent M (1987) Late Pleistocene stratigraphy and events in the Asbestos-Valcourt region, Québec. Thèse de doctorat, University of Western Ontario, London, Ontario, 320 p.

Parent M, Girard F, Fagnan N, Michaud Y, Boisvert É, Fortier R (2008) Caractérisation

géologique des formations superficielles enfouies. Dans Guide Méthodologique Pour La Cartographie Hydrogéologique Régionale Des Aquifères Granulaires, (Ministère du développement durable, de l'environnement et des parcs), pp. 23–40.

Parent M, Légaré-Couture G (2018) FT MID 6 : Champlain Sea deltas and the Saint-Narcisse Moraine in the central St. Lawrence valley, southern Quebec. 20th International Sedimentological Congress. Livret guide d'excursion. 28 p.

Parent M, Michaud Y, Boisvert E, Bolduc AM, Fagnan N, Fortier R, Cloutier M, Doiron A (1998) Cartographie hydrogéologique régionale du piémont laurentien dans la MRC de Portneuf : géologique et stratigraphie des formations superficielles. Geological Survey of Canada. Dossier public 3664a, 1 feuille. doi:10.4095/210070.

Parent M, Occhietti S (1988) Late Wisconsinan Deglaciation and Champlain Sea Invasion in the St. Lawrence Valley, Québec. *Geographie Physique Et Quaternaire* **42**: 215–246.

Parent M, Occhietti S (1999) Late Wisconsinan deglaciation and glacial lake development in the Appalachians of southeastern Québec. *Geographie Physique Et Quaternaire* **53**: 117–135.

Pawley SM, Atkinson N (2010) Application of Airborne Lidar (Light Detection and Ranging) Imagery for Surficial Geology Mapping in Densely Vegetated (Boreal Zone) Terrain, Lesser Slave Lake, Northern Alberta. Dans GeoCanada 2010, p. 1.

PDAL Contributors (2018) PDAL Point Data Abstraction Library. doi:10.5281/zenodo.2556738.

Pingel TJ, Clarke KC, McBride WA (2013) An improved simple morphological filter for the terrain classification of airborne LIDAR data. *ISPRS Journal of Photogrammetry and Remote Sensing* **77**: 21–30, doi:10.1016/j.isprsjprs.2012.12.002.

Polyak L, Korsun S, Febo LA, Stanovoy V, Khusid T, Hald M, Paulsen BE, Lubinski DJ (2002) Benthic foraminiferal assemblages from the southern Kara sea, a river-influenced Arctic marine environment. *Journal of Foraminiferal Research* **32**: 252–273, doi:10.2113/32.3.252.

Prichonnet G (1977) La déglaciation de la vallée du Saint-Laurent et l'invasion marine contemporaine. *Géographie physique et Quaternaire* **31**: 323–345.

QGIS Development Team (2014) QGIS Geographic Information System. Open Source Geospatial Foundation Project.

Rappol M (1993) Ice flow and glacial transport in Lower St. Lawrence, Quebec. Commission géologique du Canada. Dossier 90-19. 28 p. doi:10.4095/183989.

Rayburn JA, Cronin TM, Franzi DA, Knuepfer PLK, Willard DA (2011) Timing and duration of North American glacial lake discharges and the Younger Dryas climate reversal. *Quaternary Research* **75**: 541–551, doi:DOI: 10.1016/j.yqres.2011.02.004.

Rayburn JA, Franzi DA, Knuepfer PLK (2007) Evidence from the Lake Champlain Valley for a later onset of the Champlain Sea and implications for late glacial meltwater routing to the North Atlantic. *Palaeogeography, Palaeoclimatology, Palaeoecology* **246**: 62–74, doi:10.1016/j.palaeo.2006.10.027.

Rayburn JA, K. Knuepfer PL, Franzi DA (2005) A series of large, Late Wisconsinan meltwater floods through the Champlain and Hudson Valleys, New York State, USA. *Quaternary Science Reviews* **24**: 2410–2419, doi:10.1016/j.quascirev.2005.02.010.

Reimer PJ, Bard E, Bayliss A, Beck JW, Blackwell PG, Ramsey CB, Buck CE, Cheng H, Edwards RL, Friedrich M, Grootes PM, Guilderson TP, Haflidason H, Hajdas I, Hatté C, Heaton TJ, Hoffmann DL, Hogg AG, Hughen KA, Kaiser KF, Kromer B, Manning SW, Niu M, Reimer RW, Richards DA, Scott EM, Southon JR, Staff RA, Turney CSM, van der Plicht J (2013) IntCal13 and Marine13 Radiocarbon Age Calibration Curves 0–50,000 Years cal BP. *Radiocarbon* **55**: 1869–1887, doi:10.2458/azu_js_rc.55.16947.

Richard P, Occhietti S (2004) Meltwater discharge and the triggering of Younger Dryas : new data on the chronology of Champlain Sea transgression in the St-Lawrence River Valley. *American Geophysical Union, Spring Meeting*.

Richard PJH, Occhietti S (2005) 14C chronology for ice retreat and inception of Champlain Sea in the St. Lawrence Lowlands, Canada. *Quaternary Research* **63**: 353–358, doi:https://doi.org/10.1016/j.yqres.2005.02.003.

Richard PJH, Veillette JJ, Larouche AC, Hétu B, Gray JT, Gangloff P (1997) Chronologie de la déglaciation en Gaspésie : nouvelles données et implications. *Géographie physique et Quaternaire* **51**: 163–184, doi:10.7202/033116ar.

Ridge J, Bensonen M, Brochu M, Brown S, Callahan J, Cook G, Nicholson R, Toll N (1999) Varve, paleomagnetic, and 14 C Chronologies for late Pleistocene events in New Hampshire and Vermont (U.S.A.). *Géographie physique et Quaternaire* **53**: 79–107, doi:https://doi.org/10.7202/004864ar.

Rivard C, Michaud Y, Deblonde C, Boisvert V, Carrier C, Morin RH, Calvert T, Vigneault H, Conohan D, Castonguay S, Lefebvre R, Rivera A, Parent M (2008a) Canadian Groundwater Inventory: regional hydrogeological characterization of the south-central part of the Maritimes Basin. *Geological Survey of Canada, Bulletin* **589**: 1–96, doi:10.4095/223958.

Rivard C, Michaud Y, Lefebvre R, Deblonde C, Rivera A (2008b) Characterization of a Regional Aquifer System in the Maritimes Basin, Eastern Canada. *Water Resources Management* **22**: 1649, doi:10.1007/s11269-008-9247-7.

Rodrigues CG (1988) Late Quaternary glacial to marine successions in the central St. Lawrence Lowland. Dans Field Trip Guidebook, New York State Geological Association, 60th Annual Meeting, pp. 201–214.

Rodrigues CG (1992) Successions of invertebrate microfossils and the late quaternary deglaciation of the central St Lawrence Lowland, Canada and United States. *Quaternary Science Reviews* **11**: 503–534, doi:10.1016/0277-3791(92)90010-6.

Rodrigues CG, Vilks G (1994) The impact of glacial lake runoff on the goldthwait and champlain seas: The relationship between glacial lake agassiz runoff and the younger dryas. *Quaternary Science Reviews* **13**: 923–944, doi:10.1016/0277-3791(94)90009-4.

Ross M, Campbell JE, Parent M, Adams RS (2009) Palaeo-ice streams and the subglacial landscape mosaic of the North American mid-continental prairies. *Boreas* **38**: 421–439, doi:10.1111/j.1502-3885.2009.00082.x.

Ross M, Parent M, Benjumea B, Hunter J (2006) The late Quaternary stratigraphic record northwest of Montréal: Regional ice-sheet dynamics, ice-stream activity, and early deglacial events. *Canadian Journal of Earth Sciences* **43**: 461–485, doi:10.1007/s10040-004-0364-x.

Ross M, Parent M, Lefebvre R (2005a) 3D geologic framework models for regional hydrogeology and land-use management: a case study from a Quaternary basin of southwestern Quebec, Canada. *Hydrogeology Journal* **13**: 690–707.

Ross M, Parent M, Michaud Y, Boisvert E, Girard F (2005b) On the construction of 3D geological models for applications in regional hydrogeology in complex Quaternary terrains of eastern Canada. Dans Geological Models for Groundwater Flow Modeling, Workshop Extended Abstracts, p. 4.

Samson C, Barrette L, Lasalle P, Fortier J (1977) Quebec Radiocarbon Measurements I. *Radiocarbon* **19**: 96–100, doi:10.1017/S0033822200003362.

Shaw J, Piper DJW, Fader GBJ, King EL, Todd BJ, Bell T, Batterson MJ, Liverman DGE (2006) A conceptual model of the deglaciation of Atlantic Canada. *Quaternary Science Reviews* **25**: 2059–2081, doi:10.1016/j.quascirev.2006.03.002.

Shilts WW (1981) Surficial geology of the Lac Mégantic area, Québec. Geological Survey of Canada. Mémoire 397, une carte, échelle 1:100 000. 102 p. doi:10.4095/109357.

Slivitzky A, St-Julien P (1987) Compilation géologique de la région de l'Estrie-Beauce. Ministère de l'Énergie et des Ressources, Québec, Rapport MM 85-04, 48 p., 1 carte au 250 000.

Smith AM, Murray T, Nicholls KW, Makinson K, Aðalgeirsdóttir G, Behar AE, Vaughan DG (2007) Rapid erosion, drumlin formation, and changing hydrology beneath an Antarctic ice stream. *Geology* **35**: 127–130, doi:10.1130/G23036A.1.

Smith MJ, Paron P, Griffiths JS (2011) Geomorphological mapping: methods and applications (Elsevier Science).

Sookhan S, Eyles N, Putkinen N (2018) LiDAR-based mapping of paleo-ice streams in the eastern Great Lakes sector of the Laurentide Ice Sheet and a model for the evolution of drumlins and

MSGLs. *GFF* **140**: 202–228, doi:10.1080/11035897.2018.1474380.

Spagnolo M, Clark CD, Ely JC, Stokes CR, Anderson JB, Andreassen K, Graham AGC, King EC (2014) Size, shape and spatial arrangement of mega-scale glacial lineations from a large and diverse dataset. *Earth Surface Processes and Landforms* **39**: 1432–1448, doi:10.1002/esp.3532.

St-Julien P, Hubert C (1975) Evolution of the Taconian orogen in the Quebec Appalachians. *American Journal of Science* **275**: 337–362.

Stokes CR (2018) Geomorphology under ice streams: Moving from form to process. *Earth Surface Processes and Landforms* **43**: 85–123, doi:10.1002/esp.4259.

Stokes CR, Clark CD (1999) Geomorphological criteria for identifying Pleistocene ice streams. *Annals of Glaciology* **28**: 67–74, doi:10.3189/172756499781821625.

Stokes CR, Clark CD (2001) Palaeo-ice streams. *Quaternary Science Reviews* **20**: 1437–1457.

Stokes CR, Clark CD (2002) Are long subglacial bedforms indicative of fast ice flow? *Boreas* **31**: 239–249, doi:10.1111/j.1502-3885.2002.tb01070.x.

Stokes CR, Tarasov L, Blomdin R, Cronin TM, Fisher TG, Gyllencreutz R, H??ttestrand C, Heyman J, Hindmarsh RCA, Hughes ALC, Jakobsson M, Kirchner N, Livingstone SJ, Margold M, Murton JB, Noormets R, Peltier WR, Peteet DM, Piper DJW, Preusser F, Renssen H, Roberts DH, Roche DM, Saint-Ange F, Stroeven AP, Teller JT (2015) On the reconstruction of palaeo-ice sheets: Recent advances and future challenges. *Quaternary Science Reviews* **125**: doi:10.1016/j.quascirev.2015.07.016.

Taylor FB (1913) Moraine systems of southwestern Ontario (Toronto: The University Press).

Tecsult (2008) Cartographie hydrogéologique du bassin versant de la rivière Chaudière - Secteurs de la Basse-Chaudière et de la Moyenne-Chaudière Étude réalisée dans le cadre du Projet eaux souterraines de la Chaudière, financé par le Programme d'approvisionnement en eau Canada, Québec (PAECQ) et géré par le Conseil pour le développement de l'agriculture du Québec (CDAQ).

Teller JT, Leverington DW, Mann JD (2002) Freshwater outbursts to the oceans from glacial Lake Agassiz and their role in climate change during the last deglaciation. **21**: 879–887.

Thiery G (2016) Cartographie quaternaire et caractérisation de dépôts éoliens de la région de Lotbinière-Deschaillons, Basse-Terres du Saint-Laurent. Mémoire de maîtrise, Université du Québec à Montréal, Montréal, Québec, 156 p.

Thompson WB, Griggs CB, Miller NG, Nelson RE, Weddle TK, Kilian TM (2011) Associated terrestrial and marine fossils in the late-glacial Presumpscot Formation, southern Maine, USA, and the marine reservoir effect on radiocarbon ages. *Quaternary Research* **75**: 552–565, doi:DOI: 10.1016/j.yqres.2011.02.002.

Tremblay A, Pinet N (1994) Distribution and characteristics of Taconian and Acadian deformation, southern Québec Appalachians. *Geological Society of America Bulletin* **106**: 1172–1181, doi:10.1130/0016-7606(1994)106<1172:DACOTA>2.3.CO;2.

Tremblay T, Nastev M, Lamothe M (2010) Grid·based hydrostratigraphic 3D modelling of the Quaternary sequence in the Châteauguay River watershed, Québec. *Canadian Water Resources Journal* **35**: 377–389.

Veillette JJ, Cloutier M, Paradis SJ, Hétu B, Cloutier C, -A, Houde-Poirier M, Buffin-Bélanger T (2017) Géologie des formations en surface et histoire glaciaire, Bas-Saint-Laurent, Québec. Carte géoscientifique du Canada 279, 1 feuille. doi:10.4095/299135.

Veillette JJ, Nixon FM (1984) Sequence of Quaternary sediments in the Belanger sand pit, Pointe-Fortune, Quebec- Ontario. *Geographie Physique Et Quaternaire* **38**: 59–68.

de Vernal A, Goyette C, Rodrigues CG (1989) Contribution palynostratigraphique (dinokystes, pollen et spores) à la connaissance de la mer de Champlain: coupe de Saint-Césaire, Québec. *Canadian Journal of Earth Sciences* **26**: 2450–2464, doi:10.1139/e89-209.

Verville JF (2010) Paléoenvironnements et fluctuations du niveau marin relatif Holocènes dans le bassin versant de la rivière Cap-Rouge, Québec. Mémoire de maîtrise, Université Laval, 80 p.

Webster TL, Murphy JB, Gosse JC, Spooner I (2006) The application of lidar-derived digital

elevation model analysis to geological mapping: an example from the Fundy Basin, Nova Scotia, Canada. *Canadian Journal of Remote Sensing* **32**: 173–193, doi:10.5589/m06-017.

Wehr A, Lohr U (1999) Airborne laser scanning - An introduction and overview. *ISPRS Journal of Photogrammetry and Remote Sensing* **54**: 68–82, doi:10.1016/S0924-2716(99)00011-8.

Zakšek K, Oštir K, Kokalj Ž (2011) Sky-View Factor as a Relief Visualization Technique. *Remote Sensing* **3**: 398–415, doi:10.3390/rs3020398.

8 ANNEXE I – Cartes de géologie de surface

L'annexe I inclut les cartes de géologie de surface produites dans le cadre du premier article. Celles-ci ont été produites en format A0 (standard ISO 216).

En raison de la grande taille de ces cartes, le contenu réel de cette annexe est présenté dans les annexes électroniques accompagnant cette thèse. Une version en taille plus modeste est présentée ici à l'annexe 1 en format 11 x 17, mais la visibilité des éléments n'est pas idéale étant donné l'échelle d'origine de la carte. La légende géologique est présentée séparément afin d'être lisible ici.

Surficial geology legend

Landslide escarpment

Channel

Beach crest

Terrace scarp

Ravine scarp

Limit of submergence

QUATERNARY **POSTGLACIAL**

COLLUVIAL AND MASS-WASTING DEPOSITS

Ce **Scree or talus deposits**

Cg **Landslide deposits**

C **Undifferentiated colluvial or mass-wasting deposits**

ORGANIC SEDIMENTS

Ot **Peatbog sediments :** Peat, more or less decomposed, deposited in fens or bogs. Thickness varies between 0.5 and 5 m.

Om **Marsh and swamp sediments :** Organic sediments, often rich in minerals, deposited in palustre environments with open ponds. Thickness varies from 0.5 to 3 m.

O **Undifferentiated organic sediments**

EOLIAN SEDIMENTS

Ed **Dunes :** Diffuse oblique stratified fine sand set up by the wind as parabolic dunes formed on the surface of freshly exposed littoral and alluvial sediments; indicate prevailing winds from east-northeast; may contain organic horizons such as paleosols; of a thickness varying from 3 to 15 m.

ALLUVIAL SEDIMENTS

Ap **Modern floodplain alluvium :** Sand, sandy silt, gravelly sand and gravel frequently containing organic matter; from 1 to 3 m thick; current alluvial bars and plains.

Ae **Ancient estuarine alluvium :** Silt, sandy silt, sand usually containing organic fragments, mostly from aquatic plants; from 0.5 to 2 m thick; massive structure, sub-laminated; resting in unconformity on the underlying sediments and deposited during transgressive episodes.

At **Low terrace alluvium :** Sand, sandy silt, gravelly sand often containing organic matter; from 1 to 3 m thick; surface usually marked by leaflets and alluvial bars. Sometimes reworked by wind action. The lowering of the base level is manifested by terracing.

Ax **High terrace alluvium :** Sand, sandy silt and gravel containing some organic matter; from 1 to 5 m thick; deposited in overflow areas of contemporary river corridors. Estuarine facies are common in this unit. Surface generally marked by levies and alluvial bars and sometimes reworked by wind power.

MARINE SEDIMENTS

Md **Deltaïc and prodeltaïc sediments :** Sand, gravelly sand, laminated and well sorted; up to 10 m thick; set up at the mouth of streams flowing into the Champlain Sea; locally comprising prodeltaic silty-sandy sediments.

Mb/Tr **Marine beach sediments :** Sand, sandy silt, gravelly sand and stratified gravel and generally well sorted; thickness varying from 1 to 5 m; placed in shallow water by littoral cords and raised beaches. Often contains elements from the reworked till blanket underlying the beaches. These sediments generally form a thin cover and directly overly bedrock outcrops or the regional till blanket.

Mb/Trm **Marine beach sediments :** Sand, sandy silt, gravelly sand and stratified gravel and generally well sorted; thickness varying from 0.5 to 1 m; Contains elements from the reworked thin till blanket underlying the beaches. These sediments form a very thin cover and directly overly bedrock outcrops.

Mb **Littoral and near-shore sediments :** Sand, sandy silt, gravelly sand and stratified gravel and generally well sorted; thickness varying from 1 to 10 m; placed in shallow water during the Plenimarine phase and during the exondation; surface usually marked by littoral cords or prelittoral and sometimes reworked by wind power; these sediments generally form a thin cover over deep water sediments.

Ma **Deep water/offshore marine sediments :** Silty clay, dark, massive, laminated or stratified, locally comprising rhythmites; varying from less than 1 m to more than 50 m (in drilling) in thickness; put in place mainly by decantation during the post-glacial marine flood phase of the Champlain Sea.

M **Undifferentiated marine sediments**

GLACIOMARINE SEDIMENTS

MGi **Intertidal sediments :** Intertidal sediments: silt and sandy silt, generally massive or weakly stratified; thickness varying from 0.5 to 3 m; set up in intertidal or subtidal zones in bays or sheltered inlets, often near large deltaic complexes.

MGd **Deltaïc and prodeltaïc sediments :** Sand, gravelly sand, laminated and well sorted; up to 10 m thick; set up at the mouth of streams flowing into the Goldthwait Sea; locally comprising prodeltaic silty-sandy sediments.

MGb/Tr **Marine beach sediments :** Sand, sandy silt, gravelly sand and stratified gravel and generally well sorted; thickness varying from 1 to 5 m; placed in shallow water by littoral cords and raised beaches. Often contains elements from the reworked till blanket underlying the beaches. These sediments generally form a thin cover and directly overly bedrock outcrops or the regional till blanket.

MGb/Trm **Marine beach sediments :** Sand, sandy silt, gravelly sand and stratified gravel and generally well sorted; thickness varying from 0.5 to 1 m; Contains elements from the reworked thin till blanket underlying the beaches. These sediments form a very thin cover and directly overly bedrock outcrops.

MGb **Littoral and near-shore sediments :** Sand, sandy silt, gravelly sand and stratified gravel and generally well sorted; thickness varying from 1 to 10 m; placed in shallow water during the glaciomarine phase; surface usually marked by littoral cords and sometimes reworked by wind power; these sediments generally form a thin cover over deep water sediments.

MGa **Deep water/offshore glaciomarine sediments :** Silty clay, dark, massive, laminated or stratified, locally comprising rhythmites; varying from less than 1 m to more than 50 m (in drilling) in thickness; put in placemainly by decantation during the glaciomarine flood phase of the Goldthwait Sea

MG **Undifferenciated glaciomarine sediments**

GLACIOFLUVIAL SEDIMENTS

Go **Proglacial outwash sediments :** Sand, peebles and blocs put in place in broad, outspread flat or gently sloping alluvial outwash in front of or beyond the terminal moraine of a glacier. Granulometry is generally downgrading downstream. The deposit often forms spreading plains whose surface is often marked by ancient sinuous and shallow channels.

Gs **Proglacial subaqueous outwash sediments :** Sand and silty sand, some gravel. Forms heaps set up in relatively shallow water plans at the end of sub- or intra- glacial tunnels opening up in the Goldthwait Sea. Sometimes exposed under marine sediments, in sand or gravel pits.

Gx **Glaciofluvial ice-contact sediments :** Mainly composed of sand, gravel and peebles, although glaciomarine deposits may contain a greater proportion of fine sediments. Deposited in subglacial or supraglacial environments, or in an ice-marginal position. These sediments take the form of eskers, kames, deltas-kames and morainic ridges.

GxT **Glaciofluvial ice-contact sediments associated with the St. Antonin Moraine:** Mainly composed of sand, gravel and peebles, although glaciomarine deposits may contain a greater proportion of fine sediments. Deposited in the context of the an ice-marginal position of the St. Antonin Moraine. These sediments take the form of eskers, kames, deltas-kames and morainic ridges.

G **Undifferenticated proglacial sediments**

GLACIAL SEDIMENTS

Trm **Reworked till, veneer :** Thin and discontinuous diamictic sediment in which has been reworked by the action of waves and sea currents, under the maximum elevation of the post-glacial Goldthwait Sea. Often fossiliferous.

Tr **Reworked till, blanket :** Diamictic sediment in which the upper unit has been reworked by the action of waves and sea currents, under the maximum elevation of the post-glacial Goldthwait Sea. Often fossiliferous. Can contain levels of stratified sand and peebles.

Tc **Till Blanket:** Thick and continuous till layer. Contains lodgment and ablation facies. Unstratified drift, deposited directly by a glacier without reworking by meltwater, and consisting of a mixture of clay, silt, sand, gravel, and boulders ranging widely in size and shape. Thickness varies between 0.5 and 10 m.

Tm **Till veneer :** Thin and discontinuous till that may include areas of rock outcrop. Diamictic unit includes mostly ablation facies till. Thickness is usually below 1 m.

T **Till :** Continuous layer of till put in place by the St-Lawrence Ice Stream (SLIS) by ice flowing towards the northeast

PRE-QUATERNARY

R **Bedrock**

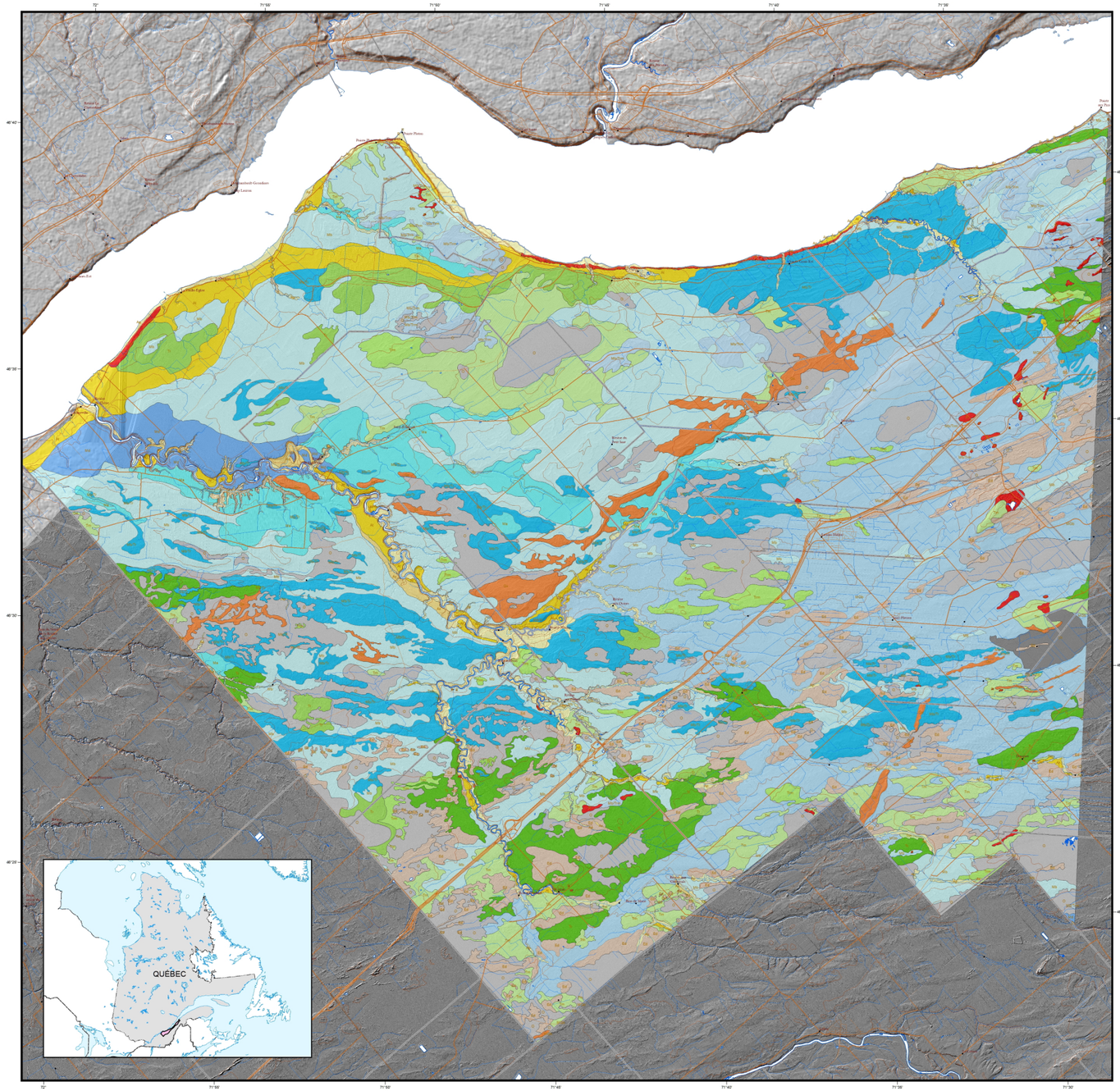

Surficial geology of the Lower Chaudière-Appalaches and Kamouraska areas, Province of Québec

Guillaume Légaré-Couture[1], Michel Parent[2] and René Lefebvre[1]

[1] Institut National de la Recherche Scientifique – Centre Eau, Terre et Environnement (INRS-ETE)
[2] Geological Survey of Canada, Natural Resources Canada

0 2.5 5 10 kilometers

Projection : Modified Transverse Mercator zone 7
Datum : North American Datum 1983

N
W E
S

Surficial geology legend

Landslide escarpment
Channel
Beach crest
Terrace scarp
Ravine scarp
Limit of submergence

QUATERNARY **POSTGLACIAL**

COLLUVIAL AND MASS-WASTING DEPOSITS

Ce **Scree or talus deposits**
Cg **Landslide deposits**
C **Undifferentiated colluvial or mass-wasting deposits**

ORGANIC SEDIMENTS

Ot **Peatbog sediments :** Peat, more or less decomposed, deposited in fens or bogs. Thickness varies between 0.5 and 5 m.
Om **Marsh and swamp sediments :** Organic sediments, often rich in minerals, deposited in palustre environments with open ponds. Thickness varies from 0.5 to 3 m.
O **Undifferentiated organic sediments**

EOLIAN SEDIMENTS

Ed **Dunes :** Diffuse oblique stratified fine sand set up by the wind as parabolic dunes formed on the surface of freshly-exposed littoral and alluvial sediments; indicate prevailing winds from east-northeast; may contain organic horizons such as paleosols; of a thickness varying from 3 to 15 m.

ALLUVIAL SEDIMENTS

Ap **Modern floodplain alluvium :** Sand, sandy silt, gravelly sand and gravel frequently containing organic matter; from 1 to 3 m thick; current alluvial bars and plains.
Ae **Ancient estuarine alluvium :** Silt, sandy silt, sand usually containing organic fragments, mostly from aquatic plants; from 0.5 to 2 m thick; massive structure, sub-laminated; resting in unconformity on the underlying sediments and deposited during transgressive episodes.
At **Low terrace alluvium :** Sand, sandy silt, gravelly sand often containing organic matter; from 1 to 3 m thick; surface usually marked by leafets and alluvial bars. Sometimes reworked by wind action. The lowering of the base level is manifested by terracing.
Ax **High terrace alluvium :** Sand, sandy silt and gravel containing some organic matter; from 1 to 5 m thick; deposited in overflow areas of contemporary river corridors. Estuarine facies are common in this unit. Surface generally marked by levees and alluvial bars and sometimes reworked by wind power.

MARINE SEDIMENTS

Mld **Deltaic and prodeltaic sediments :** Sand, gravelly sand, laminated and well sorted; up to 10 m thick; set up at the mouth of streams flowing into the Champlain Sea; locally comprising prodeltaic silty-sandy sediments.
Mb/Tr **Marine beach sediments :** Sand, sandy silt, gravelly sand and stratified gravel and generally well sorted; thickness varying from 1 to 5 m; placed in shallow water by littoral cords and raised beaches. Often contains elements from the reworked till blanket underlying the beaches. These sediments generally form a thin cover and directly overly bedrock outcrops or the regional till blanket.
Mb/Tm **Marine beach sediments :** Sand, sandy silt, gravelly sand and stratified gravel and generally well sorted; thickness varying from 0.5 to 1 m; Contains elements from the reworked thin till blanket underlying the beaches. These sediments form a very thin cover and directly overly bedrock outcrops.
Mb **Littoral and near-shore sediments :** Sand, sandy silt, gravelly sand and stratified gravel and generally well sorted; thickness varying from 1 to 10 m; placed in shallow water during the Plenimarine phase and during the exondation; surface usually marked by littoral cords or prelittoral and sometimes reworked by wind power; these sediments generally form a thin cover over deep water sediments.
Ma **Deep water/offshore marine sediments :** Silty clay, dark, massive, laminated or stratified, locally comprising rhythmites, varying from less than 1 m to more than 50 m (in drilling) in thickness; put in place mainly by excantation during the post-glacial marine flood phase of the Champlain Sea.
M **Undifferentiated marine sediments**

GLACIOMARINE SEDIMENTS

MGi **Intertidal sediments :** Intertidal sediments: silt and sandy silt, generally massive or weakly stratified; thickness varying from 0.5 to 3 m; set up in intertidal or subtidal zones in bays or sheltered inlets, often near large deltaic complexes.
MGd **Deltaic and prodeltaic sediments :** Sand, gravelly sand, laminated and well sorted; up to 10 m thick; set up at the mouth of streams flowing into the Goldthwait Sea; locally comprising prodeltaic silty-sandy sediments.
MGb/Tr **Marine beach sediments :** Sand, sandy silt, gravelly sand and stratified gravel and generally well sorted; thickness varying from 1 to 5 m; placed in shallow water by littoral cords and raised beaches. Often contains elements from the reworked till blanket underlying the beaches. These sediments generally form a thin cover and directly overly bedrock outcrops or the regional till blanket.
MGb/Tm **Marine beach sediments :** Sand, sandy silt, gravelly sand and stratified gravel and generally well sorted; thickness varying from 0.5 to 1 m; Contains elements from the reworked thin till blanket underlying the beaches. These sediments form a very thin cover and directly overly bedrock outcrops.
MGb **Littoral and near-shore sediments :** Sand, sandy silt, gravelly sand and stratified gravel and generally well sorted; thickness varying from 1 to 10 m; placed in shallow water during the glaciomarine phase; surface usually marked by littoral cords and sometimes reworked by wind power; these sediments generally form a thin cover over deep water sediments.
MGa **Deep water/offshore glaciomarine sediments :** Silty clay, dark, massive, laminated or stratified, locally comprising rhythmites; varying from less than 1 m to more than 50 m (in drilling) in thickness; put in placemainly by excantation during the glaciomarine flood phase of the Goldthwait Sea.
MG **Undifferenciated glaciomarine sediments**

GLACIOFLUVIAL SEDIMENTS

Go **Proglacial outwash sediments :** Sand, peebles and blocs put in place in broad, subplanar flat or gently sloping alluvial outwash in front of or beyond the terminal moraine of a glacier. Granulometry is generally downgrading downstream. The deposit often forms spreading plains whose surface is often marked by ancient sinuous and shallow channels.
Gs **Proglacial subaqueous outwash sediments :** Sand and silty sand, some gravel. Forms heaps set up in relatively shallow water plains at the end of sub- or intra- glacial tunnels opening up in the Goldthwait Sea. Sometimes exposed under marine sediments, in sand or gravel pits.
Gx **Glaciofluvial ice-contact sediments :** Mainly composed of sand, gravel and peebles, although glaciomarine deposits may contain a greater proportion of fine sediments. Deposited in subglacial or supraglacial environments, or in an ice-marginal position. These sediments take the form of eskers, kames, deltas-kames and moranic ridges.
GxT **Glaciofluvial ice-contact sediments associated with the St. Antonio Moraine:** Mainly composed of sand, gravel and peebles, although glaciomarine deposits may contain a greater proportion of fine sediments. Deposited in the context of the an ice-marginal position of the St. Antonin Moraine. These sediments take the form of eskers, kames, deltas-kames and moranic ridges.
G **Undifferenciated proglacial sediments**

GLACIAL SEDIMENTS

Trm **Reworked till, veneer :** Thin and discontinuous diamictic sediment in which has been reworked by the action of waves and sea currents, under the maximum elevation of the post-glacial Goldthwait Sea. Often fossiferous.
Tr **Reworked till, blanket :** Diamictic sediment in which the upper unit has been reworked by the action of waves and sea currents, under the maximum elevation of the post-glacial Goldthwait Sea. Often fossiferous. Can contain levels of stratified sand and peebles.
Tg **Till Blanket:** Thick and continuous till layer. Contains lodgment and ablation facies. Unstratified drift, deposited directly by a glacier without reworking by meltwater, and consisting of a mixture of clay, silt, sand, gravel, and boulders ranging widely in size and shape. Thickness varies between 0.5 and 10 m.
Tm **Till veneer :** Thin and discontinuous till that may include areas of rock outcrop. Diamictic unit includes mostly ablation facies till. Thickness is usually below 1 m.
T **Till :** Continuous layer of till put in place by the St-Lawrence Ice Stream (SLIS) by ice flowing towards the northeast

PRE-QUATERNARY

R **Bedrock**

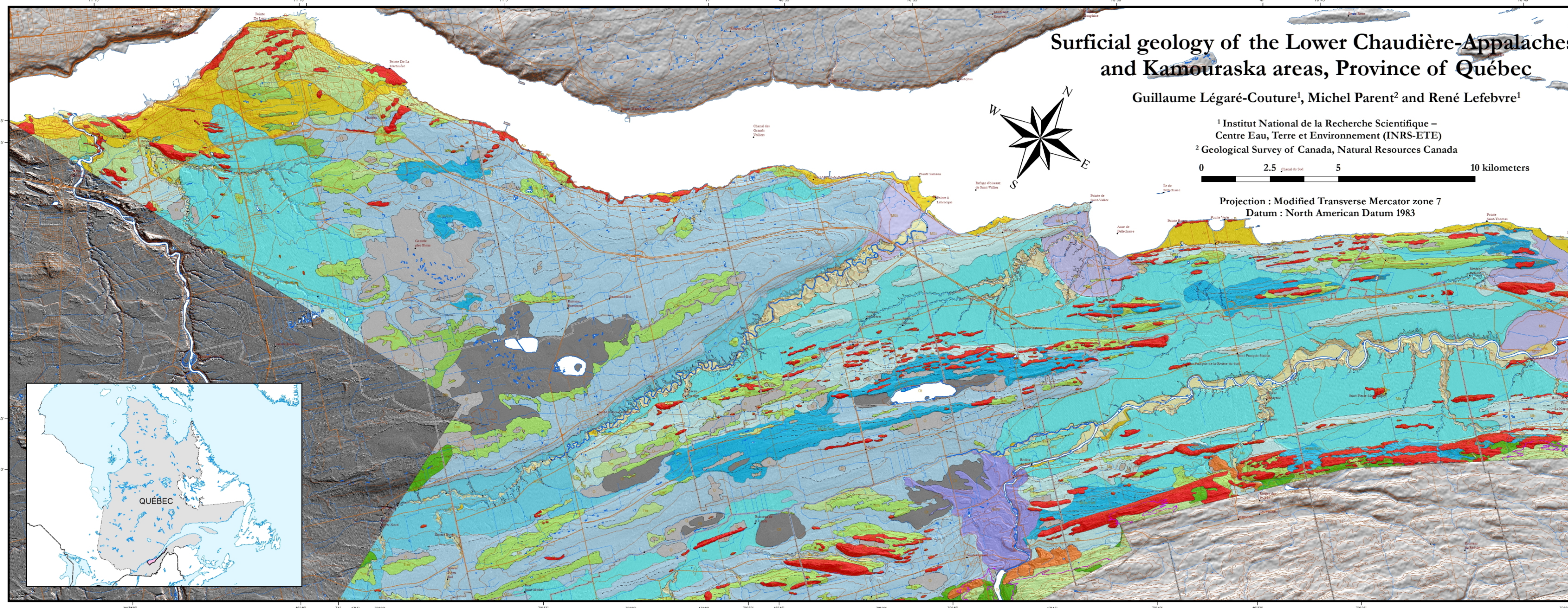

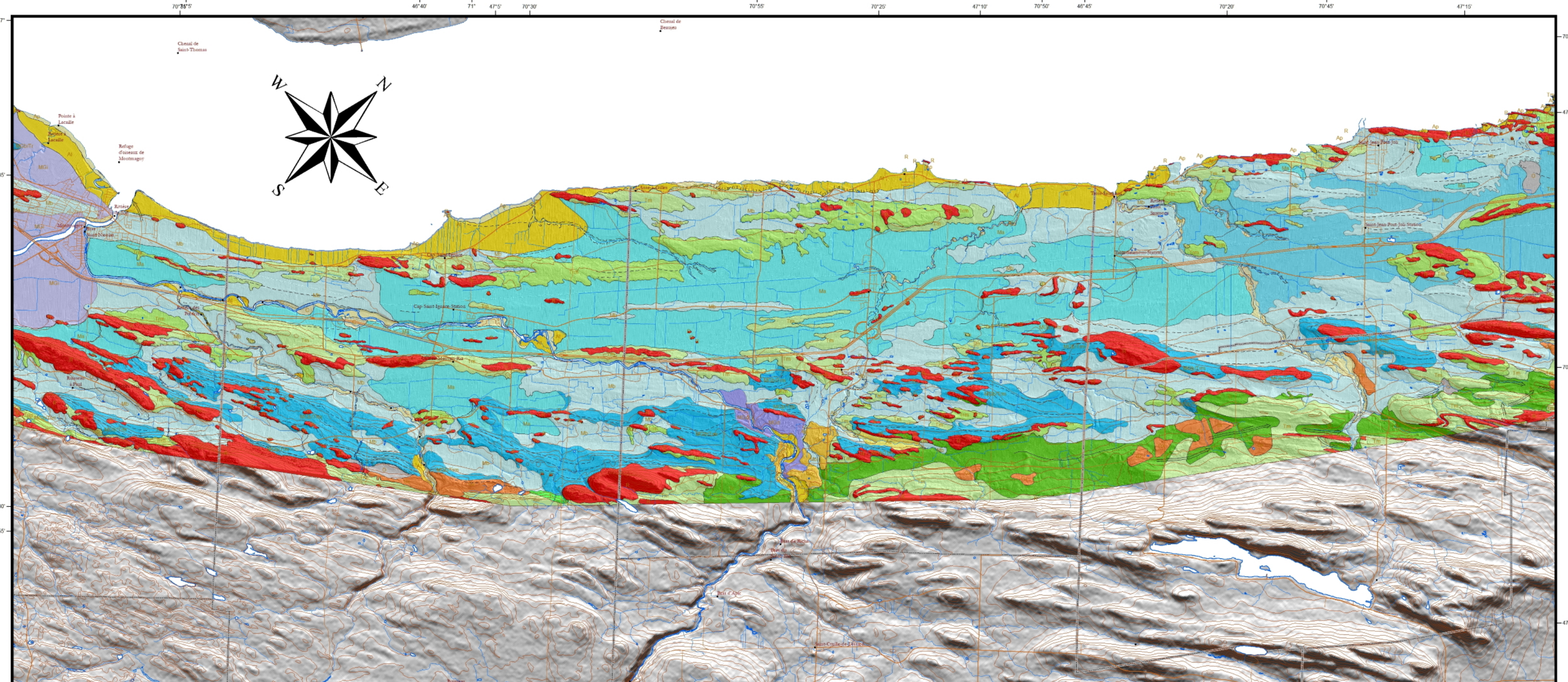

Surficial geology legend

- Landslide escarpment
- Channel
- Beach crest
- Terrace scarp
- Ravine scarp
- Limit of submergence

QUATERNARY **POSTGLACIAL**

COLLUVIAL AND MASS-WASTING DEPOSITS

- Ce — **Scree or talus deposits**
- Cg — **Landslide deposits**
- C — **Undifferentiated colluvial or mass-wasting deposits**

ORGANIC SEDIMENTS

- Ot — **Peatbog sediments :** Peat, more or less decomposed, deposited in fens or bogs. Thickness varies between 0.5 and 5 m.
- Om — **Marsh and swamp sediments :** Organic sediments, often rich in minerals, deposited in palustre environments with open ponds. Thickness varies from 0.5 to 3 m.
- O — **Undifferentiated organic sediments**

EOLIAN SEDIMENTS

- Ed — **Dunes :** Diffuse oblique stratified fine sand set up by the wind as parabolic dunes formed on the surface of freshly exposed littoral and alluvial sediments; indicate prevailing winds from east-northeast; may contain organic horizons such as paleosols; of a thickness varying from 3 to 15 m.

ALLUVIAL SEDIMENTS

- Ap — **Modern floodplain alluvium :** Sand, sandy silt, gravelly sand and gravel frequently containing organic matter; from 1 to 3 m thick; current alluvial bars and plains.
- Ae — **Ancient estuarine alluvium :** Silt, sandy silt, sand usually containing organic fragments, mostly from aquatic plants; from 0.5 to 2 m thick; massive structure, sub-laminated; resting in unconformity on the underlying sediments and deposited during transgressive episodes.
- At — **Low terrace alluvium :** Sand, sandy silt, gravelly sand often containing organic matter; from 1 to 3 m thick; surface usually marked by leaflets and alluvial bars. Sometimes reworked by wind action. The lowering of the base level is manifested by terracing.
- Ax — **High terrace alluvium :** Sand, sandy silt and gravel containing some organic matter; from 1 to 5 m thick; deposited in overflow areas of contemporary river corridors. Estuarine facies are common in this unit. Surface generally marked by levies and alluvial bars and sometimes reworked by wind power.

MARINE SEDIMENTS

- Md — **Deltaïc and prodeltaïc sediments :** Sand, gravelly sand, laminated and well sorted; up to 10 m thick; set up at the mouth of streams flowing into the Champlain Sea; locally comprising prodeltaic silty-sandy sediments.
- Mb/Tr — **Marine beach sediments :** Sand, sandy silt, gravelly sand and stratified gravel and generally well sorted; thickness varying from 1 to 5 m; placed in shallow water by littoral cords and raised beaches. Often contains elements from the reworked till blanket underlying the beaches. These sediments generally form a thin cover and directly overly bedrock outcrops or the regional till blanket.
- Mb/Trm — **Marine beach sediments :** Sand, sandy silt, gravelly sand and stratified gravel and generally well sorted; thickness varying from 0.5 to 1 m; Contains elements from the reworked thin till blanket underlying the beaches. These sediments form a very thin cover and directly overly bedrock outcrops.
- Mb — **Littoral and near-shore sediments :** Sand, sandy silt, gravelly sand and stratified gravel and generally well sorted; thickness varying from 1 to 10 m; placed in shallow water during the Plenimarine phase and during the exondation; surface usually marked by littoral cords or prelittoral and sometimes reworked by wind power; these sediments generally form a thin cover over deep water sediments.
- Ma — **Deep water/offshore marine sediments :** Silty clay, dark, massive, laminated or stratified, locally comprising rhythmites; varying from less than 1 m to more than 50 m (in drilling) in thickness; put in place mainly by decantation during the post-glacial marine flood phase of the Champlain Sea.
- M — **Undifferentiated marine sediments**

GLACIOMARINE SEDIMENTS

- MGi — **Intertidal sediments :** Intertidal sediments: silt and sandy silt, generally massive or weakly stratified; thickness varying from 0.5 to 3 m; set up in intertidal or subtidal zones in bays or sheltered inlets, often near large deltaic complexes.
- MGd — **Deltaïc and prodeltaïc sediments :** Sand, gravelly sand, laminated and well sorted; up to 10 m thick; set up at the mouth of streams flowing into the Goldthwait Sea; locally comprising prodeltaic silty-sandy sediments.
- MGb/Tr — **Marine beach sediments :** Sand, sandy silt, gravelly sand and stratified gravel and generally well sorted; thickness varying from 1 to 5 m; placed in shallow water by littoral cords and raised beaches. Often contains elements from the reworked till blanket underlying the beaches. These sediments generally form a thin cover and directly overly bedrock outcrops or the regional till blanket.
- MGb/Trm — **Marine beach sediments :** Sand, sandy silt, gravelly sand and stratified gravel and generally well sorted; thickness varying from 0.5 to 1 m; Contains elements from the reworked thin till blanket underlying the beaches. These sediments form a very thin cover and directly overly bedrock outcrops.
- MGb — **Littoral and near-shore sediments :** Sand, sandy silt, gravelly sand and stratified gravel and generally well sorted; thickness varying from 1 to 10 m; placed in shallow water during the glaciomarine phase; surface usually marked by littoral cords and sometimes reworked by wind power; these sediments generally form a thin cover over deep water sediments.
- MGa — **Deep water/offshore glaciomarine sediments :** Silty clay, dark, massive, laminated or stratified, locally comprising rhythmites; varying from less than 1 m to more than 50 m (in drilling) in thickness; put in placemainly by decantation during the glaciomarine flood phase of the Goldthwait Sea
- MG — **Undifferenciated glaciomarine sediments**

GLACIOFLUVIAL SEDIMENTS

- Go — **Proglacial outwash sediments :** Sand, peebles and blocs put in place in broad, outspread flat or gently sloping alluvial outwash in front of or beyond the terminal moraine of a glacier. Granulometry is generally downgrading downstream. The deposit often forms spreading plains whose surface is often marked by ancient sinuous and shallow channels.
- Gs — **Proglacial subaqueous outwash sediments :** Sand and silty sand, some gravel. Forms heaps set up in relatively shallow water plans at the end of sub- or intra- glacial tunnels opening up in the Goldthwait Sea. Sometimes exposed under marine sediments, in sand or gravel pits.
- Gx — **Glaciofluvial ice-contact sediments :** Mainly composed of sand, gravel and peebles, although glaciomarine deposits may contain a greater proportion of fine sediments. Deposited in subglacial or supraglacial environments, or in an ice-marginal position. These sediments take the form of eskers, kames, deltas-kames and morainic ridges.
- GxT — **Glaciofluvial ice-contact sediments associated with the St. Antonin Moraine:** Mainly composed of sand, gravel and peebles, although glaciomarine deposits may contain a greater proportion of fine sediments. Deposited in the context of the an ice-marginal position of the St. Antonin Moraine. These sediments take the form of eskers, kames, deltas-kames and morainic ridges.
- G — **Undifferenticated proglacial sediments**

GLACIAL SEDIMENTS

- Trm — **Reworked till, veneer :** Thin and discontinuous diamictic sediment in which has been reworked by the action of waves and sea currents, under the maximum elevation of the post-glacial Goldthwait Sea. Often fossiliferous.
- Tr — **Reworked till, blanket :** Diamictic sediment in which the upper unit has been reworked by the action of waves and sea currents, under the maximum elevation of the post-glacial Goldthwait Sea. Often fossiliferous. Can contain levels of stratified sand and peebles.
- Tc — **Till Blanket:** Thick and continuous till layer. Contains lodgment and ablation facies. Unstratified drift, deposited directly by a glacier without reworking by meltwater, and consisting of a mixture of clay, silt, sand, gravel, and boulders ranging widely in size and shape. Thickness varies between 0.5 and 10 m.
- Tm — **Till veneer :** Thin and discontinuous till that may include areas of rock outcrop. Diamictic unit includes mostly ablation facies till. Thickness is usually below 1 m.
- T — **Till :** Continuous layer of till put in place by the St-Lawrence Ice Stream (SLIS) by ice flowing towards the northeast

PRE-QUATERNARY

- R — **Bedrock**

Surficial geology of the Lower Chaudière-Appalaches and Kamouraska areas, Province of Québec

Guillaume Légaré-Couture[1], Michel Parent[2] and René Lefebvre[1]

[1] Institut National de la Recherche Scientifique – Centre Eau, Terre et Environnement (INRS-ETE)
[2] Geological Survey of Canada, Natural Resources Canada

0 2.5 5 10 kilometers

Projection : Modified Transverse Mercator zone 7
Datum : North American Datum 1983

Surficial geology legend

Landslide escarpment
Channel
Beach crest
Terrace scarp
Ravine scarp
Limit of submergence

QUATERNARY **POSTGLACIAL**

COLLUVIAL AND MASS-WASTING DEPOSITS

Ce **Screes or talus deposits**
Cg **Landslide deposits**
C **Undifferentiated colluvial or mass-wasting deposits**

ORGANIC SEDIMENTS

Ot **Peatbog sediments :** Peat, more or less decomposed, deposited in fens or bogs. Thickness varies between 0.5 and 5 m.
Om **Marsh and swamp sediments :** Organic sediments, often rich in minerals, deposited in palustre environments with open ponds. Thickness varies from 0.5 to 2 m.
O **Undifferentiated organic sediments**

EOLIAN SEDIMENTS

Ed **Dunes :** Diffuse oblique stratified fine sand set up by the wind as parabolic dunes formed on the surface of freshly exposed littoral and alluvial sediments. Indicate prevailing winds from east-northeast; may contain organic horizons such as paleosols; of a thickness varying from 3 to 15 m.

ALLUVIAL SEDIMENTS

Ap **Modern floodplain alluvium :** Sand, sandy silt, gravelly sand and gravel frequently containing organic matter; from 1 to 3 m thick; current alluvial bars and plains.
Aa **Ancient estuarine alluvium :** Silt, sandy silt, sand usually containing organic fragments, mostly from aquatic plants; from 0.5 to 2 m thick; massive structure, sub-laminated; resting in uncomformity on the underlying sediments and deposited during transgressive episodes.
At **Low terrace alluvium :** Sand, sandy silt, gravelly sand often containing organic matter; from 1 to 3 m thick; surface usually marked by leaflets and alluvial bars. Sometimes reworked by wind action. The lowering of the base level is manifested by terracing.
Ax **High terrace alluvium :** Sand, sandy silt and gravel containing some organic matter; from 1 to 5 m thick; deposited in overflow areas of contemporary river corridors. Estuarine facies are common in this unit. Surface generally marked by levees and alluvial bars and sometimes reworked by wind power.

MARINE SEDIMENTS

Md **Deltaic and prodeltaic sediments :** Sand, gravelly sand, laminated and well stratified, up to 10 m thick; set up at the mouth of streams flowing into the Champlain Sea; locally comprising prodeltaic silty-sandy sediments.
Mb/Tr **Marine beach sediments :** Sand, sandy silt, gravelly sand and stratified gravel and generally well sorted; thickness varying from 1 to 3 m; placed in shallow water by littoral cords and raised beaches. Often contains elements from the reworked till blanket underlying the beaches. These sediments generally form a thin cover and directly overly bedrock outcrops or the regional till blanket.
Mb/Tm **Marine beach sediments :** Sand, sandy silt, gravelly sand and stratified gravel and generally well sorted; thickness varying from 0.5 to 1 m; Contains elements from the reworked thin till blanket underlying the beaches. These sediments form a very thin cover and directly overly bedrock outcrops.
Mb **Littoral and near-shore sediments :** Sand, sandy silt, gravelly sand and stratified gravel and generally well sorted; thickness varying from 1 to 10 m; placed in shallow water during the Pleniramire phase and during the esondation; surface usually marked by littoral cords or prairilloral and sometimes reworked by wind power; these sediments generally form a thin cover over deep water sediments.
Ma **Deep water/offshore marine sediments :** Silty clay, dark, massive, laminated or stratified, locally comprising rhythmites; varying from less than 1 m to more than 50 m (in drilling) in thickness; put in place mainly by decantation during the post-glacial marine flood phase of the Champlain Sea.
M **Undifferentiated marine sediments**

GLACIOMARINE SEDIMENTS

MGi **Interbital sediments :** Intertidal sediments; silt and sandy silt, generally massive or weakly stratified; thickness varying from 0.5 to 3 m; set up in intertidal or subtidal zones in bays or sheltered inlets, often near large deltaic complexes.
MGd **Deltaic and prodeltaic sediments :** Sand, gravelly sand, laminated and well stratified, up to 10 m thick; set up at the mouth of streams flowing into the Goldthwait Sea; locally comprising prodeltaic silty-sandy sediments.
MGb/Tr **Marine beach sediments :** Sand, sandy silt, gravelly sand and stratified gravel and generally well sorted; thickness varying from 1 to 5 m; placed in shallow water by littoral cords and raised beaches. Often contains elements from the reworked till blanket underlying the beaches. These sediments generally form a thin cover and directly overly bedrock outcrops or the regional till blanket.
MGb/Trm **Marine beach sediments :** Sand, sandy silt, gravelly sand and stratified gravel and generally well sorted; thickness varying from 0.5 to 1 m; Contains elements from the reworked thin till blanket underlying the beaches. These sediments form a very thin cover and directly overly bedrock outcrops.
MGb **Littoral and near-shore sediments :** Sand, sandy silt, gravelly sand and stratified gravel and generally well sorted; thickness varying from 1 to 10 m; placed in shallow water during the glaciomarine phase; surface usually marked by littoral cords and sometimes reworked by wind power; these sediments generally form a thin cover over deep water sediments.
MGa **Deep water/offshore glaciomarine sediments :** Silty clay, dark, massive, laminated or stratified, locally comprising rhythmites; varying from less than 1 m to more than 50 m (in drilling) in thickness; put in placeramainy by decantation during the glaciomarine flood phase of the Goldthwait Sea
MG **Undifferenciated glaciomarine sediments**

GLACIOFLUVIAL SEDIMENTS

Go **Proglacial outwash sediments :** Sand, peebles and blocs put in place in broad, subplanar flat or gently sloping alluvial outwash in front of or beyond the terminal moraine of a glacier. Granulometry is generally downgrading downstream. The deposit often forms spreading plains whose surface is often marked by ancient sinuous and shallow channels.
Gs **Proglacial subaqueous outwash sediments :** Sand and silty sand, some gravel. Forms heaps set up in relatively shallow water plains at the end of sub- or intra-glacial tunnels opening up in the Goldthwait Sea. Sometimes exposed under marine sediments, in sand or gravel pits.
Gx **Glaciofluvial ice-contact sediments :** Mainly composed of sand, gravel and peebles, although glaciomarine deposits may contain a greater proportion of fine sediments. Deposited in subglacial or supraglacial environments, or in an ice-marginal position. These sediments take the form of eskers, kames, deltas-kames and moranic ridges.
GxT **Glaciofluvial ice-contact sediments associated with the St. Antonin Moraine:** Mainly composed of sand, gravel and peebles, although glaciomarine deposits may contain a greater proportion of fine sediments. Deposited in the context of the an ice-marginal position of the St. Antonin Moraine. These sediments take the form of eskers, kames, deltas-kames and moranic ridges.
G **Undifferentiated proglacial sediments**

GLACIAL SEDIMENTS

Trm **Reworked till, veneer :** Thin and discontinuous diamictic sediment in which has been reworked by the action of waves and sea currents, under the maximum elevation of the post-glacial Goldthwait Sea. Often fossiliferous.
Tr **Reworked till, blanket :** Diamictic sediment in which the upper unit has been reworked by the action of waves and sea currents, under the maximum elevation of the post-glacial Goldthwait Sea. Often fossiliferous. Can contain levels of stratified sand and peebles.
Tt **Till Blanket:** Thick and continuous till layer. Contains lodgment and ablation facies. Unsrarified drift, deposited directly by a glacier without reworking by meltwater, and consisting of a mixture of clay, silt, sand, gravel, and boulders ranging widely in size and shape. Thickness varies between 0.6 and 10 m.
Tm **Till veneer :** Thin and discontinuous till that may include areas of rock outcrop. Diamictic unit includes mostly ablation facies till. Thickness is usually below 1 m.
T **Till :** Continuous layer of till put in place by the St-Lawrence Ice Stream (SLIS) by ice flowing towards the northeast

PRE-QUATERNARY

R **Bedrock**

9 ANNEXE II – Forages, sondages et diagraphies

L'annexe II inclue les journaux (logs) des sondages CPT, forages et diagraphies géophysiques réalisés dans le cadre de cette thèse. Ils sont présentés en format tabloïd (11x17, format ANSI B) dans l'ordre suivant :

Sondage GLC-01 (CPT – identifié comme « CPT-PA04 »)

Sondage GLC-02 (CPT)

Log géologique GLC-02 (RPSS)

Sondage GLC-03 (CPT)

Log géologique GLC-03 (RPSS)

Sondage GLC-04 (CPT – identifié comme « GLC-05 »)

Log géologique et diagraphie géophysique GLC-04 (roto-sonic)

Log sismique GLC-04 (roto-sonic)

SONDAGE AU PIÉZOCÔNE (CPTu/SMR)

INRS Université d'avant-garde

Identifiant

Sondage : CPT-PA04
Fichier : G21L1401C.DAT

Projet

Nom : Chaudière-Appalaches
No. : _____

Coordonnées

X : 338931.12 m
Y : 5173579.78 m
Z : 90.32 m (p/r sol)
Syst. de coord.: UTM NAD83 z19

Informations générales

Date : 2014-07-21 (_____)
Sondage CPTu/SMR: 15 cm² ASTM
N° Sonde : 3405.101XX
Type de foreuse: Geotech 605-D

Client : INRS-ETE
Entrepreneur: INRS-ETE
Municipalité : Saint-Henri
Remarque: _____

Détails de construction

Prof. forage: 19.15 m
Diam. forage: 44.5 mm
Long. tubage: - m
Long. crépine: - m

Margelle: _____
Type de tubage: -
Diam. tubage: - mm
Échantillon: - m

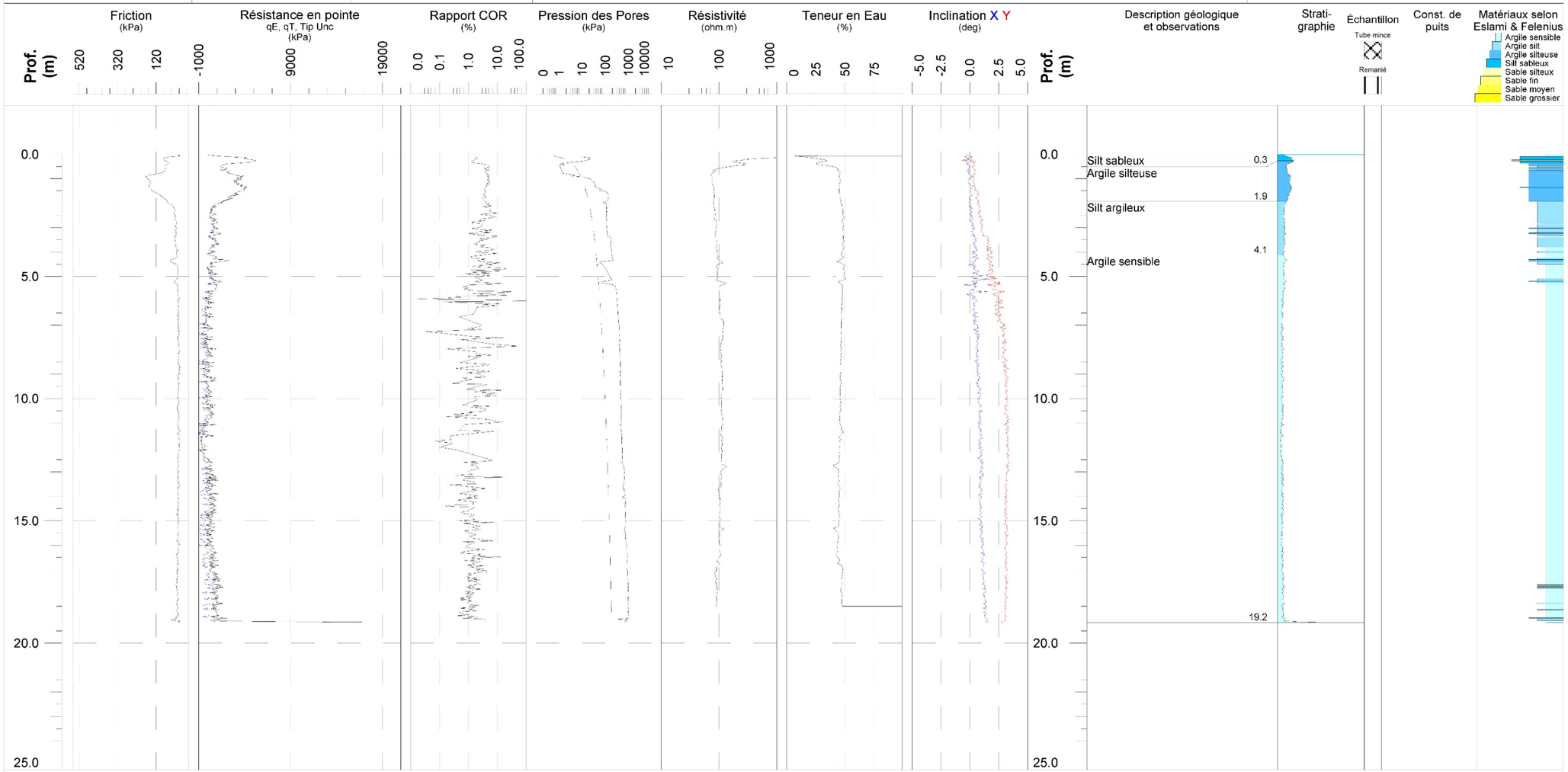

Supervisé par: J.-M. Ballard et: G. L.-Couture Vérifié par: _____ Préparé par: X. Malet Date de modification: 2014-08-05

SONDAGE AU PIÉZOCÔNE (CPTu/SMR)

INRS Université d'avant-garde

Identifiant
Sondage : GLC-02
Fichier : G2701501C

Projet
Nom : CA
No. :

Coordonnées (NAD83 Zone19)
X : _____ m
Y : _____ m
Z*: _____ m
*(niveau du sol)

Informations générales
Date : 2015-10-27
Sondage CPTu/SMR : 15 cm² ASTM
N° Sonde : 3405.101XX
Type de foreuse : Geotech 605D
Client : Michel Parent
Entrepreneur : _____
Municipalité : ST-Vallier
Remarque : Soleil,CPT

Détails de construction
Prof. Forage: 30 m
Diam. Forage: 0 mm
Long. tubage: _____ m
Long. crépine: _____ m
Margelle: _____ m
Type de tubage: _____
Diam. tubage: _____ mm
Échantillon: _____

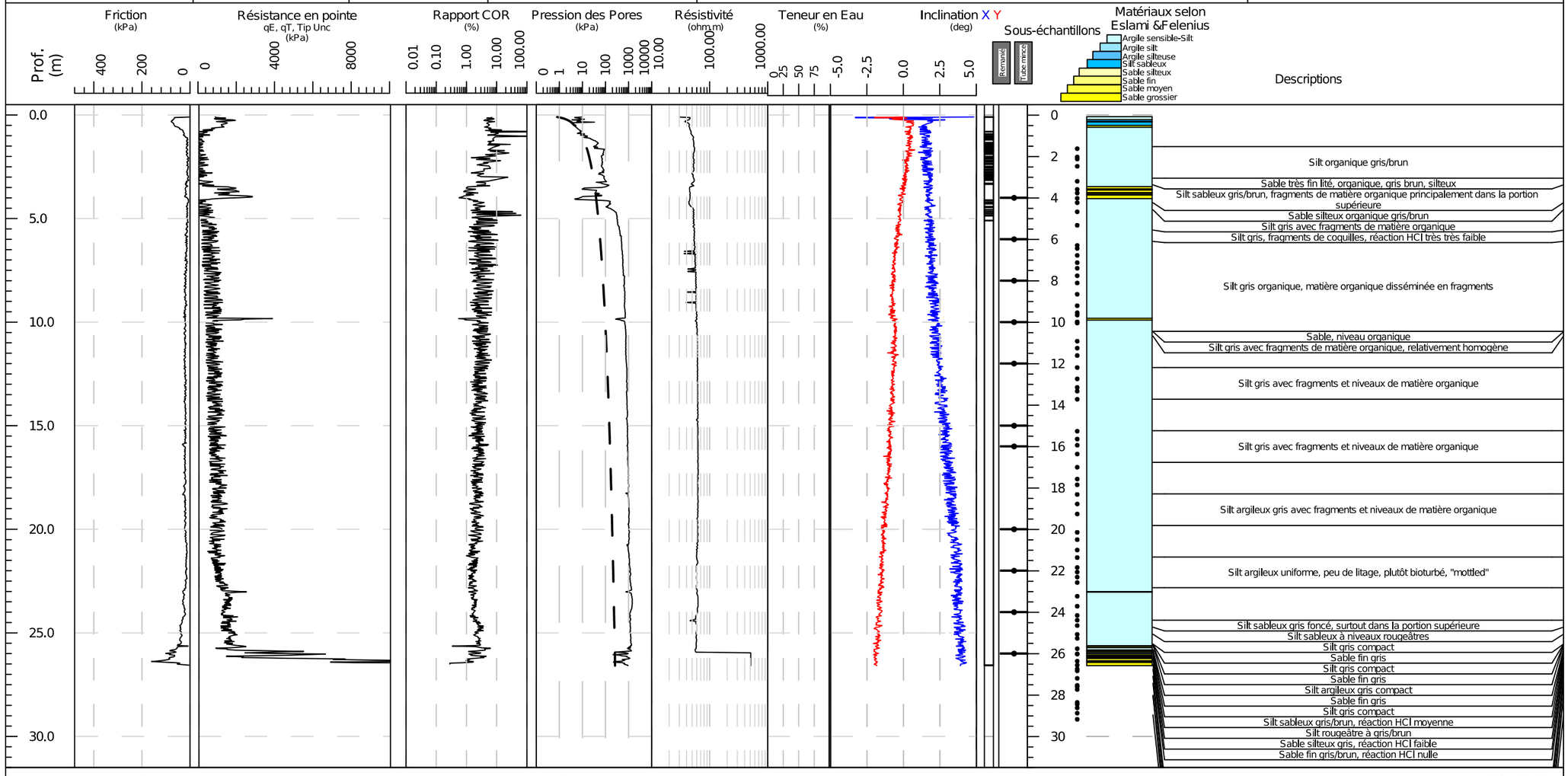

Supervisé par: J-M.Ballard et: Guillaume Vérifié par: Michel Parent Préparé par: _____ Date de modification: 2014-07-23

SONDAGE AU PIÉZOCÔNE (CPTu/SMR)

INRS
Université d'avant-garde

Identifiant
Sondage : GLC-02
Fichier : G2701501C

Projet
Nom : CA
No. :

Coordonnées (NAD83 Zone19)
X : _____ m
Y : _____ m
Z*: _____ m
*(niveau du sol)

Informations générales
Date : 2015-10-27
Sondage CPTu/SMR : 15 cm² ASTM
N° Sonde : 3405.101XX
Type de foreuse : Geotech 605D
Client : Michel Parent
Entrepreneur: _____
Municipalité : ST-Vallier
Remarque: Soleil,CPT

Détails de construction
Prof. Forage: 30 m
Diam. Forage: 0 mm
Long. tubage: _____ m
Long. crépine: _____ m
Margelle: _____ m
Type de tubage: _____
Diam. tubage: _____ mm
Échantillon: _____

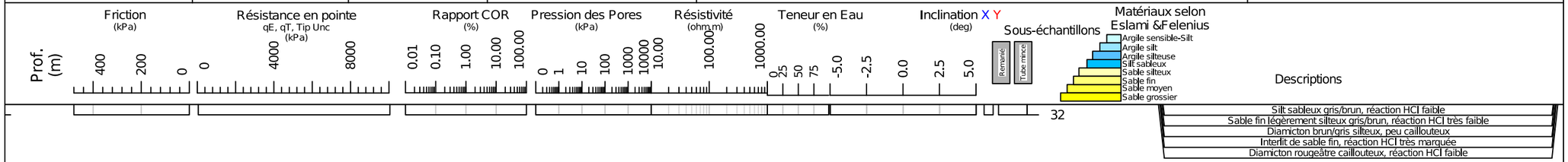

Supervisé par: J-M.Ballard et: Guillaume Vérifié par: Michel Parent Préparé par: _____ Date de modification: 2014-07-23

Rapport de forage

Forage : GLC-02 Date :
Localisation : Saint-Vallier

X : 364294.363
Y : 5196010.733
Z : 10.93
Système de coordonnées : UTM fuseau 19N

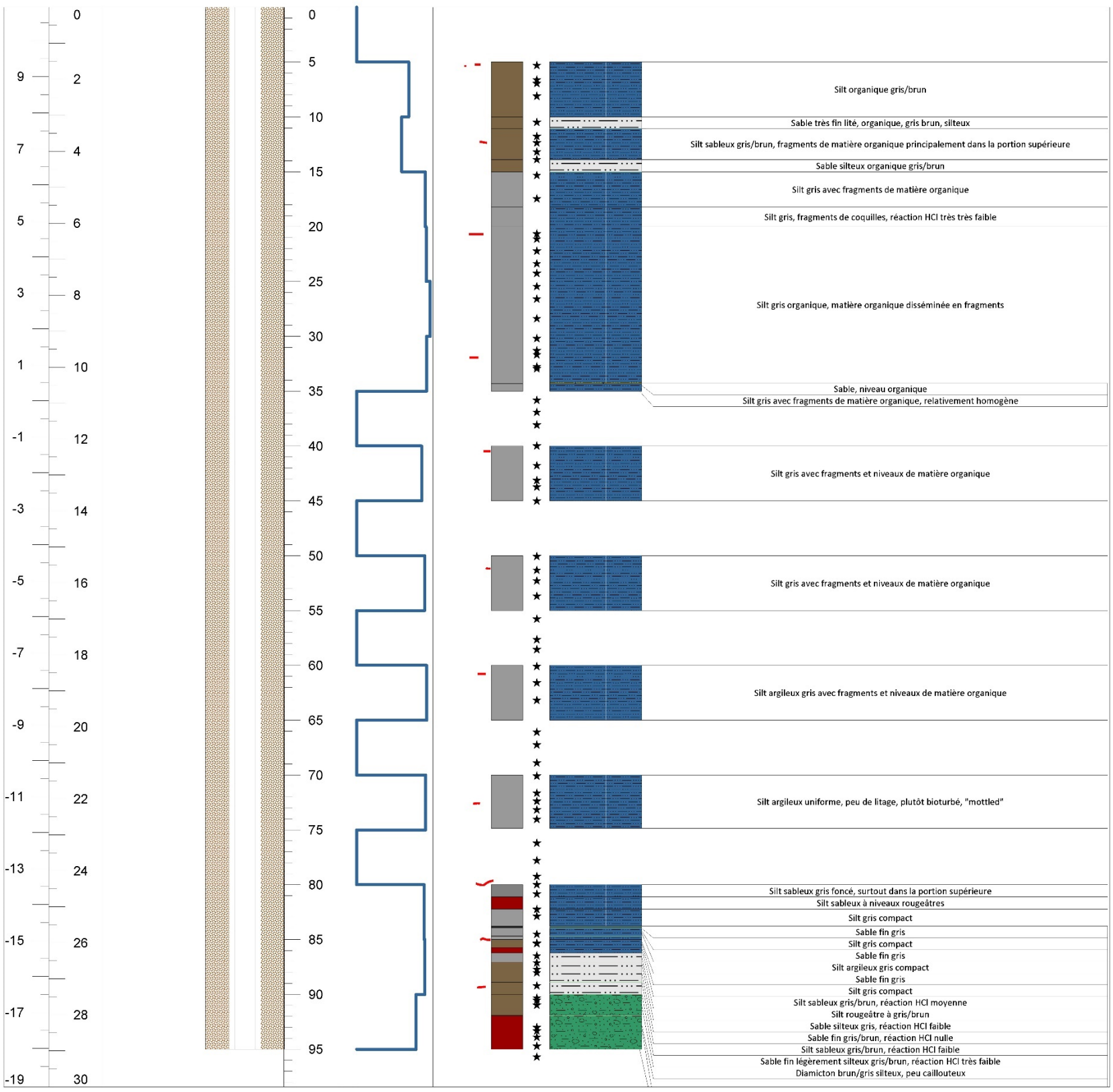

Surveillance des travaux : JMB/MP/GLC
Rapport de forage : GLC
Date de réalisation du schéma de forage : 2016-07-18

SONDAGE AU PIÉZOCÔNE (CPTu/SMR)

INRS Université d'avant-garde

Identifiant
Sondage : GLC-03
Fichier : G2801501C

Projet
Nom : CA
No. :

Coordonnées (NAD83 Zone19)
X : _____ m
Y : _____ m
Z*: _____ m
*(niveau du sol)

Informations générales
Date : 2015-10-27
Sondage CPTu/SMR : 15 cm² ASTM
N° Sonde : 3405.101XX
Type de foreuse : Geotech 605D
Client : Michel Parent
Entrepreneur : _____
Municipalité : St-Michel
Remarque : Soleil,CPT

Détails de construction
Prof. Forage : 30 m
Diam. Forage : 0 mm
Long. tubage : _____ m
Long. crépine : _____ m
Margelle : _____ m
Type de tubage : _____
Diam. tubage : _____ mm
Échantillon : _____

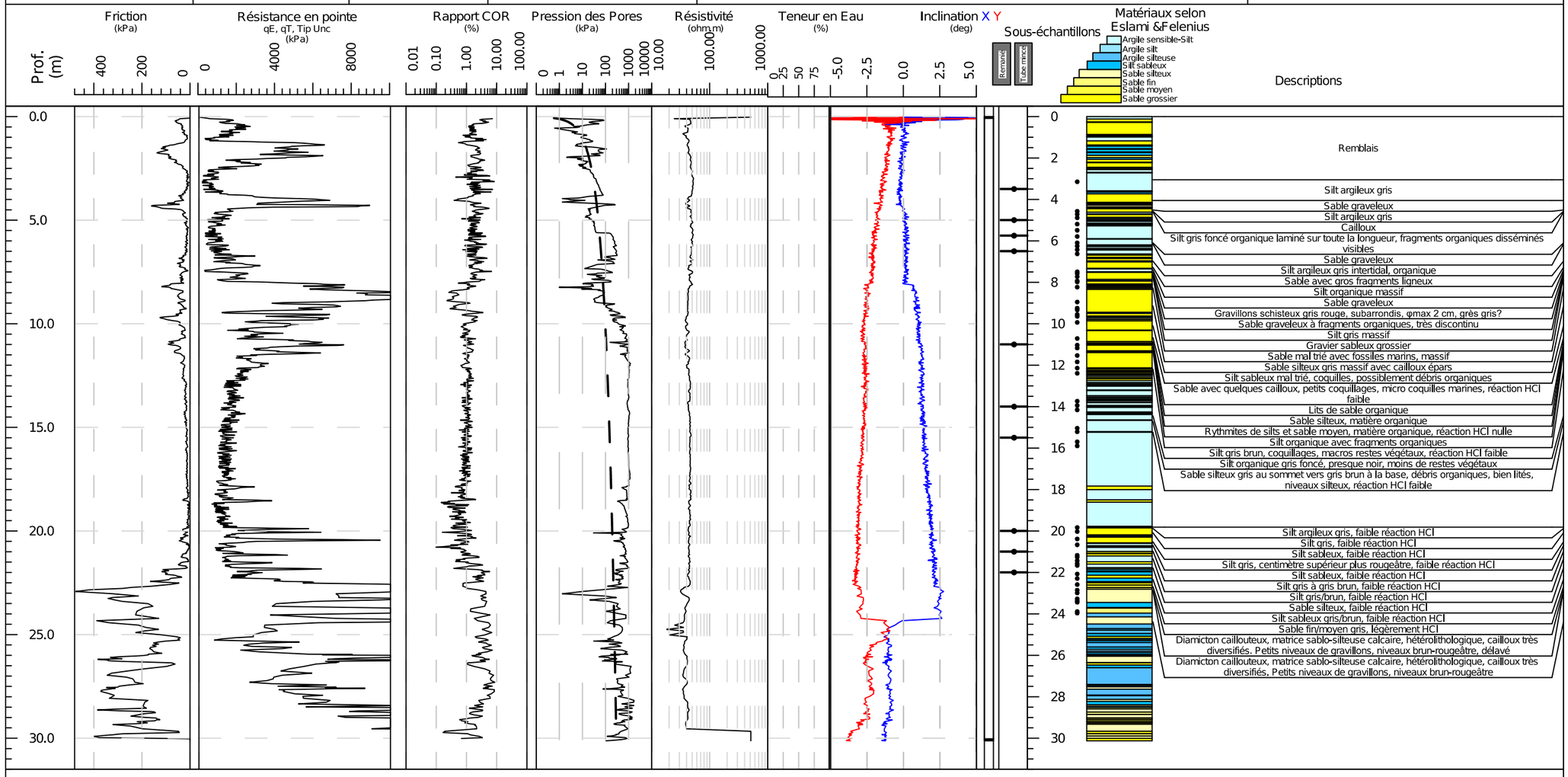

Supervisé par: J-M.Ballard et: Guillaume
Vérifié par: Michel Parent
Préparé par: _____
Date de modification: 2014-07-23

Rapport de forage

Natural Resources Canada / Ressources naturelles Canada — Canada

Forage : GLC-03 Date :
Localisation : Saint-Michel

X : 358739.45
Y : 5193991.057
Z : 9
Système de coordonnées : UTM fuseau 19N

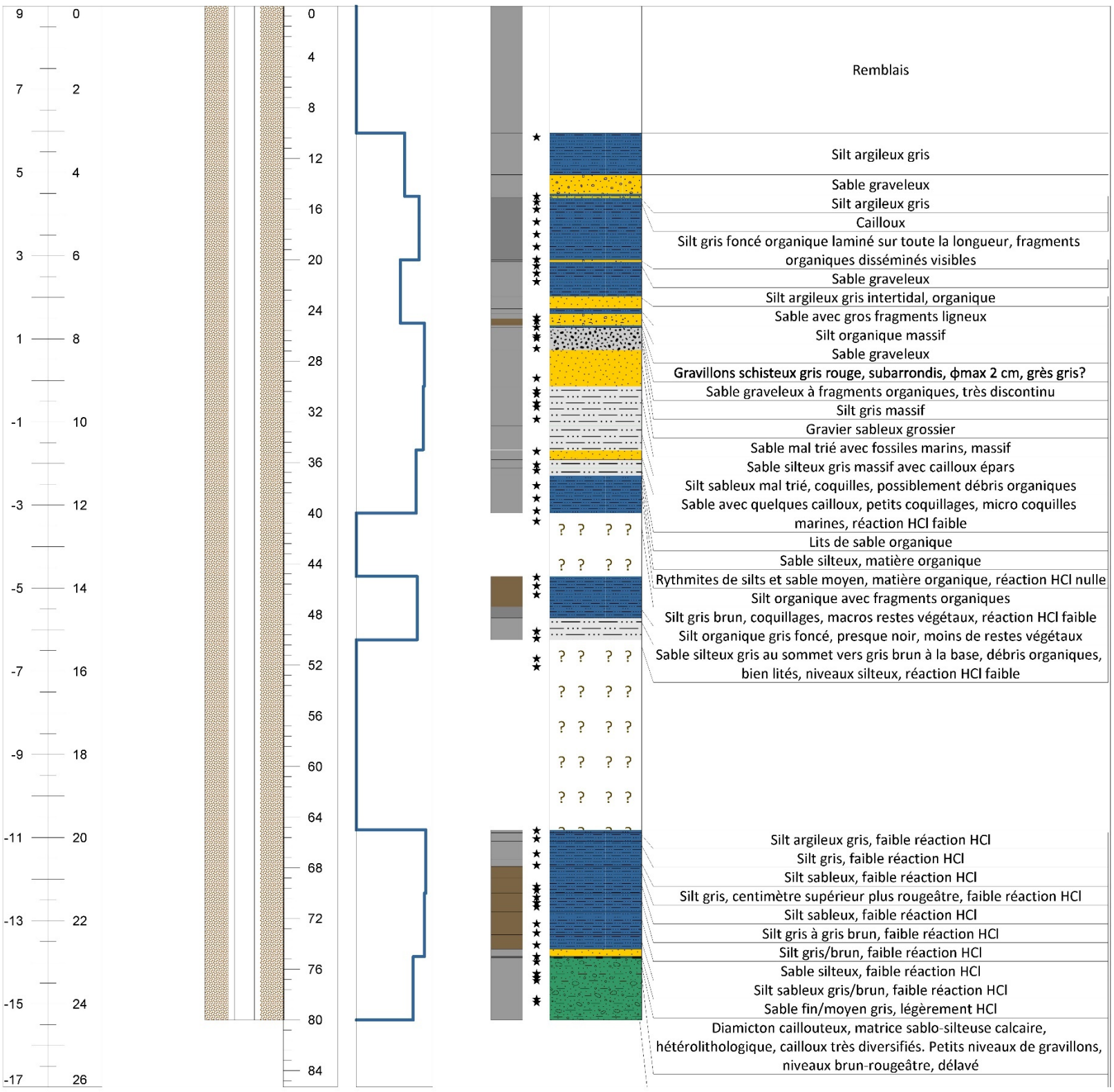

Surveillance des travaux : JMB/MP/GLC
Rapport de forage : GLC
Date de réalisation du schéma de forage : 2016-07-18

SONDAGE AU PIÉZOCÔNE (CPTu/SMR)

INRS Université d'avant-garde

Identifiant
Sondage : GLC-05
Fichier : G19L1601C

Projet
Nom : CA
No. :

Coordonnées (NAD83 Zone19)
X : _____ m
Y : _____ m
Z*: _____ m
*(niveau du sol)

Informations générales
Date : 2016-07-17
Sondage CPTu/SMR : 15 cm² ASTM
N° Sonde : 3405.101XX
Type de foreuse: Geotech 605D
Client : Michel Parent
Entrepreneur: _____
Municipalité : Montmagny
Remarque: Soleil,CPT

Détails de construction
Prof. Forage: 30 m
Diam. Forage: 0 mm
Long. tubage: _____ m
Long. crépine: _____ m
Margelle: _____ m
Type de tubage: _____
Diam. tubage: _____ mm
Échantillon: _____

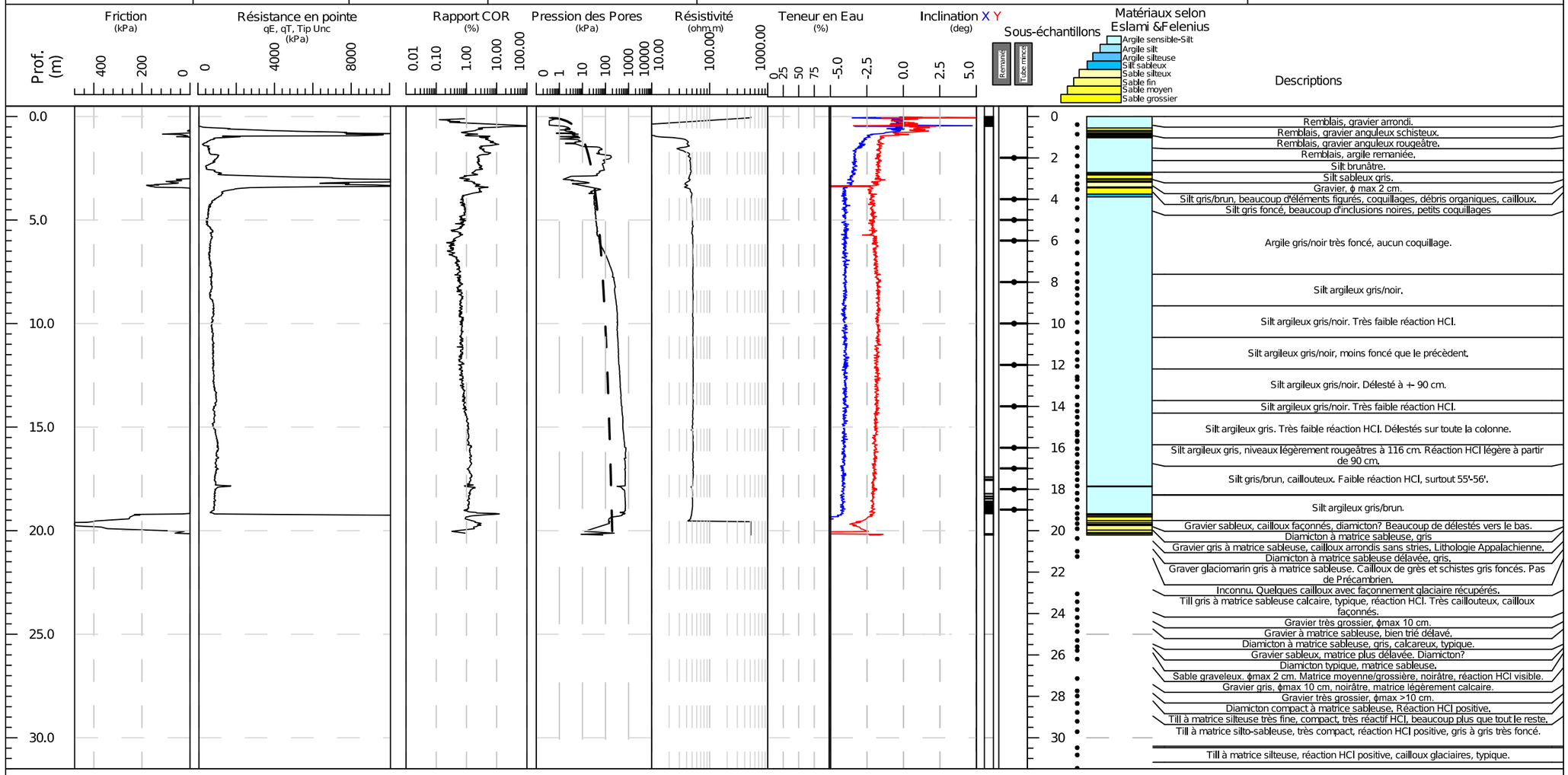

Supervisé par: J-M.Ballard et: Guillaume
Vérifié par: Michel Parent
Préparé par: _____
Date de modification: 2014-07-23

SONDAGE AU PIÉZOCÔNE (CPTu/SMR)

INRS
Université d'avant-garde

Identifiant
Sondage : GLC-05
Fichier : G19L1601C

Projet
Nom : CA
No. :

Coordonnées (NAD83 Zone19)
X : _____ m
Y : _____ m
Z*: _____ m
*(niveau du sol)

Informations générales
Date : 2016-07-17
Sondage CPTu/SMR : 15 cm² ASTM
N° Sonde : 3405.101XX
Type de foreuse : Geotech 605D
Client : Michel Parent
Entrepreneur: _____
Municipalité : Montmagny
Remarque: Soleil,CPT

Détails de construction
Prof. Forage: 30 m
Diam. Forage: 0 mm
Long. tubage: _____ m
Long. crépine: _____ m
Margelle: _____ m
Type de tubage: _____
Diam. tubage: _____ mm
Échantillon: _____

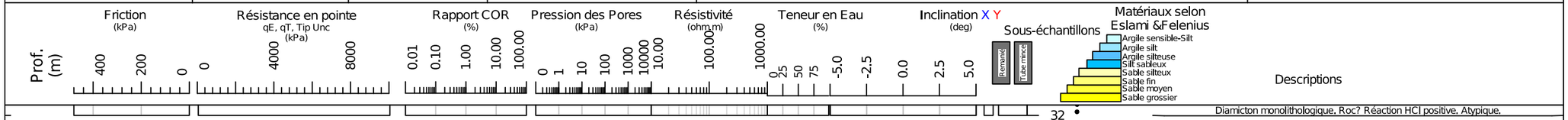

Supervisé par: J-M.Ballard et: Guillaume Vérifié par: Michel Parent Préparé par: _____ Date de modification: 2014-07-23

Rapport de forage

Forage : GLC-04 Date : 8-9 mars 2016
Localisation : Montmagny

X : 381398
Y : 5202867
Z : 15.81
Système de coordonnées : UTM fuseau 19N

Surveillance des travaux : JMB/MP/GLC
Rapport de forage : GLC
Date de réalisation du schéma de forage : 2016-07-18

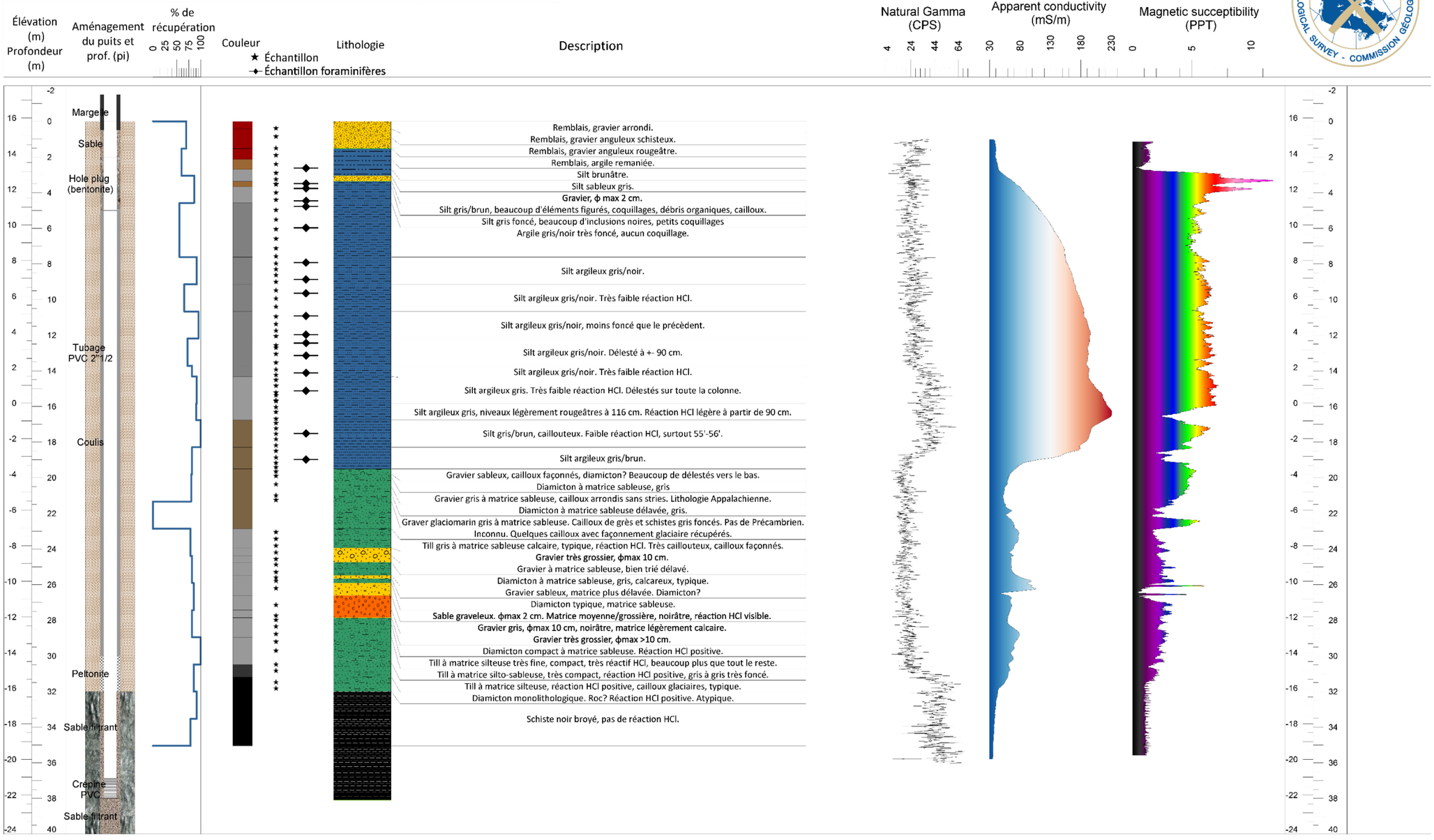

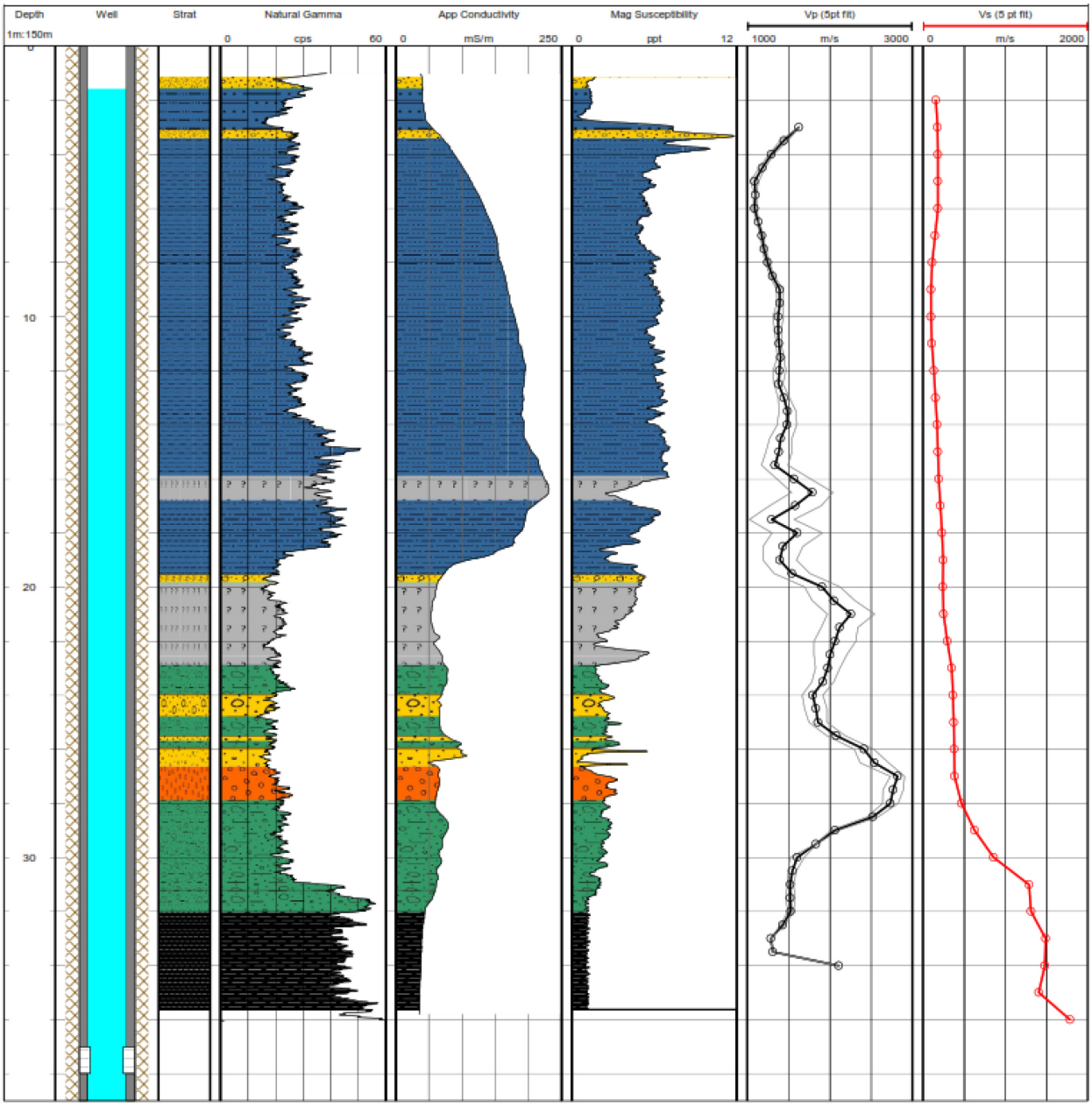
Depth
1m:150m
Well
Strat
Natural Gamma
0
cps
60
App Conductivity
0
mS/m
250
Mag Susceptibility
0
ppt
12
Vp (5pt fit)
1000
m/s
3000
Vs (5 pt fit)
0
m/s
2000
10
20
30

10 ANNEXE III – Modèle géologique 3D

L'annexe III inclue les grilles du contact supérieur de chaque unité du modèle 3D présenté au chapître 3. Pour chaque couche, les grilles sont continues et couvrent entièrement les limites du modèle géologique, même si les unités n'existent pas partout. Lorsqu'une unité géologique n'existe pas, son élévation rapportée est celle du contact supérieur de la couche sous-jacente.

Le format GeoTIFF (.tif) a été préféré pour la diffusion du modèle afin d'assurer une compatibilité maximale et un accès facile. Les grilles sont compressées (sans perte) à l'aide de la méthode Deflate (ZIP).

11 ANNEXE IV – Compilation des données de linéations glaciaires

L'annexe IV inclue la compilation des données de linéations glaciaire présentées à l'article 3. La compilation est fournie en format Shapefile (.shp) et GeoJSON (.json).